AD-A045 034   MCDONNELL AIRCRAFT CO ST LOUIS MO   F/G 9/3

INTRASYSTEM ELECTROMAGNETIC COMPATIBILITY ANALYSIS PROGRAM (IEM--ETC(U)

SEP 77   R A PEARLMAN   F30602-76-C-0193

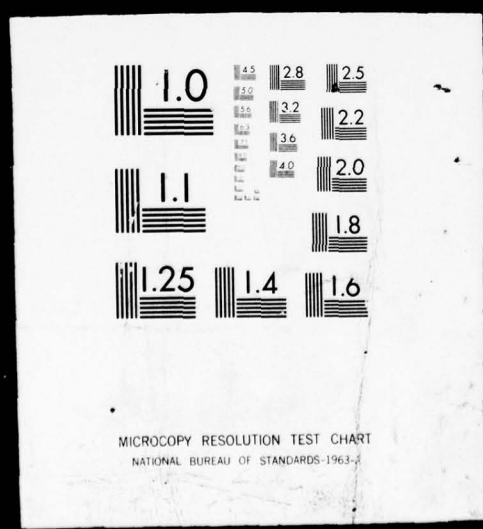UNCLASSIFIED   RADC-TR-77-290-PT-1   NL

1 OF 3

AD.
A045 034

AD

A045034

1.0
1.1
1.25
4.5
5.0
5.6
3.6
4.0
2.8
3.2
4.0
1.4
2.5
2.2
2.0
1.8
1.6

MICROCOPY RESOLUTION TEST CHART
NATIONAL BUREAU OF STANDARDS-1963-A

AD A045034

ADÑO.—
DDC FILE COPY

RADC-TR-77-290, Part I (of two)
Final Technical Report
September 1977

INTRASYSTEM ELECTROMAGNETIC COMPATIBILITY ANALYSIS PROGRAM
(IEMCAP) F-15 VALIDATION
Validation and Sensitivity Study

McDonnell Aircraft Company

Approved for public release; distribution unlimited.

D D C
RECEIVED
OCT 7 1977
A

ROME AIR DEVELOPMENT CENTER
Air Force Systems Command
Griffiss Air Force Base, New York 13441
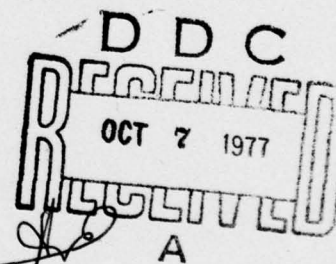
This report contains a large percentage of machine-produced copy which is not of the highest quality but because of economical consideration, it was determined in the best interest of the Government that they be used in this publication.

This report has been reviewed by the RADC Information Office (OI) and is releasable to the National Technical Information Service (NTIS). At NTIS it will be releasable to the general public, including foreign nations.
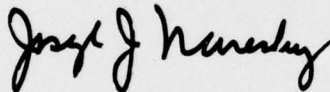
This report has been reviewed and is approved for publication.

APPROVED: *Daniel J. Kenneally*
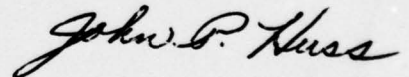
DANIEL J. KENNEALLY
Project Engineer

APPROVED: *Joseph J. Naresky*

JOSEPH J. NARESKY
Chief, Reliability & Compatibility Division

FOR THE COMMANDER: *John P. Huss*

JOHN P. HUSS
Acting Chief, Plans Office

If your address has changed or if you wish to be removed from the RADC mailing list, or if the addressee is no longer employed by your organization, please notify RADC (DAP) Griffiss AFB NY 13441. This will assist us in maintaining a current mailing list.

Do not return this copy. Retain or destroy.

UNCLASSIFIED

SECURITY CLASSIFICATION OF THIS PAGE *(When Data Entered)*

REPORT DOCUMENTATION PAGE	READ INSTRUCTIONS BEFORE COMPLETING FORM

1. REPORT NUMBER	2. GOVT ACCESSION NO.	3. RECIPIENT'S CATALOG NUMBER
RADC-TR-77-290, Part I (of two)		

4. TITLE *(and Subtitle)*	5. TYPE OF REPORT & PERIOD COVERED
INTRASYSTEM ELECTROMAGNETIC COMPATIBILITY ANALYSIS PROGRAM (IEMCAP) F-15 VALIDATION- Part I. Validation and Sensitivity Study.	Final Technical Report.
	6. PERFORMING ORG. REPORT NUMBER
	N/A

7. AUTHOR(s)	8. CONTRACT OR GRANT NUMBER(s)
Dr. R. A. Pearlman	F30602-76-C-0193

9. PERFORMING ORGANIZATION NAME AND ADDRESS	10. PROGRAM ELEMENT, PROJECT, TASK AREA & WORK UNIT NUMBERS
McDonnell Aircraft Company McDonnell Douglas Corporation P. O. Box 516, Saint Louis MO 63166	62702F 45400139

11. CONTROLLING OFFICE NAME AND ADDRESS	12. REPORT DATE
Rome Air Development Center (RBCT) Griffiss AFB NY 13441	September 1977
	13. NUMBER OF PAGES
	196

14. MONITORING AGENCY NAME & ADDRESS *(if different from Controlling Office)*	15. SECURITY CLASS. *(of this report)*
Same	UNCLASSIFIED
	15a. DECLASSIFICATION/DOWNGRADING SCHEDULE
	N/A

16. DISTRIBUTION STATEMENT *(of this Report)*

Approved for public release; distribution unlimited.

17. DISTRIBUTION STATEMENT *(of the abstract entered in Block 20, if different from Report)*

Same

18. SUPPLEMENTARY NOTES

RADC Project Engineer:
Daniel J. Kenneally (RBCT)

19. KEY WORDS *(Continue on reverse side if necessary and identify by block number)*

EMC Simulation	Computer Program Validation
Electromagnetic Compatibility	Intrasystem Analysis
Electromagnetic Interference	Aircraft Avionics
Radio Frequency Interference	
Computer Programs	

20. ABSTRACT *(Continue on reverse side if necessary and identify by block number)*

The validity and usefulness of the Intra-system Electromagnetic Compatibility Analysis Program (IEMCAP) is assessed, based on its predictions for the F-15 air superiority fighter aircraft. The aircraft was simulated using a combination of known, measured and approximated data. A sensitivity study is also performed, indicating the effects of approximating unknown IEMCAP input parameters. Finally, a physical interpretation of the integrated EMI margin is given, and an assessment is made of its validity as an EMC figure merit.

(cont'd)

DD FORM 1473 EDITION OF 1 NOV 65 IS OBSOLETE
1 JAN 73

UNCLASSIFIED

SECURITY CLASSIFICATION OF THIS PAGE *(When Data Entered)*

The IEMCAP is shown to successfully predict the known overall compatibility of the F-15, and is also shown to predict interference between equipments in cases where receiver blanking is provided by the system. Cases in which the program incorrectly predicted interference are generally attributed to uncertainties in modeling non-required spectra rather than program inaccuracy.

The results supports a judgment that the integrated EMI margin is a valid figure of merit for most equipment used on aircraft systems, with the exception of threshold vulnerable devices.

This report is divided into Part I and Part II. The first part of the report describes how the F-15 aircraft was used as a data base for a shakedown of the IEMCAP code and an assessment of its predictions. The results of an imput parameter sensitivity study are also presented. The second part of the report is devoted to a detailed exposition on the meaning and physical significance of the integrated EMI margin, the quantity calculated by the IEMCAP as a measure of interference.

EVALUATION

This validation effort effectively demonstrates that the IEMCAP code
can successfully predict the EMC performance characteristics of a modern
Air Force weapon system. In this validation, using the F-15 aircraft as
the measured baseline for comparison, the IEMCAP predicted the overall
system compatibility, some isolated cases of interference, and the
compatibility effectiveness of the subsequent fixes. Numerically, this
means that for 353 coupling pairs in some three major coupling modes (wire-
to-wire, antenna-to-antenna, and antenna-to-wire), IEMCAP successfully
predicted 303 cases of compatibility, 7 cases of interference, (and the
effectiveness of their subsequent fixes), and 43 Type I errors in which
the code predicted interference when actual compatibility was present.
There were no Type II errors in the analysis in which compatibility was
predicted when interference was present. With this validated computerized
analysis program, Air Force product divisions and their system contractors
can facilitate the practical implementation of EMC design-to-cost at all
stages of an Air Force system's life cycle with the attendant scheduling,
testing, and cost benefits. This effort supports technical program
objective C^3 Survailability, (TPO #R1C).

DANIEL J. KENNEALLY
Project Engineer

iii

PREFACE

This report documents work conducted by McDonnell Aircraft Company, St. Louis, Missouri, on the Intrasystem Electromagnetic Compatibility Analysis Program (IEMCAP) F-15 validation effort, sponsored by Rome Air Development Center, Griffiss Air Force Base, New York, under Contract F30602-76-C-0193 from 8 April 1976 to 8 April 1977. Dr. Ronald A. Pearlman was the MCAIR principal investigator and Mr. Daniel J. Kenneally (RBCT) was the RADC Project Engineer.

This report is divided into Part I and Part II. The first part of the report describes how the F-15 aircraft was used as a data base for a shakedown of the IEMCAP code and an assessment of its predictions. The results of an input parameter sensitivity study are also presented. The second part of the report is devoted to a detailed exposition on the meaning and physical significance of the integrated EMI margin, the quantity calculated by the IEMCAP as a measure of interference.

Contributions to this contract effort from Dr. J. L. Bogdonar, Mr. G. Koester, Mr. R. E. Plummer and Mr. G. L. Weinstock are gratefully acknowledged. The timely and helpful suggestions of Dr. D. Weiner of Syracuse University are also acknowledged.

TABLE OF CONTENTS

TABLE OF CONTENTS

FIGURES

TABLES

5

TABLES

1. INTRODUCTION AND SUMMARY

1.1 <u>Introduction</u>. This report documents a one-year effort undertaken to assess the performance of the Intra-system Electromagnetic Compatibility Program (IEMCAP)[1] on the basis of its predictions for a compatible F-15 aircraft. The major effort was devoted to the Comparative Electromagnetic Analysis Routine (CEAR) survey option, in which the program is used to predict EMI margins for a baseline system. Representative F-15 equipments were incorporated into several mini-systems serving as a baseline for the IEMCAP analysis, using a combination of known, measured, and approximated data. The simulation included 10 F-15 antenna ports associated with the UHF, IFF, TACAN, auxiliary UHF, ADF and ILS subsystems, 50 equipments located throughout the aircraft, and 170 wire ports including signal/control lines, power lines, and electro-explosive device lines.

The IEMCAP was repeatedly run with these mini-systems, revealing several code errors that were subsequently corrected by RADC. The mini-system were then rerun for an assessment of IEMCAP interference predictions on the baseline system. This assessment was made by comparing the predicted EMI margins with the known compatibility of the F-15 aircraft. Thus, receptors known to be compatible should have an integrated EMI margin equal to or less than zero, since a positive margin corresponds to interference. For example, if the program predicts a positive margin of +15 dB for that receptor, there is at least a 15 dB inaccuracy in the IEMCAP prediction; however, if the program predicts a negative margin, all that can be said is that the code correctly predicts compatibility, since measured data on negative margins is generally not available. A possible experiment is proposed in Part II in which the integrated EMI margin calculated by IEMCAP could be evaluated quantitatively on the basis of measured power and susceptibility.

All cases for which the IEMCAP predicted positive margins were investigated in detail, and conclusions were drawn on the probable cause of each discrepancy. Because of the many approximations associated with the input data, as well as the built-in approximations in the IEMCAP, predicted margins between -15 dB and +15 dB were considered to be in a grey area, indicating that there may or may not be interference.

This overall assessment based on known F-15 compatibility was supplemented by a number of cases where more detailed information was available. Measured antenna coupling data was used to evaluate the IEMCAP antenna-to-antenna coupling calculation and provide a quantitative basis for the assessment of antenna-coupled interference predictions. In addition, 4 former cases of EMI on the F-15 production aircraft, subsequently corrected by shielding or filtering, were simulated in IEMCAP runs to see whether the program predicted the original problem and its subsequent fix, using IEMCAP filter and shielding models.

The Specification Generation Routine (SGR) option of IEMCAP was also exercised, and an overall evaluation of its performance is presented in this report.

---

[1] For those readers unfamiliar with the IEMCAP, a description of the program itself and its conceptual basis is provided in Appendix A of Part II.

To determine the effect of approximating IEMCAP input parameters, a sensitivity study was performed in which 18 types of input parameters were varied and correlated with changes in IEMCAP output parameters. The results of the study are included in this report and give a good overall assessment of the sensitivity of the input parameters.

In Part I of this report, Section 2 documents how the F-15 equipments were selected and modeled to create a data base for the IEMCAP. A description of the mini-systems used as a baseline is given, along with a listing of the input data and a record of the IEMCAP code errors that were corrected. Section 3 presents an assessment of IEMCAP predictions for the mini-systems, with conclusions on the applicability of the integrated margin concept to systems similar to the F-15. The results of the sensitivity analysis are presented in Section 4.

Part II of this report is devoted to a detailed explanation of the meaning and physical significance of the integrated EMI margin. This quantity is shown to be a measure of the interference at a receptor, the ratio of the interference at the receptor input to a threshold level of interference. It is also shown how this threshold is relatable to measured receiver performance characteristics and the minimum signal-to-noise levels required for satisfactory operation. The purpose of this discussion is to demonstrate the physical significance of the integrated margin as an indicator of system performance and to show how the IEMCAP can be applied to various types of equipments.

1.2 <u>Summary</u>. For the most part the IEMCAP mini-system runs were successful in predicting the known compatibility of the F-15 aircraft.

For coupling between antenna ports, the program predicts positive integrated margins in 16 out of 49 cases. Of the 16 positive margins, 7 are considered to be correct predictions of interference, accounted for by system-provided blanking or receiver suppression. Figure 1 shows the distribution of predicted integrated margins for antenna-to-antenna coupling, between -100 dB and +60 dB, and also shows the number of cases correctly predicted as interference or compatibility. For the cases of incorrectly predicted interference, the probable cause is over-predicted antenna coupling in six cases, simulated susceptibility levels that are to low in two cases, and simulated emission levels that are too high in the remaining case. The IEMCAP calculations for antenna coupling generally compare favorably with measured coupling data, with the exception of coupling between antennas on opposite sides of the fuselage.

For coupling between wire ports involving a pair of wires with a common run length, the program predicts positive integrated margins in 29 out of 177 cases, with a distribution as illustrated in Figure 2. The most probable causes for the positive margins are the worst case simulation of spurious emission levels by an envelope based on the MIL-STD-461 specification curve, and errors introduced by the approximation of unknown susceptibility levels.

For coupling between antenna ports and wire ports, the program predicts positive margins in 5 out of 120 cases involving coupling to an exposed wire, with a distribution as illustrated in Figure 3. All of these cases involve coupling to DC magnetic relays, where the simulated susceptibility threshold at UHF and L-band frequencies is probably much lower than the actual susceptibility level, considering the eddy current and hysteresis losses.

8
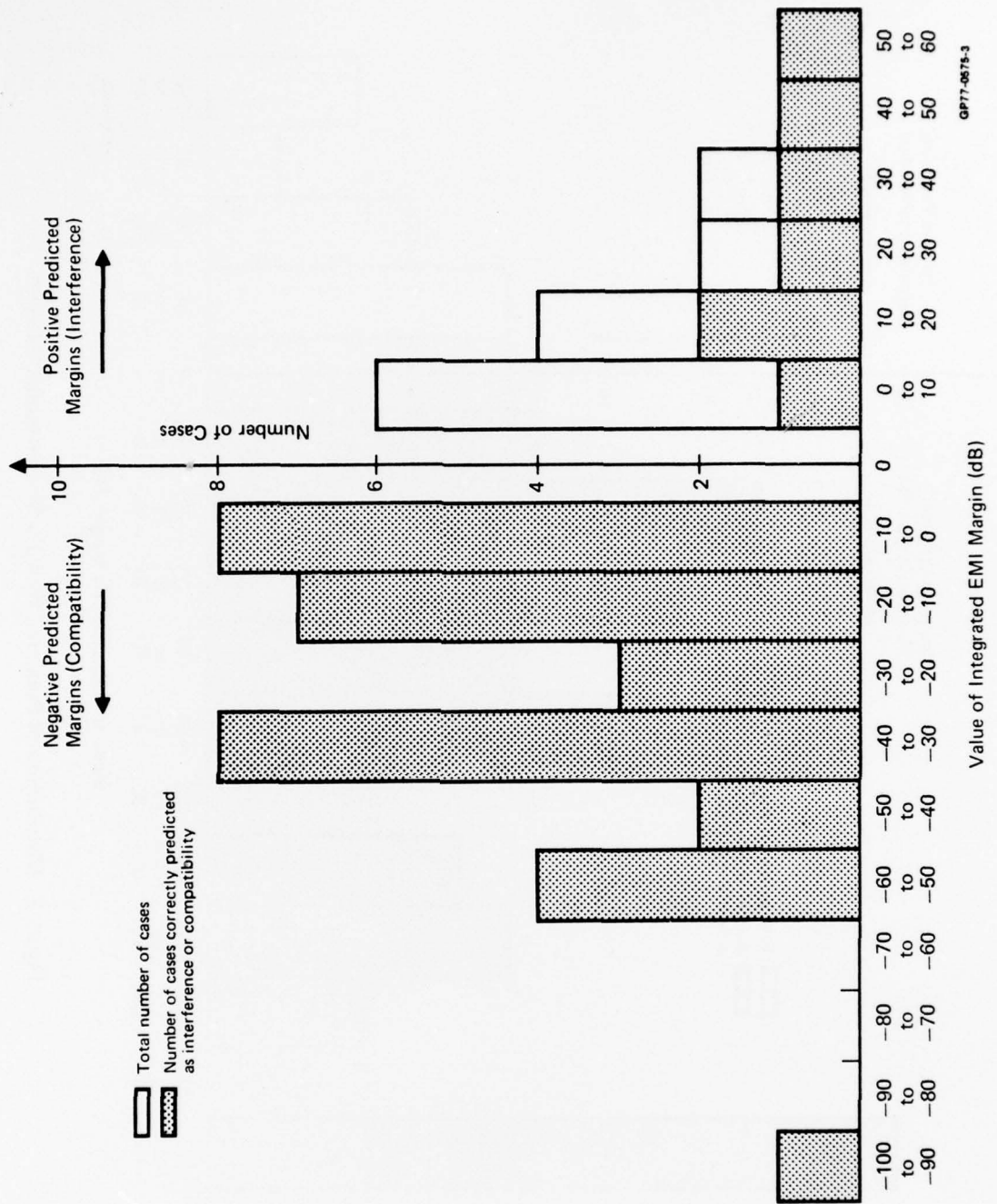
Figure 1. Distribution of Predicted Antenna-To-Antenna Integrated Margins

GP77-0875-3

9
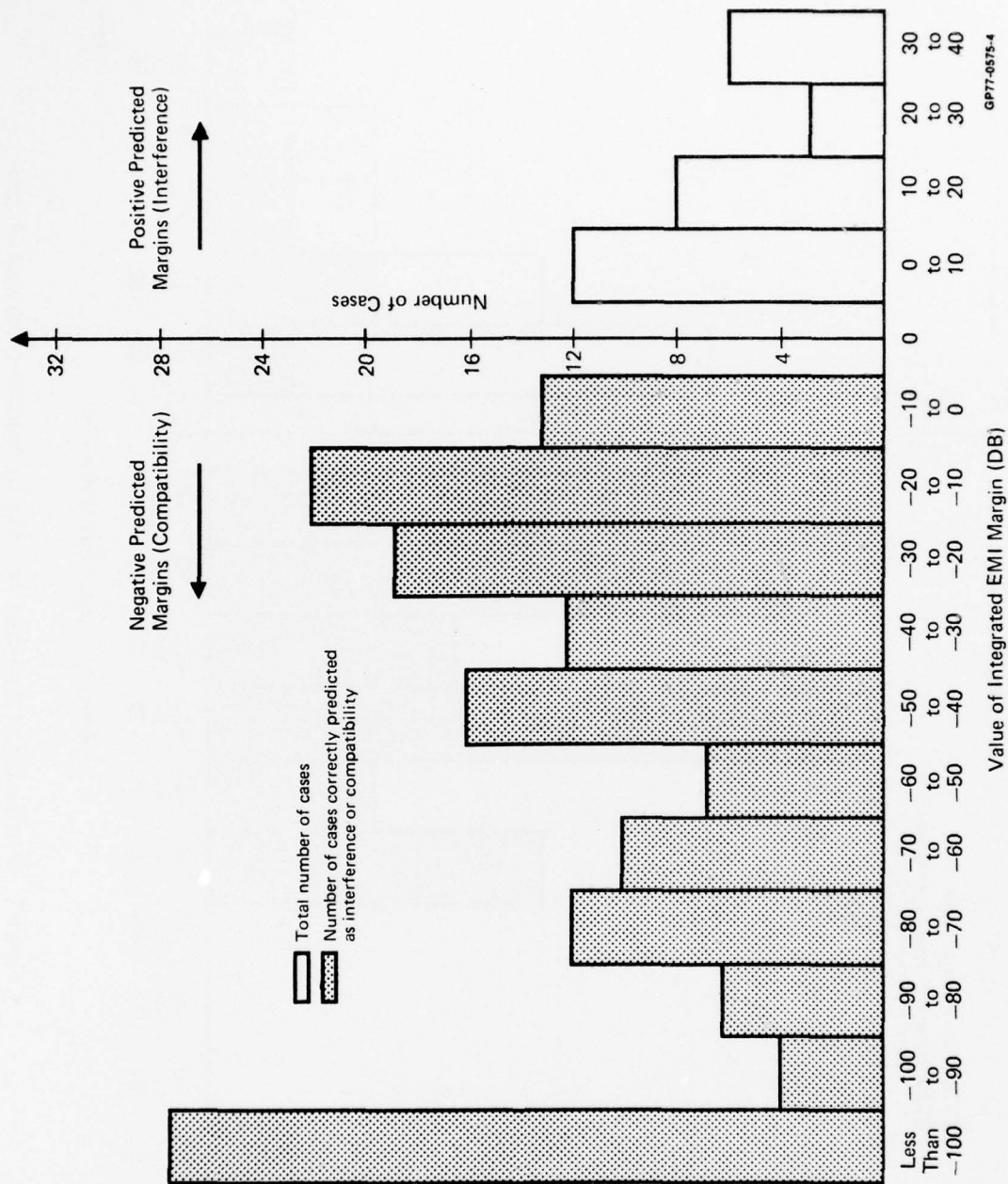
Figure 2. Distribution of Predicted Wire-To-Wire Integrated Margins

GP77-0575-4

10
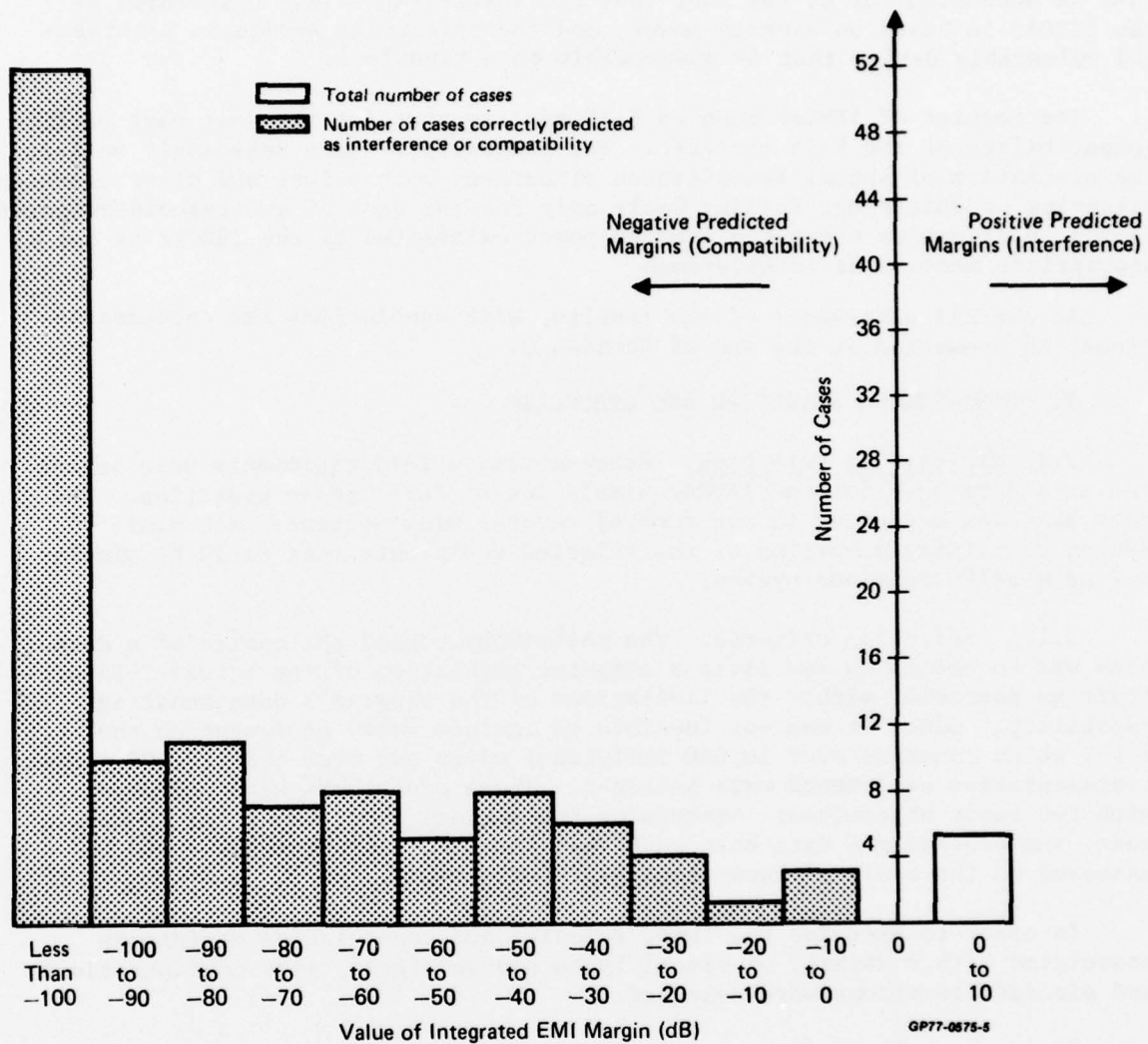
Figure 3 Distribution of Predicted Antenna-To-Wire Integrated Margins

11

The results of simulating actual cases of EMI are reasonably favorable in 3 out of 4 cases. In 2 cases, the program predicts the original interference and also predicts the elimination of the interference in the shielded or filtered configuration simulating the actual fix. In one case the program does not predict the interference, but is only in error by about 8 dB in the integrated margin. In the remaining case, however, the program fails to predict the interference by a wide margin, an error of about 60 dB. The latter case is accounted for by the fact that the integrated margin calculated by the IEMCAP is based on average power, and the particular device is a threshold vulnerable device that is susceptible to a transient.

The results of IEMCAP runs on F-15 mini-systems for the most part confirm the compatibility of the F-15 aircraft. The program performed reasonably well in the simulation of actual interference situations both before and after connector filtering or shielding, failing badly only for the case of a threshold-vulnerable device, a situation where the average power calculated by the IEMCAP is not an appropriate measure of interference.

An overall assessment of the results, with conclusions and recommendations, is presented at the end of Section 3.

2. MINI-SYSTEM SELECTION AND DEBUGGING

2.1 Mini-system selection. Representative F-15 equipments were selected as a data base for the IEMCAP simulation of full system operation. The data base was organized in the form of several mini-systems, each mini-system containing a portion of the selected equipments that could be simulated as a self-contained system.

2.1.1 Selection criteria. The philosophy behind the choice of a data base was to obtain as realistic a computer simulation of the actual F-15 aircraft as possible, within the limitations of the program's data handling capability. Since it was not feasible to include every equipment on the F-15, which contains over 10,000 individual wires and more than 20,000 ports, representative equipments were selected. These equipments were selected with two basic objectives: exercising the various portions of the IEMCAP code, and providing a data base such that the IEMCAP predictions could be assessed on the basis of known equipment performance.

In order to exercise the code, avionics and non-avionics equipments associated with a variety of signal types and waveforms, wire configurations and aircraft locations were selected.

Since the bulk of the ports in F-15 equipments are interconnected by wires, the mini-system selection process centered primarily on choosing the various wires. To meet the basic objectives, a systematic procedure was used to select wires according to the following considerations:

(a) Common run length. Wires with common parallel run lengths, thus permitting electromagnetic coupling between wires, were selected from actual F-15 wire bundles, with 3 or 4 wires representing each bundle. Since the IEMCAP is used as a system EMC tool for analysis of compatibility between different equipments and subsystems rather than within an equipment, each bundle representa-

12

tion or "mini-bundle" was made up of parallel-running wires interfacing different subsystems, rather than wires all inter-facing equipments in the same subsystem. To select wires inherently suspect from an EMI standpoint, such wires with long common run lengths, preferably 10 feet or more, were sought. Wires with short common run lengths or wires all running between the same two boxes were generally avoided.

(b) Wire configuration. To exercise IEMCAP coupling models as fully as possible, various wire types used in F-15 wire bundles were selected. These included unshielded, shielded and double-shielded wires, untwisted and twisted, and wires in balanced and unbalanced configurations.

(c) Location. Wires were selected from bundles in many different air-craft locations (nose, cockpit, forward and aft fuselage, wing, rudder, etc.) and compartments. To exercise the antenna-to-wire routines, wires running in exposed sections such as the nose wheel well and speedbrake compartment were also selected.

(d) Variety of equipments. In order to obtain a good mix in the mini-system representation, virtually all of the F-15 avionics sub-systems were represented, such as the UHF Transmitter/Receiver, TACAN and Automatic Flight Control Set, and many non-avionics subsystems, such as hydraulics control lines, fuel gauge, engine control, generator and weapons system lines. Both signal/control and power lines were selected, including voice communication lines, DC switches and relays, and AC and DC power lines.

The selection of the other kinds of ports, namely, antennas and equip-ment cases, could be done in a more straightforward way. The selection of wires essentially dictated the selection of the equipment cases associated with them, i.e., some 50 "black boxes" distributed in about a dozen individual compartments. Almost all of the equipment cases on the F-15 were selected. Switches, panels and breakers, etc., although not considered to be legitimate equipment cases, were also modeled.

Because of the relatively few numbers of antennas on the F-15, it would have been possible to include all of them. However, the classified F-15 antennas such as the radar antenna and jamming antennas were not included because they would have necessitated both classified computer runs and a classified technical report. All 10 unclassified F-15 antennas were included in the mini-systems.

Finally, equipments were selected with a known history of EMI problems, since corrected, providing an excellent test of IEMCAP's ability to correctly predict actual interference situations, as well as their subsequent correc-tion through shielding or filtering.

2.1.2 Data collection. The most difficult part of the selection pro-cess was to collect and organize the F-15 wire data in a form suitable for selection according to the above criteria. This was particularly true in obtaining information on wire common run lengths. Although a computer-based information system was available for tracking down the schematic routing of individual wires from connector to connector, there was no com-parable source of information on wire common run lengths. Wires that happen to run close together physically, but are not part of the same bundle assem-

13

bly, are so difficult to trace that they were not even considered. All wires were selected on the basis of common run length with other wires in the same bundle assembly so that scaled bundle assembly layout photos (before installation in the aircraft) could be used. It was possible then to measure the distance between bundle break-out points for the individual wires and calculate from that the common run length between wires. This information was correlated with information from subsystem basic schematic diagrams indicating the function of a particular line, its source and destination and its unique wire identification. This last item was used in conjunction with the computer-based information system and the F-15 wire installation manual to obtain the routing of the wires through the aircraft from connector to connector through various compartments and bulkheads, and the length of each wire segment.

After the selection of wires in this manner, MIL-STD-462 test data on the individual subsystems was used to obtain measured emission and susceptibility of the emitter and receptor ports associated with the wires. Subsystem interface control sheets were used to obtain waveform and impedance information associated with the wire ports.

Information on the non-wire ports, antenna ports and equipment cases, was relatively easy to obtain from available drawings. This type of information was fairly well documented and could be collected and organized in a strightforward way.

2.1.3 Mini-system description. The F-15 mini-systems selected were eventually combined into one large mini-system as a data base for the validation itself, although the smaller component mini-systems were initially run individually so that a systematic program shakedown could be performed starting with a very small mini-system and gradually working up to the large mini-system. The large mini-system is composed of 11 antenna ports, 170 selected wire ports, and 50 selected equipment cases, for a total of 231 ports. Figure 4 is an overall system diagram indicating the locations of the boxes and most of the interfaces between them. A key to the abbreviations used to identify many of the boxes is provided in Figure 4a. As seen in the diagram, most of the avionics equipments are located in the right hand No. 1 equipment bay or the cockpit area, but there are boxes located in compartments all over the aircraft. All of the boxes with antenna ports are located in the right hand No. 1 equipment bay, as indicated, however. Hard-wired interfaces are indicated by solid lines, and compartment boundaries by dashed lines. As an example, the Interference Blanker (IB) in the right hand No. 1 equipment bay interfaces with the Radar Warning Receiver (RWR) in the right hand No. 2 equipment bay.

The large mini-system, Mini-system B, was constructed out of Mini-system I, consisting of the 11 antenna ports, Mini-system II, consisting of 22 wire ports, Mini-system III with 38 wire ports, and an additional 110 wire ports. Table 1 is a listing of all the Mini-system B wire ports, listed by port number (ID). Each port number is followed by; first a wire number (ID) identifying the mini-system wire to which it is connected, second the name of the equipment with which the port is associated, and third a brief description of the port's particular function, also indicating whether the port is a source (S), receptor (R) or both (S/R). Ports originally from Mini-system II are listed by port numbers 2-1 through 2-22 with wire numbers taking on values anywhere between 2-1 and 2-11. Ports originally from Mini-system III are listed by port numbers 3-1 through 3-38 with wire numbers anywhere between

14
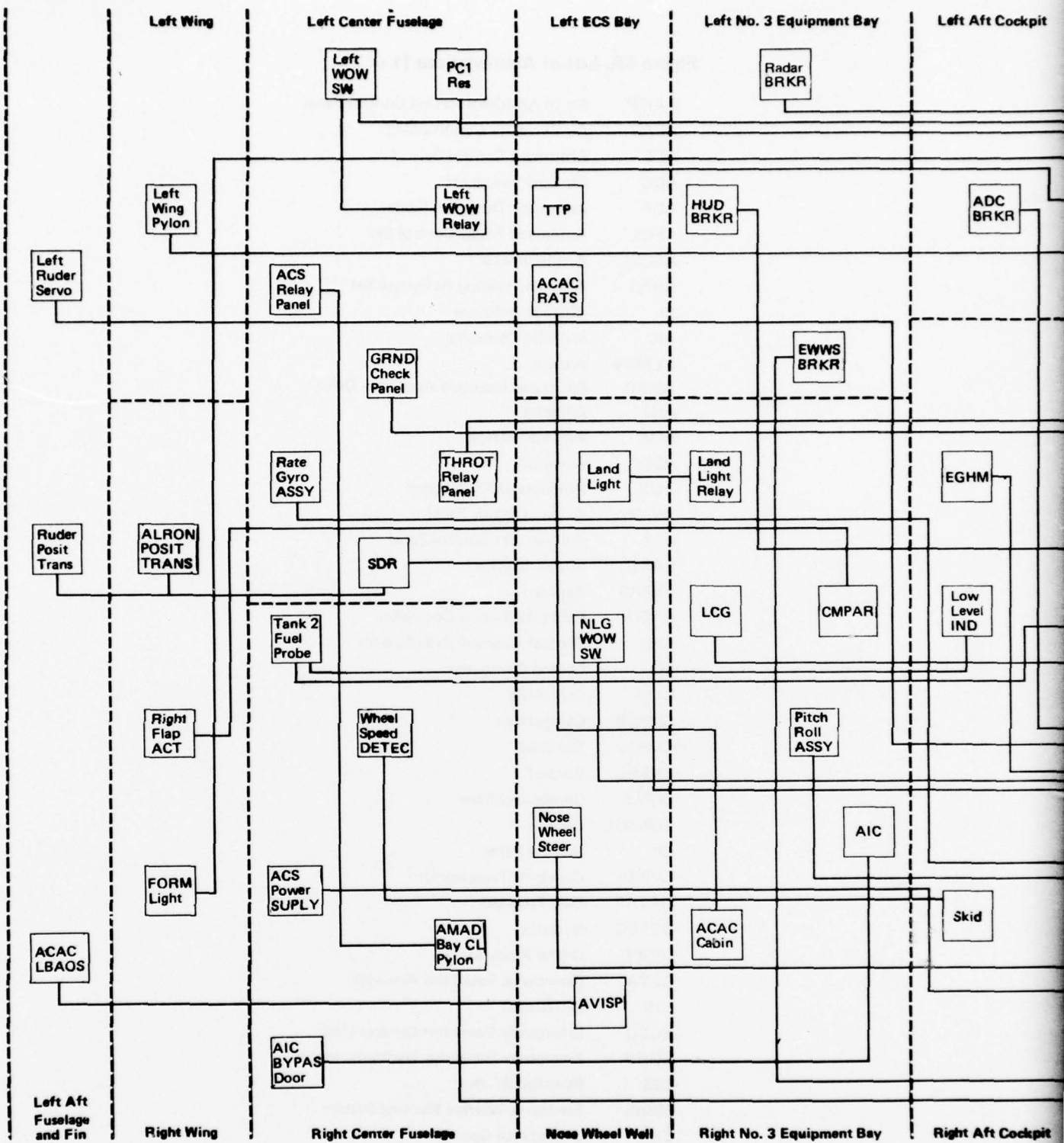
Figure 4   Mini-System B System Diagram

Form Light CP

CAS CNTRL

Fire IND

Radar RFOSC

Radar Xmtr

DFTA BRKR

BCP

FIRED

Radar DIGPR

ADC BRKR

AOA IND

NLG BRKR

Left MLG BRKR

Radar DATAP

Radar ANT

THROT QUAD

Steer Mode SW

ACS CVPGR

Radome

ILS BRKR

IB

IFFCP

INACP

UHF BRKR

INS

ESS DC Bus

TACAN

GHM

AAICP

ICCP

HUDSP

CC

ADF

ILS

HUD Power Supply

Consol Light Trim

Tank 2 Fuel IND

VSDSP

AUX

UHF

ow evel ND

IFT

HUDCP

INS IND Panel

ADC

HSI FDA

EGCU

RWR

Roll

Nose Gear BRKR

Comm DIS

Pitch

Stick

AHRS CMPAS CP

EXC

IFFRE

DFTA

AI

AFCS ACCEL

AHRS

EWWS

Figure 4A. List of Abbreviations (1 of 2)

AAICP	Air to Air Identification Control Panel
ACAC	Air Cycle/Air Conditioning
ACS	Armament Control Set
ADC	Air Data Computer
ADF	Automatic Direction Finder
AFCS	Automatic Flight Control Set
ACCEL	Accelerometer
AHRS	Attitude/Heading Reference Set
AI	Altitude Indicator
AIC	Air Inlet Controller
ALRON	Aileron
AMAD	Air Frame Mounted Accessory Drive
ANT	Antenna
AOA	Angle of Attack
ASSY	Assembly
AUX	Auxiliary UHF Receiver
AVISP	Avionics Status Panel
BCP	Built-in-Test Control Panel
BRKR	Circuit Breaker
BYPAS	Bypass
CABIN	Cabin Air Circuit Controller
CAS	Control Augmentation System
CC	Central Computer
CL	Centerline
CMPAR	Comparator
CMPAS	Compass
CNTRL	Control
COMM	Communications
CONSOL	Console
CP	Control Panel
CVPGR	Converter Programmer
DATAP	Data Processor
DETEC	Detector
DIGPR	Digital Processor
DFTA	Directional Feel Trim Actuator
DIS	Disconnect
EGCU	Emergency Generator Control Unit
EGHM	Emergency Generator Hydraulic Motor
ESS	Essential DC Bus
EWWS	Electronic Warfare Warning System
EXC	Exceedance Counter
FDA	Flight Director Adapter
FIRED	Fire Detector
FORM	Formation
GRND	Ground

16

HUD	Head Up Display
HUDCP	Head Up Display Control Unit
HUDSP	Head Up Display Signal Processor
IB	Interference Blanker
ICCP	Integrated Communications Control Panel
IFF	Identification/Friend or Foe
IFFCP	IFF Control Panel
IFFRE	IFF Reply Evaluator
IFT	IFF Transponder
IFFX	IFF Transponder
ILS	Instrument Landing System
INACP	Integrated Navigational Aids Control Panel
IND	Indicator
INS	Inertial Navigation System
LAND	Landing
LBAOS	Left Bleed Air Overpressure Sensor
LCG	Lead Computing Gyro
MLG	Main Landing Gear
NLG	Nose Landing GGar
PITCH	Pitch Computer
POSIT	Position
QUAD	Quadrant
RATS	Ram Air Temperature Sensor
RES	Reservoir
RFOSC	Radio Frequency Oscillaotr
ROLL	Roll Computer
RUDER	Rudder
RWR	Radar Warning Receiver
SDR	Signal Data Recorder
SERVO	Servo Actuator
SKID	Skid Control Box
STICK	Stick Force Sensor
SUPLY	Supply
SW	Switch
TACAN	Tactical Air Navigation Set
THROT	Throttle
TRANS	Transducer
TTP	Total Temperature Probe
UHF	UHF Communications Receiver/Transmitter
UHFCO	UHF Communications Receiver/Transmitter
VSDSP	Vertical Situation Display Signal Processor
WOW	Weight on Wheels
XMTR	Transmitter

Table 1. Mini-System Wire Ports

Port ID	Wire ID	Box	Description
1	12	Emergency Generator Control Unit (Right No. 3 Bay)	Hydraulic Motor Control (S)
2	12	Hydraulic Motor (Right Duct Area)	Hydraulic Motor Control (R)
3	1	Tank 2 Fuel Probe (Right Center Fuselage)	Tank 2 Fuel Quantity (S)
4	1	Tank 2 Fuel Indicator (Cockpit)	Tank 2 Fuel Quantity (R)
5	2	Tank 2 Fuel Probe (Right Center Fuselage)	Tank 2 Low Level Warning (S)
6	2	Tank 2 Low Level Indicator (Cockpit)	Tank 2 Low Level Warning (R)*
7	48	PC1 Reservoir (Left Center Fuselage)	Hydraulic Pressure Warning (S)
8	55	Fire Detection Controller (Left No. 2 Bay)	Fire Warning Light (S)
9	55	Indicator (Cockpit)	Fire Warning Light (R)
10	44	Landing Lights (Nose Wheel Well)	28V DC Landing Lights Power (R)
11	44	Relay (Right No. 3 Bay)	28V DC Landing Lights Power (S)
12	13	Formation Lights (Right Wing Tip)	115V AC Formation Lights Power (R)
13	13	Formation Lights Control Panel (Cockpit)	115V AC Formation Lights Power (S)
14	28	Trim Panel (Cockpit)	5V AC Panel Lights Power
15	31	Left W.O.W. Switch (Left Center Fuselage)	Left W.O.W. Power (R)
16	32		Left W.O.W. Switch (S)
17	31	Breaker Panel (Left No. 2 Bay)	Left W.O.W. Power (S)
18	32	W.O.W. Relay (Left Center Fuselage)	Left W.O.W. Switch (R)
19	43	Nose W.O.W. Switch (Nose Wheel Well)	Nose W.O.W. Switch (S)
20	43	Breaker Panel (Left No. 7 Bay)	Nose W.O.W. Switch (R)
2-1	2-11	Breaker (Cockpit)	Nose Wheel Steering Disconnect (R)
21	42	Steering Unit (Nose Wheel Well)	Nose Wheel Steering Engage (R)
22	30	Right Wheel Speed Detector (Right Center Fuselage)	Right Wheel Speed Detector (S)
23	30	Skid Control Box (Cockpit)	Right Wheel Speed Detector (R)
24	15	Comparator (Right No. 3 Bay)	Right Flap Power (S)
25	14		Right Flap Extend (S)
26	15	Right Flap Actuator (Right Wing)	Right Flap Power (R)
27	14		Right Flap Extend (S)
28	33	ACS Converter Programmer (Left No. 2 Bay)	Left Wing Inboard Pylon eject (S)
29	34		MER Fire - Left Wing Pylon (S)
30	35		MER/MAU Nose Arm (S)
31	36		Center-Line Pylon Eject (S)
32	37		Center-Line Tank Eject (S)
33	40		Radar Signal Reference (R)
34	45		Simulated Doppler Reference (R)
35	3		Hydraulic Motor Solenoid (S)
36	3	Gatling Gun (Right Center Fuselage)	Hydraulic Motor Solenoid (R)

*These receptor ports are threshold responsive devices rather than average power.

GP77-0221-2

18

3-1 and 3-15. The remaining ports are listed by port numbers 1 through 110 with wire numbers between 1 and 55.

For more information on the wire ports, such as voltage level, type of waveform, impedance, wire configuration and a schematic indicating wire connections between a given port and other ports, the unique wire number in Table 1 can be used as a reference to the appropriate mini-system bundle in Figures 18 through 20. Each bundle is drawn schematically, with port terminations on individual wires designated by port number. Wires 2-1 through 2-11, 3-1 through 3-15, 55 and 56 are referenced in Figure 18, wires 1 through 29 in Figure 19 and wires 30 through 53 in Figure 20.

Shielded wires are designated by "S", unshielded by "U" and double shielded by "DS". Wires with a twisted wire return are also designated "TP", for twisted pair. Additional information on the results of the IEMCAP simulation is provided, to be discussed in a later section of this report.

Antenna port information is provided in Figure 5, indicating the locations of each antenna and the transmitter and receiver operating characteristics. These antenna ports consist of the upper and lower UHF receiver/transmitter antennas (UHF), the upper and lower IFF transponder antennas (IFF), the upper and lower TACAN receiver/transmitter antennas (TACAN), the auxiliary UHF receiver antenna (AUX), the Automatic Direction Finder Antenna (ADF), and the Instrument Landing System (ILS) localizer, glideslope and marker beacon antennas. Water line, fuselage station, antenna type, antenna gain, transmitter power and harmonic levels, receiver sensitivity and bandwidth, and tuned frequency range data are provided. All antennas are located at zero butt line, the symmetry plane of the aircraft.

2.2 Mini-system modeling. In order to perform IEMCAP simulations of F-15 operation based on the mini-system data base, the various equipments had to be modeled. The task of representing a complex real-world weapons system with a system of relatively simple mathematical models for purposes of simulation required a considerable amount of judgement and discretion on the part of the principal investigator. The F-15 geometry had to be fitted as closely as possible to the cylinder-cone aircraft model used by the IEMCAP, antenna radiation patterns had to be fitted to 3-level quantized antenna models, signal waveforms had to be fitted to the most appropriate IEMCAP modulation models, missing data had to be approximated or estimated, and many other similar tasks had to be performed. The task was a learning process, and some of the problems encountered are therefore documented for the benefit of those who at some time may be using IEMCAP as an EMC tool on a different weapons system. Even though the problems that arise in different systems will be different, it is still instructive to describe some of the experiences and difficulties encountered in the course of modeling the F-15 equipments.

2.2.1 System modeling. This effort had to do with modeling the system environment seen by F-15 electronic and electrical equipment, the medium affecting the coupling of energy between source of electromagnetic emissions and the receptors of such emissions. The system to be modeled consisted of the following elements:

Table 1. Mini-System Wire Ports (Continued)

Port ID	Wire ID	Box	Description
37	33	Left Wing Inboard Pylon (Left Wing)	Left Wing Inboard Pylon Eject (R)
38	34		MER Fire - Left Wing Pylon (R)
39	35		MER/MAU Nose Arm (R)
40	36	AMAD Bay Centerline Pylon (Right Center Fuselage)	Center-Line Pylon Eject (R)
41	37		Center-Line Tank Jettison (R)
42	38		External Tank Air Pressure Regulator (S)
43	38	Relay Panel (Left Center Fuselage)	External Tank Air Pressure Regulator (R)
3-1	3-15	Lead Computing Gyro (Right No. 3 Bay)	Multiplex Bus (S/R)
44	45	Radar RF Oscillator (Left No. 1 Bay)	Simulated Doppler Reference (S)
45	46	Radar Transmitter (Left No. 1 Bay)	115V AC Power to Radar (R)
46	41	Radar Digital Processor (Left No. 1 Bay)	Mode X Ident Command (R)
47	39		Display Command A (S)
3-2	3-14	Radar Data Processor (Left No. 1 Bay)	Data Initiate Line (S)
48	40		Radar Signal Reference (S)
49	47		Linear Pot Excitation (S)
50	47	Radar Antenna (Radome)	Linear Pot Excitation (R)
51	46	Breaker (Left No. 3 Bay)	115V AC Power to Radar (S)
3-3	3-12	Radar Warning Receiver (Right No. 2 Bay)	BIT No-Go to HSI and BCP (S)
3-4	3-15		Multiplex Bus (S/R)
3-5	3-11		Blanking Pulse (R)
3-6	3-12	BIT Control Panel (Cockpit)	BIT No-Go- from RWR (R)
3-7	3-5		BIT Acknowledge from ADF (R)
2-2	2-10		Reset Line to Central Computer (S)
52	48		Hydraulic Pressure Warning from PC1 (R)*
53	9	Avionics Status Panel (Nose Wheel Well)	Left Bleed Air Overpressure Sensor (R)
3-8	3-11	Interference Blanker (Right No. 1 Bay)	Blanking Pulse (S)
3-9	3-14	Inertial Navigation Set (Right No. 1 Bay)	Data Initiate Line from Radar (R)
54	5		INS BIT No-Go to HSI (S)
3-10	3-15	INS Indicator Panel (Cockpit)	Multiplex Bus (S/R)
2-3	2-1	TACAN (Right No. 1 Bay)	Serial Data Train (S)
55	6	Instrument Landing System (Right No. 2 Bay)	28V DC Power (R)
56	6	Breaker (Left No. 3 Bay)	28V DC Power (S)
3-11	3-5	Automatic Direction Finder (Right No. 1 Bay)	ADF BIT Acknowledge (S)
2-4	2-2	UHF (Right No. 1 Bay)	Modulation Audio (R)
2-5	2-4		UHF Frequency Control (R)
3-12	3-9		28V DC Power to Antenna Select (R)
3-13	3-9	Breaker (Left No. 2 Bay)	28V DC Power to Antenna Select (S)
3-14	3-2	AUX (Right No. 1 Bay)	AUX BIT No-Go Signal (S)

GP77-0221-3

Table 1. Mini-System Wire Ports (Continued)

Port ID	Wire ID	Box	Description
57	50	Integrated Communications Control Panel (Cockpit)	Ground Crew Mike Line (R)
3-15	3-6		Mode 4 Audio from IFF Transponder (R)
3-16	3-2		AUX BIT No-Go (R)
2-6	2-7		Headset Audio (S)
2-7	2-2		Modulation Audio (S)
2-8	2-4		UHF Frequency Control (S)
2-9	2-8		Comm Channel 10-1 from HUD (R)
2-10	2-9		28V DC Power to ICCP (R)
2-11	2-3	IFF Control Panel (Cockpit)	Mode 1 Select to IFF Transponder (S)
2-12	2-1	Integrated NAVAIDS Control Panel (Cockpit)	Serial Data Train from TACAN (R)
2-13	2-5	AAI Control Panel (Cockpit)	Automatic Challenge Enable to IFFRE (S)
2-14	2-7	Disconnect Panel (Cockpit)	Headset Audio (R)
58	53	Ground Check Panel (Left Center Fuselage)	Ground Crew Mike Line (S)
59	4	IFF Transponder (Right No. 1 Bay)	AIMS Code C4 from ADC (R)
2-15	2-3		Mode 1 Select from IFFCP (R)
3-17	3-6		Mode 4 Audio to ICCP (S)
3-18	3-15	Central Computer (Left No. 2 Bay)	Multiplex Bus (S/R)
2-16	2-10		Central Computer Reset Line (R)*
3-19	3-14	Attitude Heading Reference Set (Right No. 2 Bay)	Data Initiate Line from Radar (R)
3-20	3-15		Multiplex Bus (S/R)
60	21		Annunciator Drive (S)
61	21	Compass Control Panel (Cockpit)	Annunciator Drive (R)
3-21	3-15	Air Data Computer (Right No. 1 Bay)	Multiplex Bus (S/R)
62	20		115V AC Power to ADC (R)
63	22		Altitude Data Bus (S)
64	19		Total Temperature Probe Excitation (R)
65	4		AIMS Code Cr to IFF Transponder (S)
66	20	Breaker (Cockpit)	115V AC Power to ADC (S)
2-17	2-6	AoA Indicator (Cockpit)	Angle-of-Attack Indicator (R)
67	19	Total Temperature Probe (Left ECS Bay)	Total Temperature Probe Excitation (R)
68	25	HUD Signal Processor (Left No. 2 Bay)	Display x - Deflection (S)
69	26		60V DC Power to HVPS (S)
70	24		Display y-Deflection (S)
71	23		28V DC Power Relay (R)
3-22	3-14		Data Initiate Line from Radar (R)*
3-23	3-15		Multiplex Bus (S/R)
72	23	HUD Control Panel (Cockpit)	28V AC Power Relay (S)

Table 1 Mini-System Wire Ports (Continued)

Port ID	Wire ID	Box	Description
73	24	HUD Control Panel (Cockpit)	Display y-Deflection (R)
74	26		60V DC Power to HVPS (R)
75	25		Display x-Deflection (R)
76	28		5V AC Panel Lights Power (R)
77	29		28V DC Power to HUDCP (R)
78	27		Master Caution Light (R)*
2-18	2-8		Comm Channel 10-1 to ICCP (S)
79	29	Breaker	28V DC Power to HUDCP (S)
80	27	Interior Lights Power Supply (Cockpit)	Master Caution Light (S)
81	39	VSD Signal Processor (Left No. 2 Bay)	Display Command A from Radar (R)
3-24	3-13		61-Fwd Cockpit Fail from HSI (R)
3-25	3-3	HSI Flight Director Adapter (Right No. 1 Bay)	ILS/TAC Mode (R)*
3-26	3-12		BIT No-Go from RWR (R)
3-27	3-13		61-Fwd Cockpit Fail to VSD (S)
82	5		BIT No-Go from INS (R)
3-28	3-3	HSI Steer Mode Switch (Cockpit)	ILS/TAC Mode (S)
83	49	Throttle Quadrant (Cockpit)	Throttle Switch (S)
84	49	Relay Panel (Left Center Fuselage)	Throttle Switch (R)
85	7	AFCS Roll/Yaw Computer (Right No. 1 Bay)	Rudder Servo Engage Signal (S)
86	10		Yaw Rate Sensor A BIT Signal (R)
87	53		Forward Roll B Signal from Stick (R)
88	51	AFCS Pitch Computer (Right No. 1 Bay)	Forward Pitch A Signal from Stick (R)
89	52		Forward Pitch A Excitation to Stick (S)
3-29	3-1		Attitude Engage A (R)*
3-30	3-4		Altitude Engage A (R)*
3-31	3-7		CAS Interconnect Servo A CMD LO (S)
3-32	3-10		Normal Accelerometer Sensor B Signal (S)
2-19	2-6		Angle-of-Attack Reference to AoA Indicator (S)
2-20	2-11	AFCS Stick Force Sensor (Cockpit)	Nose Gear Steering Disconnect (S)
90	42		Nose Gear Steering Engage (S)
91	51		Forward Pitch A Signal from Stick (S)
92	52		Forward Pitch A Excitation to Stick (R)
93	53		Forward Roll B Signal from Stick (S)
94	7	Left Rudder Servoactuator (Left Aft Fuselage)	Rudder Servo Engage Signal (R)
95	10	Rate Gyro Assembly (Left Center Fuselage)	Yaw Rate Sensor A BIT Signal (S)
3-33	3-10	Acceleration Sensor (Right No. 2 Bay)	Normal Accelerometer Sensor B Signal (R)
3-34	3-1	CAS Control Panel (Cockpit)	Attitude Engage A (S)
3-35	3-4		Altitude Engage A (S)
3-36	3-7	Pitch/Roll Channel Assembly (Right No. 3 Bay)	CAS Interconnect Servo A, Cmd LO (R)

GP77-0221-5

Table 1. Mini-System Wire Ports (Concluded)

Port ID	Wire ID	Box	Description
96	54	Directional Feel Trim Actuator (Cockpit)	115V AC Power to DFTA (R)
97	54	Breaker (Cockpit)	115V AC Power to DFTA (S)
98	22	Altitude Indicator (Cockpit)	Altitude Data Bus (R)
99	11	Exceedance Counter (Right No. 2 Bay)	Vertical Acceleration, Filtered (S)
100	18	Air Inlet Controller (Right No. 3 Bay)	Right Bypass RAM Servo (S)
101	18	Right Bypass Door Actuator (Right Center Fuselage)	Right Bypass RAM Servo (R)
2-21	2-5	IFF Reply Evaluator (Right No. 1 Bay)	Reply Evaluator Enabler (R)
102	11	Signal Data Recorder (Left Center Fuselage)	Vertical Acceleration, Filtered (R)
103	8		Rudder Deflection (R)
104	16		Right Aileron Deflection (R)
105	8	Rudder Position Transducer (Left Aft (Fuselage)	Rudder Deflection (S)
106	16	Aileron Position Transducer (Right Wing)	Right Aileron Deflection (S)
107	9	Left Bleed Air Overpressure Sensor (Left Aft Fuselage)	Left Bleed Air Overpressure (S)
108	17	Cabin Air Circuit Controller (Right No. 3 Bay)	RAM Air Temperature Sensor (S)
109	17	RAM Air Temperature Sensor (Left ECS Bay)	RAM Air Temperature Sensor (R)
110	41	Electronic Warfare Warning Set (Right No. 1 Bay)	Mode X IDENT Command to Radar (S)
3-37	3-8		115V AC Power to EWWS (R)
3-38	3-8	Breaker (Left No. 3 Bay)	115V AC Power to EWWS (S)
2-22	2-9	Breaker (Left No. 2 Bay)	28V DC Power to ICCP (S)

GP77-0221-6

Figure 5 F-15 Mini-System Antenna Ports
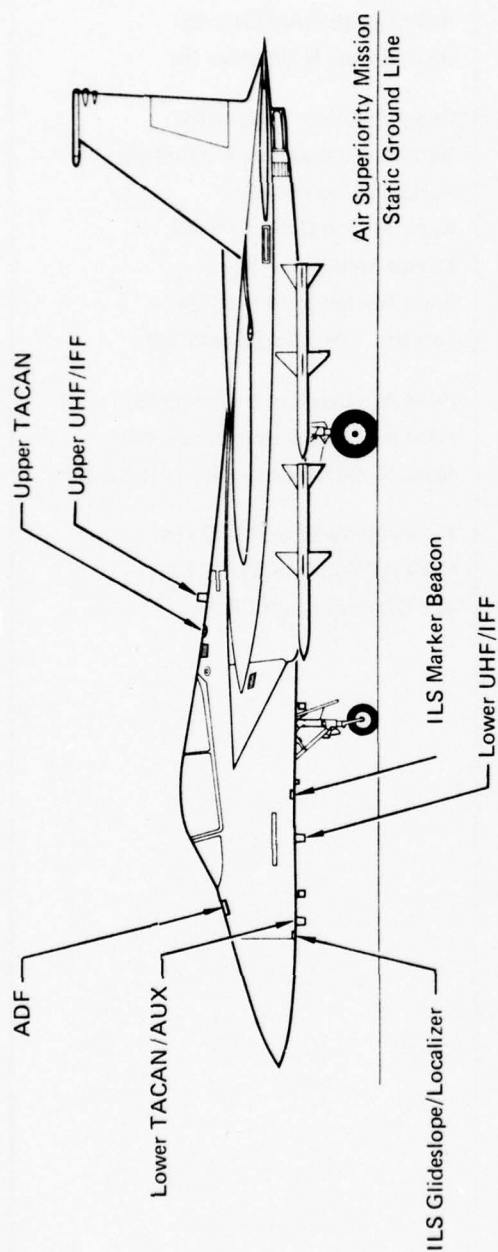
Antenna	WL	FS	Type	Gain (dB)	Transmitter Power (W)	Transmitter Harmonics (dB)	Receiver Sensitivity (dBm)	Receiver Bandwidth (kHz)	Frequency Range (mHz)
Upper UHF	168	464	Blade	2.1	100	−73, −73	−101	44	225-400
Lower UHF	87	284	Blade	2.1					
Upper IFF	158	464	Blade	2.1	1000	−90, −90	−77	8000	1090 (Transmit)
Lower IFF	87	284	Blade	2.1					1030 (Receive)
Upper TACAN	160	436	Annular Slot	2.1	4000	−93, −93	−96	1000	1025-1150 (Transmit)
Lower TACAN	87	222	Blade	2.1					962-1213 (Receive)
AUX	87	222	Blade	2.1	N/A	N/A	−101	44	225-400
ADF	140	229	Array	−16	N/A	N/A	−101	44	225-400
ILS Localizer	93	196	Dipole	2.1	N/A	N/A	−90	26	108.1-111.9
ILS Glideslope	93	196	Dipole	2.1	N/A	N/A	−90	48	329.5-335
ILS Marker Beacon	92	312	Slot	−8	N/A	N/A	−53	40	75.0-75.1

Upper TACAN

Upper UHF/IFF

Lower UHF/IFF

ILS Marker Beacon

Air Superiority Mission
Static Ground Line

ADF

Lower TACAN/AUX

ILS Glideslope/Localizer

GP77-0342-19

24

(a) Aircraft structure (surface geometry, compartments, apertures)
(b) Antennas
(c) Filters
(d) Wires.

2.2.1.1 Aircraft structure modeling. The aircraft surface geometry, affecting the propagation of radiated energy between antennas and other antennas or exposed wires, had to be simulated in terms of the IEMCAP cylinder-cone aircraft model for the fuselage and also for wing diffraction. The structure of the airframe including bulkheads, conducting and non-conducting panels, access doors, seams, etc., had to be simulated in terms of IEMCAP models for compartments and apertures.

Figure 6 shows the principal dimensions of the F-15 aircraft in side, front, and top views. The striking features are the squared off appearance of the engine ducts, the twin tails, and the 45° sweep of the wings. The fuselage was modeled as a flat-bottomed cylinder, Figure 7, with a radius of 46 inches. Each wing was modeled as a trapezoid in a plane slanting downward going away from the fuselage, with the leading edge slanting back about 45° and the trailing edge slanting back only about 7°. As seen in Figure 7, the top of the cylinder used to represent the fuselage is tangent to the top of the fuselage at a point just behind the canopy. The flat bottom of the cylinder is tangent to the bottom of the fuselage below that point. The wing coordinates were taken from the scale drawing in a straightforward way. The choice of a variable radius region, in which the fuselage is modeled as a cone rather than as a cylinder, was not as straightforward, however. This was taken to be from the tip of the nose, fuselage station 116.3, to the bottom edge of the engine ducts, fuselage station 415.0, close to the point where the cylinder is tangent to the fuselage. In this region the fuselage gradually tapers toward the nose of the aircraft, except for the protuberances of the canopy and the engine ducts. Since the canopy is constructed of an insulating type of material, it was not considered to be a barrier to the propagation of electromagnetic energy, even though it extends about a foot higher than the top of the cylinder. The engine ducts, seen from the side, taper forward like a wedge, in keeping with the variable radius representation.

The modeling of compartments was reasonably straightforward, since most equipments on the F-15 are located in well-defined compartments, separated from other compartments by bulkheads. Most of the mini-system equipments are located in the right and left hand No. 1, No. 2, and No. 3 equipment bays, and the cockpit; equipments are also located in the Environmental Control System (ECS) bay, the left duct area, the wheel wells and the right hand center fuselage area.

Finally, there are 4 areas in the aircraft surface through which mini-system wires are exposed to external radiation: the transparent plastic canopy, the composite speedbrake door, the nose wheel well opening and the left wheel well opening. All of these were modeled as rectangular apertures. Except for the canopy these areas are in fact approximately rectangular and were therefore modeled by their actual dimensions. The canopy is roughly oval-shaped, and was modeled by circumscribing a rectangle about the oval.

25

12.08 ft

18.45 ft

Air Superiority Mission

Static Ground Line

17.79 ft

42.81 ft

9.03 ft

28.25 ft

63.75 ft
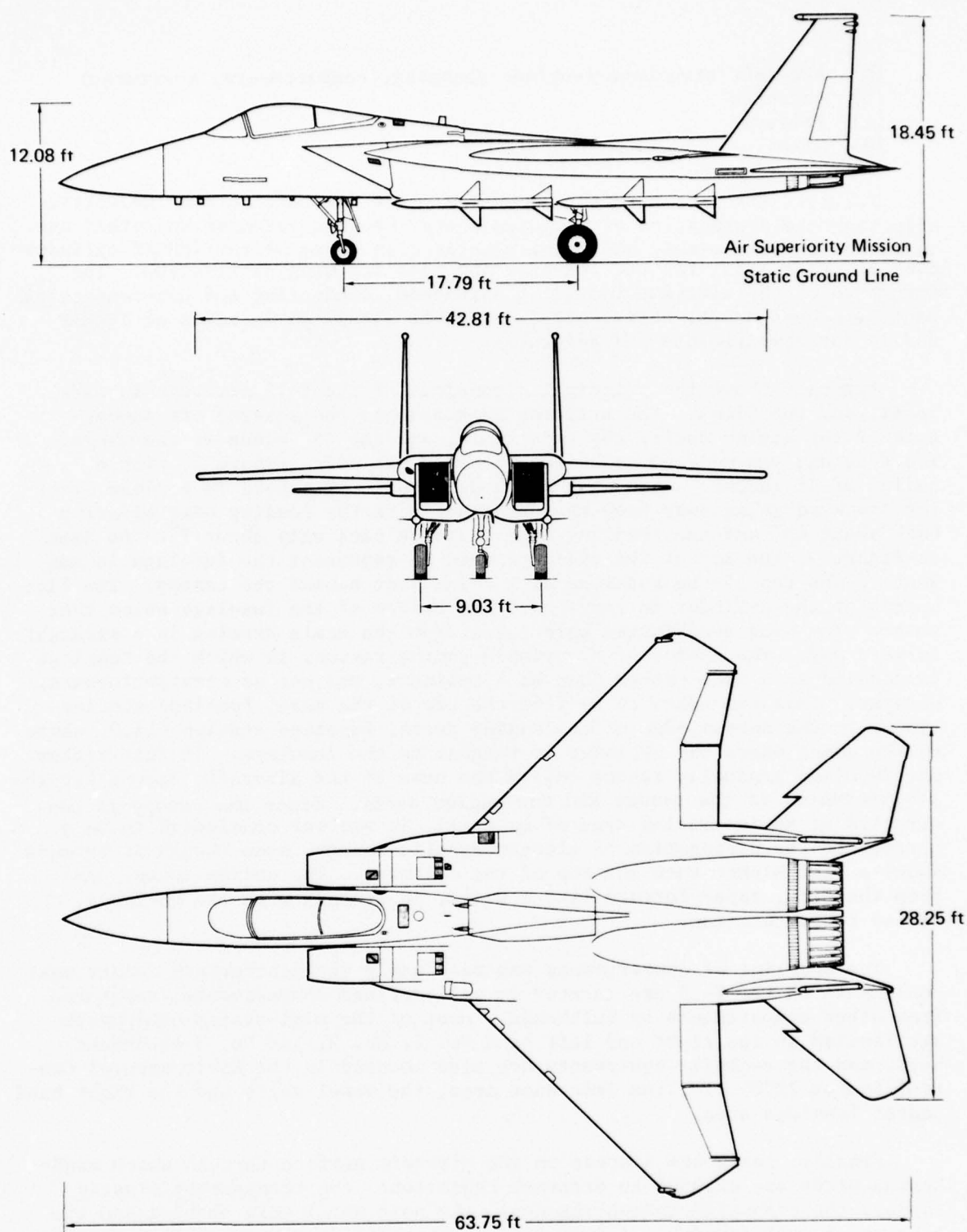
GP77-0342-15

Figure 6 F-15 Principal Dimensions

26

WL$_T$ - Water Line of Cylinder Top (163)

WL$_C$ - Water Line of Cylinder Centroid (117)

WL$_B$ - Water Line of Truncated Flat Bottom (93)

(a) Side View
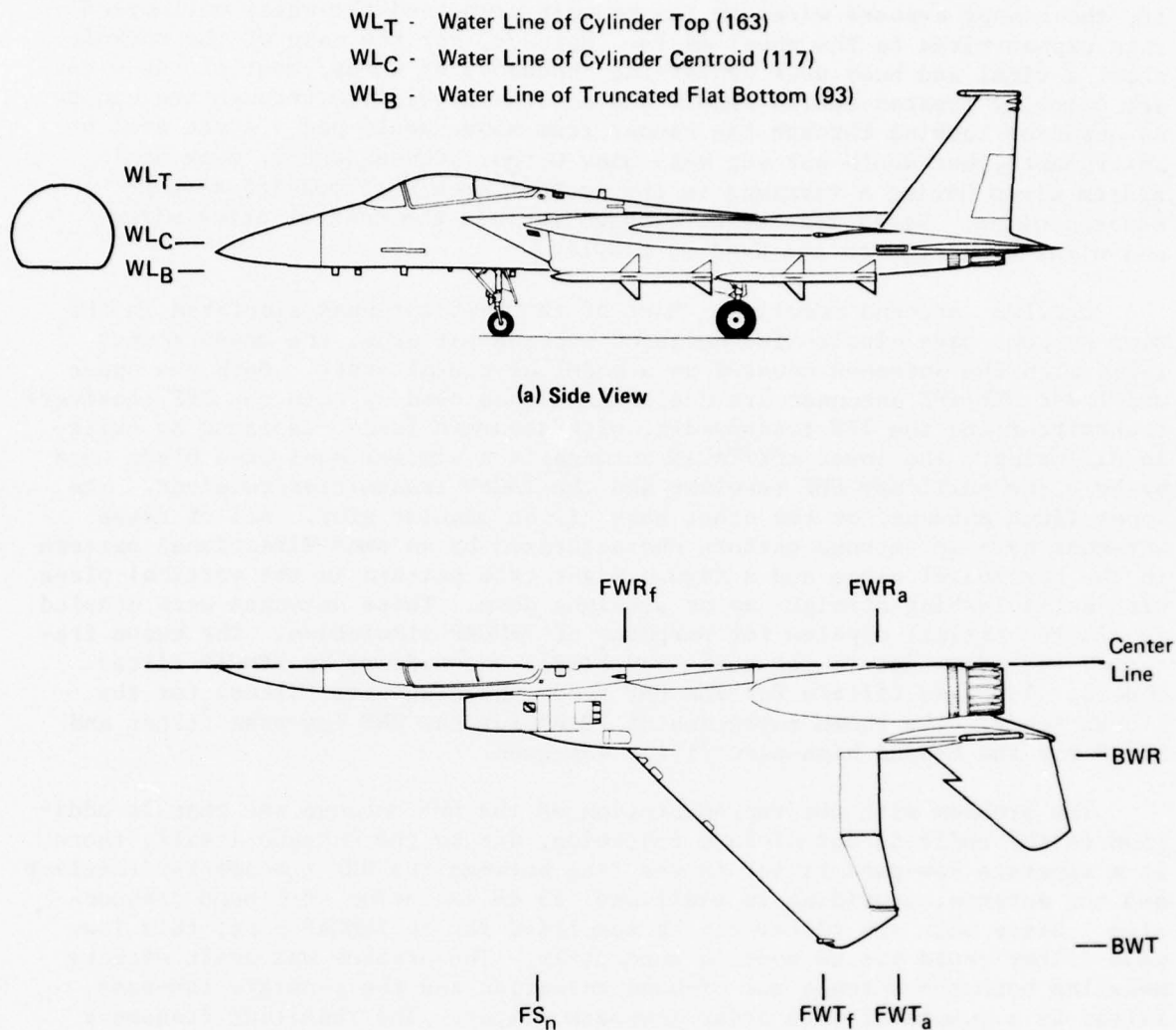
FS$_n$ - Fuselage Station of Variable Radius Region Limit (415)

FWT$_f$ - Fuselage Station of Wing Tip Leading Edge (655)

FWT$_a$ - Fuselage Station of Wing Tip Trailing Edge (732)

FWR$_f$ - Fuselage Station of Wing Root Leading Edge (457.5)

FWR$_a$ - Fuselage Station of Wing Root Trailing Edge (707)

BWR - Butt Line of Wing Root ($\pm$ 46)

BWT - Butt Line of Wing Tip ($\pm$ 260)

GP77-0342-26

(b) Top View

Figure 7 Modeling of F-15 Aircraft Geometry

27

The speedbrake door exposes wires in the speedbrake compartment below it, the canopy exposes wires in the cockpit area, and the wheel well openings expose wires in the wheel wells. However, for the case of the cockpit area, a vital and busy area containing thousands of wires, most of the wires are actually located behind panels and not really visible through the canopy. An observer looking through the canopy from above would see a great deal of instruments, but would not see very many wires. Consequently, many minisystem wires having a terminus in the cockpit area were modeled as non-exposed wires. Wires modeled as exposed include the control stick wires and wires connected to the Head-Up Display.

2.2.1.2 Antenna modeling. Most of the F-15 antennas simulated in the mini-systems have dipole-like measured antenna patterns, the measurements taken with the antennas mounted on a model of the aircraft. Both the upper and lower UHF/IFF antennas are dual-band blades used by both the UHF receiver/transmitter and the IFF transponder, with separate feeds, isolated by built-in diplexing. The lower AUX/TACAN antenna is a similar dual-band blade used by both the auxiliary UHF receiver and the TACAN transmitter/receiver. The upper TACAN antenna, on the other hand, is an annular slot. All of these antennas have an antenna pattern characterized by an omni-directional pattern in the horizontal plane and a figure eight type pattern in the vertical plane with nulls looking straight up or straight down. These antennas were modeled as simple vertical dipoles for purposes of IEMCAP simulation. The known frequency rejection due to the dual-band blades was modeled by IEMCAP filter models: low pass filters for the UHF feeds and high-pass filters for the L-band feeds. The known rejection of 70 dB for the UHF low-pass filter and 50 dB for the L-band high-pass filter was used.

The problem with the representation of the UHF antenna was that in addition to the built-in out-of-band rejection, due to the antenna itself, there is a separate low-pass filter in the line between the UHF transmitter/receiver and the antenna, providing an additional 45 dB isolation at L-band frequencies. Since only one filter can be specified for an IEMCAP port, this low-pass filter could not be modeled separately. The problem was dealt with by modeling both the antenna out-of-band rejection and the separate low-pass filter by a composite 16th order low-pass filter. The resulting frequency rejection of the UHF antenna port is 0 dB at 400 MHz, increasing at a rate of 320 dB per decade above 400 MHz and reaching its maximum rejection of 115 dB at 962 MHz, the lowest L-band frequency.

There was no measured data on the out-of-band rejection of the upper TACAN antenna, the annular slot. Based on the recommendation of engineering personnel familiar with this antenna, the rejection of UHF frequencies was approximated at 20 dB as a worst case, and modeled as a high-pass filter.

The remaining antennas are the Automatic Direction Finder (ADF) and the ILS localizer, glideslope and marker beacon. The ADF antenna is an eight element vertically polarized fixed array with a cardioid radiation pattern in the horizontal plane, steerable electronically a full 360 degrees. Since this antenna can be pointed in any horizontal direction, it was modeled as a simple dipole with an omni-directional pattern in the horizontal plane. How-

28

ever, the ADF is a relatively inefficient antenna with a maximum gain of -14 dBI (relative to an isotropic). Unfortunately, the IEMCAP dipole model makes no provision for specifying the gain of a dipole; the code assumes that a dipole has a nominal gain of about 2 dBI. This problem was solved by using an IEMCAP low-pass filter model with an insertion loss of 16 dB, with the pass band extending all the way to 18 GHz. Thus, the insertion loss of the filter, flat across the entire spectrum, simulated the inefficiency of the antenna, bringing the maximum gain down from 2 dBI to -14 dBI.

The Instrument Landing System (ILS) glideslope/localizer antenna is an integrated half-wave dipole antenna with common radiating elements for the localizer (108 to 112 MHz) and the glideslope (329 to 335 MHz) channels of the ILS receiver. It does not have an omni-directional pattern in the horizontal plane for either the glideslope or the localizer. However, since all mini-system antennas are located on the same vertical plane, its gain in the direction of any other mini-system antenna is determined solely by its vertical pattern. This can be seen by referring back to the diagram of antenna locations in Figure 5. The vertical patterns of both glideslope and localizer are similar, a dipole-like pattern with nulls looking straight up or down but with additional nulls looking back towards the tail. It was difficult to represent this type of pattern with a 3-level quantized IEMCAP model; instead, the antenna was modeled as a dipole, simulating the nulls looking up or down but over predicting the gain in the aft direction. This error was responsible for over predictions in coupling to this antenna from the lower UHF, IFF and TACAN antennas, discussed in a later section.

The ILS marker beacon antenna is a flush-mounted, electrically short single element antenna used by the marker beacon channel (75 MHz) of the ILS receiver. Its principal measured patterns are given in Figure 8. Unlike the other antennas, the marker beacon is oriented with its main beam pointing down instead of forward. In the aircraft coordinate system, this corresponds to a vertical angle of $\theta = 180^{\circ}$ and an indeterminate azimuthal angle $0 \leq \phi \leq 360^{\circ}$. Either one of the two principal patterns could be considered to be the "vertical" pattern in the coordinate system of the antenna itself; the orthogonal pattern would then be considered to be the "azimuthal" pattern in the coordinate system of the antenna. The pattern on the right of Figure 8 is the pattern of interest and was consequently chosen to be the azimuthal pattern, modeled by two quantized levels as shown by the dashed line. The main beam gain is only -8 dBI, relatively low because the antenna is electrically short, and the secondary lobe gain is down to -18 dBI. The quantized model in this case is a very good fit to the envelope of the measured pattern. In the coordinate system of the antenna, all other mini-system antennas are in the same azimuthal plane. The "vertical" pattern in the orthogonal plane was modeled by a single quantized level as shown.

2.2.1.3 Filter modeling. There are two identifiable filters included on mini-system equipments. One of them, the low-pass filter at the UHF receiver/transmitter was modeled in conjunction with the built-in antenna rejection, as discussed previously. The other is a low-pass filter at the stick force sensor, designed to prevent RF interference on the stick wires, induced by radiation through the canopy, from getting into the sensitive stick force sensor amplifier. The actual filter is constructed out of a 2000
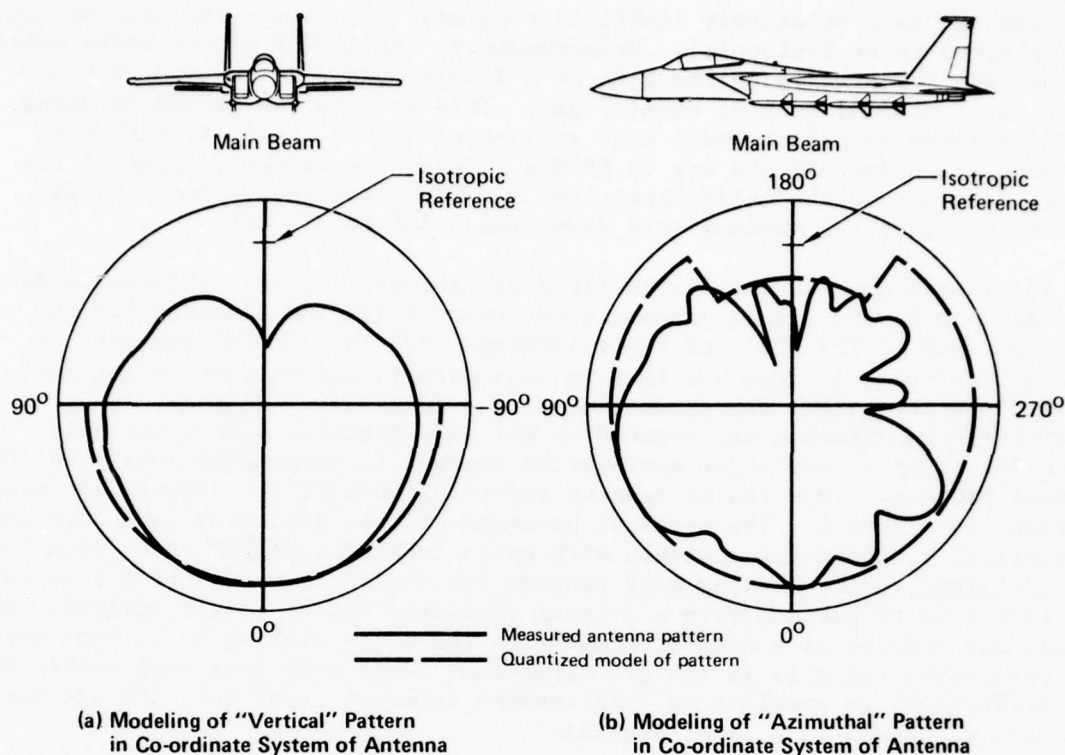
Figure 8 Modeling of Marker Beacon Antenna Radiation Pattern

GP77-0342-27

pf feedthrough capacitor, inserted into the equipment case through a well-grounded plate. At UHF frequencies, the dynamic impedance of the receptor is estimated at about 50 ohms, so the frequency at which the shunting reactance becomes comparable to the impedance is about 1.6 MHz. The filter's characteristic was modeled as a low-pass filter of 4th order with a break point of 1.6 MHz. The model brings the isolation from 0 dB insertion loss below 1.6 MHz up to a maximum isolation of 53.3 dB, the measured filter rejection at UHF frequencies.

2.2.1.4 Wire modeling. The physical construction and configuration of individual wires, as well as the relationship of each wire to other wires in the same bundle and the routing of each wire in the aircraft, all had to be modeled for simulation purposes. Specifications on the wire diameter, insulation thickness, shield diameter and thickness, conductivity and permittivity, etc., were available on each of 24 different types of wires contained in the mini-systems, plus an additional eleven (11) wire types required for the sensitivity study. This data was applied directly to the IEMCAP wire model. Information on grounding and balance configurations was similarly applied to the wire model in a straightforward way. The only item of data not generally available was the shield to wire capacitance for shielded

30
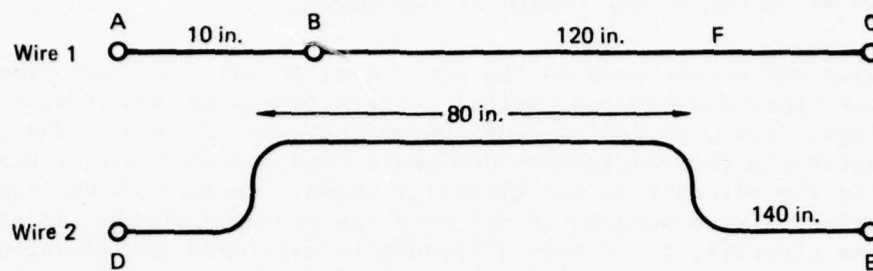
(a) Organized Wire Routing Data
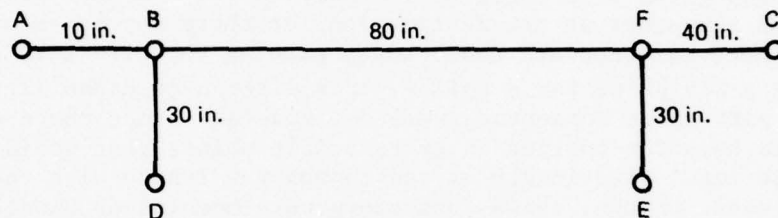
(b) Bundle Representation

GP77-0342-28

Figure 9 Modeling of Wire Bundles

twisted wires; a default value of 0 pf/ft was used, requiring the IEMCAP code to calculate the value of this capacitance from the other data. Hand calculations were used to verify that the simple algorithm used by the code to compute this capacitance is a reasonably good approximation to the detailed analytic solution for a pair of wires circumscribed by a shield. Otherwise it would have been necessary to write a computer program to calculate the value of this IEMCAP input parameter for some 20 different wire types.

Modeling of wire routing and the relationship between wires in a bundle was a more involved process. However, the bulk of the effort was collecting and correlating the wire routing data, discussed previously, after which the actual modeling was relatively easy. A sample format for the organized wire routing data is shown in Figure 9(a), for two wires with a common run length. Wire 1 has two segments, as indicated, a 10 inch segment between connectors A and B, and a 120 inch segment between connectors B and C. Wire 2 has a single 140 inch segment between connectors D and E, and a common run length of 80 inches with Wire 1. Figure 9(b) illustrates how the IEMCAP wire bundle is represented. Wire 1 follows route ABFC, while Wire 2 follows the route

31

DBFE, so that both wires share the segment BF. The sum of the bundle segments for Wire 1 corresponds to the actual length of 130 inches, and the segments of Wire 2 add up to the actual length of 140 inches.

A major difference between the upper diagram and the lower diagram, is that in the upper diagram the capital letters designate actual wire connectors - plugs, jacks, or splice boxes whose location is known - and in the lower diagram the capital letters designate bundle branch points whose actual location in the aircraft is not generally known. Because of the complex, tortuous routing of wire bundles up and down and around obstacles as they wind through the aircraft, it is very difficult to determine the locations of these branch points. However, it was not necessary to designate the actual coordinates of the bundle branch points. This was true because the IEMCAP code uses these coordinates only to calculate the length of each bundle segment when the lengths are not given directly in the input data. Since the lengths are known, they could be entered as input without the need for the program to calculate them.

For any given wire there may be only two wire connectors, one at the source and the other at the destination, or there may be as many as a half dozen or more intermediate connectors, passing the wire through bulkheads, providing a tie point for a splice, or a disconnect capability, etc. For the most part these connectors were not modeled, since there was no way to model them save for putting in extra bundle points that would not affect either the total wire length or the common run length with the other wire. In some cases, though, these connectors were modeled as bundle points. This was done for bulkhead connectors joining to aperture-exposed segments so that the actual length of the exposed segment was used. In one case, the fuel gauge wire running through the speedbrake compartment, the length of the exposed portion of the segment was known and consequently the exposed portion was modeled as a separate segment.

Mini-system bundles of 3 or more wires were modeled in a way similar to the example just illustrated, with the additional complication of more branch points and bundle segments to model the different common run lengths between any given pair of wires in the same bundle. All bundle segments were modeled as having a height above ground of four inches.

Since it was not necessary to designate the coordinates of the bundle branch points, an arbitrary location of (0,0,0) was assigned to them. However, the actual location of connectors at receptor or source terminations was used, as an aid to catch errors in the data that would show up if a wire appeared to go to the wrong location in the aircraft.

2.2.2 Source/Receptor modeling. Each mini-system source or receptor port had to be modeled as best as possible with one of the mathematical spectrum models used by the IEMCAP, to simulate its required emission or susceptibility spectra. Unrequired emission and susceptibility also had to be simulated.

In some cases, the actual signal waveform of a port corresponds closely with one of the IEMCAP models. For example, there are ports with audio, amplitude modulation, pulse train and pulse code modulation signals that fit in with existing IEMCAP spectrum models. For cases like these, the modeling consisted simply of matching the known characteristics of the signals, such as pulse width and rise time, with the corresponding IEMCAP input parameters.

In most cases, though, the actual waveforms did not correspond closely with IEMCAP models, and it was necessary to pick a model that was most representative of a particular waveform with an appropriate choice of model parameters.

2.2.2.1 Modeling RF ports. The RF ports consist of all the antenna-connected ports associated with the UHF, IFF transponder, TACAN, AUX, ADF, and ILS equipments. All of these ports are receptors, and the ports associated with the UHF, IFF and TACAN are also emitters.

The required susceptibility of the RF ports was modeled by assuming a flat response over the receiver bandwidth, the level being approximated by the known receiver sensitivity. This approximation was used because in each case the receiver response is relatively flat within its required bandwidth, and the sensitivity seemed to be a reasonable approximation to the unknown susceptibility level at the tuned frequency. The 6 dB receiver bandwidth was used as the required bandwidth for RF receptors. It should be noted that if the IEMCAP is used on RF equipments whose actual required susceptibility is known, the value of the susceptibility rather than the sensitivity should be used in the input data.

The required emission of the UHF transmitter antenna ports is an amplitude modulated signal between 225 and 400 MHz carrying voice information. Although a limiter is used on the modulating signal, it does not affect the signal when a normal speaking voice is used at the microphone input. Consequently, the modulating signal was modeled by the IEMCAP stochastic voice model, and the RF waveform was modeled as AM (double sideband plus carrier) with voice modulation.

The required emission of the IFF transponder antenna ports operating in Mode 4, the military mode, is an RF signal at 1090 MHz modulated by a train of pulses half a microsecond wide with 8 microseconds between pulses, the train being repeated every 64 microseconds. The waveform was modeled as a radar rectangular pulse train with a period of 8 microseconds and a pulse width of 0.5 microseconds, a simulation that closely represents the actual signal.

The required emission of the TACAN antenna ports in the air-to-air ranging mode is an RF signal between 1025 and 1150 MHz modulated by a pair of pulses, each 7 microseconds wide, 12 microseconds apart, repeated 100 times per second. The signal was originally modeled as a radar rectangular pulse train with a period of 12 microseconds and a pulse width of 7 microseconds. This was done as a kind of worst case, replacing the pair of pulses by an infinite train of pulses, which was probably too pessimistic a representation. Since the TACAN puts out a relatively narrow bandwidth, 1 MHz, com-

33

pared with its tuned frequency in the vicinity of 1 GHz, the exact shape of the emission spectrum is not as important as the average power contained in the bandwidth. Because the way the TACAN emission was modeled resulted in a higher duty cycle than the true duty cycle, it also resulted in a higher calculated value for the average power contained in the TACAN bandwidth. For this reason, the TACAN was subsequently modeled as a pulse train with a period of 10 milliseconds and a pulse width of 14 microseconds.

Unrequired RF emissions include broadband and narrowband noise between 14 kHz and 18 GHz, and spurious emissions at harmonics of the operating frequencies. Procurement specifications for conducted interference on antenna leads were used to simulate the noise and the second and third harmonics. They were modeled by simply specifying the harmonic levels and specifying whether the equipment was designed to MIL-STD-461A or MIL-I-6181D, the IFF and TACAN being designed to the former and the UHF to the latter, and letting the IEMCAP models for these specifications generate the appropriate spectrum.

The unrequired susceptibility levels for these equipments was modeled in the same way, since the IEMCAP models automatically generate the susceptibility limits associated with MIL-STD-461A or MIL-I-6181D. The unrequired susceptibility of the remaining RF receptor ports was modeled in a similar way, the AUX by MIL-I-6181D and the ADF and ILS ports by MIL-STD-461A.

Modeling the unrequired emission and susceptibility of these ports by their specification limits amounts to a worst case simulation. Although the actual emission level at a given frequency is not known, it is known that it does not exceed the specification limit at that frequency.

2.2.2.2 Modeling equipment cases. Avionics and other electrical equipment integrated into a weapons system are subject to limits on the amount of emission the equipment can radiate into the environment. In addition, they must be able to withstand some amount of radiated interference, so there is a lower limit on its radiated susceptibility level. Tests to these specifications are performed in the screen room on an entire subsystem, with the subsystem boxes connected by wire cables to other boxes, and antenna leads connected to dummy loads in a simulation of actual operation. Radiated emissions are measured by a test antenna at some fixed distance, usually 1 meter from the "center" of the subsystem. Similarly, radiated susceptibility is tested by irradiating the subsystem with a field generated by a test antenna, gradually increasing the level until the subsystem performance is adversely affected or the specification limit is reached. Since the antenna leads, if any, are connected to dummy loads that do not radiate energy or receive radiated energy, the measured radiated emission and susceptibility relates to energy leaking through equipment cases and wire interfaces. Since the subsystem is tested as a whole, it is not known precisely where the measured emission is coming from within the subsystem or where the vulnerability to radiated interference is greatest. In IEMCAP, radiated emission and susceptibility is simulated by assuming that the equipment cases themselves are both sources of interference, and victims of

34

interference from other equipment cases. The code treats each box as if it were a simple magnetic dipole putting out the measured level of radiation 1 meter from the center of the box and falling off as the cube of the distance.

Each equipment case in the F-15 mini-systems was modeled as if it radiated the level that was measured for the particular subsystem as a whole, and was susceptible to the level that the subsystem as a whole was tested to. The spectrum displacement factor was used to shift the MIL-STD-461A or MIL-I-6181D limits generated by IEMCAP up or down so that the spectrum was just tangent to the measured emission levels, the displaced spectrum serving as an envelope to measured levels. This procedure is illustrated in Figure 10. In this example, the measured emission level at frequency f_o exceeds the MIL-STD-461A limit by 10 dB, so the entire specification spectrum is shifted up 10 dB such that it is just tangent to the measured level at f_o and is an upper limit to measured levels at all other frequencies. Susceptibility levels were modeled in a similar way, shifting the IEMCAP-generated spectrum up or down so that it was tangent to the measures susceptibility level from below, a lower limit to the measured susceptibility levels.

The IEMCAP as structured requires every wire port to be associated with an equipment case. Therefore, it was necessary to create dummy equipment cases for terminations that were not associated with legitimate equipment cases, such as switches, breakers, panels, probes, etc. Since these dummy equipment cases did not correspond to real boxes, they were not modeled as such. For purposes of simulation, each dummy equipment case was modeled as if it were the only equipment case located in its own separate compartment, thus avoiding any interactions with other equipment cases.

GP77-0342-29
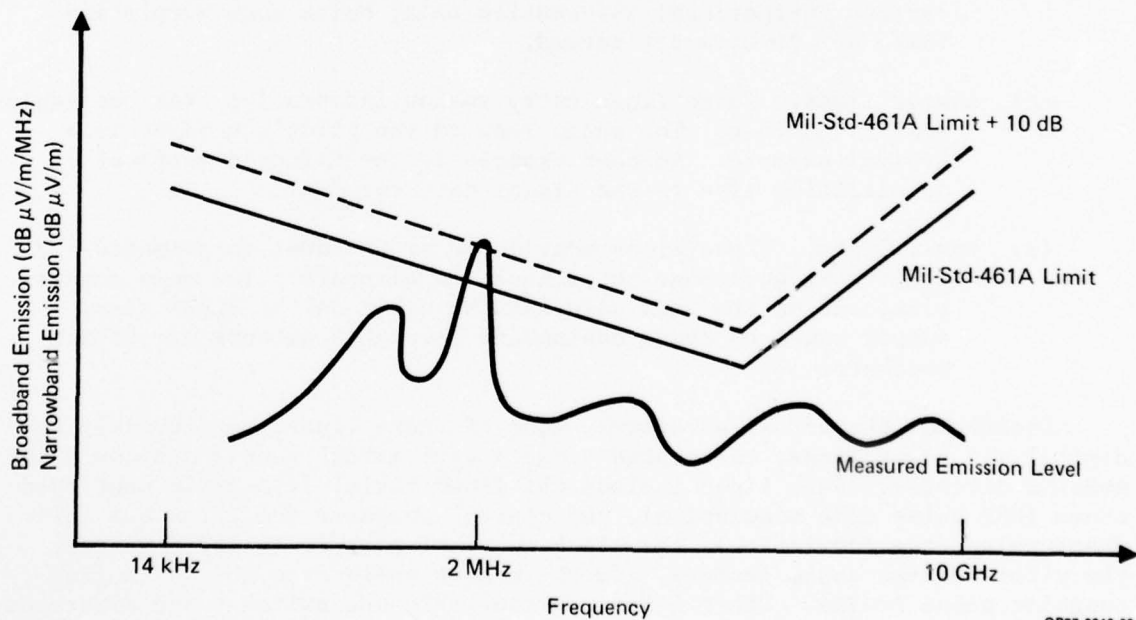
Figure 10 Modeling of Equipment Case Radiated Emission

35

2.2.2.3 Modeling signal/control and power lines. The wire interfaces represented in the mini-systems make up a broad cross section of the types of signal/control and power lines used on the F-15 aircraft. These lines tend to fall in one of five general categories as follows:

(a) Switches. These lines consist of mechanical switches, magnetic relays, or solid state switches whose function is to enable some sort of device or function. Typical examples of these are the switch that engages the nose wheel steering mechanism and the switch that resets the central computer.

(b) Discretes. These lines carry a constant AC or DC voltage level in one of two possible states, V_1 or V_2. The binary information thus provided is used either by itself, or, more commonly, in conjunction with parallel lines, each line providing one bit of information. These are classed differently than digital lines, however, because they maintain the same state for a relatively long period of time, whereas digital lines carry a steady flow of information at some bit rate. A typical example is the AIMS code C4 line from the air data computer to the IFF transponder. The voltage on this line is either 18 or 30 volts DC, providing in conjunction with 10 parallel wires, BCD coded information on the altitude of the aircraft in 100 foot increments.

(c) Digital lines. These lines carry digital information at some bit rate from one equipment to another, using some kind of pulse modulation. The serial data train from the TACAN, for example, carries navigational information using pulse code modulation (NRZ) at 400 bits per second.

(d) Analog lines. These lines carry analog information from one equipment to another. The audio line to the pilot's headset is a typical example. Another example is the filtered vertical acceleration line to the signal data recorder.

(e) Power lines. These lines provide AC or DC power to avionics and electrical equipment throughout the aircraft. Two main generators, one on the left side and the other on the right side, supply power to these equipments through a network of circuit breakers.

Looking at the actual waveforms, some of these lines, particularly the digital and power lines, correspond closely with IEMCAP models and could be modeled directly. Such lines include the TACAN serial data train mentioned above (NRZ pulse code modulation), the central computer multiplex bus (bi-phase pulse code modulation), the black modulation audio (clipped voice), the pilot headset audio (voice), and the mode 4 audio from the TACAN (rectangular pulse train). Other lines, particularly the switches and discretes, did not correspond closely with IEMCAP models, and an effort had to be made to model each of these with the most representative IEMCAP model.

36

Modeling the required susceptibility of these lines involved estimating acceptable signal-to-noise margins. As a general rule of thumb, the susceptibility of signal/control lines in their required frequency range was approximated as being 20 dB less than the normal operating level. Thus a signal/control line operating at 10 volts was assumed to be susceptible to an interfering signal of 1 volt at any frequency within its required frequency range.

The unrequired emission levels on signal/control and power lines, emissions at frequencies outside the required operating range, were modeled on the basis of measured MIL-STD-462 or MIL-I-6181 test data on conducted emissions. These measurements are performed in the screen room with the particular equipments hooked up in a manner simulating normal operation. For signal/control lines, a current probe is usually placed around a group of wires so that the reading is the sum of the currents on all the wires in a particular group, with a few noisy wires probably dominant. However, power line readings are performed on individual lines, both the high side and the return. For the case of 3-phase AC lines, each phase is measured individually. These unrequired emissions were modeled using the IEMCAP-generated limits for MIL-STD-461A or MIL-I-6181D, displaced up or down to serve as an envelope for the measured emissions similar to the way the unrequired emission of equipment cases was modeled.

The unrequired susceptibility levels of power lines were modeled on the basis of measured MIL-STD-462 and MIL-I-6181 test data on conducted susceptibility. The IEMCAP-generated specification limits were shifted up or down as a lower envelope to the measured levels. However, comparable information is not available on the susceptibility of signal/control lines. These lines are not measured as part of MIL-STD-462 susceptibility tests for several reasons, among them the lack of a standard of comparison for the multitude of signal types. The susceptibility of these lines was modeled at a constant level of 1 watt in the unrequired frequency range, so that the induced current in a victim signal/control receptor had to exceed an interference threshold corresponding to 1 watt of power, $I^2R=1$, $I^2=1/R$. Thus low impedance lines were modeled with a higher susceptibility level in terms of current, and high impedance lines were modeled with a lower current susceptibility level.

2.2.2.3.1 Modeling of switches and discretes. Of all the types of lines on the F-15, these are the most difficult to model within the framework of IEMCAP. The IEMCAP system model, based on the integrated margin concept, uses power spectral density over a frequency range to compute average power at a receptor. Technically, a switch operating only once during operation of the aircraft on a line maintaining a constant voltage, is essentially a DC line for which there is no power spectral density, as such, except for a spike at 0 Hz. This is not to say that these lines have no frequency components above DC, however. When a switch is thrown, or a discrete line changes state, it generates a transient on a one-shot basis. Such transients can be particularly bothersome when switching large currents very quickly on or off. The problem is that the average power of a single transient over a long period of time goes to zero.

37

In the laboratory, such lines are often tested by switching them on and off rapidly and observing whether they cause any malfunctions at other equipments or devices. For purposes of simulation, switches and discretes were represented as if they were turned on and off at the rate of once every second. Lines such as the nose wheel disconnect and built-in test initiate were modeled as rectangular pulse trains with a bit rate of 1 pulse per second and a pulse width of 0.5 seconds. The lines were modeled as rectangular rather than trapezoidal because the actual rise time of such lines, though unknown, is generally extremely fast, less than 10^{-6} seconds.

The question of required frequency range for such devices posed a problem. Many of these lines interface directly with the pilot, whose reaction time is of the order of a fraction of a second. In these cases, a required frequency response of about 10 Hz is usually sufficient for satisfactory operation; a circuit response of up to 1 MHz does not buy very much when the pilot initiating the signal or responding to the signal is only capable of responding at 1/5th of a second.

However, the discretes and switches, modeled as rectangular pulses repeated once every second, nevertheless have components at frequencies greater than 10 Hz even though they may not actually be required for satisfactory operation. The IEMCAP program does not compute interference below 30 Hz. In order to simulate the emissions of these types of lines, the upper limit of the "required" frequency range was extended to 1 kHz, simulating the modulation spectrum of the rectangular pulse between 30 Hz and 1 kHz. The arbitrary upper limit of 1 kHz was chosen as the approximate break point, above which the displaced MIL-STD-461A specification limit used to approximate measured spurious emissions generally exceeds the modulation spectrum.

2.2.2.3.2 Modeling digital lines. Most of the mini-system digital lines could be modeled directly with an IEMCAP spectrum model for the particular modulation scheme. These included rectangular pulse trains, NRZ pulse code modulation, and biphase pulse code modulation. There were two digital lines, however, that did not correspond directly with IEMCAP spectrum models as follows:

(a) Blanking pulse. This line blanks the radar warning receiver during transmission of pulses from the TACAN and the IFF transponder. It has a 0.5 microsecond rise time, a pulse duration anywhere between 2 and 50 microseconds and a repetition rate between 1000 and 10,000 pulses per second.

The IEMCAP model for pulse duration modulation (PDM) seemed to be the most representative model for this type of signal. In normal PDM, however, while the duration of each pulse is varied, the leading edge of all the pulses are synchronized at regular intervals, so that the pulse repetition rate is fixed. The duration of each pulse can then take on values anywhere between zero and the pulse period. As a compromise, the blanking pulse was simulated as a PDM signal with a period of 25 microseconds, corresponding to an average pulse duration of 12.5 microseconds

38

and a repetition rate of 40,000 pulses per second. To represent the modulation envelope, the required frequency range was extended out to 2 MHz.

(b) HUD x-deflection. The HUD x- and y-deflection lines carry the horizontal and vertical voltages to the CRT display. These voltages, generated by the HUD symbol generator, vary the beam deflection to trace out small amplitude strokes on the screen, making up preprogrammed symbols, and may be considered as a pulse modulated signal, at a rate of 10^6 bits per second, with a rise time of 0.1 microseconds. Both the x- and y-deflection lines were simulated as rectangular pulse trains with 10^6 pulses per second, an average pulse amplitude of one-half the full deflection voltage, a pulse width of 0.5 microseconds, and a rise time of 0.1 microseconds. The required frequency range of these lines was taken to be 0-10 MHz, and the required susceptibility was approximated as the amount of deflection voltage required to produce a visible change in the HUD display.

2.2.2.3.3 Modeling analog lines. There are only three IEMCAP models for analog signals on signal/control lines: voice, clipped voice, and user-input spectrum. The voice and clipped voice models were used to simulate pilot headset audio and modulation audio, respectively. Other analog signals represented in the mini-systems were fit to a user-input spectrum or approximated by digital modulation models. The following examples illustrate how this was done:

(a) Angle of attack indicator. This line carries a signal indicating the angle of attack generated by a rotating potentiometer with a frequency response (Laplace Transform) $1/(1 + .075 \text{ S})$. The potentiometer can respond to changes in the aircraft's angle of attack that are slow compared with a frequency of about 2 Hz, and its response to faster changes falls off at 20 dB per decade. The maximum voltage is 12 volts, corresponding to a maximum current of 3.4 mA in the line. The current spectral level of the line was approximated by dividing 3.4 mA by 2 Hz to get 1.7×10^{-3} amps per hertz as the baseline level at a frequency of 2 Hz, or 184.6 dBμA/MHz, falling off above 2 Hz at the rate of 20 dB/decade. To represent this spectrum in the "required" range between 30 Hz and 1 kHz, the calculated value of this log-linear curve only needed to be specified at 30 Hz and 1 kHz, using the SPECT option for user-input spectra. Other lines modeled in a similar way include the normal accelerometer sensor B signal, the CAS interconnect servo A signal, and the filtered vertical acceleration signal.

(b) Fuel quantity indicator. This line carries a 4000 Hz signal applied to a probe inside the fuel tank. As the level in the tank changes, it changes the capacitance of the probe, the change in capacitance causing a shift in phase that is detected at the indicator. The waveform on this line is essentially a

39

4 kHz phase-modulated sine wave, whose modulation signal is
very slowly varying compared with the carrier frequency. Al-
though there is no IEMCAP spectrum model for phase modulation
per se, phase modulation can always be considered as a form of
frequency modulation, for which there is an IEMCAP spectrum
model. A phase-modulated waveform $V(t) = A \sin [\omega t + g(t)]$
where $g(t)$ is a unit amplitude modulation signal, is equivalent
to a frequency-modulated waveform $v(t) = A \sin [\omega_0 t + h(\tau) d\tau]$
where the modulation signal $h(t)$ is equal to dg/dt. The instantaneous
phase $g(t)$ is related in a simple manner to the level of fuel in
the tank, and the instantaneous frequency shift dg/dt is similarly
related to the rate of change of the fuel level. Since the
variation of the fuel level is extremely slow compared with the
4 kHz carrier, the bandwidth of the modulated waveform is very
small, and for all practical purposes the spectrum could be con-
sidered as a spike. Thus, the fuel quantity indicator signal
could be modeled either as CW or an FM signal centered about
4 kHz.

Unfortunately, the IEMCAP spectrum models for CW and FM can
only be specified for RF ports in the frequency range 14 kHz to
18 MHz, and consequently could not be used to simulate the fuel
quantity indicator emission spectrum in the vicinity of 4 kHz.

An approximation to the spectrum of this signal was obtained by
simulating the line as a rectangular pulse train with a 4 kHz
bit rate, each pulse 125 microseconds wide, with a required fre-
quency range between 30 Hz and 4 kHz. The narrow band signal was
thus simulated as a broadband signal with a uniform power spec-
tral density between 30 Hz and 4 kHz, cutting off harmonics
above 4 kHz.

In hindsight, a more accurate representation might have been
obtained with a user-input spectrum, representing the narrow
band spectrum with a very high, narrow rectangle in the frequency
domain, centered about 4 kHz.

Lines from the stick force sensor to the automatic flight control
set that also carry phase-modulated signals were simulated a
similar way, using a digital model to represent an analog signal.

Lines like the fuel quantity indicator and stick force sensor have
a record of being particularly sensitive to RF interference. They
strip off the modulation, acting as non-linear detectors of RF
energy. These particular lines originally exhibited a suscepti-
bility to interference at UHF frequencies; the problem in each
case was subsequently corrected by shielding or filtering. To
simulate the detection at UHF frequencies, these lines were modeled
as RF receptor ports with a window between 225 and 400 MHz, trans-
lating the susceptibility at low frequencies to the RF frequency
with the assumption of 100% demodulation efficiency.

40

(c) Annunciator drive to compass control panel. This line carries a signal from the attitude and heading reference set (AHRS) indicating the error between the flux valve true magnetic heading and the gyro-stabilized heading put out by the AHRS. During steady flight this error is zero, but sudden maneuvers by the pilot cause the gyro-stabilized heading to lag the true magnetic heading, the error persisting for several seconds. This signal was simulated as a rectangular pulse train, one pulse per second, the leading edge representing the sudden error introduced by a maneuver. In retrospect, an exponential spike might have been a more representative model, although its spectrum differs very little from that of the pulse train.

2.2.2.3.4 Modeling power lines. Power lines were modeled on the basis of measured unrequired emission and susceptibility obtained from MIL-STD-462 and MIL-I-6181 tests. These levels were modeled similar to the way unrequired spectra were modeled for signal/control lines and equipment cases, using the shifted MIL-STD-461A or MIL-I-6181D specification limits as an envelope to the measured emission and susceptibility levels.

2.3 Listing of mini-system input data. The input deck for Mini-system I, consisting of all the F-15 mini-system antenna ports, is listed in Figure 11. This mini-system was used for the evaluation of IEMCAP predictions for antenna-coupled interference, and also provided a basis for comparing the calculated values of antenna coupling with measured antenna isolation data. Mini-system I was also used as a baseline for the sensitivity study of antenna-related input parameters and as a baseline for an assessment of IEMCAP SGR runs.

The input decks for Mini-systems B1, B2, and B3 are listed in Figures 12 through 14. These three mini-systems include all the simulated F-15 equipments broken up into three mini-systems because of limitations on the number of wire types, equipment cases, bundles, etc., permitted in a single run. They were used for the evaluation of all remaining coupled interference predictions by IEMCAP: antenna-to-wire, wire-to-wire, and case-to-case. Mini-system B2 was also used as a baseline for the sensitivity study of input parameters relating to wire-to-wire and antenna-to-wire coupled interference.

2.4 IEMCAP Program shakedown. Experience in debugging the IEMCAP program with F-15 mini-systems underscored the lesson that one does not throw data at the computer and expect it to run the first time. With a large, complex data base, it takes repeated runs to screen out input data errors. Almost all of these errors, fortunately, tend to be caught by checks built into IDIPR, and the others usually show up in the TART results. The latter tend to be errors like missing or misspelled filter or wire types whose absence quickly makes itself known.

During the assessment phase of the validation effort, simulation of the filter on the stick force sensor wire, exposed to an environmental field, revealed an error in the TART program, such that the total received signal in microamps is squared twice. This error was corrected so that the received signal is only squared once.

41

```
COMMENT=ANTENNA TO ANTENNA VALIDATION RUN
TITLE=MINISYSTEM I
EXEC=CEAR,NEW,SURVEY
OUTPUT=ISF
SYSTEM=AIR,0,0,0,-6,-199
FUSLGE=415,46,5,117,93,FLAT
WNGRT=46,129,457,5,707
WGTIP=260,120,655,732
EFQ=14E3,20EQ
DOEFL=-100,-100
APER=CNOPY,0,158,292,35,150,NOW
APER=SPRRK,0,163,530,40,114,NOW
APER=NSWEL,0,93,350,15,82,NOW
APER=LMLG,41,93,571,38,80,NOW
ANT=UHFUP,DIPOLE,VE,(8.00)
ANT=UHFL1,DIPOLE,VE,(8.00)
ANT=UHFL2,DIPOLE,VE,(8.00)
ANT=TACLO,DIPOLE,VE,(8.00)
ANT=TACUP,DIPOLE,VE,(8.00)
ANT=IFFUP,DIPOLE,VE,(8.00)
ANT=IFFLO,DIPOLE,VE,(11.0)
ANT=ILSGL,DIPOLE,VE,(13.0,-8,90,145,-18,180,-18)
ANT=ILSMB,PSDAR,VE,(12.0)
ANT=ADF,DIPOLE,VE,(12.0)
FILTER=LPAS,LOWPAS,16,(400E6,0,-115)
FILTER=ADF,LOWPAS,2,(1E9,-16,-16)
FILTER=HPAS,HIPAS,13,(900E6,0,-50)
FILTER=TACUP,HIPAS,13,(900E5,0,-20)
SUBSYS=COMM
EQOPT=UHFCO,M6181D,FIX,R1BAY,NOTCLS,10,111,236
FREQ=14E3,18E9,1,40
FQTBL=320624359,320624679,320645600,320646000,320649000,320649800,320649900,
      320650000,320650100,320650200,320651000,320654000,320654400,
      320675321,320675641
PORT=CASE,6,0
```

Figure 11 Mini-System I Input Deck

```
SOURCE=CASE,30,MILSPC,MILSPC
PORT=CASE,30,MILSPC,MILSPC
RCEPT=COMUP,ANT,(UHFUP,90,0,2158,464,NOW),50,0,0,0,LPAS
SOURCE=RF,500,3200,65FF6,320,0,65E6,100,0,5044E3,AM(VOICE,50E3,1),(-73,-73)
RCEPT=RF,500,3200,65FF6,320,0,65E6,287,0,5044E3,AM(VOICE,50E3,1),0
PORT=COMLN,ANT,(UHFLN,90,0,0,284,NOW),50,0,0,0,LPAS
SOURCE=RF,500,3200,65E6,320,0,65E6,100,0,5044E3,AM(VOICE,50E3,1),(-73,-73)
RCEPT=RF,500,3200,65E6,320,0,55FF6,10,0,5044E3,AM(VOICE,50E3,1),0
EQPT=AUX,M6181E9,FIX,RIBAY,NOTCLS,10,111,244
FREQ=14E3,363327274,36335000,363372363,363372726
FQTBL=363327274,36335000,363372363,363372726
SOURCE=CASE,30,MILSPC,MILSPC
PORT=CASE,30,MILSPC,MILSPC
RCEPT=AUXLN,ANT,(UHFLL2,90,0,047,222,NOW),50,0,0,0,LPAS
EQPT=ADF,M461A,FIX,RIBAY,NOTCLS,10,121,219
PORT=RF,500,363,35E6,363,35E6,-1014,44F3,AM(CVOICE,50E3,1),0
FREQ=14E3,218E9,14E3,363327274,36335000,363372363,363372726
FFQTBL=363327274,36335000,363372363,363372726
PORT=CASE,30,MILSPC,MILSPC
SOURCE=CASE,30,MILSPC,MILSPC
RCEPT=ADFRF,ANT,(ADF,900,0,0140,229,NOW),50,0,0,0,ADF
PORT=ADFRF,ANT,(ADF,900,0,0140,229,NOW),50,0,0,0,ADF
RCEPT=RF,50,363,35E6,353,-101,44E3,CW,0
SUBSYS=IDFNT
EQPT=IFFX,M461A,FIX,RIBAY,NOTCLS,10,102,218
FREQ=14E3,2187940,10259,94970,1030E6,10340010030,10340002060,
10459097820,10859098910,10871352112,10887267602,1089363380,
1090E6,10906366619,1091273240,10928647892,10940010902,1094002180
```

```
PORT=CASE,29,0
SOURCE=CASE,30,MILSPC,MILSPC
RCEPT=CASE,30,MILSPC,MILSPC
```

Figure 11 Mini-System I Input Deck (Continued)

43

```
PORT=IFFUP,ANT,(IFFUP,90,0,0,159,464,NOW),50,0,0,0,HPAS
SOURCE=RF,50,1030E6,1090E6,177,CO,8E6,RADAR(RECTPL,125E3,,5E-6),(-90,-90)
RCEPT=RF,50,1030E6,1090E6,177,284,8E6,RADAR(RECTPL,125E3,,5E-6),0
PORT=IFFLP,ANT,(IFFLP,90,0,0,87,200,NOW),50,0,0,0,HPAS
SOURCE=RF,50,1030E6,1090E6,77,3E6,RADAR(RECTPL,125E3,,5E-6),(-90,-90)
RCEPT=RF,50,1030E6,1030E6,77,8E6,RADAR(RECTPL,125E3,,5E-6),0
SUBSYS=NAV
EQPT=TACAN,M461A,FIX,R1BAY,NOTCLS,10,122,238
FREQ=14E3,18E9,1,40
FQTBL=9614980760,9614499038,962E6,962500962,962501924,
1024495273,1024454527,1024547272,1024479537,1025090946,1025204628,1025454728,
1025501025,1025502050

PORT=CASE,52,MILSPC,MILSPC
SOURCE=CASE,30,MILSPC,MILSPC
RCEPT=TACUP,ANT,(TACUP,90,0,0,160,436,NOW),50,0,0,0,TACUP
SOURCE=RF,50,1062E6,962E6,21E-6,2,1E6,RADAR(RECTPL,100,14E-6),(-93,-93)
RCEPT=RF,50,1062E6,962E6,87,2000,1E6,RADAR(RECTPL,100,14E-6),0
PORT=TACLO,ANT,(TACLO,90,0,0,222,NOW),50,0,0,0,HPAS
RCEPT=RF,50,1062E6,962E6,1E6,RADAR(RECTPL,100,14E-6),0
EQPT=ILS,M461A,FIX,R1BAY,NOTCLS,10,102,213
FREQ=14E3,18E9,1,40
FQTBL=7467,7467,9925,75E6,20075,750201500,
1099867800,1099868900,1E6,11001311011100013220,
3319753336,3319756669,332E6,332024332,332024664

PORT=CASE,-3,0,MILSPC,MILSPC
SOURCE=CASE,30,MILSPC,MILSPC
RCEPT=LOCAL,ANT,(ILSGL,110E6,0,90,93,196,NOW),50,0,0,0,0,0
RCEPT=GLIDE,ANT,(ILSGL,110E6,0,90,93,196,NOW),50,0,0,0,0,0
SOURCE=RF,50,332E6,332E6,180,48E3,CW2O
PORT=MARK,ANT,(ILSMR,180,0,90,92,312,NOW),50,0,0,0,0,0
RCEPT=RF,50,75E6,75E6,-53,40E3,CW,0
EODATA
```

Figure 11 Mini-System I Input Deck (Concluded)

44

GP77-0221-78

Figure 12 Mini-System B1 Input Deck

45

```
SOURCE="CASE..MILSPC
RCEPT=CASE..MILSPC
PORT=FIREWIRE..0..GND..NONE..NOTEX)..280..0..0..0..0
RCEPT=(III4..855..RECTPL(.125..4)..1..AMPS..1E3
EQPT=DUMYO..NOTCLS..0..0..0
FREQ=SIGNAL..0..30..1E3
PORT=

SOURCE="CASE..MILSPC
RCEPT=CASE..MILSPC
PORT=DIST..0..GND..NONE..EX)..78..0..0..0..0
RCEPT=(III0..RECTPL(.14..1)..111..316
EQPT=R3BAY..NOTCLS..14..111..316
FREQ=SIGNAL..0..30..1E3..1..AMPS..1E3
PORT=

SOURCE="CASE..MILSPC
RCEPT=CASE..MILSPC
PORT=LG..0..BAL..GND..NOTEX)..1CE3..0..0..25..0..0
RCEPT=(III5..BPPCM(.5E6..1)..6E-3..AMPS..2.E6
EQPT=LIBAY..NOTCLS..-10..113..234
FREQ=SIGNAL..0..30..2.E3..5E6..1)..1E-3..AMPS..2.E6
PORT=

SOURCE="CASE..MILSPC
RCEPT=CASE..MILSPC
PORT=INIT..WIRE..0..BAL..GND..NOTEX)..300..0..0..23..0..0
RCEPT=(III5..30..1E6..RECTPL(60..210E-6)..15..AMPS..1E6
EQPT=R2BAY..NOTCLS..10..112..265
FREQ=SIGNAL..0..30..50E6..1..90
PORT=

SOURCE="CASE..MILSPC
RCEPT=CASE..MILSPC
PORT=BNOGO..GND..NONE..NOTEX)..500..0..0..18..0..0
RCEPT=(III4..1E3..RECTPL(1..0..5)..0067..1OE3..0..18..0..0
PORT=MBUS3..WIRE..0..BAL..GND..NOTEX)..1OE3..0..18..0..0
RCEPT=(III5..2E6..BPPCM(.5E6..1)..6E-3..AMPS..2E6
SOURCE="CASE..MILSPC
RCEPT=(III4..30..2E6..BPPCM(.5E6..1)..1E-3..AMPS..2E6
PORT=BLANK..WIRE..0..UNBAL..GND..NOTEX)..68..0..0..0..0
EQPT=(III1..30..2E6..PDM(.40E3)..588..AMPS..2E3
FREQ=30..50E6..1..90
```

Figure 12 Mini-System B1 Input Deck (Continued)

46

```
P.
        PORT=CASE,0,0,MILSPC,MILSPC
        SOURCE=CASF,0,0,MILSPC,MILSPC
        PORT=RFSET,WIRE,0,(IIII4,IIIO,TP,ZNC(L0F,5E-6),2.5E-3,21E3,0,0,0,0
        SOURCE=SIGNAL,0,(IIII2,III304,1E3,GND,NOTEX),10,0,AMPS,0,0,0,0
        PORT=3NOGN,WIRE,0,(IIII2,III305,RECTPL(1,0.5),1.33E-3,AMPS,1E3
        PORT=BIT,WIRE,0,(III12,III305,RECTPL(1,0.5),1.33E-3,AMPS,1E3
        RCEPT=IB,M461A,FIX,RIBAY,NOTCLS,4,120,213
    EQPT=IB,M461A,FIX,RIBAY,NOTCLS,4,120,213
    FRFQ=30,50E6,1,90
        PORT=CASE,12,0,MILSPC,MILSPC
        SOURCE=CASF,0,0,MILSPC,MILSPC
        PORT=BLANK,WIRE,0,(IIII4,2E6,PDM(40E3),58B,AMPS,2F6
        SOURCE=SIGNAL,0,30,2E6,UNBAL,GND,NOTEX),68,0,0,24,0,0
        RCEPT=INS,M461A,FIX,RIBAY,NOTCLS,10,113,217
    EQPT=INS,M461A,FIX,RIBAY,NOTCLS,10,113,217
    FRFQ=30,50E6,1,90
        PORT=CASE,31,0,MILSPC,MILSPC
        SOURCE=CASF,0,0,MILSPC,MILSPC
        PORT=INIT,WIRE,0,(IIII5,IIII4E,RECTPL(60,10F-6),05,AMPS,1E6
        RCEPT=INIT,WIRE,0,30,1E5,BAL,GND,NOTEX),300,0,0,0,0,0
    EQPT=TACAN,M461A,FIX,RIBAY,NOTCLS,10,122,238
    FRFQ=30,50E6,1,90
    FQTBL=1024497527,1025502050,1024545272,1024795372,1024909054,
          1025501000,1024945427,1025E6,1025204628,1025454728,
        PORT=CASE,52,0,MILSPC,MILSPC
        SOURCE=CASE,0,0,MILSPC,MILSPC
        PORT=TACUB,ANT,(TACUP,30,1E5,RADAR(RECTPL,100,14E-6),(-93,-93)
        SOURCE=RF,ANT,30,1025E6,900,222,NOW),50,0,0,0,0,0
        PORT=TACLD,ANT,(TACLD,30,1025E6,400,436,NOW),50,RADAR(RECTPL,100,0,HPAS
        SOURCE=RF,ANT,30,1025E6,400,222,NOTEX),50,RADAR(RECTPL,100,14E-6),(-93,-93)
        PORT=SDATA,WIRE,0,(IIII1,IIIO,GND,NP7,PCM(400),2.0E-3,AMPS,10E3
        SOURCE=SIGNAL,0,30,IIO,IIIO,GND,NP7,PCM(400),2.0E-3,AMPS,10E3
    EQPT=ILS,M461A,FIX,RIBAY,NOTCLS,10,102,213
    FRFQ=30,50E6,1,90
        PORT=CASE,13,0,MILSPC,MILSPC
        SOURCE=CASE,30,MILSPC,MILSPC
        RCEPT=ADF,M461A,FIX,RIBAY,NOTCLS,10,121,219
    EQPT=ADF,M461A,FIX,RIBAY,NOTCLS,10,121,219
    FREQ=30,50E6,1,90
```

Figure 12 Mini-System B1 Input Deck (Continued)

```
PORT=CASE,3C,0,MILSPC,MILSPC
SOURCE=CASE,0,MILSPC,MILSPC
RCEPT=CASE,0,MILSPC,MILSPC

PORT=BITAK,WIRE,(III2,III5,R,UNBAL,NONE,NOTEX),500,0,0,0,0,0
EQPT=SOURCE=SIGNAL,FIX,RIBAY,RECTPL(1,0,5),1,33E-3,AMPS,1E3
*FREQ=M6E1D,NOTCLS,10,111,236
FCTBL=3206245,3206245,73,3206460CO,3206460CO,3206549800,3206649CO,
      3206545200,3206545200,3206551000,3206545400CO,3206544400,
      3206675321,3206675541

PORT=CASE,0,MILSPC,MILSPC
SOURCE=CASE,0,0,0,158,464,NOW),50,0,0,0,0,LPAS
    (UHF),0,0,320,65E6,10E3,AM(VOICE),0,50E3,1),(-73,-73)
PORT=LOOP,WIRE,(III2,UNBAL,NONE,NOTEX),50,AM(VOICE),0,50,0,LPAS
SOURCE=SIGNAL,0,0,320,65E6,AM(VOICE),0,500,-44,7,0,(-73,-73)
PORT=BLACK,WIRE,(III4,C,VOICE,GND,NOTEX),0,300E3,1500,0,0,0,-61,7,0
RCEPT=SIGNAL,0,112,III4,RECTPL(1),1500,0,0,0,0,150E3
PORT=CEPT,WIRE,(III3,III,C,GND,NOTEX),0,1026,AM,0,187,0,0,0,0
PORT=ANTSL,WIRE,0,2X,(1),NOTFX),OX),187,0,0,0,0,0
EQPT=III2,M61A,FIX,M6181D
*FREQ=30,5CE6,1,90

PORT=CASE,0,MILSPC,MILSPC
SOURCE=CASE,0,MILSPC,MILSPC
RCEPT=ANTSL,WIRE,0,0,(III9,F,GND,NONE,NOTEX),0,1,0,0,17,0,0
PORT=MBUS3,WIRE,3,(III5,BAL,GND,NOTEX),10E3,2,0,9,0,0
EQPT=SOURCE=SIGNAL,0,30,BPBCM(5E6,1),6E-3,AMPS,2E6
*FREQ=50E6,2,90
PORT=AUX,WIRE,(III2,BPPCM(5E6,1),1E-3,AMPS,2E6
RCEPT=SIGNAL,FIX,RIBAY,NOTCLS,10,111,244

PORT=CASE,0,MILSPC,MILSPC
SOURCE=CASE,0,MILSPC,MILSPC
RCEPT=3ND,WIRE,(III2,B,GND,NONE,NOTEX),25,0,0,0,0,0
SOURCE=SIGNAL,0,30,1E3,RECTPL(1,0,5),02,AMPS,1E3
PORT=TCCP,M61A,FIX,CKBIT,NOTCLS,-15,125,302
```

Figure 12 Mini-System B1 Input Deck (Continued)

GP77-0221-81

GP77-0221-82

Figure 12 Mini-System B1 Input Deck (Continued)

GP77-0221-83

Figure 12 Mini-System B1 Input Deck (Continued)

GP77-0221-84

```
PORT=CASE,0,0
SOURCE=CASE,0,MILSPC,MILSPC
RCE=CASE,0,MILSPC,MILSPC
PORT=ADC,IH6,FUNBAL,GND,NOTEX),3500,0,0,0,0,0
RCEPT=WIRE,(IH2,IH6,1200,SPECT(30,50,72)00,50,7),3,43E-3,AMPS,1E3
EOPT=ADC,M461A,FIX,RIBAY,NOTCLS,10,132,246
FREQ=30,5CE6,1,90

OPT=CASE,0,MILSPC,MILSPC
SOURCE=CASE,MILSPC,MILSPC
RCE=CASE,IH15,FBAL,GND,NOTEX),10E3,0,0,5,0,0
RCEPT=WIRE,(IH6,RPPC,5E6,1,6E-1,1E3,AMPS,2E6
EOPT=SIGNAL,M461A,FIX,L2BAY,NOTCLS,0,109,275
FREQ=30,2E6,90

OPT=CASE,MILSPC,MILSPC
SOURCE=WIRE,IH4,RECTPL,GND,NOTEX),300,0,0,0,0
RCEPT=SIGNAL,IH6,RHPPC,5E6,1,6E-1,1E3,AMPS,2E6
EOPT=SIGNAL,M461A,FIX,CKBIT,NOTCLS,0,135,259
FREQ=30,2E6,90

OPT=CASE,0,MILSPC,MILSPC
SOURCE=WIRE,IH8,TPZD,GND,NONE,NOTEX),30000,0,0,14,0,0
RCEPT=SIGNAL,IH3,1E3,TPL,25E-3,AMPS,1E3
EOPT=SIGNAL,M461A,FIX,L2BAY,NOTCLS,9,109,293
FREQ=30,50E6,1,90

OPT=CASE,0,MILSPC,MILSPC
SOURCE=WIRE,IH13,K,GND,NONE,NOTEX),280,0,0,0,0
RCEPT=FAIL,IH13,1E3,RECTPL,1,1,AMPS,1E3
EOPT=FDA,M461A,FIX,RIBAY,NOTCLS,12,129,224
FREQ=30,50E6,1,90
SOURCE=CASE,0,MILSPC,MILSPC
```

Figure 12 Mini-System B1 Input Deck (Continued)

51

```
PORT=ACCEL,WIRE,(IIT4,IIIIO,A,UNBAL,NONE,NOTEX),100,0,0,C,0,0,0
ESOURC=SIGNAL,0,100,SPECT(30,214,100,214,1000,174),.05,AMPS,1E3
EFREQ=30,FIX,CKPIT,NOTCLS,0,125,288
PORT=CASE,0,MILSPC

PORTSOURC=WIRE,DISCH,GND,NONE,NOTEX),1,1,C,C,1,0,C
EFREQ=30,1000,HZ,ZNL,TRZD(1,.5,1E-6),1,AMPS,1E3
PORT=IITI4,IIIIO,E,ZBAY,NOTCLS,10,100,270
ESOURC=CASE,0,MILSPC

PORT=ACCEL,WIRE,(IIT4,IIIIO,E,UNBAL,NONE,NOTEX),100,0,0,0,0,C
ESOURC=SIGNAL,0,C,SPECT(30,74,100,74,1000,114),.C5,AMPS,1E3
EFREQ=30,FIX,NOTCLS,0,0,0
PORT=CASE,0,MILSPC

PORTSOURC=WIRE,CHLGND,NONE,NOTEX),1,C,0,C,0,C
EFREQ=ENG,1,.5),2E3, RFCTPL(1,.5),2E3,0,0,0
PORT=IITI4,IIIIO,E,GND,NONE,NOTEX),2,C,0,0,0,0
ESOURC=AJENG,ZNTRCLA,FIX,L3BAY,NOTCLS,-13,120,359

PORT=SERVA,WIRE,(IIII3,D,UNBAL,GND,NOTEX),190,0,0,0,0,0
EFREQ=30,2E3,SPECT(30,71,891,71,2E3,851,.35E-3,AMPS,2E3
PORT=CASE,0,MILSPC

PORTSOURC=CHAL,WIRE,(IIT2,II5,D,GND,NONE,NOTEX),224,0,0,C,0,0
EFREQ=30,5OE6,1.90,RECTPL(1,0,.5),.125,AMPS,1000
PORTSOURC=CASE,0,MILSPC,MILSPC
```

Figure 12 Mini-System B1 Input Deck (Continued)

GP77-0221-86

Figure 12 Mini-System B1 Input Deck (Continued)

```
PORT=ACPWR,WIRE,(III3,III5,R,GND,NONE,NOTEX),1,6,0,0,0,0,0
PORT=POWER,0,II5,4C0,3,1,M461A
FPORT=III5,M461A,FIX,III5,NOTCLS,0,0,0
FRED=30,50EE6,1,90
PORT=CASE,0,MILSPC
SOURCE=CASE,0,MILSPC,MILSPC
PORT=ACPWR,CASE,0,MILSPC
PORT=ACPWR,(III3,III8,E,GND,NONE,NOTEX),0,1,0,0,0,0,0
SOURCE=POWER,0,II5,400,3,1,M461A
BUNDLE=III1
BPTS=A,-14,125,281,R,-15,125,302,C,-21,133,302,D,-2,122,240,F,15,111,239,
BSEG=F,13,102,279,G,0,0,0,H,0,0,0,I,0,0,0,J,0,0,0
      G,21,100,254,CKPIT,0,G,32,4,CKPIT,0,C,H,71,4,CKPIT,0,
      H,22,122,4,R1BAY,0,I,J,15,4,R1BAY,0,E,J,32,4,R1BAY,0,
WIRE=III1,STP26,A,B,C,D
WIRE=III2,U26,C,H,I,E
BUNDLE=III2
BPTS=A,-16,125,302,B,-20,126,301,F,-24,125,247,C,15,111,239,D,15,112,229,
BSEG=E,15,132,241,G,0,0,0,H,0,0,0,I,0,0,0,J,0,0,0
      G,24,C,CKPIT,0,G,42,4,CKPIT,0,F,H,43,4,CKPIT,0,
      H,I,43,4,R1BAY,0,I,J,24,4,R1BAY,0,D,J,43,4,R1BAY,0,
WIRE=III4,U26,A,G,H,I,C
WIRE=III5,U26,B,F,H,I,J,D
WIRE=III6,STP26,F,H,I,E
BUNDLE=III3
BPTS=A,-14,120,302,B,-16,125,302,C,14,126,303,D,2,135,259,E,0,0,0,F,0,0,0,
BSEG=G,20,254,H,31,4,CKPIT,C,E,F,60,4,CKPIT,0,D,F,32,4,CKPIT,0,
      F,C,44,CKPIT,0,H,E,6,4,CKPIT,0,F,G,6,4,CKPIT,0
WIRE=III7,STP26,A,E,F,C
WIRE=III8,U22,B,E,F,D
WIRE=III6,B54,U22,H,E,F,G
BUNDLE=III4
BPTS=A,-16,125,302,B,-20,125,306,C,3,120,279,D,-17,109,304,E,-15,110,260,
BSEG=A,G,27,4,CKPIT,0,B,G,58,4,CKPIT,0,C,H,105,4,CKPIT,0,
      H,I,60,4,L2BAY,0,F,I,106,4,L2BAY,0,L2BAY,0,E,J,59,4,
```

Figure 12 Mini-System B1 Input Deck (Continued)

```
WIRE=III19,U22,A,G,H,I,J,D
WIRE=III1C,STP26,B,G,I,J,F
WIRE=III11,U24,C,H,I,F
BUNDLE=III1
RPTS=A,15,111,241,B,15,111,245,C,15,129,225,D,-13,125,285,E,-16,125,302,
      F,12,132,270,G,32,4,R1BAY,O,A,O,J,O,C,H,39,4,R1BAY,O,
RSEG=A,G,130,4,R1BAY,O,G,I,330,4,P1BAY,O,C,H,39,4,R1BAY,O,
      H,100,4,CKPIT,O,E,I,IC,4,CKPIT,O,F,J,32,4,CKPIT,O,

WIRE=III12,U26,C,H,I,F
RSEG=A,F,130,4,CKPIT,O,F,I,I,J,E

WIRE=III13,U24,D,E,H,I
RPTS=A,15,111,216,C,13,1C2,220,D,-13,125,285,E,-20,125,306,
      F,12,132,267,G,32,4,P1BAY,O,C,H,56,4,R1BAY,O,
RSEG=A,G,130,4,R1BAY,O,G,I,172,4,R1BAY,O,C,H,56,4,R1BAY,O,
      H,57,4,CKPIT,O,E,I,18,4,CKPIT,O,E,J,43,4,CKPIT,O,

WIRE=III14,U26,C,H,I,F
RSEG=A,F,130,4,CKPIT,O,F,I,J,E

WIRE=III15,U26,C,H,I,F
RPTS=A,15,111,234,C,15,111,239,D,-13,120,359,E,-16,120,332,
      F,17,132,264,G,19,4,R1BAY,O,C,H,36,4,R1BAY,O,
RSEG=A,C,130,4,R1BAY,O,G,I,172,4,R1BAY,O,C,H,36,4,R1BAY,O,
      H,18,4,L3BAY,O,F,I,18,4,L2BAY,O,E,J,20,4,L3BAY,O,

WIRE=III16,STP26,C,H,I,F
WIRE=III17,U22,A,G,H,I,J,D
WIRE=III18,U22,B,G,H,I,J,E
WIRE=III19,U26,C,H,I,F
BUNDLE=III4
RPTS=A,15,132,237,B,11,120,213,C,15,129,225,D,18,112,270,F,8,100,279,
RSEG=A,H,18,112,267,G,-20,125,305,H,O,C,I,40,4,R2BAY,O,I,G,104,4,CKPIT,O
RSEG=A,H,31,4,R1BAY,O,R,H,40,4,R1BAY,O,D,H,54,4,R2BAY,O,

WIRE=III50,4,R1BAY,O,I,E,32,4,R2BAY,O,I,F,40,4,R2BAY,O,I,G,104,4,CKPIT,O
WIRE=III10,UT26,A,H,I,E
WIRE=III11,STP26,B,H,I,F
BUNDLE=III5,U26,C,H,D,I,G
RPTS=A,18,111,320,B,17,113,297,C,14,125,289,D,18,112,267,E,15,132,246,
```

Figure 12 Mini-System B1 Input Deck (Continued)

```
   F,-15,110,260,G,-15,109,280,J,-16,113,241,K,-15,109,213,
   H,0,0,I,0,0,0
BSEG=A,H,72,4,R3BAY,0,B,H,7,4,R2BAY,C,C,4,60,4,CKPIT,0,J,H,6,4,L1BAY,0,
     K,H,64,4,L2BAY,C,H,IC,4,L2BAY,C,I,D,43,4,R2BAY,0,I,E,41,4,R1BAY,0,
     I,F,177,4,L2BAY,0,I,G,6,4,L2BAY,0
WIPE=IIII13,U26,K,H,I,E
WIPE=IIII14,STP24,B,H,J,I,E,G
WIPE=IIII15,STP22,A,B,C,H,I,D,E,F,G
ENDATA
```

Figure 12 Mini-System B1 Input Deck (Concluded)

56

GP77-0221-90

Figure 13 Mini-System B2 Input Deck

```
FREQ=30,5CF6,1,90
POPT=CASE=17,0,,MILSPC,MILSPC
SOURCE=CASE,0,,MILSPC,MILSPC
RCEPT=HYD,MC,WIRE,(M4,B12,MF,GND,NONE,NOTEX),72C,0,0,0,0,0
PORT=MC,CNTRL,0,30,1E3,RECTPL(1,,5),,0333,AMPS,1E3
EQPT=B1A,FIX,B1,NOTCLS,0,C,0
FREQ=30,50E6,1,90
SOURCE=CASE,0,,MILSPC,MILSPC
OPT=CASE,0,,MILSPC,MILSPC
SOURCE=SIGNAL,(B1,B1,A,UNBAL,GND,EX),11,0,0,0,0,0
OPT=T2UL=WIRE,(B1,30,4CC),RECTPL(4E3,1,25E-4),,455,AMPS,4E3
SOURCE=SIGNAL,(B1,32,A,UNBAL,GND,FX),280,0,0,,0
OPT=T2UL=WIRE,(B1,30,400),RECTPL(4E2,1,25E-4),,1,AMPS,4E3
EQPT=R2,M461A,FIX,B2,NOTCLS,0,0,0
FEQTBL=30,18,35E6,
FEQTBL=363,35E6
SOURCE=CASE,0,,MILSPC,MILSPC
OPT=CASE,0,,MILSPC,MILSPC
RCEPT=T2QNT,WIRE,(B1,B1,C,UNBAL,GND,EX),11,0,0,0,-53,6,0

RCEPT=RF,0,225E6,400E6,13,6,100E3,CW,0,0,0,0,0,0
PORT=T2LOW,WIRE,(B1,B2,B),UNBAL,GND,EX),280,0,0,0,0,0
RCEPT=SIGNAL,0,30,4000,RECTPL(4E3,1,25E-4),,1,AMPS,4E3
FOPT=B4,M461A,FIX,B4,NOTCLS,0,0,0
FREQ=30,50E6,1,90
SOURCE=CASE,0,,MILSPC,MILSPC
RCEPT=FLITE,WIRE,(B5,B13,D,GND,NONE,NOTEX),8,C,C,0,0,0
EQPT=B5,M461A,FIX,B5,NOTCLS,0,0,0
FREQ=30,5CE6,1,90
SOURCE=CASE,0,,MILSPC,MILSPC
RCEPT=PNLIT,WIRE,(B9,B28,B,GND,GND,EX),,1,0,0,13,0,0
SOURCE=POWER,0,5,400,3,1,M461A
PORT=FLITE,WIRE,(B5,B13,A,GND,NONE,NOTEX),,1,0,C,G,0
.SOURCE=POWER,0,115,400,3,1,M461A
```

Figure 13 Mini-System B2 Input Deck (Continued)

GP77-0221-91

GP77-0221-92

```
EQPT=PAR,M461A,FIX,R3BAY,NDTCLS,11,109,332
EFREQ=30,50,0
EPORT=CASE=0,,MILSPC,MILSPC
ERCEPT=CASE=214,,0,,MILSPC,MILSPC
EPORT=PWR=CHIP-ELEC,NONE,NOTEX),1,0,0,6,0,0
ERCEPT=PWR=(B5,B15,B14,R,UNBAL,NONE,NOTEX),1,0,0,22,0,0
ESOURCE=EXTND,WIRE,(B5,B14,R,RECT,PL(1,,5),2.8E-3,AMPS,1E3
ESOURCE=SIGNAL,0,3C,1E3,NOTCLS,0,0,0
EQPT=B9,M461A,FIX,B9,NOTCLS,...
EPORT=CASE=0,,MILSPC,MILSPC
ERCEPT=CASE=30,M461A,...,0,,MILSPC,MILSPC
EPORT=AFT=PWR,0,3C,UNBAL,NONE,NOTEX),3,6,0,0,0,0
ERCEPT=EXTND,PWR,(B5,B15,B14,R,UNBAL,NONE,NOTEX),10F3,0,0,11,0
ESOURCE=TRIG,WIRE,(B5,2C,1E3,2.8E-3,AMPS,1E3
ESOURCE=SIGNAL,0,91,2,B3,1E3,GND,RECTPL(1,,5),0,0,40,0,0
EQPT=TRIG,SIGNAL,0,91,2,B3,1E3,GND,RECTPL(1,,5),55,AMPS,1E3
EFREQ=30,M461A,FIX,A9BAY,RECTPL(1,,5),89,497
EPORT=CASE=0,,MILSPC,MILSPC
ERCEPT=CASE=21,,0,,MILSPC,MILSPC
EPORT=GUN,WIRE,(B1,B3,B9,GND,NONE,NOTEX),11,0,0,0,0,0
ERCEPT=EXTND,WIRE,(B1,B3,30,1E3,RECT,NOTCLS,-7,100,355
EPORT=AVISP,M461A,FIX,B9,...90
EFREQ=30,18E9,10
EPORT=CASE=0,,MILSPC,MILSPC
ERCEPT=CASE=40,,0,,MILSPC,MILSPC
EPORT=LBAC,WIRE,(B3,B9,GND,NONE,EX),50,0,0,0,0,0
ERCEPT=INS,M461A,FIX,(B3,30,1E3,RECTPL(1,,5),56,AMPS,1E3
EFREQ=30,50E6,10
EPORT=CASE=31,,0,,MILSPC,MILSPC
ERCEPT=CASE=0,,MILSPC,MILSPC
EPORT=BNDGD,WIRE,(B2,B5,B,GND,NONE,NOTEX),500,0,0,14,0,0
ESOURCE=SIGNAL,0,30,1E3,FIX,R1BAY,NDTCLS,10,122,238
EQPT=TACAN,M461A,FIX,R1BAY,NOTCLS,10,122,238
EFREQ=30,18E9,18E92,90
FQTRL=10244098050.1024498075.1024545272.1024795372.1024909054.
```

Figure 13 Mini-System B2 Input Deck (Continued)

59

```
PORT=CASE,5,0
SOURCE=CASE,30,MILSPC,MILSPC
RCEPT=CASE,30,MILSPC,MILSPC
PORT=TACCUP,ANT(TACCUP,90,0,160,436,NOW),50,0,0,0,0
SOURCE=ANT,30,1025E6,1025E6,400,1E6,RADAR(RECTPL,83333,7E-6),(-93,-93)
PORT=TACCLO,ANT(TACCLO,90,0,222,NOW),50,0,1E6,RADAR(RECTPL,83333,7E-6),(-93,-93)
SOURCE=RF,30,1025E6,1025E6,400,
EQPT=ILS,M461A,FIX,RIBAY,NOTCLS,10,102,213
FREQ=30,5CE6,1,90
PORT=CASE,-3,0
SOURCE=CASE,0,MILSPC,MILSPC
RCEPT=CASE,0,MILSPC,MILSPC
PORT=CCPWR,WIRE(VR2,B6,CIG7M,NONE,NOTEX),15,0,0,0,0,0
RCEPT=PWR,0,2A,0,M461A
EQPT=UHFCO,M61B1D,FIX,RIBAY,NOTCLS,10,111,236
FREQ=30,1RE9,1,90
FQTBL=3206243679,3206245600,3206246000,3206649000,3206649800,3206649900,
      3206750100,3206750200,3206651000,3206654000,3206654400,
      3206753212,3206675641
PORT=CASE,30,MILSPC,MILSPC
SOURCE=CASE,30,MILSPC,MILSPC
PORT=COMUP,ANT(UHFUP,90,0,158,464,NOW),50,0,0,0,0,LPAS
SOURCE=RF,30,50F3,100,50E3,AM(VOICE,50F3,1),(-73,-73)
PORT=COMLO,ANT(UHFLO,90,0,65F6,323,0,87,284,NOW),50,0,0,0,0,LPAS
SOURCE=RF,30,65F6,320,65E6,AM(VOICE,50E3,1),(-73,-73)
EQPT=AUX,M61B1D,FIX,RIBAY,NOTCLS,10,111,244
FREQ=30,1RE9,1,90
PORT=CASE,6,0
SOURCE=CASE,30,MILSPC,MILSPC
RCEPT=CASE,30,MILSPC,MILSPC
PORT=ADF,M461A,FIX,RIBAY,NOTCLS,10,121,219
FREQ=30,18E9,1,90
SOURCE=CASE,30,MILSPC,MILSPC
RCEPT=CASE,30,MILSPC,MILSPC
EQPT=B14,M461A,FIX,B14,NOTCLS,0,0,0
FREQ=30,50F6,1,90
PORT=CASE,0,0
```

Figure 13 Mini-System B2 Input Deck (Continued)

60

GP77-0221-94

Figure 13 Mini-System B2 Input Deck (Continued)

GP77-0221-95

Figure 13 Mini-System B2 Input Deck (Continued)

```
EQPT=B17,M461A,FIX,H17,NOTCLS,0,0,0
FREQ=50E6,1,90
PORCEPT=CASE,0,MILSPC
SOURCE=CASE,0,MILSPC,MILSPC
PORT=DCPWR,WIRE,(A0,B29,C,GND,GND,EX),1,0,0,41,0,0

EQPT=...,M461A
FREQ=...,GND,EX),1,0,0,-7,0,0
...27E3,RECTPL(1,5),,16,AMPS,1E3
...2IBAY,NOTCLS,12,128,,224

SOURCE=...,MILSPC
...,MILSPC
PORT=...,NONE,NOTEX),500,0,0,0,0,0
...2E3,RECTPL(,5),,056,AMPS,1E3
...RIBAY,NOTCLS,2,128,231

...MILSPC
...MILSPC
...NONE,NOTEX),9,0,0,48,0,0
...15E3,RECTPL(1,5),2,15,AMPS,1E3
...310E3,NOTEX),15,0,0,10,0,0,0
...RECTCLS,0,2,0...,0333,AMPS,1E3

EQPT=...,MILSPC,MILSPC
...GND,NONE,NOTEX),13,0,0,0,0,0
...B7,0,1E3,RECTPL(1,5),2,15,AMPS,1E3
...FIX,LDUCT,NOTCLS,-34,91,505

EQPT=...,MILSPC,MILSPC
...B10,GND,UNRAL,GND,NOTEX),80,0,0,0,0,0
...B4,0,30,1E3,RECTPL(1,5),,0333,AMPS,1E3
EQPT=AI,M461A,FIX,CKPIT,NOTCLS,8,128,270
FREQ=30,50E6,1,90
```

Figure 13 Mini-System B2 Input Deck (Continued)

63

GP77-0221-96

```
PORT=ALTBS,WIRAL,FIX,R23BAY,NOTCLS,10,105,299
  PORT=EXC,WIRAL,GND,NOTEX),5E3,C,0,C,0,0
  PORT=EXC,M461A,.3C,.F,TPZD(10E3,50E-6,10E-6),.004,AMPS,100E3
FREQ=30,50E6,10
SOURCE=CASE,0,MILSPC,MILSPC

  PORT=VERTX,WIRAL,GND,NOTEX),300,C,0,-2,0,0
  PORT=VERTX,M461A,.3C,.F,SPECT(30,248,5,1000,112),R.25E-4,,AMPS,1E3
  PORT=VERTX,WIRAL,FIX,B3BAY,NOTCLS,14,109,351
FREQ=30,50E6,10
SOURCE=CASE,0,MILSPC,MILSPC

  PORT=BYRA,WIRAL,GND,NOTEX),10,0,C,-10,0,0
  PORT=BYRA,M461A,.3C,.F,TPZD(43,11.5E-3,1E-3),.072,AMPS,1E3
  PORT=BYRA,WIRAL,FIX,B22,NOTCLS,0,0,0
FREQ=30,50E6,10
SOURCE=CASE,0,MILSPC,MILSPC

  PORT=BYRA,M461A,.3C,.F,BAL,GND,NOTEX),125,0,C,C,0
  PORT=BYRA,M461A,.3C,.F,TPZD(43,11.5E-3,1E-3),.072,AMPS,1F3
  PORT=SR,M461A,FIX,LRDUCT,NOTCLS,-38,89,439
FREQ=30,50E6,4
SOURCE=CASE,0,MILSPC,MILSPC

  PORT=VERTX,WIRE,.3C,.F,UNBAL,GND,NOTEX),10E3,0,0,0,0
  PORT=VERTX,WIRE,.30,.F,UNBAL,SPECT(30,38,3,1000,3B,3,1000,3B,3),8.25E-4,,AMPS,1E4
  PORT=RUD,WIRE,.30,.F,UNBAL,SPECT(30,24,1,100,24,1),16E-5,,AMPS,1E3
  PORT=AILPO,WIRE,.3C,.F,SPECT(30,24,1,1000,24,1),16E-5,,AMPS,1F3
FREQ=B20A,M461A,FIX,B20A,NOTCLS,0,0,0
SOURCE=CASE,0,MILSPC,MILSPC
```

Figure 13 Mini-System B2 Input Deck (Continued)

64

```
PORT=C,CASE,MILSPC
BPTS=C,UNBAL,GND,NOTEX),10C,0,0,0,0,0,0,1E3
PORT=B2,SIGNAL,RECTRAL(40DD,5,AMPS,2,1E3
       C,A,1E3,F,UNBAL,RECTPL(G7DD,1,10E-5,AMPS,2,0
       C,A,16E0,1E3,RECTPL(400,,CO125),16E-5,AMPS,1E3
EQPT=B23,NOTCLS,0,0,0,0

PORT=C,CASE,MILSPC
BPTS=C,UNBAL,NOTEX),50,0,AMPS,0,22,0,0
PORT=B5,SIGNAL,RECTPL(1,5),56,AMPS,1E3
       C,C,1E3,F,UNBAL,RECTPL(1,5),160,0,AMPS,0,0,0
       C,A,30,1E3,BAL,RECTPL(1,5),24,67E-03,AMPS,1E3
EQPT=B23,NOTCLS,17,120,341

PORT=C,CASE,MILSPC
BPTS=C,UNBAL,GND,NOTEX),10C,0,0,0,22,0,C
PORT=B17,SIGNAL,RECTPL(1,5),4,67E-3,AMPS,1E3
       B30,1E3,RECTPL(1,5),4,67E-3,AMPS,1E3
EQPT=B17
BPTS=A,0,125,535,30,19,C,487,C,12,125,270,D,15,125,353,E,-14,103,266,
       F,A,0,G,0,SBRK,R,F,142,4,AMRAY,0,F,G,192,4,ECSBY,0,E,G,142,4,L2BAY,
       O,G,108,4,CKPIT,0,H,76,4,CKPIT,0,H,C,175,4,CKPIT,0
WIRE=B1,ST626,A,F,G,H,D
WIRE=R2,U26,A,F,G,H
WIRE=R3,U20,B,F,G
BUNDLE=B2
BPTS=A,15,132,246,B,15,113,216,C,13,102,213,D,13,102,220,E,15,129,225,
       F,16,124,332,G,0,C,G,0,C,RIBAY,0,C,G,H,10,4,RIBAY,0,4,RIBAY,C,C,H,99,4,RIBAY,0,
       H,10,47,RIBAY,0,0,RIBAY,0,4,RIBAY,0,I,J,10,4,RIBAY,0,E,J,93,4,RIBAY,0,
WIRE=B4,U26,A,G,H,I,J
WIRE=B5,U26,B,G,H,I,J
BUNDLE=B6
BPTS=A,15,128,234,B,-29,89,491,C,-5,100,341,D,-68,130,904,E,-68,130,800,
       F,A,-68,39,B,4,RIBAY,0,80,4,LCFUS,0,G,291,4,LDUCT,0,G,H,10,4,LCFUS,0,C,H,231,4,NSWEL,
       NSWEL,H,I,80,4,LCFUS,0,J,231,4,LAFUS,0,I,J,10,4,LCFUS,0,
       F,J,291,4,LAFUS,0,J,H,309,4,LAFUS,0
```

Figure 13 Mini-System B2 Input Deck (Continued)

65

```
WIRE=H7,U20,A,G,H,I,J,E
WIRE=H9,STP26,B,G,H,I,J,F
WIRE=U26,C,H,I,F
BUNDLE=B4
BPTS=A,15,128,234,R,14,105,295,C,14,105,305,D,-34,91,505,E,-29,89,241,
          H,-30,GIBAY,0,C,0,C,
          G,F,145,142,R2BAY,0,G,H,80,4,R2BAY,0,C,H,149,4,R2BAY,0,
RSEG=H1,162,ECSBY,0,F,I,140,4,RCFUS,0,I,J,80,4,LCFUS,0,E,J,46,4,LCFUS,0,
          LCFUS,
WIRE=B10,ST26,A,G,H,I,J
```

```
WIRE=B11,STP26,B,G,H,I,J,E
WIRE=U12,U2C,C,H,I,F
BUNDLE=B5
BPTS=A,-17,125,299,R,16,107,333,C,-29,89,241,D,-29,89,241,
          H,-30,BAY,0,C,
RSEG=A,G7,577,RWING,0,G,H,135,4,ECSBY,0,C,H,124,125,535,
          H,J,22,4,RWING,0,I,J,28,4,RWING,0,E,J,135,4,RWING,0,
WIRE=B13,STP25,A,G,H,I,J
WIRE=U14,U2,B,G,H,I,F
WIRE=B15,ST25,C,H
BUNDLE=B5
BPTS=A,17,120,341,R,18,109,353,C,15,132,246,D,-15,120,400,E,44,110,461,
          H,0,C,0,G,H,110,4,R3BAY,0,
RSEG=A,G,259,4,R3BAY,0,C,H,5,4,R3BAY,0,C,H,112,4,ECSBY,0,
          H,J,260,4,ECSBY,0,F,I,112,4,ECSBY,0,E,J,110,4,RCFUS,0,
WIRE=R17,STP22,A,G,H,I,J,E
WIRE=R18,STP26,B,G,H,I,J
WIRE=B19,ST22,C,H,I,F
BUNDLE=B7
BPTS=A,15,132,244,R,17,113,293,C,15,132,246,D,20,125,368,E,13,127,302,
          H,0,C,0,G,H,2,4,R1BAY,0,C,H,7,4,R1BAY,0,
BSEG=A,G7,4,R1BAY,0,G,F,155,4,CKPIT,0,I,J,6,4,CKPIT,0,E,J,48,4,CKPIT,0,
WIRE=R20,U26,A,G,H,I,J,E
WIRE=B21,ST626,B,G,H,I,F
BUNDLE=R8
```

Figure 13 Mini-System B2 Input Deck (Continued)

66

GP77-0221-100

```
RPTS=A,-15,109,275,5,-1,135,259,C,0,0,C
 BSEG=A,C,85,4,L2RAY,0,C,3,60,4,CKPIT,CNOPY
WIREF=R23,2,U26,A,B,C
WIREF=R24,2,TRIAX,A,B,C
WIREF=B26,9,UTP22,A,B,C
BUNDLE=B26,9
RPTS=A,15,125,202,8,16,125,316,C,-16,120,332,D,2,135,259,E,0,0,F,0,0,0
 BSEG=A,E,227,4,CKPIT,CNOPY,9,E,38,4,CKPIT,CNOPY,F,96,4,CKPIT,CNOPY,
 CSEG=A,E,227,4,CKPIT,CNOPY,F,0,36,4,CKPIT,CNOPY
WIREF=R27,2,U22,A,E,F,D
WIREF=R28,2,U22,B,E,F,D
WIREF=R29,2,U22,C,E,F,D
ERDATA
```

Figure 13 Mini-System B2 Input Deck (Concluded)

67

GP77-0221-101

```
TITLE=MINISYSTEM B3
EXEC=CLEAR,NEW,SURVEY
OUTPUT=ISF
SYSTEM=AIR,0,0,0,-6,-199
FUSLGE=415,46,12,457.5,117.93,FLAT
```

Figure 14 Mini-System B3 Input Deck

68

```
EQPT=PRESS,(B16,R43,0,GND,NONE,NOTEX),280,0,0,0,0,0
SOURCE=SIGNAL,0,3C,1E3,RECTPL(1,.5),.1,AMPS,1E3
PORT=B4,30,FIX,B4,NOTCLS,0,0,0
FREQ=M461A,90
SOURCE=WIRE,MILSPC
PORT=CASE,MILSPC
EQPT=B5,30,R44,R44,C,M461A
SOURCE=WIRE,R14,0,C,NOTCLS,0,0,0
PORT=CASE,28,85
FREQ=FIX,90

EQPT=...,MILSPC
SOURCE=WIRE,MILSPC
PORT=B14,B44,F,UNBAL,GND,EX),.1,0,0,0,0,0
SOURCE=WIRE,0,0,C,NOTCLS,0,0,0
PORT=CASE,86
FREQ=FIX,90

EQPT=...,MILSPC
SOURCE=CASE,MILSPC
PORT=WIRE,(B14,R43,E,UNBAL,GND,EX),1,0,0,0,0,0
FREQ=NWSW,WIRE

SOURCE=SIGNAL,0,30,1E3,RECTPL(1,.5),.01,AMPS,1E3
PORT=EPT,0,R31,B,RECTPL(1,.5),.68,.412,AMPS,1E3
PORT=WOUT,0,R3C,1E3,RECTPL(1,.5),.412,1,AMPS,1E3
SOURCE=M461A,B7,RECTPL(1,.5),.412,AMPS,1E3
FREQ=B7,30,18E9,NOTCLS,0,0,0
PORT=CASE,0,MILSPC
SOURCE=CASE,0,MILSPC
PORT=WIRE,(B10,R31,D,UNBAL,GND,EX),1,0,0,0,0,0
PORT=SOURCE,WIRE,(R1C,R32,E,RECTPL(1,.5),.68,.412,AMPS,1E3
PORT=CASE,WIRE,(B1C,R32,F,UNBAL,GND,EX),.412,1,AMPS,1E3
PORT=NWSW,SIGNAL,(B14,R43,RECTPL(1,.5),.412,.2800,0,0,0,0
EQPT=STEER,M461A,FIX,NSWEL,NOTCLS,.85,361
PORT=CASE,18E9,1,90
FREQ=30,18E9,1,0
PORT=CASE,-16,0
```

Figure 14 Mini-System B3 Input Deck (Continued)

69

Figure 14 Mini-System B3 Input Deck (Continued)

```
PORT=THERFR,WIRE,(B11,B34,0,GND,GND,NOTEX),2.5,0,0,0,0,0,0
RCEPT=EFD,0.1,4,.75,(30,2.5,0,1E6,2.5,0)

EQPT=NSARM,WIRE,(B11,B35,0,GND,NONE,NOTEX),6.5,0,0,0,0
RCEPT=CNTRL,0,30,1E3,RECTPL(1,.5),4,.31,AMPS,1E3
FREQ=30,.50E6,1,90
PORT=B11,M461A,FIX,B11,NOTCLS,0,0,0
PORT=CASE=MILSPC

RCEPT=CASE=,0,MILSPC
PORT=CLD,WIRE,(B12,0,0,GND,NOTEX),2.5,0,0,0,0,0
RCEPT=CLD,0,30,1E6,2.5,0),2.5,0,0,0,0,0,0
PORT=CLTJ,WIRE,(B12,75,30,0,NONE,NOTEX),2.5,0,0,0,0,0
RCEPT=CLTJ,0,30,1E6,2.5,0),1.0,0,.34,0,0
PORT=TANK,WIRE,(B12,0,0,NONE,NOTEX),1,AMPS,1E3
SOURCE=B12,M461A,FIX,B12,NOTCLS,0,0,0
FREQ=30,.50E6,1,90

PORT=CASE=,0,MILSPC,MILSPC
RCEPT=CASE=,0,MILSPC,MILSPC
PORT=PREG,WIRE,(B12,B33,0,GND,NONE,NOTEX),28,0,0,0,0,0
EQPT=RFOSC,CNTRL,0,30,1E3,RECTPL(1,.5),13,AMPS,1E3
FREQ=30,.50E6,1,90
PORT=CASE=,0,MILSPC,MILSPC
SOURCE=CASE=,0,MILSPC,MILSPC
PORT=DPREG,WIRE,(R15,B45,A,UNBAL,GND,NOTEX),200,0,0,23,0,0
EQPT=XMTR,SIGNAL,0,30,1E3,RECTPL(100,.005),.002,AMPS,1E3
FREQ=30,.50E6,1,90
PORT=CASE=,0,MILSPC,MILSPC
SOURCE=CASE=,0,MILSPC,MILSPC
PORT=ACPWR,WIRE,(B15,B46,B,UNBAL,NONE,NOTEX),3,2,0,0,0,0
EQPT=DIGPR,POWER,0,115,400,3,2,M461A
FREQ=30,.50E6,1,90
PORT=CASE=,0,MILSPC,MILSPC
RCEPT=CASE=,0,MILSPC,MILSPC
```

Figure 14 Mini-System B3 Input Deck (Continued)

GP77-0221-104

```
PORT=MODEX,WIRE,(E13,841,C,GND,NONE,NOTEX),100,0,0,0,0
PRCEPT=SIGNAL,0,30,1E3,RECTPL(1,,5),28,AMPS,1E3
PORT=DISPA,WIRE,(B13,B39,A,UNBAL,GND,NOTEX),68,0,25,0,0
SOURCE=SIGNAL,0,30,1E3,RECTPL(1,,5),4E-4,AMPS,1E3
EQPT=DATAP,M461A,FIX,LIBAY,NOTCLS,-10,113,234
 FREQ=30,50E6,1,90
 SOURCE=CASE,27,-3
 PRCEPT=CASE,0,,MILSPC
PORT=RDRRE,WIRE,(B18,B40,A,UNBAL,GND,NOTEX),130,0,0,23,0,0
PRCEPT=SIGNAL,0,30,1E3,RECTPL(1,,5),1.79E-3,AMPS,1E3
SOURCE=SIGNAL,0,30,1E3,RECTPL(1,GND,EX)1,1,0,0,23,0,0
EQPT=ANT,M461A,FIX,NOTCLS,0,113,198
 FREQ=30,50E6,1,90
 SOURCE=CASE,27,-3
 PRCEPT=CASE,0,,MILSPC
PORT=POTEX,SIGNAL,(B15,B47,F,UNBAL,GND,NOTEX),500,0,0,0,0
SOURCE=SIGNAL,0,30,1E3,RECTPL(1,,5),.02,AMPS,1E3
EQPT=POT,M451A,FIX,NOTCLS,0,0,0
 FREQ=30,50E6,1,90
 SOURCE=CASE,0,,MILSPC,MILSPC
 PRCEPT=CASE,0,,MILSPC,MILSPC
PORT=RDPWR,WIRE,(B15,B46,E,UNBAL,NONE,NOTEX),,3,0,0,36,0,0
SOURCE=POWER,0,115,400,3,M461A
PRCEPT=PRESS,WIRE,(B16,B44,A,GND,NONE,NOTEX),280,0,0,0,0
EQPT=UHFCO,M461B1D,FIX,RIBAY,NOTCLS,10,111,235
 FREQ=30,1E9,1,90
 SOURCE=SIGNAL,0,30,1E3,RECTPL(1,,5),1,AMPS,1E3
 FQTBL=30,320645600,320645900,320646000,320649000,320649800,320649900,
       320650200,320650100,320651000,320654000,320654400,
       320675321,320675541
 PORT=CASE,6,0,,MILSPC,MILSPC
 SOURCE=CASE,30,,MILSPC,MILSPC
PRCEPT=COMUP,ANT,30,0,158,464,NOW1,50,0,0,0,LPAS
SOURCE=RF,30,.65E6,320,0,65E6,100,.50E3,AM(VOICE,50E3,1),(-73,-73)
PORT=COMLD,ANT,30,0,287,284,NOW1,50,0,0,0,LPAS
SOURCE=RF,30,.65E6,320,.65E6,100,.50E3,AM(VOICE,50E3,1),(-73,-73)
```

Figure 14 Mini-System B3 Input Deck (Continued)

72

```
EQPT=ADX,M461AD,FIX,RIPAY,NOTCLS,1C,111,244
FREQ=30,CASE=1,90
PORT=CASE=646,CASE=30,MILSPC,MILSPC
SOURCE=ADF,CASE=30,FIX,RIBAY,NOTCLS,10,121,219
FREQ=30,CASE=1,90

EQPT=CCASE=30,MILSPC
SOURCE=CCASE=30,FIX,RIPAY,NOTCLS,10,102,218
FREQ=30,CASE=1,90
EQPT=IFFX,M461A,FIX,RIPAY,NOTCLS,10,102,218
FREQ=30,1REQ=1,90
FQTBL=1085997826,1085998910,1087135211,1088726760,1089363380,
       10906365619,109127324C,10928647989,1094001090,1094002180

PORT=CASE=29C,MILSPC,MILSPC
SOURCE=CCASE=30,MTLUP(IFFUP,50,0,0,0,HPAS
PORT=IFFUP=ANT,(IFFLC,100,0,0,RL,125E3,.5E-6),(-90,-90)
SOURCE=ANT,(IFFLC,100,0,0,C,0,HPAS
PORT=IFFLC=ANT,(IFFLC,100,0,0,RL,125E3,.5E-6),(-90,-90)
SOURCE=ANT,(IFFLC,100,0,0,C,0,HPAS
EQPT=TACAN,M461A,FIX,RIBAY,NOTCLS,10,122,234
FQTBL=18EQ=1,90
FQTBL=1024497952,1024454272,1024795372,1024909054,
       102454452C,10545473,1025090946,1025204628,1025454728,
       10255C100
       10255020C

PORT=CASE=52C,MILSPC,MILSPC
SOURCE=CASE=30,MILSPC
PORT=TACUP=ANT,(TACL3,90,0,0,0,0,436,NOW),50,0,0,0,0
SOURCE=RF,CASE=30,(TACL3,100,0,0,1F6,RADAR(RECTPL,100,14E-6),(-93,-93)
PORT=TACL3=ANT,(TACL3,100,0,0,87,222,NOW),50,0,0,0,0
SOURCE=RF,CASE=30,FIX,(TACL3,100,0,1E6,RADAR(RECTPL,100,14E-6),(-93,-93)
EQPT=ILS,M461A,FIX,RIBAY,NOTCLS,10,102,213
FREQ=30,CASE=1,90

PORT=CASE=30,MILSPC,MILSPC
SOURCE=CASE=30,FIX,CKPIT,NOTCLS,-15,125,302
FREQ=30,50FF6,113,90
EQPT=ICCCP,M461A,FIX,CKPIT,NOTCLS,-15,125,302
PORT=CASE=0,MILSPC,MILSPC
SOURCE=CASE=0,MILSPC,MILSPC
PORT=GCMIK,WIRE,(B16,R50,C,UNBAL,GND,NOTEX),5,C,0,0,0,0
```

Figure 14 Mini-System B3 Input Deck (Continued)

73

```
RCEPT=SIGNAL,0,30,6J00,VLICE,2E-4,A1PS,6E3
EQPT=B15,M461A,FIX,B15,N0TCLS,0,0,0.0
FREQ=30,50E6,1,90
PORT=CASE,0,MILSPC,MILSPC
RCEPT=CASE,0,MILSPC,MILSPC

PORT=MIKE,(B16,R50,F,UNBAL,GND,NOTEX),5,0,0,0,0,0
VSDSP=SIGNAL,M461A,FIX,30,6J00,VCICE,2E-4,AMPS,6E3
EQPT=M461A,FIX,L23BAY,N0TCLS,-9,109,283
FREQ=30,10
SOURCE=CASE,0,MILSPC,MILSPC
RCEPT=CASE,0,MILSPC,MILSPC

PORT=DISPLAY,(B13,R39,D,UNBAL,GND,NOTEX),10E3,0,0,0,0,C
SIGNAL,M461A,FIX,30,1E3,RECTPL(1,.5),4E-4,AMPS,1E3
EQPT=M461A,FIX,B13,N0TCLS,0,0,0.0
FREQ=30,50E6,1,90
SOURCE=CASE,0,MILSPC,MILSPC
RCEPT=CASE,0,MILSPC

PORT=THROT,(B18,R40,B,GND,NONE,NOTEX),1,0,0,9,0,0
CUR=70X,M461A,FIX,30,1E3,RECTPL(1,.5),1.4,AMPS,1E3
EQPT=M461A,FIX,B19,N0TCLS,0,0,0.0
FREQ=30,50E6,1,90
SOURCE=CASE,0,MILSPC,MILSPC
PORT=CASE,0,MILSPC

PORT=ENGINE,CNTROL,(B16,R40,E,GND,NONE,NOTEX),20,0,0,0,0,0
WIRE,M461A,FIX,30,1E3,RECTPL(1,.5),1.4,AMPS,1E3
EQPT=M461A,FIX,RIBAY,N0TCLS,9,128,231
FREQ=30,50E6,1,90
SOURCE=CASE,0,MILSPC,MILSPC

PORT=ROLL,PITCH,(B17,R53,C,UNBAL,NONE,EX),50E3,0,0,0,0,FTHRU
WIRE,M461A,FIX,30,25E6,400E6,-21,4,100E3,CW,0
EQPT=M461A,FIX,RIBAY,N0TCLS,9,132,239
FREQ=30,50E6,1,90
FQTBL=363,35E6
SOURCE=CASE,0,MILSPC,MILSPC
```

Figure 14 Mini-System B3 Input Deck (Continued)

74

```
PORT=CASE,0,MILSPC
PORT=PASIG,(B17,B51),B,UNBAL,NONE,EX),50E3,C,C,C,0,FTHRU
PORT=PASIG,(B25),6,R,B52,4,NONE,CW),10,0,0,-1,0,0,
PORT=PAE,0,MILSPC,4,NONE,EX),10,0,0,-1,0,0,
PORT=PAE,(B17,B52),R,RECTPL(400,,CO125),,OC9,AMPS,2E3
EQPT=SOURCE,SIGNAL,0,30,RECTCLS,125,289
FREQ=X,CKPIT,FIX,
PORT=STIC,X18,90
PORT=SOURCE,0,MILSPC
PORT=QE,I,C,1,C,0
PORT=QE,I,AMPS,1E3
PORT=CE,(EX),1,AMPS,1E3
PORT=RE,CUTPL,(EX),10,2,4,-1,AMPS,0,0,
PORT=PAE,I,(EX),100,0,0,C,0,FTHRU
PORT=PAE,(B25),R,RECTPL(125),1,2E-4,C,0,AMPS,2E3
PORT=SOURCE,0,MILSPC
PORT=QE,I,C,2,C,C
PORT=QE,(EX),100,C,-2,C,C
PORT=CE,(EX),1,2E-4,AMPS,2E3
PORT=PAE,R,RECTPL(400,,CO122,,CO122,229
EQPT=CASE,0,MILSPC
PORT=SOURCE,SIGNAL,0,30,RECTPL(1,,5),,2R,AMPS,1E3

BUNDLE=B10
BPTS=A,-31,90,538,B,-41,90,568,C,20,137,338,D,-16,100,304,E,-11,100,626,
BSEG=A,F,217,4,LMLG,B,F,88,4,LMLG,LMLG,F,G,90,4,LCFUS,O,E,G,88,4,LMLG,
LMLG,G,H,240,4,LCFUS,O,D,H,44,4,L2BAY,O,H,C,175,4,CKPIT,O

WIRE=B30,UTP20,A,F,G,H,C
WIRE=B31,ST620,B,F,G,H,D
WIRE=B32,ST620,B,F,G,E
PBUNDL=B11
BPTS=A,-14,103,266,B,-14,103,268,C,-14,103,270,D,-115,120,648,E,0,0,0
BSEG=A,E,37,4,L2BAY,O,B,E,7,4,L2BAY,O,C,C,E,3,4,L2BAY,O,E,D,550,4,LWING,O
WIRE=B33,S20,A,F,E,D
WIRE=B34,S16,C,E,D
WIRE=B35,U16,C,E,D
BUNDLE=B12
BPTS=A,-14,103,266,B,-14,103,268,C,-50,120,275,D,0,90,675,E,0,90,604,
```

Figure 14 Mini-System B3 Input Deck (Continued)

75

```
         F,G,0,0,G,0,0,L2BAY,0,0,0
BSEG=A,F,230,4,LCFUS,0,B,F,100,4,L2BAY,0,F,G,240,4,ECSBY,0,C,G,86,4,LCFUS,0,
         G,H,120,4,FLGAP,0,E,T,86,4,RCFUS,0,H,D,100,4,RCFUS,0,
WIRE=B36,S16,4,G,H,E
WIRE=B37,S16,4,F,G,H
WIRE=B38,U22,4,C,G,H
BUNDLE=B13,C,G,H,E
RPTS=A,-15,132,241,C,-15,132,236,D,-15,109,273,E,-14,103,262,
         J,-16,113,241,C,-16,113,241,C,-10,0,0,C
BSEG=A,G,122,4,L2BAY,0,C,G,180,4,L1BAY,0,C,H,64,4,L1BAY,0,
         H,I,246,4,L2BAY,0,F,I,65,4,R1BAY,0,E,J,89,4,L2BAY,0,C,
WIRE=B39,STP26,4,H,I,J,D
WIRE=B40,STP26,4,B,C,H,I,J,E
WIRE=B41,U26,4,C,H,I,J
BUNDLE=B14,C,H,I,J
RPTS=A,-85,361,D,0,125,288,E,-16,120,304,F,10,120,371,
BSEG=A,H,88,4,NSWEL,NSWEL,G,H,45,4,ECSBY,0,I,2,45,4,L2BAY,0,
         C,H,76,4,NSWEL,0,F,I,90,4,ECSBY,0,F,I,2,4,R3BAY,0,
WIRE=B42,U26,4,L2BAY,0,C,J,65,4,CKPIT,0,
WIRE=B43,STP42,4,G,H,I,F
WIRE=B44,ST616,4,C,H,I,F
BUNDLE=B15,C,H,I,F
RPTS=A,-12,103,248,B,-17,124,229,C,-16,113,250,D,-14,103,262,E,-18,120,334,
BSEG=A,G,58,4,L1BAY,0,R,G,0,0,C,0,0,C,H,36,4,L1BAY,0,
         H,I,59,4,L2BAY,0,F,I,56,4,L1BAY,0,H,30,4,L1BAY,0,E,J,56,4,L3BAY,0,
WIRE=B45,STP26,4,A,G,H,I,D
WIRE=B46,STT12,4,B,C,H,I,E
WIRE=B47,U26,4,C,H,I
BUNDLE=B16,C,H,I
RPTS=A,-20,125,305,B,-13,125,290,C,-15,125,302,D,-26,130,574,E,-50,110,525,
BSEG=A,G,135,4,CKPIT,0,0,0,G,3,63,4,CKPIT,0,C,H,79,4,CKPIT,0,C,H,143,4,CKPIT,0,
         H,I,170,4,ECSBY,0,F,I,143,4,LCFUS,0,I,J,80,4,LCFUS,0,E,J,64,4,LCFUS,0,
WIRE=B48,U26,4,G,H,I,J,D
WIRE=B49,U22,4,B,G,H,I,J,E
WIRE=B50,STP22,4,C,H,I,J
BUNDLE=B17,C,H,I,F
RPTS=A,0,125,288,B,15,132,241,C,15,128,229,D,0,0,0
```

Figure 14 Mini-System B3 Input Deck (Continued)

76

```
$BSEG=A,0,26,4,CKPIT,C,D,19,4,R1BAY,0,0,B,175,4,R1BAY,0
WIRE=R51,UTP26,A,0,B
WIRE=R52,U26,A,0,B
WIRE=B53,UTP26,A,0,C
ENDATA
```

Figure 14 Mini-System B3 Input Deck (Concluded)

All of these code corrections are summarized in Table 2, indicating each line of code that was changed, and the reason for each change. These changes, implemented by McDonnell Aircraft at the St. Louis computer facility, were approved by RADC.

In addition to these code corrections, approximately 25 lines of code were affected to implement code corrections proposed by RADC. Many of these corrections were the result of RADC cooperation and assistance in tracking down various bugs uncovered during mini-system runs, affecting the results for antenna-to-antenna, antenna-to-wire and wire-to-wire coupling. The sensitivity study was particularly helpful in exercising the wire coupling routine with a large number of different configurations, and was instrumental in cleaning up this large, complex portion of the IEMCAP program.

Table 2. Summary of IEMCAP Code Corrections

Code Change	Reason for Change
1. Remove extra "END" card in subroutine REPORT in IDIPR	The extra END card prevented successful compilation of IDIPR
2. Change the following statement in subroutine CTLVAR in TART: DATA ISHA/1,2,0,0,0,0, 2,2,0,0,0,0, 0,0,1,3,2,4 A 0,0,3,3,4,4, 0,0,2,4,2,4, 0,0,4,4,4,4/ to DATA ISHA/1,2,0,0,0,0, 2,2,0,0,0,0, 0,0,1,3,2,4, A 0,0,3,3,4,4, 0,0,2,4,2,4, 0,0,4,4,4,4/	The missing comma presented successful compilation of TART
3. Move the following statement in subroutine CEAR in TART: EQUIVALENCE (IDCDE(1), SBIDE(1)), (RSIGM(1),ADJS(1,1)), 1 (IDCDR(1),SBIDR(1)), (ICHGEQ(1), ICHG(1,1)) 2, (RSIGEF(1),TRNSFE(1)) so that it immediately proceeds this statement DATA ANYL/4HBASE, 4HLINE, 4H SYS, 4H TEM, 4HANAL, 4HYSIS,	The compiler would not accept data statements that preceded equivalence statements
4. Move the following statement in subroutine WFREAD in TART: DATA IENDR, IENDS, ISMOV, IRMOV, IGRP, IDSSPV/ 0,0,0,0,0,0/ so that it immediately follows the following statement: EQUIVALENCE (IPPRM2 (1, 10), ITYPE(1))	

5. Change the following statement two lines below statement 100 in subroutine TEMPNT in CEAR:
 	
IF (RSGN·NE·O) RSGDB = 8.686 * ALOG(RSGN)
          to
IF (RSGN·NE·O) RSGDB = 4.343 * ALOG(RSGN)
	The program was erroneously squaring a quantity that had already been squared

GP77-0342-30

78

3.   IEMCAP ASSESSMENT WITH MINI-SYSTEMS

The results of IEMCAP runs on the F-15 mini-systems form the basis of an
overall assessment of the program, using the code (Version 03) supplied by RADC.
These results were compared with the known electromagnetic compatibility of
the F-15 aircraft and four former cases of EMI that have been corrected by
filtering or shielding. Each of the four interference situations was simu-
lated in its original configuration in an IEMCAP run, and compared with an
IEMCAP run in which the "fix", filtering or shielding, was also simulated.
The IEMCAP results were further evaluated by comparison with measured antenna
coupling data.

The IEMCAP calculates interference from one equipment case to another,
from one antenna terminal to another, from one wire terminal to another, and
from an antenna terminal to a wire terminal. It is therefore convenient to
look at the results for each type of interference separately, before making
an overall assessment of the program. Accordingly, the antenna-to-antenna,
wire-to-wire, antenna-to-wire, and case-to-case results are presented in
Sections 3.1 through 3.4, respectively. An assessment of the SGR option is
given in Section 3.5, and the overall assessment is given in Section 3.6.

3.1   Antenna-to-Antenna Assessment. The IEMCAP was used to predict
interference margins in a mini-system comprised of the upper and lower UHF,
IFF, and TACAN, plus the ADF, UHF AUX, glideslope, localizer, and marker bea-
con. All 11 of these antenna ports are receptor ports, but only the upper
and lower UHF, IFF, and TACAN are also emitter ports. Neglecting those
combinations involving ports of the same equipment or the same antenna loca-
tion, which IEMCAP does not consider, there are a total of 49 emitter-
receptor combinations to be analyzed.

A summary of the predicted EMI margins for these 49 emitter-receptor
combinations is given in Table 3. A study of the table will show that pair-
wise compatibility (negative integrated EMI margin) is predicted for 33
combinations and pair-wise incompatibility (positive integrated EMI margin)
is predicted for the remaining 16 combinations. Since the F-15 system being
modeled did not exhibit any actual interference, the cases for which IEMCAP
predicted positive margins were examined to determine the cause of the
discrepancies.

In most of the cases of predicted interference, the predominant
interference mode was required emission to unrequired reception, although
there were a few cases where the predominant mode was unrequired emission to
required reception. In each case, however, the dominant interference mode
well over-shadowed the other mode and the integrated margin was within 1 dB
of the dominant point margin. The point margin was thus a very useful quan-
tity, and allowed the IEMCAP results to be evaluated in a fairly straight
forward way. Positive integrated margin values were directly relatable
to the appropriate point margins, and were clearly due to inaccuracies in
modeling non-required spectra and/or the coupling models, rather than in
integration.

The required emission of the UHF, IFF and TACAN ports, as computed by
IEMCAP, was consistent with simple hand calculations. The total received
signal at any port due to required UHF, IFF or TACAN emission was found to be

Table 3. Antenna to Antenna Validation Results

Receiver	Transmitter					
	UHF Upper	UHF Lower	IFF Upper	IFF Lower	TACAN Upper	TACAN Lower
UHF Upper	Same Equipment	Same Equipment	Co-Located Antennas	−34.0 −35.4 U→R	36.2 35.6 U→R	−33.5 −34.7 U→R
UHF Lower	Same Equipment	Same Equipment	−34.0 −35.4 U→R	Co-Located Antennas	−4.6 −6.1 U→R	−0.6 −1.2 U→R
Aux	16.6 15.3 R→U	50.1 48.8 R→U	−35.7 −37.0 U→R	−2.2 −2.3 U→R	−5.9 −7.3 U→R	Co-Located Antennas
ADF	2.1 0.1 R→U	−27.0 −28.8 R→U	−10.5 − 9.5 R→U	−57.0 −58.8 R→U	1.2 1.1 U→R	−90.2 −91.0 U→R
IFF Upper	Co-Located Antennas	−55.0 −56.4 R→U	Same Equipment	Same Equipment	22.6 21.5 U→R	−30.9 −31.8 U→R
IFF Lower	−55.0 −56.4 R→U	Co-Located Antennas	Same Equipment	Same Equipment	−33.8 −34.8 U→R	15.7 14.7 U→R
TACAN Upper	15.9 14.6 R→U	−25.8 −27.1 R→U	41.2 41.4 U→R	−14.2 −14.2 U→R	Same Equipment	Same Equipment
TACAN Lower	−54.2 −55.7 R→U	−19.7 −22.2 R→U	−11.3 −11.4 U→R	34.3 34.2 U→R	Same Equipment	Same Equipment
Localizer	−14.5 −17.8 R→U	6.4 4.7 R→U	−38.4 −40.9 R→U	−5.9 −5.0 R→U	−9.4 −9.6 U→R	3.6 2.3 R→U
Glidescope	−16.5 −17.8 R→U	6.0 4.7 R→U	−41.8 −40.9 R→U	−5.9 −5.0 R→U	−27.1 −27.4 U→R	3.3 2.3 R→U
Marker Beacon	−15.0 −16.2 R→U	25.5 24.3 R→U	−42.5 −41.5 R→U	13.6 14.6 R→U	−36.9 −39.3 U→R	−4.3 −5.2 R→U

Legend:

GP77-0276-1

Upper Number = Integrated EMI Margin
Lower Number = Highest Point Margin
R = Required
U = Unrequired

80

consistent with the actual average transmitter power times the calculated value of coupling to that port. Each EMI point margin overprediction involving required emission must therefore be due to overpredicted coupling or an underpredicted susceptibility threshold level.

For the six cases of positive margins where the predominant interference (primary interference mode) involves unrequired emission to required suscep- tibility, four of them were correct predictions of situations where receiver blanking is provided in the system. One case involved an unrequired emission from the TACAN to the upper UHF antenna, only 2 feet away. The required susceptibility of the UHF was, like all of the antenna-connected ports, appro- ximated by its sensitivity, and is probably not too greatly in error. The positive margin for this case, therefore, is probably caused by an over- predicted unrequired emission level and/or an over-predicted coupling factor involving a near field condition. The remaining case, a positive margin at the ADF due to unrequired TACAN emission, is probably also caused by a combination of inaccuracies in the simulation of unrequired emission and in coupling.

For all cases of predicted interference, then, the problem is either with the coupling models or with the unrequired spectrum levels for emission and susceptibility. These unrequired spectrum levels were obtained from the MIL- STD-461A and MIL-I-6181D specification limits to which the equipments were designed. Unfortunately, these numbers represent only the maximum emission levels and the minimum susceptibility levels for the equipments; the equipments may have emissions well below the spec limits and susceptibility levels well above the spec limits. Discrepancies in the IEMCAP-computed unrequired spectra are not due to any error in the IEMCAP code but to the lack of more detailed knowledge of the actual spurious levels.

In order to further evaluate the antenna-to-antenna results to determine whether the problems reside mainly in the data or in the coupling models, available measured antenna coupling data, taken in the operating range of transmitting antenna, was compared with the IEMCAP-computed transfer function. The results, as tabulated in Table 4, are mixed. The predicted transfer func- tion between antennas on the same side of the fuselage is in reasonably good agreement with measured data, with 75% of the predicted numbers within 10 dB and 83% within 15 dB of the measured data. The only serious discrepancy between predicted and measured antenna coupling involving antennas on the same side of the fuselage is the -25.7 dB predicted versus the -70 dB measured coupling between the lower UHF and the ILS marker beacon antenna. This particular case, however, is most likely due to inaccurate modeling of the antenna response, either a null in one of the patterns or the out of band frequency rejection of the marker beacon antenna.

This can be seen by looking at the coupling between the lower IFF and the marker beacon, where the predicted coupling of -36.4 dB compares very favor- ably with the measured value of -40 dB, only off by 3.6 dB. The lower IFF however is physically co-located with the lower UHF antenna, a dual UHF/L-band blade. Since the measured coupling between the lower IFF and the marker beacon is -40 dB and agrees with the IEMCAP prediction, everything else being equal, one would expect that there would be more coupling at the lower frequency of the UHF antenna according to the Friis transmission law, and that the coupling

81

Table 4. Comparison of Predicted vs Measured Antenna Coupling (dB)

Receiver	Transmitter					
	UHF Upper	UHF Lower	IFF Upper	IFF Lower	TACAN Upper	TACAN Lower
UHF Upper					−95.4 −90 (-5.4)	−148.8 −115 (−33.8)
UHF Lower						−102.3 −96 (−6.3)
AUX		−22.2 −30 (+7.8)		−101.2 −105 (+3.8)		
ADF	−49.9 −40 (−9.9)	−78.8 −50 (−28.8)	−60.5 −70 (+9.5)	−109.7 −70 (−39.7)	−58.9 −75 (+16.1)	−139.8 −70 (−69.8)
Localizer		−45.3 −60 (+14.7)		−56.0 −65 (+9)		−38.2 −45 (+6.8)
Glide Slope		−45.3 −50 (+4.7)		−56.0 −65 (+9)		−38.2 −50 (+11.8)
Marker Beacon		−25.7 −70 (+44.3)		−36.4 −40 (+3.6)		−45.7 −50 (+4.3)

Legend:
    Upper Number ≈ Predicted Antennas Coupling
    Lower Number ≈ Measured Antenna Coupling
    Number in Parenthesis ≈ Difference

GP77-0276-3

82

would be close to the -25.7 dB predicted by IEMCAP instead of -70 dB. Clearly this interaction is an isolated case not amenable to prediction, and on the whole the predicted coupling compares favorably with measurements between antennas on the same side of the fuselage.

On the other hand, the predicted coupling between antennas on opposite sides of the fuselage, where the program uses a cylindrical fuselage shading model, does not compare very favorably with the measured data. The most accuracy prediction, between the lower UHF and the ADF, under predicts coupling by 29 dB and the least accurate, between the lower TACAN and the ADFADF, under predicts by 70 dB. These discrepancies are probably the result of trying to simulate a real airplane geometry with an idealized cylindrical shading model. The aircraft engine ducts present a large cross section, simulated as a cylinder, but probably allow more energy to pass than a solid cylinder. A histogram showing the overall distribution of the error between predicted and measured antenna coupling is given in Figure 15.

Since the predicted antenna-to-antenna interference involves, in all but one instance, coupling between antennas on the same side of the fuselage where the computed coupling factor is in fairly good agreement with measured data, it can generally be said that the difference between MIL-SPEC and actual spurious spectrum levels is the reason for the prediction of positive margins in the IEMCAP simulation. A summary of all cases of predicted interference is given in Table 5, showing the integrated margin, the point margin at the transmitter frequency (required to unrequired interference) and the point margin at the receiver frequency (unrequired to required interference). The table is organized by emitter, followed by receptors interfered with by the particular emitter.

The point margin for the primary mode of interference, usually the required to unrequired mode, is indicated with a single asterisk. In most cases, the margin for the secondary mode of interference is negative, but in a few cases, indicated with a double asterisk, the margin for the secondary mode is positive. In the latter situations, the positive secondary mode does not usually contribute significantly to the integrated margin, since the primary point margin is much greater, but the positive secondary margin is still a prediction of interference which must be accounted for.

Looking in Table 5 at the interference prediction from the lower UHF to the AUX, a required to unrequired point margin of 48.8 dB is indicated. The antenna coupling factor at the frequency of interest is only overpredicted by 7.8 dB, however, as indicated in Table 4. If the measured antenna coupling factor were substituted for the IEMCAP-predicted antenna coupling factor, the predicted point margin would be 48.8 dB minus 8.8 dB or 40 dB.

The only explanation for such a large positive margin given an accurate received interfering signal level, is a discrepancy between the MIL-SPEC susceptibility level and the actual susceptibility level of at least 40 dB. Upon consultation with the system engineers familiar with the situation, it was determined that there is a built-in audio suppression of the AUX receiver whenever the UHF transmitter is keyed, and that there actually was interference before this had been done. This also accounts for the positive margin at the AUX due to the upper UHF transmitter. The ADF has a similar suppression circuit, accounting for the positive margin at the ADF due to the upper UHF transmitter.

83

GP77-0276-4

Difference Between Predicted and Measured Coupling (dB)
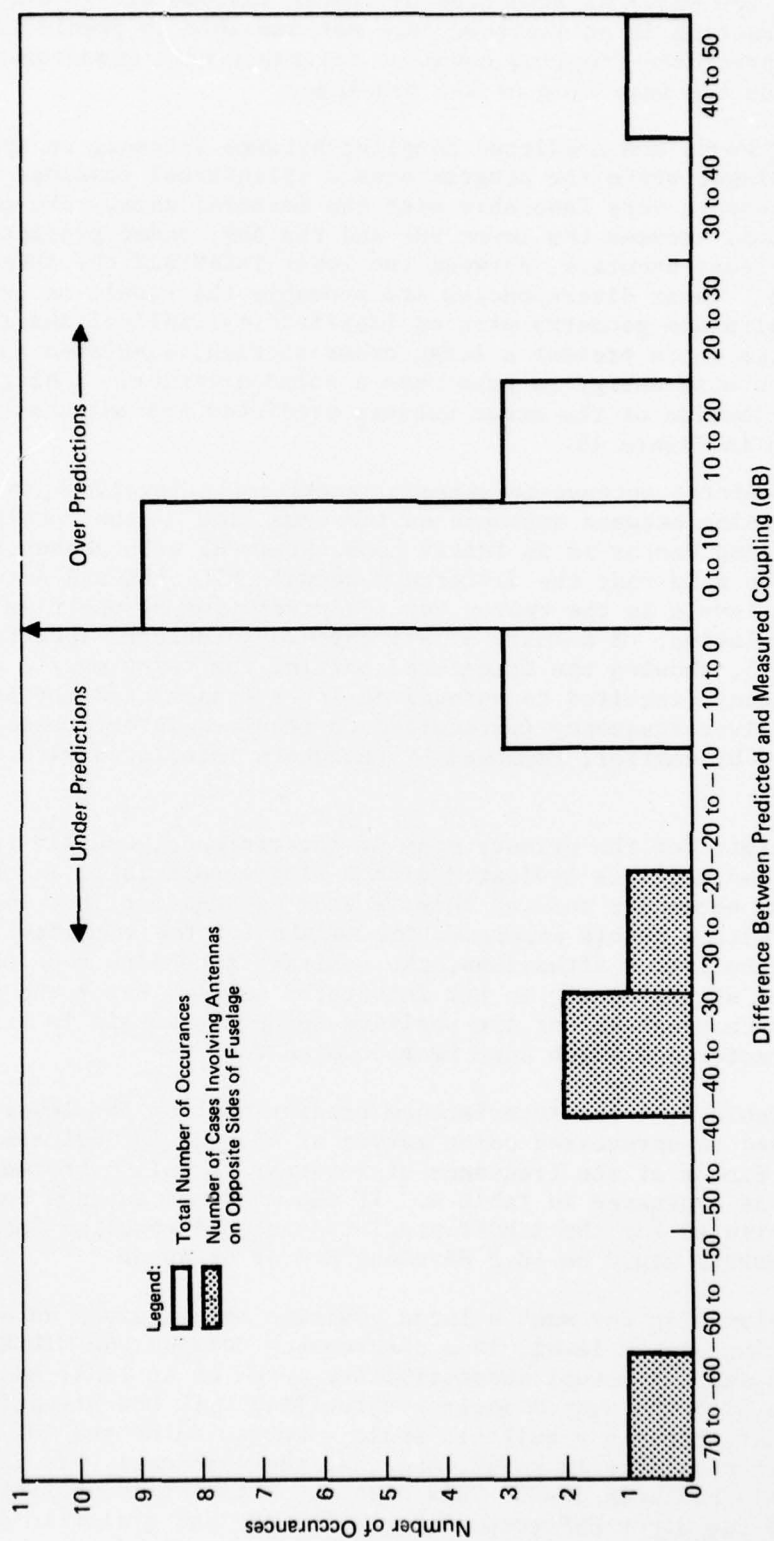
Figure 15. Distribution of Antenna Coupling Differences Between IEMCAP
Predictions and Measured Data

84

Table 5. Summary of Antenna-to-Antenna Interference Predictions

Interfering Transmitter	Victim Receiver	Integrated EMI Margin	Max Point Margin at Xmtr Freq (R→U)	Max Point Margin at Rcvr Freq (U→R)	Comments
Upper UHF	AUX	16.6	15.3*	−13.2	Audio Suppression[1]
	ADF	2.1	0.1*	−6.2	Audio Suppression
	Upper TACAN	15.9	14.6*	−22.5	Simulated Susceptibility Threshold Is Too Low
Lower UHF	AUX	50.1	48.8*	21.5**	Audio Suppression
	Localizer	6.4	4.7*	−4.5	15 dB Coupling Over Prediction
	Glidescope	6.0	4.7*	−19.6	5 dB Coupling Over Prediction
	Marker Beacon	25.5	24.3*	−15.3	44 dB Coupling Over Prediction
Upper IFF	Upper TACAN	41.2	25.0**	41.1*	Blanking
Lower IFF	*Lower TACAN*	34.3	18.1**	34.2*	Blanking
	Marker Beacon	13.6	14.6*	−40.1	Simulated Susceptibility Threshold Is Too Low
Upper TACAN	Upper UHF	36.2	−79.0	35.6*	Simulated Emission Is Too High
	ADF	1.2	−18.4	1.1*	16.1 dB Coupling Over Prediction
	Upper IFF	22.6	15.0**	21.5*	Blanking
Lower TACAN	Lower IFF	15.7	8.2**	14.7*	Blanking
	Localizer	3.6	2.3*	−8.8	6.8 dB Coupling Over Prediction
	Glidescope	3.3	2.3*	−18.4	11.8 dB Coupling Over Prediction

*Primary Interference Mode
**Secondary Interference Mode (if Present)
[1]Cases involving system - provided audio suppression or blanking are considered to be successful predictions of interference.

GP77-0276-2

85

Going down the list in Table 5 and looking at each case of IEMCAP-predicted interference, the upper UHF causes a 14.6 dB margin in the unrequired range of the upper TACAN. Measured antenna coupling data between these antennas only exists at L-band, where the difference between measured and predicted is about 5 dB. It is believed that the positive margin is due to a combination of inaccuracies in the modeling of unrequired TACAN susceptibility and antenna coupling.

According to IEMCAP, the lower UHF causes interference to the ILS localizer, glideslope and marker beacon. The computed antenna coupling to the localizer over predicts the measured value by 15 dB, more than enough to account for the 4.7 dB margin. The computed coupling to the glideslope over predicts by 4.7 dB, just enough to account for the positive margin of 4.7 dB. Finally, the computed coupling to the marker beacon over predicts by 44 dB, more than accounting for the 25.5 dB margin. As discussed previously, the over prediction is a special case for which IEMCAP cannot be faulted.

The upper IFF is correctly predicted to interfere with the upper TACAN, and receiver blanking is provided in this case.

The lower IFF is correctly predicted to interfere with the lower TACAN, a situation again accounted for by receiver blanking. The lower IFF is also predicted to interfere with the marker beacon, with a margin of 14.6 dB. The predicted coupling for this case is only 3.6 dB greater than the measured value, so that actual susceptibility threshold of the marker beacon at L-band must be 11 dB higher than the MIL-STD-461A limit.

The upper TACAN is predicted to interfere with the upper UHF antenna with a margin of 35.6 dB through unrequired emission to required susceptibility. Measured antenna coupling between these antennas is only available at L-band, as indicated in the above discussion of interference from the UHF to the TACAN, where the deviation of predicted versus measured is only 5 dB. It is believed that the positive margin is due to a combination of inaccuracies in the modeling of unrequired TACAN emission and antenna coupling.

The upper TACAN is also predicted to interfere with the ADF with a margin of 1.1 dB, unrequired to required. This discrepancy could be caused by a small error in any of the many approximations used by the program.

The upper TACAN, finally, is also predicted to interfere with the upper IFF, compatibility being achieved by receiver blanking.

The lower TACAN is predicted to interfere with the lower IFF, again accounted for by receiver blanking. The lower TACAN is also predicted to interfere with the ILS localizer and glideslope, required to unrequired, by 2.3 dB in both cases. The coupling overpredictions of 6.8 dB between the TACAN and the localizer and 11.8 dB between the TACAN and the glideslope are more than enough to account for the 2.3 dB positive margins. Inaccuracies in the modeling of unrequired ILS susceptibility are probably also a factor.

86

3.1.1 Summary of antenna-to-antenna assessment. The various instances
of antenna-coupled interference predicted by IEMCAP can be explained by
receiver blanking or suppression, by simulated emissions that are too high,
by simulated susceptibility levels that are too low, or by over predicted
antenna coupling. Except for the isolated case of coupling from the lower
UHF to the marker beacon, where the measured coupling is much less than would
be expected, the amount of EMI margin over prediction due to coupling over
prediction appears to be relatively small.

The predicted coupling between antennas on opposite sides of the fuselage
is much less than the measured coupling, and is probably due to the limita-
tions of the idealized cylindrical diffraction model.

Figure 16 shows the distribution of integrated EMI margins for antenna-
to-antenna coupling, the smallest margins taking on values between -100 dB and
-90 dB and the largest margins taking on values between 50 dB and 60 dB. As
previously stated, there are a total of 33 negative margins (between -80 dB
and 0 dB) and a total of 16 positive margins (between 0 dB and 60 dB). Also
indicated in Figure 16 are the number of positive margins where interference
is correctly predicted, accounted for by blanking or receiver suppression. Both
of the 2 positive margins greater than 40 dB are seen to be correctly predicted.
Of the 2 positive margins between 30 and 40 dB, one is correctly predicted as
interference and the other is an incorrect interference prediction, probably
the result of inaccuracy in simulating unrequired TACAN emission. Of the 2
positive margins between 20 and 30 dB one is correctly predicted as interference,
and the other is an incorrect interference prediction, probably the result of
the unpredictable marker beacon antenna frequency rejection at UHF frequencies,
discussed previously.

Between 10 and 20 dB, 2 out of 4 positive margins are correct predictions
of interference and between 0 and 10 dB, 1 out of 6 positive margins is
correctly predicted as interference.

Thus it is seen that all positive margins greater than 40 dB correspond
to correct interference predictions, and two of the margins between 20 and 40 dB
are correct interference predictions, the other two due to over-pessimistic
simulation of emission spectra or unpredictable out of band antenna response.
All of the negative margins are taken to be correct predictions of compatibility.
Taken as a whole, these antenna-to-antenna results appear quite favorable.

3.2 Wire-to-Wire Assessment. The wire-to-wire assessment is based on the
results of IEMCAP runs on F-15 mini-systems with a total of 26 different wire
bundles (all assumed to be 4 inches above a ground plane), made up of power lines,
signal lines, control lines and electro-explosive device lines known to be
electromagnetically compatible in normal operation on the F-15 aircraft. The
great majority of these wires connect to devices that are vulnerable to average
power and are consequently amenable to the integrated EMI margin representation
as a measure of interference. The IEMCAP-predicted integrated margins for
wire-coupled interference are presented in Figures 17 through 19. For each
wire bundle, all of the wire-connected receptors are tabulated with the
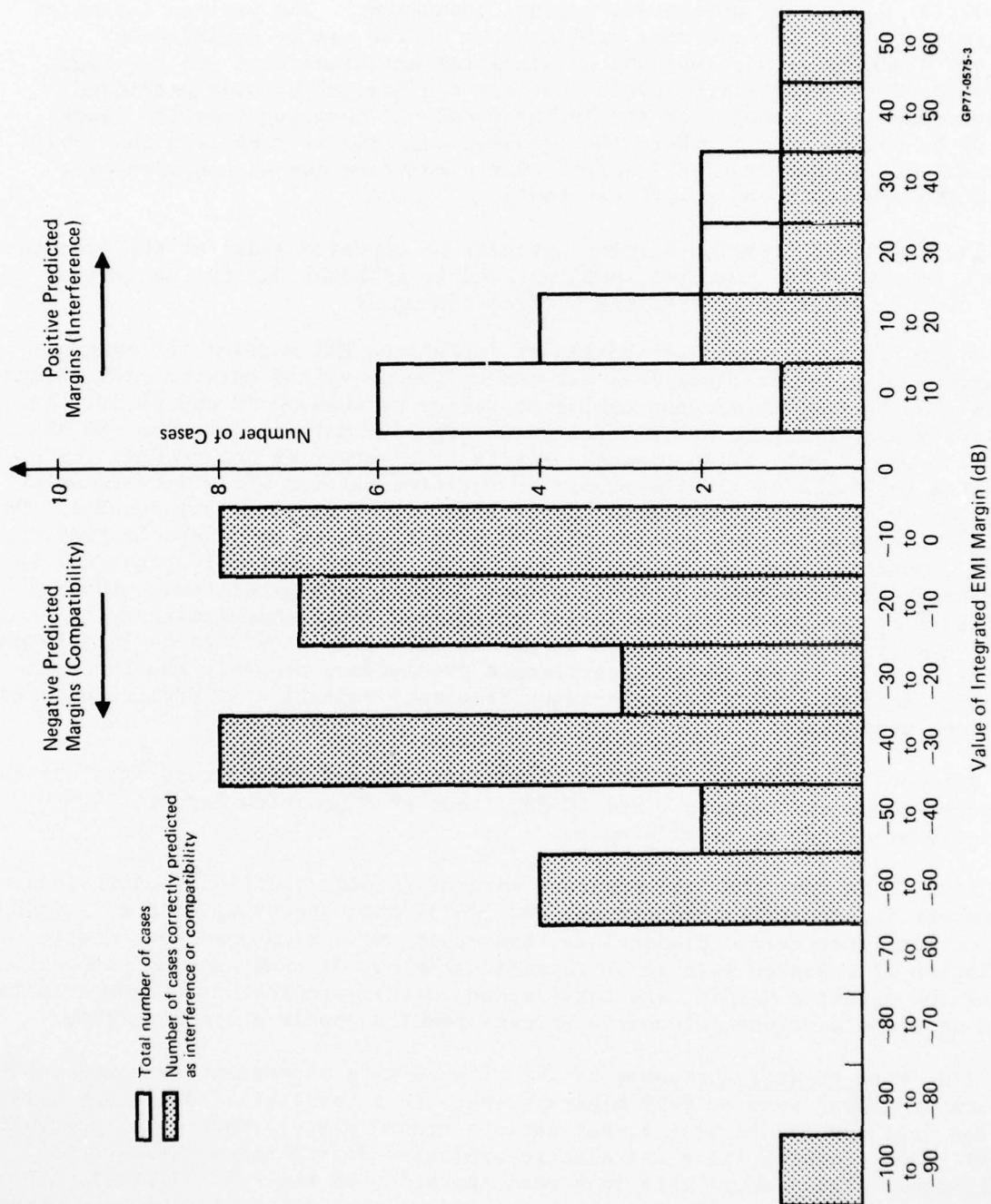
Figure 16. Distribution of Predicted Antenna-to-Antenna Integrated Margins

88

individual integrated margins due to each coupled emitter, as well as the total integrated margin. Figure 17 contains the wire bundles associated with Mini system B1 (Bundles 2-1 through 3-5), and Figure 18 the bundles associated with Mini-system B2 (Bundles B1 through B9) and Figure 19 the bundles associated with Mini-system B3 (Bundles B10 through B17). Along with the tabulated margins for each bundle, there is a schematic diagram of the bundle with each wire termination referenced by the 5-character alphanumeric ID used in the input card deck, in addition to the port number and description as documented in the Mini-system Lists.

Receptor	Source	Integrated Margin (dB)
S Data	Black	−126.0
	Mode 1	−29.3
	Total	−29.3

Receptor	Source	Integrated Margin (dB)
Black	S Data	−43.8
	Mode 1	−73.5
	Total	−43.8

Receptor	Source	Integrated Margin (dB)
Mode 1	S Data	−7.6
	Black	−58.4
	Total	−7.6

[1]Wire Configuration: U = Unshielded, S = Shielded, DS = Double Shielded
TP = Twisted Pair, TT = Twisted Triplet, T6 = Twisted sextuplet

GP77-0221-49

Figure 17 Mini-System B1 Wire-to-Wire Results
Bundle II-1

Port 2-8   UHF Frequency Control (S) → Fqcon
Fqcon o—
30^V Discrete, 40 KΩ
Automatic Challenge Enable   2-4 U   Port 2-5 — Fqcon o
Port 2-13   to IFF Reply Evaluator (S) 2-5 U   15 KΩ Receptor
Chall o— →   2-6 STT Port 2-21 — Chall o
28^V Discrete, 10 Ω   224 Ω Receptor

Port 2-17   Angle of Attack Reference   Port 2-19
AOA In o—   AOA In o
3,500 Ω Receptor   −12^V DC With Response T(S) = 1/(1 + 0.075s)
                                        Generated by Rotating Potentiometer, 2200 Ω

Receptor	Source	Integrated Margin (dB)
Fqcon	Chall	2.8
	AOA In	−10.6
	Total	3.0

Receptor	Source	Integrated Margin (dB)
Chall	Fqcon	−0.8
	AOA In	1.8
	Total	3.7

Receptor	Source	Integrated Margin (dB)
AOA In	Fqcon	−79.6
	Chall	−95.0
	Total	−79.5

GP77-0221-50

Figure 17   Mini-System B1 Wire-to-Wire Results (Continued)
Bundle II-2

Port 2-6   Headset Audio to Disconnect (S)   Port 2-14
Inter o— →   Hdset o
1.55^V, 300-3000 Hz, Voice   2-7 STP   8 Ω Receptor
Port 9-7   AC Power (S)   54   U   Port 96
AC Pwr o—   2-8 U   AC Pwr o
115^V, 400 Hz 0.1 Ω   319 Ω Receptor

Port 2-9   Comm Channel 10-1 (S)   Port 2-18
CH101 o—   CH101 o
20 KΩ Receptor   5v Discrete, 30 KΩ

Receptor	Source	Integrated Margin (dB)
Hdset	AC Pwr	−87.4
	CH101	−62.8
	Total	−62.7

Receptor	Source	Integrated Margin (dB)
AC Pwr	Inter	−39.4
	CH101	6.7
	AC Pwr	39.5
	Total	39.5

Receptor	Source	Integrated Margin (dB)
CH101	Inter	Same Equip
	AC Pwr	−5.1
	Total	−5.1

GP77-0221-51

Figure 17   Mini-System B1 Wire-to-Wire Results (Continued)
Bundle II-3

MICROCOPY RESOLUTION TEST CHART
NATIONAL BUREAU OF STANDARDS-1963-A

Port 2-10
DC Pwr O—
28 Ω Receptor

DC Power to ICNICP (S)   Port 2-22
                                 —O DC Pwr
28^V DC, 0.1 Ω

Port 2-2 Reset Line to Central Computer (S)
Reset O—
5^V DC Switch, 1sec, 1μsec Rise, 10 Ω

Port 2-16
                                 —O Reset
1,000 Ω Receptor

2-9   U
2-10 STP
2-11   U
55   U

Port 2-1
Nwdis O—
28 Ω Receptor   Canopy

Nose Gear Steering Disconnect (S) Port 2-20
                                 —O Nwdis
28^V DC Switch, Disengages Steering Unit

Port 9
Firew O—
280 Ω Receptor

Fire Warning Light (S)   Port 8
                                 —O Firew
28^V Pulse Train, 240 Flashes/Min, 1 Ω

Receptor	Source	Integrated Margin (dB)
DC Pwr	Reset	−29.0
	Nwdis	−20.7
	Firew	−1.5
	DC Pwr	31.0
	Total	31.0

Receptor	Source	Integrated Margin (dB)
Reset	DC Pwr	−85.4
	Nwdis	−104.0
	Firew	−92.8
	Total	−84.7
Nwdis	DC Pwr	−41.2
	Reset	−46.9
	Firew	0.6
	Total	0.6

Receptor	Source	Integrated Margin (dB)
Firew	DC Pwr	−40.9
	Reset	−43.8
	Nwdis	−19.9
	Total	−19.9

GP77-0221-52

Figure 17 Mini-System B1 Wire-to-Wire Results (Continued)
Bundle II-4
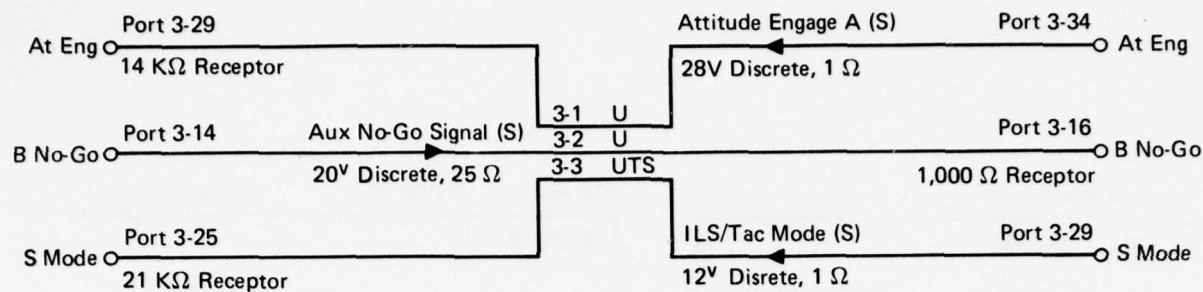
91

Figure 17 (Bundle III-1)

Diagram labels:

- At Eng — Port 3-29 — 14 KΩ Receptor
- Attitude Engage A (S) — Port 3-34 — At Eng — 28V Discrete, 1 Ω
- 3-1 U
- 3-2 U
- 3-3 UTS
- B No-Go — Port 3-14 — Aux No-Go Signal (S) — 20^V Discrete, 25 Ω
- B No-Go — Port 3-16 — 1,000 Ω Receptor
- S Mode — Port 3-25 — 21 KΩ Receptor
- ILS/Tac Mode (S) — Port 3-29 — S Mode — 12^V Disrete, 1 Ω

Receptor	Source	Integrated Margin (dB)
At Eng	B No-Go	−42.0
	S Mode	−28.3
	Total	−28.1

Receptor	Source	Integrated Margin (dB)
B No-Go	At Eng	−9.7
	S Mode	6.4
	Total	6.5

Receptor	Source	Integrated Margin (dB)
S Mode	At Eng	−53.0
	B No-Go	−78.3
	Total	−53.0

GP77-0221-53

Figure 17 Mini-System B1 Wire-to-Wire Results (Continued)
Bundle III-1
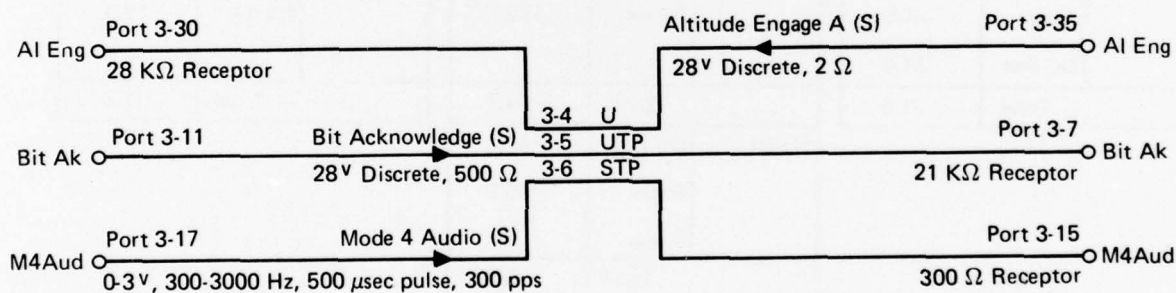
Figure 17 (Bundle III-2)

Diagram labels:

- Al Eng — Port 3-30 — 28 KΩ Receptor
- Altitude Engage A (S) — Port 3-35 — Al Eng — 28^V Discrete, 2 Ω
- 3-4 U
- 3-5 UTP
- 3-6 STP
- Bit Ak — Port 3-11 — Bit Acknowledge (S) — 28^V Discrete, 500 Ω
- Bit Ak — Port 3-7 — 21 KΩ Receptor
- M4Aud — Port 3-17 — Mode 4 Audio (S) — 0-3^V, 300-3000 Hz, 500 μsec pulse, 300 pps
- M4Aud — Port 3-15 — 300 Ω Receptor

Receptor	Source	Integrated Margin (dB)
Al Eng	Bit Ac	−37.9
	M4Aud	−28.2
	Total	−27.8

Receptor	Source	Integrated Margin (dB)
Bit Ak	Al Eng	1.5
	M4Aud	−38.0
	Total	1.5

Receptor	Source	Integrated Margin (dB)
M4Aud	Al Eng	−65.0
	Bit Ak	−68.4
	Total	−63.3

GP77-0221-54

Figure 17 Mini-System B1 Wire-to-Wire Results (Continued)
Bundle III-2

Port 3-31 CAS Interconnect Servo A Cmd Lo (S)

Serv A ○ ⟶

35 mA Analog Signal with Response

$T(S) = 1/(1 + 0.3s/5600 + s^2/5600^2)$, 1 Ω

3-7	STP
3-8	U
3-9	U

Port 3-36

Serv A ○

190 Ω Receptor

115V Power Line (S)   Port 3-38

AC Pwr ○

Port 3-37

AC Pwr ○

1.6 Ω Receptor

115V AC, 400 Hz, 0.1 Ω

Port 3-12

Ant Sl ○

187 Ω Receptor

Power to Antenna Select (S)   Port 3-13

Ant Sl ○

28V DC Power 0.1 Ω
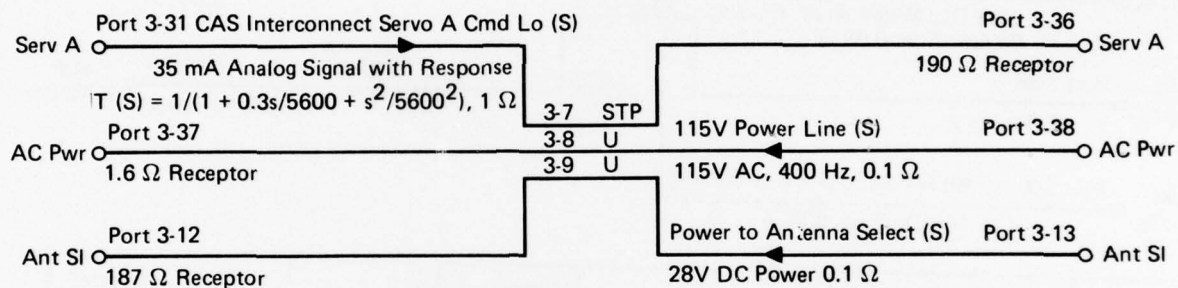
Receptor	Source	Integrated Margin (dB)
Serv A	AC Pwr	−50.6
	Ant Sl	−72.3
	Total	−50.6

Receptor	Source	Integrated Margin (dB)
AC Pwr	Serv A	−12.7
	Ant Sl	−0.5
	AC Pwr	28.5
	Total	28.5

Receptor	Source	Integrated Margin (dB)
Ant Sl	Serv A	47.6
	AC Pwr	14.6
	Ant Sl	59.7
	Total	60.0

GP77-0221-55

Figure 17   Mini-System B1 Wire-to-Wire Results (Continued)
Bundle III-3

93

Port 3-32 Normal Acclerometer Sensor B Signal (S)
Accel O——
−5V to +5V Analog Signal with
Bandwidth Approximately 100 Hz, 100 Ω

Port 3-73
Accel O
100 Ω Receptor

3-10 UTP

Port 3-8 Blanking Pulse (S)
Blank O——
0.4V DC, Minimum of 0.5 μsec,
30 ηsec Rise, 0.68 Ω

3-11 STP
3-12 U

Port 3-5
Blank O
0.68 Ω

HSI
B No-Go O
Port 3-26
21 KΩ Receptor

Port 3-6
21K Ω Receptor
BCP
B No-Go

Rwr
B No-Go O
Port 3-3 Bit No-Go to HSI and BCP (S)
28V Discrete, 500 Ω

Receptor	Source	Integrated Margin (dB)
Accel	Blank	−79.6
	B No-Go	19.4
	Total	19.4

Receptor	Source	Integrated Margin (dB)
Blank	Accel	−136.2
	B No-Go	Same Equip
	Total	−136.2

Receptor	Source	Integrated Margin (dB)
B No-Go (HSI or BCP)	Accel	−51.0
	Blank	−115.0
	Total	−51.0

GP77-0221-56

Figure 17   Mini-System B1 Wire-to-Wire Results (Continued)
Bundle III-4

94

Figure 17   Mini-System B1 Wire-to-Wire Results (Concluded)
Bundle III-5

Receptor	Source	Integrated Margin (dB)	Receptor	Source	Integrated Margin (dB)	Receptor	Source	Integrated Margin (dB)
Fail	D Init	−35.5	D Init	Fail	−38.8	M Bus 3	Fail	−20.5
	LCG M Bus 3	−29.4		LCG M Bus 3	−2.0	(Any Receptor)	D Init	−12.4
	AHRS M Bus 3	−42.4		AHRS M Bus 3	−17.7			
	INS M Bus 3	−45.4		INS M Bus 3	−17.7			
	Rwr M Bus 3	−36.4		Rwr M Bus 3	−9.0			
	ADC M Bus 3	−52.0		ADC M Bus 3	−42.2			
	CC Bus 3	−43.4		CC Bus 3	−15.8			
	Hud SP M Bus 3	−24.4		Hud SP M Bus 3	0.2			
	Total	−22.6		Total	2.7		Total	−11.8

[1] All MBUS 3 ports are both emitters and receptors.

GP77-0221-57

95

Bundle B1

Port 3 — Tank 2 Fuel Quantity (S) — T2QNT
0-5^V, 4000 Hz Discrete, 11 Ω

Speedbrake — Port 4 — T2QNT
11 Ω Receptor

Port 5 — Tank 2 Low Level Warning (S) — T2LOW
28^V DC Discrete, 280 Ω

Port 6 — T2LOW
280 Ω Receptor

1 U
2 U
3 U

Gun — Port 36
11 Ω Receptor

Hydraulic Motor Solenoid (S) — Port 35 — TRIGG
28^V DC Switch, Fires Gatling Gun, 11 Ω
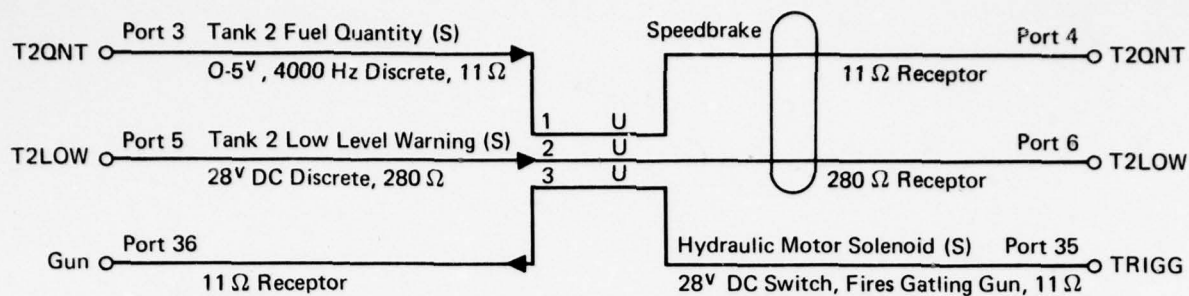
Receptor	Source	Integrated Margin (dB)
T2QNT	T2LOW	−80.4
	Trigg	−62.0
	Total	−61.9

Receptor	Source	Integrated Margin (dB)
T2LOW	T2QNT	−40.5
	Trigg	14.5
	Total	14.5

Receptor	Source	Integrated Margin (dB)
Gun	T2QNT	−66.3
	T2LOW	−29.5
	Total	−29.5

GP77-0221-58

Figure 18   Mini-System B2 Wire-to-Wire Results
Bundle B1

Bundle B2

Port 65 — AIMS Code C4 (S) — AIMS4
18 - 30^V Discrete, 100 KΩ

Port 59 — AIMS4
10 KΩ Receptor

Port 54 — INS BIT No - Go (S) — BNOGO
28^V Discrete, 500 Ω

Port 82 — INSNG
500 Ω Receptor

4 U
5 U
6 U

Port 55 — DCPWR
15 Ω Receptor

28^V DC Power (S) — Port 56 — ILSPR
28^V DC, 0.1 Ω
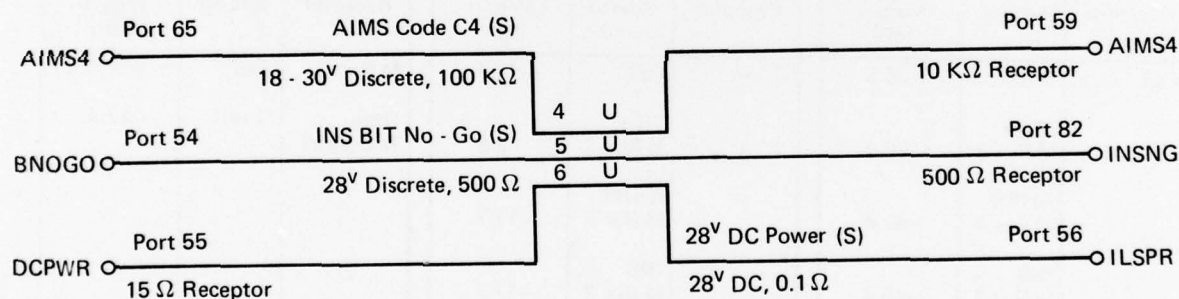
Receptor	Source	Integrated Margin (dB)
AIMS4	BNOGO	12.4
	ILSPR	−21.3
	Total	12.4

Receptor	Source	Integrated Margin (dB)
INSNG	AIMS4	6.6
	ILSPR	−31.1
	Total	6.6

Receptor	Source	Integrated Margin (dB)
DCPWR	AIMS4	−20.4
	BNOGO	−12.4
	ILSPR	43.6
	Total	43.6

GP77-0221-59

Figure 18   Mini-System B2 Wire-to-Wire Results (Continued)
Bundle B2

96

RUDER ○— Port 85 L&R Rudder Servo Engage Signal (S)   Port 94   ○ RUDER

28^V Switch, 09 Ω   13 Ω Receptor

7   U

RUDPO ○— Port 103   8   STP   Rudder Deflection (S)   Port 105   ○ RUDPO

50, KΩ Receptor   9   U   0-8^V, 400 Hz AC, Phase Modulated, 100 Ω

LBAO ○— Port 53   Left Bleed Air Overpressure (S) Port 107   ○ LBAOS

50 Ω Receptor   28^V Discrete, 50 Ω

Nose Wheel Well
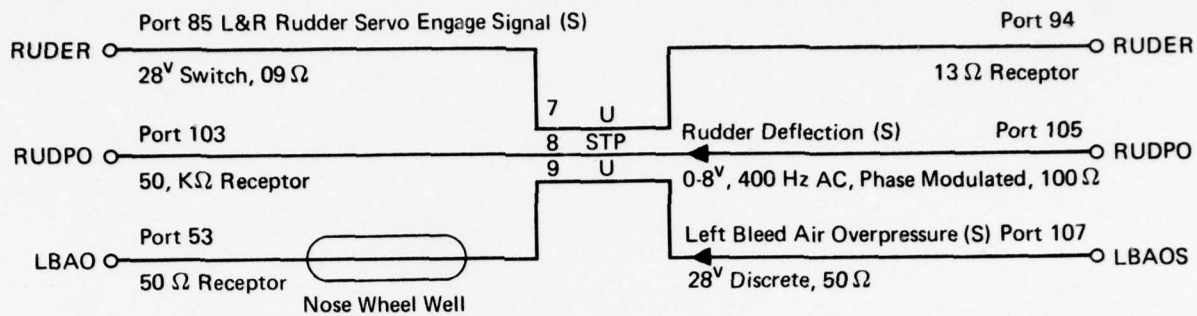
Receptor	Source	Integrated Margin (dB)
RUDER	RUDPO	−43.5
	LBAOS	−6.4
	Total	−6.4

Receptor	Source	Integrated Margin (dB)
RUDPO	RUDER	−70.0
	LBAOS	−96.1
	Total	−70.0

Receptor	Source	Integrated Margin (dB)
LBAO	RUDER	16.5
	RUDPO	−37.1
	Total	16.5

GP77-0221-60

Figure 18 Mini-System B2 Wire-to-Wire Results (Continued)
Bundle B3

YAWBT ○— Port 86   Yaw Rate Sensor A Bit Signal (S) Port 95   ○ YAWBT

150 Ω Receptor   5^V, 400 Hz Switch, 80 Ω

10   STT

VERTX ○— Port 99 Vertical Acceleration Filtered (S)   11   STP   Port 102   ○ VERTX

−3.75^V to 8.25^V Analog DC to 20 Hz, Flat to 1Hz,   17   U   10 KΩ Receptor

Down 3dB at 4 Hz, 24 dB/Octave Above 4 Hz, 300 Ω

HYDMC ○— Port 1 Hydraulic Motor Control (S)   Port 2   ○ HYDMC

24^V DC Switch, 24 Ω   120 Ω Receptor
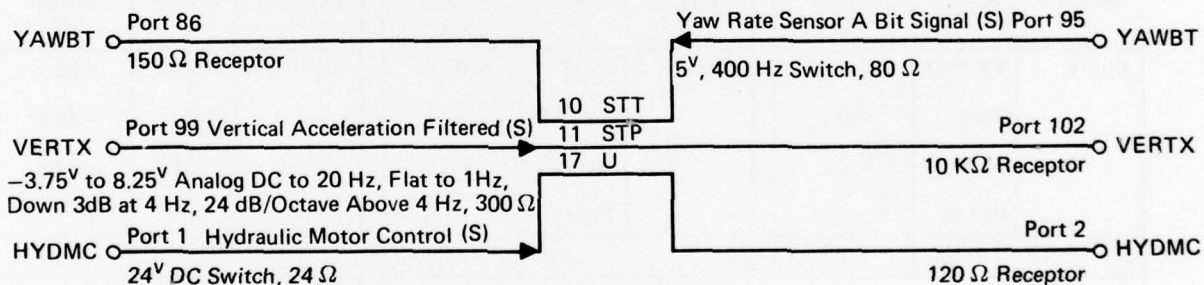
Receptor	Source	Integrated Margin (dB)
YAWBT	VERTX	−118.4
	HYDMC	−48.7
	Total	−48.7

Receptor	Source	Integrated Margin (dB)
VERTX	YAWBT	−136.8
	HYDMC	−65.2
	Total	−65.2

Receptor	Source	Integrated Margin (dB)
HYDMC	YAWBT	−39.8
	VERTX	−40.9
	Total	−37.3

GP77-0221-61

Figure 18 Mini-System B2 Wire-to-Wire Results (Continued)
Bundle B4

97

FLITE ○ Port 13 — Formation Lights Power (S) → 115^V, 400Hz, 0.1Ω

Port 12 ○ **FLITE** — 8Ω Receptor

Pwr. ○ Port 24 — Right Flap Power (S) → 115^V, 400Hz, 0.1Ω

Port 26 ○ **ACPWR** — 3.6Ω Receptor

13 U
14 UTT
15 UTT
16 STP

EXTND ○ Port 25 — Right Flap Extend (S) → 28^V DC Switch, 1Ω

Port 27 ○ **EXTND** — $10\,K\Omega$ Receptor

AILPO ○ Port 104 — $50\,K\Omega$ Receptor

Right Aileron Deflection (S) — Port 106 ○ **AILPO** — $0\text{-}8^V$, 400Hz AC Phase - Modulated, $100\,\Omega$
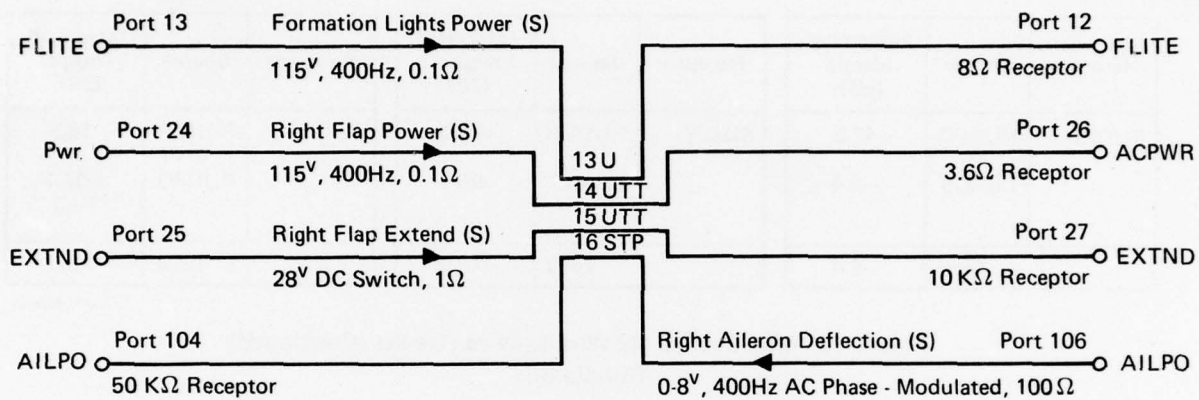
Receptor	Source	Integrated Margin (dB)
FLITE	EXTND	−3.3
	PWR	−62.2
	AILPO	−36.6
	FLITE	42.5
	Total	42.5

Receptor	Source	Integrated Margin (dB)
ACPWR	FLITE	−62.2
	EXTND	2.7
	AILPO	−70.3
	PWR	41.6
2	Total	41.6

Receptor	Source	Integrated Margin (dB)
EXTND	FLITE	−69.7
	PWR	−78.7
	AILPO	−77.9
	Total	−68.7
AILPO	FLITE	−53.9
	PWR	−140.4
	EXTND	−73.4
	Total	−53.8

GP77-0221-62

Figure 18   Mini-System B2 Wire-to-Wire Results (Continued)
Bundle B5
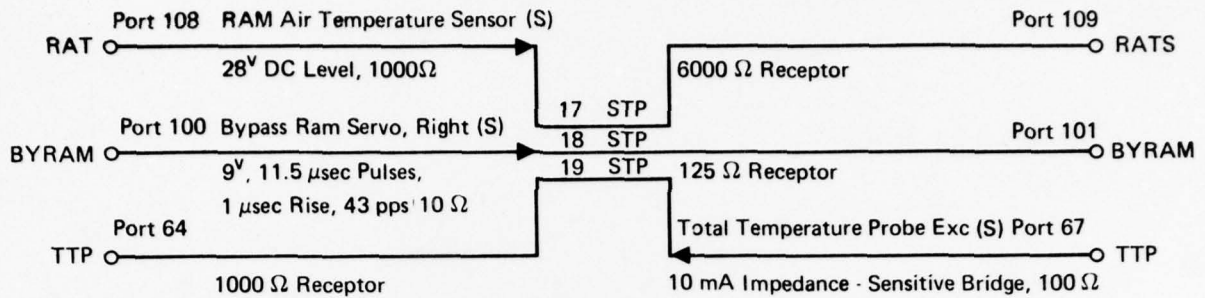
98

Port 108   RAM Air Temperature Sensor (S)   Port 109
RAT o—————————————————————————————   o RATS
         28^V DC Level, 1000Ω   6000 Ω Receptor

                                          17 STP
         Port 100 Bypass Ram Servo, Right (S)   Port 101
BYRAM o—————————————————————————   18 STP   o BYRAM
         9^V, 11.5 μsec Pulses,   19 STP   125 Ω Receptor
         1 μsec Rise, 43 pps 10 Ω

         Port 64   Total Temperature Probe Exc (S) Port 67
TTP o——————————————————————   o TTP
         1000 Ω Receptor   10 mA Impedance - Sensitive Bridge, 100 Ω

Receptor	Source	Integrated Margin (dB)
RATS	BYRAM	−162.3
	TTP	−155.6
	Total	−154.8

Receptor	Source	Integrated Margin (dB)
BYRAM	RAT	−91.9
	TTP	−118.4
	Total	−91.9

Receptor	Source	Integrated Margin (dB)
TTP	RAT	−129.0
	BYRAM	−159.8
	Total	−129.0

GP77-0221-63

Figure 18   Mini-System B2 Wire-to-Wire Results (Continued)
Bundle B6
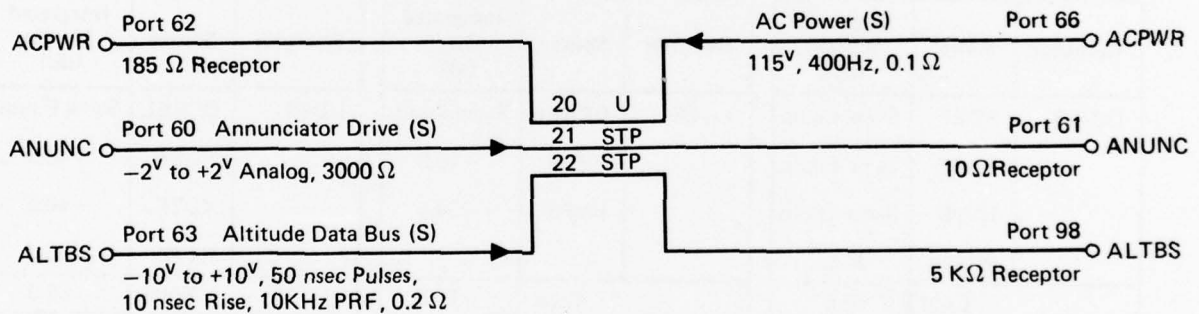
         Port 62   AC Power (S)   Port 66
ACPWR o———————————————————————   o ACPWR
         185 Ω Receptor   115^V, 400Hz, 0.1 Ω

                                          20 U
         Port 60 Annunciator Drive (S)   Port 61
ANUNC o————————————————————————   21 STP   o ANUNC
         −2^V to +2^V Analog, 3000 Ω 22 STP   10 ΩReceptor

         Port 63 Altitude Data Bus (S)   Port 98
ALTBS o————————————————————————   o ALTBS
         −10^V to +10^V, 50 nsec Pulses,   5 KΩ Receptor
         10 nsec Rise, 10KHz PRF, 0.2 Ω

Receptor	Source	Integrated Margin (dB)
ACPWR	ANUNC	−27.8
	ALTBS	Same Equip
	ACPWR	74.8
	Total	74.8

Receptor	Source	Integrated Margin (dB)
ANUNC	ACPWR	−86.5
	ALTBS	−126.4
	Total	−86.5

Receptor	Source	Integrated Margin (dB)
ALTBS	ACPWR	−59.1
	ANUNC	−200.3
	Total	−59.1

GP77-0221-64

Figure 18   Mini System B2 Wire-to-Wire Results (Continued)
Bundle B7
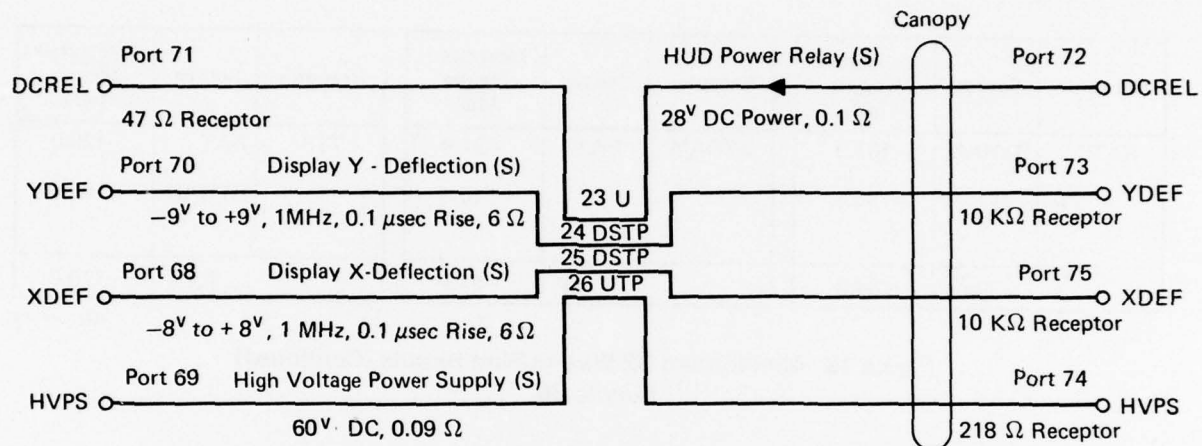
99

Port 71
DCREL o——
47 Ω Receptor

Port 70 Display Y - Deflection (S)
YDEF o——
-9^V to $+9^V$, 1MHz, 0.1 μsec Rise, 6 Ω

Port 68 Display X-Deflection (S)
XDEF o——
-8^V to $+8^V$, 1 MHz, 0.1 μsec Rise, 6 Ω

Port 69 High Voltage Power Supply (S)
HVPS o——
60^V DC, 0.09 Ω

23 U
24 DSTP
25 DSTP
26 UTP

HUD Power Relay (S)
28^V DC Power, 0.1 Ω

Canopy

Port 72
o DCREL

Port 73
o YDEF
10 KΩ Receptor

Port 75
o XDEF
10 KΩ Receptor

Port 74
o HVPS
218 Ω Receptor

Receptor	Source	Integrated Margin (dB)
DCREL	XDEF	Same Equip
	YDEF	Same Equip
	HVPS	Same Equip
	DCREL	45.5
	Total	45.5

Receptor	Source	Integrated Margin (dB)
XDEF	DCREL	Same Equip
	YDEF	−15.8
	HVPS	−34.4
	Total	−15.8

Receptor	Source	Integrated Margin (dB)
HUPS	DCREL	Same Equip
	YDEF	−40.5
	XDEF	−40.5
	HVPS	58.3
	Total	58.3

GP77-0221-65

Figure 18 Mini-System B2 Wire-to-Wire Results (Continued)
Bundle B8

100

Port 80 Master Caution Light (S)
CAUTN o——— 28^V Discrete, 1 Ω

Port 14 Panel Lighting Power (S)
PNLIT o——— 5^V, 400Hz 0.1 Ω

Port 79 DC Power (S)
DCPWR o——— 28^V DC, 0.1 Ω

27 U
28 U
29 U

Port 78
CAUTN o
175 Ω Receptor

Port 76
PNLIT o
3 Ω Receptor

Port 77
DCPWR o
5 Ω Receptor
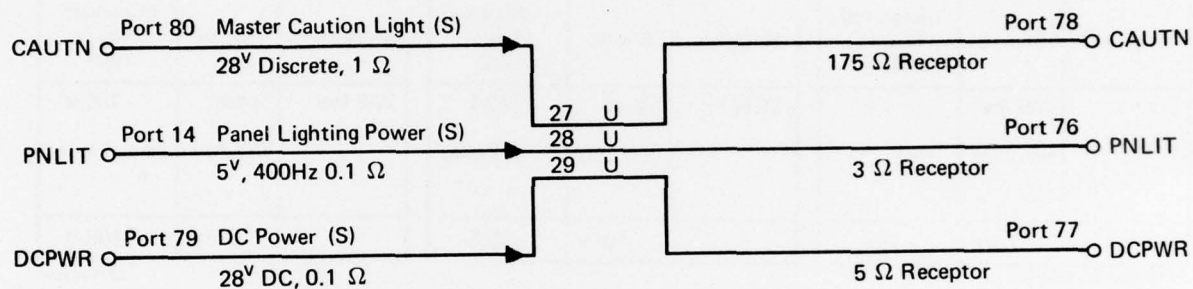
Receptor	Source	Integrated Margin (dB)
CAUTN	PNLIT	−2.5
	DCPWR	12.8
	Total	12.8

Receptor	Source	Integrated Margin (dB)
PNLIT	CAUTN	−15.8
	DCPWR	28.8
	PNLIT	62.5
	Total	62.5

Receptor	Source	Integrated Margin (dB)
DCPWR	CAUTN	−35.5
	PNLIT	−12.2
	DCPWR	67.0
	Total	67.0

GP77-0221-66

Figure 18   Mini-System B2 Wire-to-Wire Results
Bundle B9

Left MLG Wheel Well

SKID o— Port 22 Right Wheel Speed Det (S)

2.5^V, 0-4000 Hz Signal:
Frequency Relates to RPM, 1 Ω

Port 23 o SPEED
1000 Ω Receptor

30	UTP	
31	ST6	Left MLG WOW[1] Power (S)
32	ST6	28^V DC Switch, 1 Ω

WOWIN o— Port 15
68 Ω Receptor

Port 17 o WWPWR

WW Out o— Port 16 Left MLG WOW Switch (S)
28^V DC Switch, 1 Ω

Port 18 o WWREL
68 Ω Receptor

Receptor	Source	Integrated Margin (dB)
Speed	WW Pwr	4.2
	WW Out	−11.1
	Total	4.2

Receptor	Source	Integrated Margin (dB)
WOW In	Speed	−83.5
	WW Out	Same Equip
	Total	−83.5

Receptor	Source	Integrated Margin (dB)
WW Rel	Speed	−108.9
	WW Pwr	Same Equip
	Total	−108.9

1. Weight on wheels

GP77-0221-67

Figure 19 Mini-System B3 Wire-to-Wire Results
Bundle B10

Left Wing Inboard

LWIPE o— Port 28 Pylon Eject (S)
28^V DC Switch, 0.5 Ω

Port 37 o LWIPE
2.5 Ω Receptor

33	S
34	S
35	U

MERFR o— Port 29 MER Fire - Left Wing Pylon (S)
28^V DC Switch, 0.5 Ω

Port 38 o MERFR
2.5 Ω Receptor

NSARM o— Port 30 MER/MAU Nose Arm (S)
28^V DC Switch, 1 ms Rise, 1.5 Ω

Port 39 o NSARM
6.5 Ω Receptor

Receptor	Source	Integrated Margin (dB)
LWIPE	MERFR	37.7
	NSARM	37.5
	Total	40.6

Receptor	Source	Integrated Margin (dB)
MERFR	LWIPE	37.0
	NSARM	36.7
	Total	39.8

Receptor	Source	Integrated Margin (dB)
NSARM	LWIPE	28.8
	MERFR	28.6
	Total	31.7

GP77-0221-68

Figure 19 Mini-System B3 Wire-to-Wire Results (Continued)
Bundle B11

102

Port 31 CL Pylon Eject (S) — CLPE — 28V DC Switch, 0.5 Ω

Port 40 — CLPE — 2.5 Ω Receptor

36 S
37 S
38 U

Port 32 CL Tank Jettison (S) — CLTJ — 28V DC Switch, 0.5 Ω

Port 41 — CLTJ — 2.5 Ω Receptor

Port 43 — PREG — 28 Ω Receptor

Ext Tank Air Pressure Regulator Port 42 — Tank — 28V DC Switch; Closes A Valve, 1 Ω

Receptor	Source	Integrated Margin (dB)
CLPE	CLTJ	36.1
	Tank	Same Equip
	Total	36.1

Receptor	Source	Integrated Margin (dB)
CLTJ	CLPE	35.5
	Tank	Same Equip
	Total	35.5

Receptor	Source	Integrated Margin (dB)
PREG	CLPE	11.2
	CLTJ	11.0
	Total	14.1

GP77-0221-69

Figure 19   Mini-System B3 Wire-to-Wire Results (Continued)
Bundle B12

Port 47 Display Command A (S) — Disp A — 4ᵛ Discrete, 30 ns Rise, Controls Display Mode 68 Ω

Port 81 — Disp A — 10 KΩ Receptor

39 STP
40 STP
41 U

Port 48 Radar Signal Reference (S) — RDREF — 5ᵛ DC Ref, 180 Ω

Port 33 — RDREF — 2,800 Ω Receptor

Port 46 — MODEX — 100 Ω Receptor

Mode X Ident Command (S) Port 110 — MODEX — 28ᵛ Discrete, 100 Ω
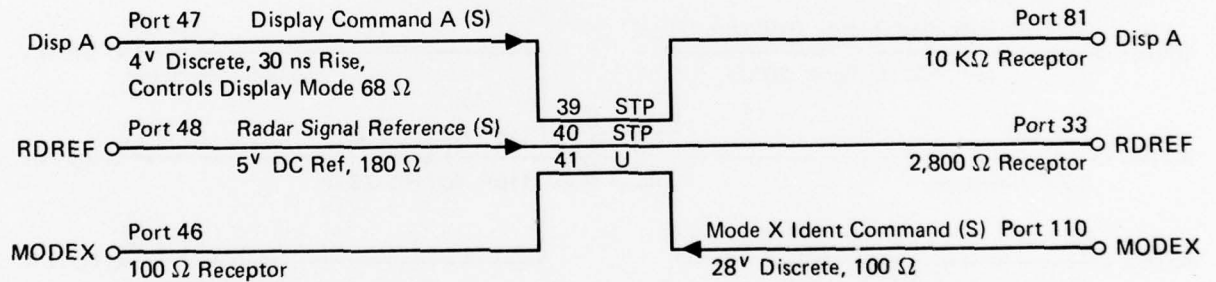
Receptor	Source	Integrated Margin (dB)
Disp A	RDREF	−143.0
	MODEX	−121.1
	Total	−121.1

Receptor	Source	Integrated Margin (dB)
RDREF	Disp A	−129.1
	MODEX	−118.1
	Total	−117.8

Receptor	Source	Integrated Margin (dB)
MODEX	Disp A	Same Equip
	RDREF	−27.8
	Total	−27.8

GP77-0221-70

Figure 19   Mini System B3 Wire-to-Wire Results (Continued)
Bundle B13
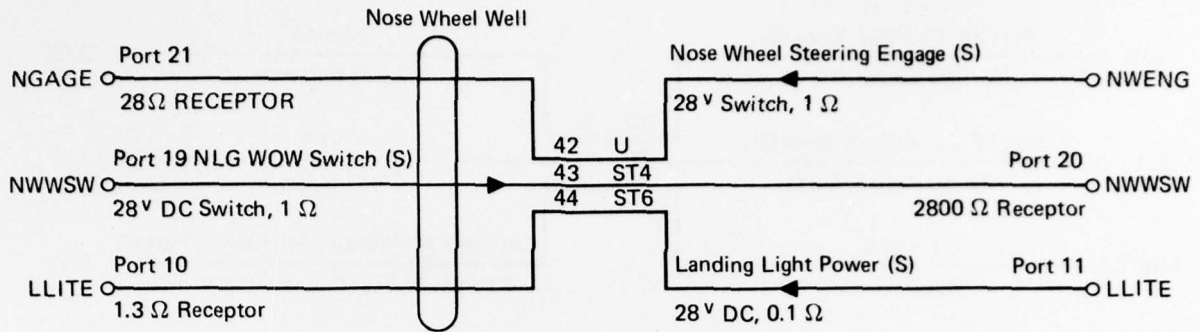
103

Nose Wheel Well

Port 21
NGAGE o—— 28 Ω RECEPTOR

Nose Wheel Steering Engage (S)
o NWENG
28 V Switch, 1 Ω

Port 19 NLG WOW Switch (S)
NWWSW o—— 28 V DC Switch, 1 Ω

42 U
43 ST4
44 ST6

Port 20
o NWWSW
2800 Ω Receptor

Port 10
LLITE o—— 1.3 Ω Receptor

Landing Light Power (S)   Port 11
o LLITE
28 V DC, 0.1 Ω

Receptor	Source	Integrated Margin (dB)
NGAGE	NWWSW	−15.0
	LLITE	−78.1
	Total	−15.0

Receptor	Source	Integrated Margin (dB)
NWWSW	NWENG	−71.6
	LLITE	< −199
	Total	−71.6

Receptor	Source	Integrated Margin (dB)
LLITE	NWENG	−84.8
	NWWSW	−108.7
	LLITE	14.3
	Total	14.3

GP77-0221-71

Figure 19   Mini-System B3 Wire-to-Wire Results (Continued)
Bundle B14
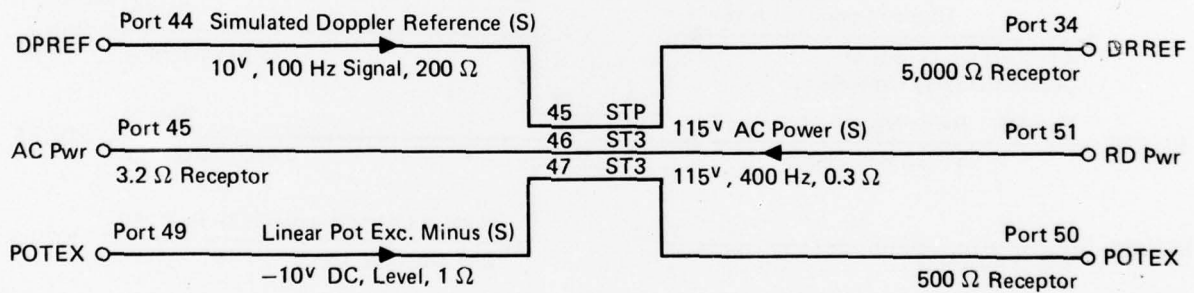
Port 44   Simulated Doppler Reference (S)   Port 34
DPREF o—— 10 V, 100 Hz Signal, 200 Ω   o DRREF
5,000 Ω Receptor

45 STP
46 ST3
47 ST3

Port 45
AC Pwr o—— 3.2 Ω Receptor

115 V AC Power (S)   Port 51
o RD Pwr
115 V, 400 Hz, 0.3 Ω

Port 49   Linear Pot Exc. Minus (S)   Port 50
POTEX o—— −10 V DC, Level, 1 Ω   o POTEX
500 Ω Receptor

Receptor	Source	Integrated Margin (dB)
DPREF	RD Pwr	−162.3
	POTEX	−144.4
	Total	−144.3

Receptor	Source	Integrated Margin (dB)
AC Pwr	DPREF	−152.3
	POTEX	−171.1
	RD Pwr	70.6
	Total	70.6

Receptor	Source	Integrated Margin (dB)
POTEX	DPREF	−175.0
	AC Pwr	< −199
	Total	−175.0

GP77-0221-72

Figure 19   Mini-System B3 Wire-to-Wire Results (Continued)
Bundle B15

Port 52
PRESS o— 280 Ω Receptor

Hydraulic Pressure Warning (S)   Port 7
—o PRESS
28ᵛ DC Discrete, 280 Ω

Port 83   Throttle Switch (S)
THROT o—
28ᵛ Switch, Starts Engines, 1 Ω

48   U
49   U
50   STP

Port 84
—o ENGIN
20 Ω Receptor

Port 57
GCMIK o—
5 Ω Receptor

Gnd Crew Mike Line (S)   Port 58
—o GMIKE
0.001ᵛ , 0-3000 Hz Audio, 5 Ω
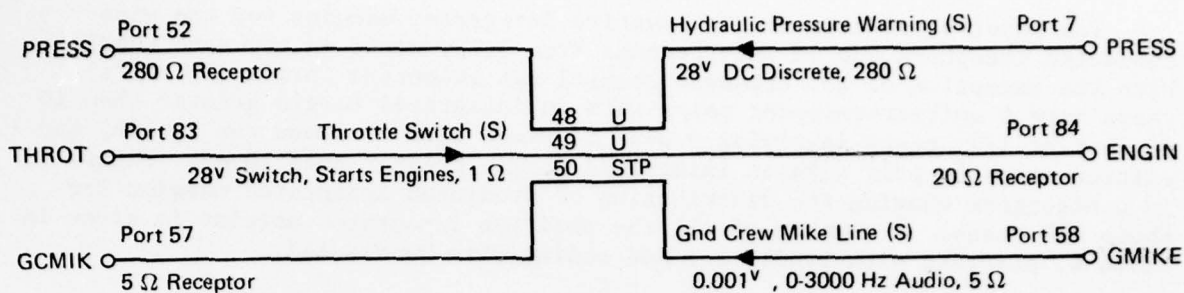
Receptor	Source	Integrated Margin (dB)
PRESS	THROT	−13.2
	GMIKE	−61.6
	Total	−13.2

Receptor	Source	Integrated Margin (dB)
ENGIN	PRESS	−17.6
	GMIKE	−7.14
	Total	−17.6

Receptor	Source	Integrated Margin (dB)
GCMIK	PRESS	−8.2
	THROT	0.9
	Total	1.4

GP77-0221-73

Figure 19   Mini-System B3 Wire-to-Wire Results (Continued)
Bundle B16

Port 91 Fwd Pitch A Signal From Stick (S)
PASIG o—
−6V to 6V, 400 Hz AC Phase Modulated, 100 Ω

Port 88
—o PASIG
50 KΩ Receptor

Canopy

51 UTP
52 U
53 UTP

Port 92
PAEXC o—
1000 Ω Receptor

Fwd Pitch A Excitation to Stick (S) Port 89
—o PAEXC
9V, 400 Hz AC Reference Phase, 10 Ω

Port 93 Fwd Roll B Signal, From Stick (S)
Roll B o—
0 to 6V, 400 Hz AC Phase Modulated, 100 Ω

Port 87
—o Roll B
50 KΩ Receptor
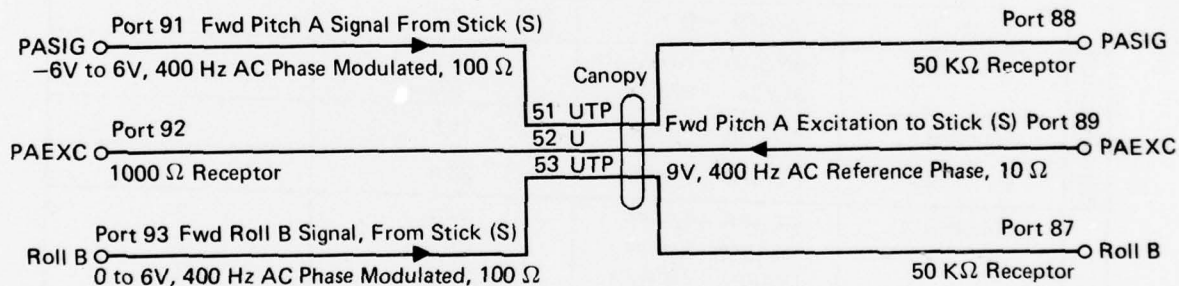
Receptor	Source	Integrated Margin (dB)
PASIG	PAEXC	Same Equip
	Roll B	5.5
	Total	5.5

Receptor	Source	Integrated Margin (dB)
PAEXC	PASIG	Same Equip
	Roll B	Same Equip
	Total	X

Receptor	Source	Integrated Margin (dB)
Roll B	PASIG	+11.3
	PAEXC	−11.6
	Total	+11.3

GP77-0221-74

Figure 19   Mini-System B3 Wire-to-Wire Results (Concluded)
Bundle B17

105

The results indicate mostly negative integrated margins for the wire-connected receptors due to interference from other wires in the same bundle. With the exception of the armament control set receptors (primarily EED's) there were 6 emitter-receptor pairs with an integrated margin greater than 10 dB (out of 177 cases involving a pair of wires with a common run length) and 1 emitter-receptor pair with an integrated margin greater than 20 dB. Figure 20 is a histogram showing the distribution of predicted integrated margins for these 177 cases. A summary of all the positive integrated margins is given in Table 6, starting with Bundle 2-1 and ending with Bundle B17.

Table 6. Summary of Wire-Coupled Interference Predictions

	Bundle	Emitter-Receptor Combination	Integrated Margin	Notes
Minisystem B1	Bundle 2-2	CHALL → FQCON AOAIN → CHALL	2.8 1.8	
	Bundle 2-3	CH101 → ACPWR	6.7	
	Bundle 2-4	FIREW → NWDIS	0.6	
	Bundle 3-1	SMODE → BNOGO	6.4	
	Bundle 3-2	ALENG → BITAK	1.5	
	Bundle 3-3	SERVA → ANTSL ACPWR → ANTSL	17.0 11.6	2 2
	Bundle 3-4	BNOGO → ACCEL	19.4	3
	Bundle 3-5	MBUS3 → DINIT	2.7	
Minisystem B2	Bundle B2	BNOGO → AIMS4 AIMS4 → BNOGO	12.4 6.6	
	Bundle B3	RUDER → LBAO	16.5	2
	Bundle B9	DCPWR → PNLIT	28.8	2,3
Minisystem B3	Bundle B11	MERFR → LWIPE NSARM → LWIPE LWIPE → MERFR NSARM → MERFR MERFR → NSARM LWIPE → NSARM	37.7 37.5 37.0 36.7 28.6 28.8	3 3 3 3 3 3
	Bundle B12	CLTH → CLPE CLPE → CLTH	36.1 35.4	3 3
	Bundle B16	THROT → GCMIK	0.9	

GP77-0342-5

Notes:
1. No interference is predicted for Bundles 2-1, B1, B4, B5, B6, B7, B8, B10, B13, B14, B15 and B17.
2. Actual susceptibility threshold is probably higher.
3. Actual emission level is probably lower.

106
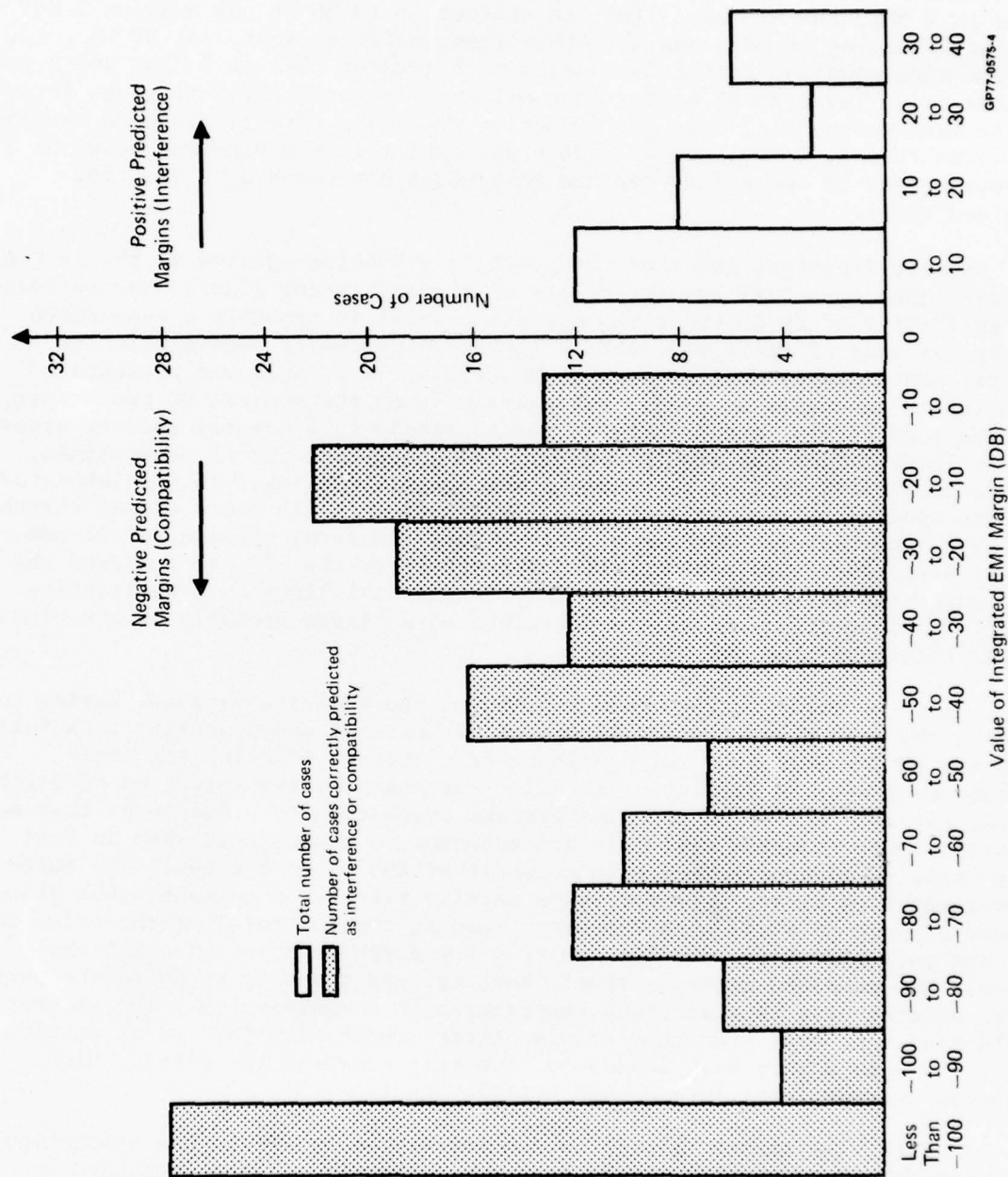
Figure 20. **Distribution of Predicted Wire-to-Wire Integrated Margins**

GP77-0575-4

107

There are a number of reasons for the existence of positive integrated margins. The major reason has to do with the fact that the measured non-required emissions were simulated by a simple displacement of MIL-STD-461 limits to the point just tangent to the highest measured level. (See Figure 10) Consequently, if an emitter has a measured noise level 30 dB above the MIL-spec limit at 2 MHz, the MIL-spec limit is shifted up by 30 dB not only at 2 MHz but also at 2 kHz, at 50 MHz, and all other frequencies as well. At 50 MHz, the wire-to-wire coupling factor is usually much greater than at 2 MHz, and a calculated noise level 30 dB higher than MIL-spec is more likely to cause interference. By the same token, at 2 kHz, the inductive shielding effectiveness is usually much less than at 2 MHz, and a 30 dB upward shift in the MIL-spec level at 2 kHz may appear to cause interference that would not occur at 2 MHz, for shielded wires.

Another important cause of the positive predicted margins is the lack of measured data on actual susceptibility of signal/control lines. The estimated susceptibility of 20 dB under the operating level is probably a reasonable figure for many of the lines, but is likely to be overly pessimistic for others, particularly devices such as DC relays. A DC solenoid presents a much larger impedance at 2 kHz, for example, than the nominal DC resistance, and the eddy current and hysteresis losses result in a greatly reduced magnetic field, insufficient to trip the relay. The susceptibility of power lines, tested to MIL-STD-461A or MIL-I-6181D susceptibility limits in the laboratory, was represented by the specification limits, even though their actual threshold may have been higher. Because of the uniform standards applied to all power lines, sensitive lines such as the power supply to the HUD are assigned the same susceptibility level as relatively insensitive lines such as lighting power. Consequently, the less susceptible power lines probably have a higher actual threshold than the MIL-specs.

There are other factors contributing to the positive margins, having to do with the generally worst-case type of assumptions and approximations built into the IEMCAP models and also arising from the way in which the mini-systems were used to simulate the F-15. For example, the selection of 3-wire bundle representations in the mini-systems automatically presupposes that an emitter wire - receptor wire pair are adjacent to each other, when in fact they could be located anywhere in a bundle of 100 or more wires. The noise measurements on wires, moreover, were usually taken by a current probe placed around a group of wires with the meter reading the sum total of the noise on all the enclosed wires, usually due to a few dominant noisy wires in the group. The measured emission level, however, was taken to apply to the particular emitter wire in that group represented in a mini-system. The assumption could result in over predicted coupled interference from that wire, particularly if it is a very high impedance line that converts the already high measured current level into a high voltage level.

Finally, the IEMCAP calculates the integrated margin on the assumption that the MIL-spec emission levels are simultaneously in every standard or measuring instrument bandwidth, so that even when the individual point margins are negative, the sum may add up to a positive integrated margin.

108

Looking at Table 6, there is no predicted interference in the first bundle, Bundle 2-1. In Bundle 2-2, there is an integrated margin of 2.8 dB at the FQCON due to the CHALL, and an integrated margin of 1.8 dB at the CHALL due to the AOAIN. Considering all the factors in the above discussion that can contribute to positive integrated margins, these results are not at all unreasonable, and the same can be said for Bundle 2-3, Bundle 2-4, Bundle 3-2, Bundle 3-4, and Bundle 3-5. Any one of the worst-case assumptions can easily account for such relatively small positive integrated margins. The remaining bundles are Bundle 2-3, with an integrated margin of 6.7 dB at the ACPWR line due to the CH101, Bundle 3-1, with an integrated margin of 6.4 dB at the BNOGO due to the SMODE, and Bundle 3-3, with an integrated margin at the ANTSL of 17.0 dB due to the SERVA and 11.6 dB due to the ACPWR. All of these positive margins are primarily due to predicted interference at 50 MHz and could be accounted for by actual emission levels below the MIL-spec limits and by actual susceptibility thresholds above the MIL-spec limits.

The only integrated margins in Mini-system B1 that could be considered large are the 17 and 11.6 dB margins at the ANTSL and the 19.4 dB margin at the ACCEL. The 17 dB integrated margin at the ANTSL corresponds to a highest point margin of 5 dB at 50 MHz, the predominant interference being predicted in the vicinity of this frequency. Since the ANTSL line is a power line to an equipment built to MIL-I-6181 specifications, its susceptibility was simulated according to the MIL-I-6181 limit for power lines, which is less stringent (a lower threshold level) than MIL-STD-461A. However the ANTSL happens to be a 28 volt DC relay, a magnetic transducer than switches the UHF to either the upper or lower antenna. Such a device, whose ferromagnetic core is not laminated, tends to have very high eddy current, as well as hysteresis losses at frequencies even as low as a few kilohertz, and its susceptibility in the vicinity of 50 MHz is bound to be much less than the MIL-I-6181 standard (i.e., a much higher threshold level). Furthermore, since this type of device has a much higher impedance at RF frequencies than the nominal DC resistance used to model it, the wire-to-wire coupling model probably over-predicts the coupled current to the ANTSL.

The 19.4 dB integrated margin at the ACCEL, due to the BNOGO, corresponds to a 17.9 dB point margin in the vicinity of 50 MHz. The positive margin in this case is probably due to inaccuracy in the simulation of unrequired BNOGO emission. The BNOGO is a high impedance line (21,000 ohms) whose conducted emission is probably much lower than the simulated current levels based on actual measurements for an entire group of wires. Additional inaccuracy results from the way the MIL-STD-461A limits are used to simulate the actual emission level, which may be quite low in the vicinity of 50 MHz.

Looking at the results for Mini-system B2, there is predicted interference in 3 of the 9 bundles. In Bundle B2, there is an integrated margin of 12.4 dB at the AIMS4 due to the BNOGO, with the dominant point margin of 6.8 dB at 2 kHz. This is probably due to the simulated emission level shifted 14 dB above the MIL-STD-461A limit at 2 kHz, with an actual emission level at 2 kHz much lower. Also, in Bundle B2, there is an integrated margin of 6.6 dB at the BNOGO due to the AIMS4. In the latter case, the likely cause of the positive margin is that the assumption of a current emission level at the AIMS4 of 5 dB above MIL-STD-461A limits is pessimistic, because of the 10K impedance at one end and 100K at the other end.

109

In Bundle B3, the RUDER causes a 16.5 dB integrated margin at the LBAO, with point margins of 3.4 dB at 2 kHz and 3.9 dB at 63 MHz. The interference at 2 kHz, which is narrowband, probably contributes more to the integrated margin than the interference at 63 MHz, which is broadband, because of the way the narrow band margins are integrated. However, the LBAO is a DC relay similar to the ANTSL, and probably has a much higher rejection at those frequencies than that used in modeling it.

In Bundle B9, the 28.8 dB integrated margin at the PNLIT due to the DCPWR corresponds to a 17 dB narrowband point margin at 2 kHz. In this case, the PNLIT is probably less susceptible than the MIL-spec limit to which it was tested, since it only functions to illuminate cockpit instruments and does not supply power to sensitive equipments.

In Mini-system B3, the only significant interference predictions involve the four EED's (LWIPE, MERFR, CLPE, and CLTH) and the DC relay (NSARM) in Bundles B11 and B12. All these cases, mostly integrated margins of about 37 dB, correspond to a narrowband interference at 2 kHz, with a point margin of about 18 dB. Predicted interference to the NSARM is again a case of a DC relay that cannot really respond to the AC interference, but the EED's present a different problem. These devices are standard ejection cartridges that respond essentially to joule heating, but the unavailability of a really good EED model makes it difficult to represent their spectrum at higher frequencies, where the dynamic impedance affects the actual susceptibility level. If the impedance at 2 kHz is not grossly at variance with the DC impedance, then the maximum no-fire current of 0.75 amps is a reasonable figure for the suscepti-bility at that frequency, and the 18 dB point margin is probably not attribut-able to error in the susceptibility data. On the other hand, the actual emission at that frequency is probably less than the level simulated in the mini-system as 34 dB greater than the MIL-STD-461A limit, and could account for the positive margin.

The GCMIK in Bundle B16 has an integrated margin of 0.9 dB due to the THROT, a very marginal situation that could be accounted for by any approxima-tion error.

The overall assessment of wire-to-wire is that the IEMCAP generally pre-dicts little or no interference among the F-15 wire-connected ports represented in the mini-systems. The exceptions could be traced to devices that are prob-ably not as susceptible or as noisy as the MIL-spec limits, and the IEMCAP does not predict any point margins in excess of 20 dB.

3.3 Antenna-to-Wire Assessment. The antenna-to-wire assessment is based upon the results of IEMCAP runs on 20 wires exposed to apertures. Four F-15 apertures were simulated: the speedbrake and the canopy, both dielectric apertures, and the nose wheel and left main landing gear wheel wells, both physical apertures. All 20 wires were subject to electromagnetic radiation from the upper and lower UHF, IFF, and TACAN antennas. Four of the wires, the fuel gauge (T2QNT) and the AFCS control stick wires (PASIG, PAEXC, ROLLB) were known to exhibit non-linear effects in the UHF frequency range, picking off modulations that were in their own operating range of 400 Hz or 4000 Hz. These 4 wires were simulated by treating them as RF receptors; their required low frequency susceptibility, approximated by 40 dB below the operating level for the fuel gauge and 20 dB below the operating level for the stick wires,

110

was translated into the UHF region as an equivalent sensitivity. Implicit in this approximation is the assumption of 100% demodulation efficiency. These wires were all simulated in the "fixed" configuration, simulating the EMI correction of shielding or filtering that was actually used to eliminate the original interference. The remaining 16 wires were simulated as having an unrequired susceptibility of 1 watt and a required susceptibility 20 dB below their normal operating level.

Out of 120 emitter-receptor combinations involving coupling to an exposed wire, the program predicted positive margins in 5 cases; the distribution of predicted margins is given in Figure 21.

Positive integrated margins were predicted for 3 wires out of the 20 wires simulated: the nose wheel disconnect (NWDIS) exposed through the canopy, the nose wheel engage (NGAGE) and left bleed air over pressure sensor (LBAO), exposed through the nose wheel well. A summary of the antenna-to-wire interference predictions is given in Table 7. The 20 exposed wires are ordered by mini-system and bundle ID, indicating each interfering transmitter and the integrated EMI margin at the receptor due to the offending transmitter. The NWDIS line shows positive integrated margins due to two of the three upper transmitting antennas radiating through the canopy, but does not show any interference from any of the lower antennas that do not have a line-of-sight path to the canopy. The NGAGE line shows a positive integrated margin due to two of the three lower antennas radiating through the nose wheel well, but does not show any interference from any of the upper antennas that do not have a line-of-sight path to the nose wheel well. The LBAO line shows interference from the lower UHF through the nose wheel well, but not from the lower IFF or any of the upper antennas.

The NWDIS has an integrated margin of 2.8 and 1.5 dB from the COMUP and IFFUP, respectively, and similarly the NGAGE has an integrated margin of 9.0 and 7.8 dB from the COMLO and IFFLO, respectively. The TACAN puts out less average power than the UHF or IFF transmitters and is not predicted to be an interferer. The LBAO has an integrated margin of 0.8 dB due to the CMLO.

All three victim wires have one thing in common - they are 28 volt DC relays and cannot really respond to the high frequency AC signals because of eddy current and hysteresis losses and high dynamic impedances. This accounts for the fact that thepredicted positive integrated margins of up to 20 dB do not correspond to actual interference situations. The 20 dB integrated margin corresponds to approximately 0.6 amps of induced current on the NGAGE line, a 1 amp DC relay, at about 1 GHz. The actual impedance of the solenoid is probably much higher than the predicted, and the B-field produced by current through the solenoid at such a high frequency is very small.

Results of the sensitivity study indicate that the integrated margin is very insensitive to the exact coordinates of the aperture location, as long as the aperture remains on the same side of the fuselage. Consequently, the antenna-to-wire results would be essentially unchanged if the apertures were assumed to be displaced several feet from their present positions.

111

Table 7. Summary of Antenna-to-Wire Interference Predictions

	Bundle	Receptor	Aperture	Interfering Emitter	Integrated Margin	Notes
Minisystem B1	II-4	NWDIS	Canopy	COMUP IFFUP	2.8 1.5	1 1
Minisystem B2	B1	T2QNT T2LOW	Speedbrake Speedbrake	(None) (None)		2
	B3	LBAO	Nose Wheel Well	COMLO	0.8	1
	B8	DCREL XDEF YDEF HVPS	Canopy Canopy Canopy Canopy	(None) (None) (None) (None)		3 3 3 3
	B9	CAUTN PNLIT DCPWR	Canopy Canopy Canopy	(None) (None) (None)		3 3 3
Minisystem B3	B10	SPEED WOWIN WWREL	Left Wheel Well Left Wheel Well Left Wheel Well	(None) (None) (None)		
	B14	NGAGE NWWSW LLITE	Nose Wheel Well Nose Wheel Well Nose Wheel Well	COMLO IFFLO (None) (None)	9.0 7.8	1 1
	B17	PASIG PAEXC ROLLB	Canopy Canopy Canopy	(None) (None) (None)		4 4 4

GP77-0342-6

Notes:

1. Receptor is a DC relay that cannot actually respond at UHF and L-band.
2. Receptor is shielded to eliminate interference from upper UHF (COMUP).
3. Receptors are shielded to eliminate interference from environmental field.
4. Receptors are filtered to eliminate UHF interference.

112
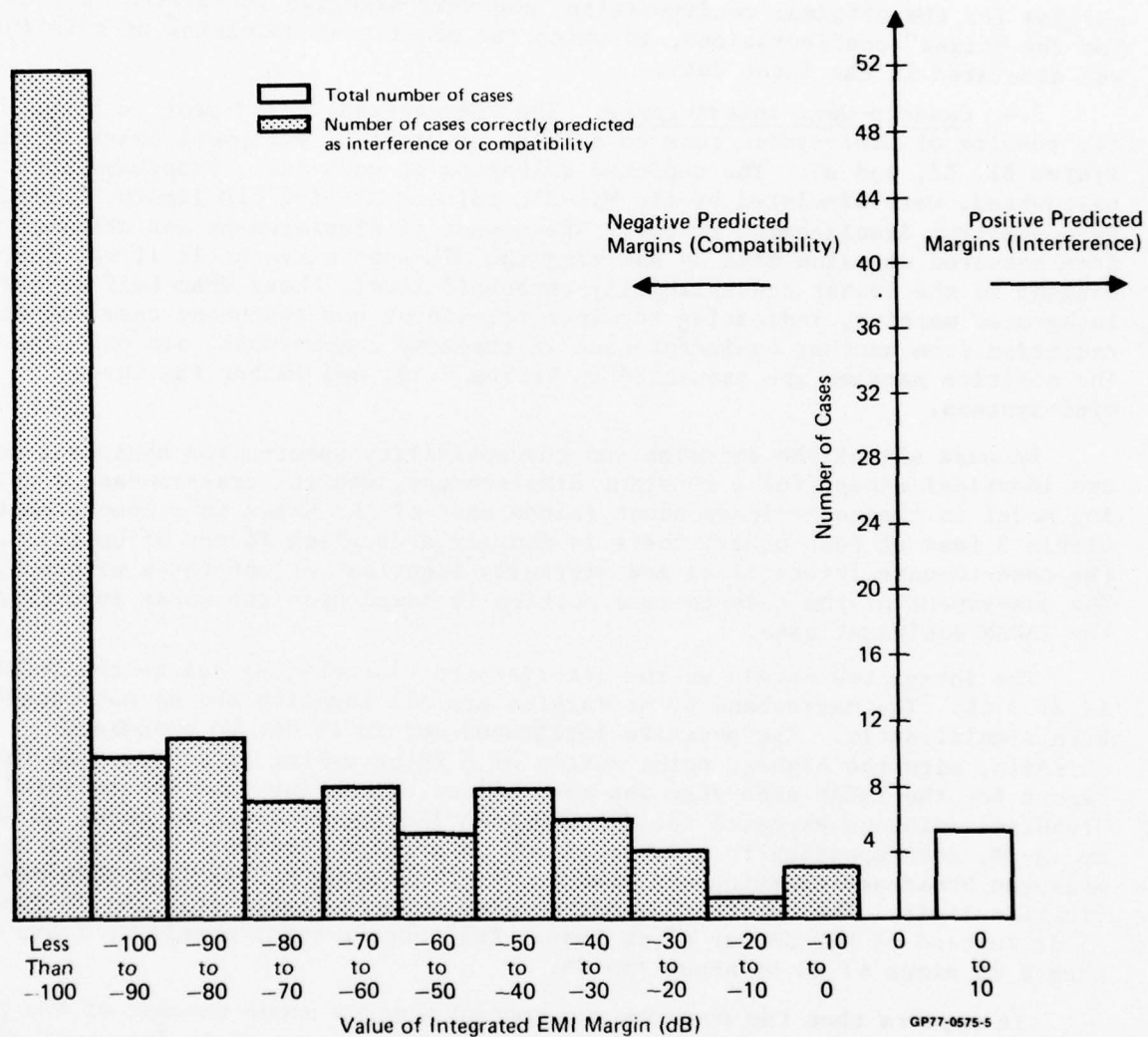
Figure 21. Distribution of Predicted Antenna-to-Wire Integrated Margins

113

The antenna-to-wire results generally confirm the compatibility of the F-15 aircraft, and the wires with positive integrated margin of up to 9 dB are explainable by the difficulty in modeling the susceptibility of devices such as a DC relay at UHF and L-band frequencies.

These results are reinforced by the simulation of the 3 actual cases of field-to-wire coupled interference described in Section 3.6. These cases involved interference from the upper UHF antenna to the fuel gauge, from an external UHF antenna (such as from another F-15 aircraft flying nearby) to the stick force sensor wires, and from environmental fields to the HUD wires. In each case, the IEMCAP predicted slightly positive or slight negative integrated margins for the original configuration, and very negative integrated margins for the "fixed" configurations, in which the additional shielding or twisting was simulated in the input data.

3.4 Case-to-Case Interference. The case-to-case assessment is based on the results of mini-system runs on a total of about 40 equipment cases in Mini-system B1, B2, and B3. The radiated emissions of each case, broadband and narrowband, were simulated by the MIL-STD-461A or MIL-I-6181D limits, shifted by a spectrum displacement factor. The amount of displacement was obtained from measured emission data by shifting the MIL-spec curve until it was just tangent to the lowest susceptibility threshold level. Less than half of the integrated margins, indicating the interference at one equipment case due to radiation from another equipment case in the same compartment, are positive. The positive margins are tabulated in Tables 8, 9, and 10 for the three mini-systems.

Because all of the emission and susceptibility spectra for equipment cases are identical except for a constant displacement, and the case-to-case coupling model is frequency-independent (since most of the boxes in a compartment are within 3 feet of each other, there is usually a coupling factor of unity), all the case-to-case interactions are virtually identical except for a constant. The assessment of the case-to-case portion is based upon the worst interferer, the TACAN equipment case.

The integrated margin at the interference blanker (IB) due to the TACAN is 27.3 dB. The narrowband point margins are all negative and do not contribute significantly. The positive integrated margin is due to broadband emission, with the highest point margin of 8 dB occurring at 1 GHz. The test report for the TACAN subsystem was re-examined, revealing that the measured broadband emission exceeded the MIL-STD-461A (Notice 3) limit at about 60 MHz by 42 dB, corresponding to a level of 102 dB μV/MHz. However, at 1 GHz, the measured broadband emission was down to 75 dB μV/MHz, or 5 dB less than specification limit. The "correct" spectrum displacement factor at 1 GHz is really -5 dB instead of +42 dB, or 47 dB less. The correct point margin at 1 GHz is then 8 dB minus 47 dB or about -39 dB.

It appears that the positive integrated margins occur because of the poor approximation of actual broadband emission levels at the upper frequency of 1 GHz, where they count more. For example, a level of 1 volt/meter/MHz distributed over a one MHz interval contributes much less to the integrated margin than the same level distributed over a one GHz interval.

The TACAN is the worst interferer, and the margins due to other equipment cases are all less than the margins due to the TACAN, and the highest point margins are generally still negative, even at 1 GHz.

114

Table 8. Mini-System B1 Case-to-Case Interference Predictions

Receptor	Emitter	Integrated Margins
IB	INS	7.3
	TACAN	27.3
	ADF	6.3
	IFT	3.1
	FDA	13.3
	IFFRE	11.3
	Total	27.6
INS	TACAN	27.3
	ADF	6.3
	IFT	3.1
	FDA	13.3
	IFFRE	11.3
	Total	27.6
TACAN	INS	6.8
	ADF	5.8
	IFT	4.3
	FDA	12.8
	IFFRE	10.8
	Total	16.3
ILS	INS	7.3
	TACAN	27.3
	ADF	6.3
	IFT	3.1
	FDA	13.3
	IFFRE	11.3
	Total	27.6
ADF	INS	7.3
	TACAN	27.3
	IFT	3.1
	FDA	13.3
	IFFRE	11.3
	Total	27.6
UHF	IB	12.4
	INS	31.4
	TACAN	51.9
	ADF	30.4
	AUX	5.1
	IFT	28.5
	ADC	15.4
	FDA	37.4
	Pitch	8.4
	IFFRE	35.4
	EWWS	0.4
	Total	52.2
ADC	FDA	13.2
	IFFRE	11.3
	Total	27.6
HUDSP	Fired	6.3
	Total	6.4
VSD	Fired	6.3
	Total	6.5

Receptor	Emitter	Integrated Margins
FDA	INS	7.3
	TACAN	27.3
	ADF	6.3
	IFT	3.1
	IFFRE	11.3
	Total	27.5
Pitch	INS	7.3
	TACAN	27.3
	ADF	6.3
	IFT	3.1
	FDA	13.3
	IFFRE	11.3
	Total	27.7
AUX	IB	13.6
	INS	32.6
	TACAN	52.3
	ADF	31.6
	UHF	4.2
	IFT	28.5
	ADC	16.6
	FDA	38.6
	Pitch	9.6
	IFFRE	36.6
	EWWS	1.6
	Total	52.7
IFT	INS	5.5
	TACAN	27.1
	ADF	4.5
	FDA	11.5
	IFFRE	9.5
	Total	27.3
CC	Fired	6.3
	Total	6.5
ADC	INS	7.3
	TACAN	27.3
	ADF	6.3
	IFT	2.0
	FDA	13.2
	IFFRE	11.3
	Total	27.6
IFFRE	INS	7.3
	TACAN	27.3
	ADF	6.3
	FDA	13.3
	Total	27.5
EWWS	INS	7.3
	TACAN	27.3
	ADF	6.3
	IFT	3.1
	FDA	13.3
	IFFRE	11.3
	Total	27.7

GP77-0276-5

115

Table 9. Mini-System B2 Case-to-Case Interference Predictions

Receptor	Emitter	Integrated Margin
INS	TACAN	27.3
	ADF	6.3
	IFT	3.1
	FDA	13.3
	Total	27.5
TACAN	INS	6.8
	ADF	5.8
	IFT	4.3
	FDA	12.8
	Total	14.8
ILS	INS	7.3
	TACAN	27.3
	ADF	6.3
	IFT	3.1
	FDA	13.3
	Total	27.5
UHFCO	INS	31.4
	TACAN	51.9
	AUX	5.1
	ADF	30.4
	IFT	28.5
	ADC	15.4
	FDA	37.4
	Roll	8.4
	Total	52.1
AUX	INS	32.6
	TACAN	52.3
	UHFCO	4.2
	ADF	31.6
	IFT	28.5
	ADC	16.6
	FDA	38.6
	Roll	9.6
	Total	52.5
ADF	INS	7.3
	TACAN	27.3
	IFT	3.1

Receptor	Emitter	Integrated Margin
ADF	FDA	13.3
	Total	27.5
IFT	INS	5.5
	TACAN	27.1
	ADF	4.5
	FDA	11.5
	Total	27.3
ADC	INS	7.3
	TACAN	27.3
	ADF	6.3
	IFT	2.0
	FDA	13.3
	Total	27.5
FDA	INS	7.3
	TACAN	27.3
	ADF	6.3
	IFT	3.1
	Total	27.4
Roll	INS	7.3
	TACAN	27.3
	ADF	6.3
	IFT	3.1
	FDA	13.3
	Total	27.5

GP77-0276-7

116

Table 10. Mini-System B3 Case-to-Case Interference Predicitons

Receptor	Emitter	Integrated Margin
RFOSC	XMTR	0.3
	DIGPR	0.3
	DATAP	0.3
	Total	5.1
XMTR	RFOSC	0.3
	DIGPR	0.3
	DATAP	0.3
	Total	5.1
DIGPR	RFOSC	0.3
	XMTR	0.3
	DATAP	0.3
	Total	5.1
DATAP	RFOSC	0.3
	XMTR	0.3
	DIGPR	0.3
	Total	5.1
UHFCO	AUX	5.1
	ADF	30.4
	IFFX	28.5
	TACAN	51.9
	Roll	8.4
	Pitch	8.0
	EWWS	0.4
	Total	51.9
AUX	UHFCO	4.2
	ADF	31.6
	IFFX	28.5
	TACAN	52.3
	Roll	9.6
	Pitch	7.7
	EWWS	1.6
	Total	52.4

Receptor	Emitter	Integrated Margin
ADF	IFFX	3.1
	TACAN	27.3
	Total	27.3
IFFX	ADF	4.5
	TACAN	27.1
	Total	27.1
TACAN	ADF	5.8
	IFFX	4.3
	Total	8.5
ILS	ADF	6.3
	IFFX	3.1
	TACAN	27.3
	Total	27.3
Roll	ADF	6.3
	IFFX	3.1
	TACAN	27.3
	Total	27.3
Pitch	ADF	5.4
	IFFX	3.7
	TACAN	27.1
	Total	27.2
EWWS	ADF	6.3
	IFFX	3.1
	TACAN	27.3
	Total	27.3

GP77-0276-8

117

Integrated margins at the UHF and AUX equipment cases are about 25 dB greater than at the other boxes because the MIL-I-6181D susceptibility limits are about 25 dB lower than the MIL-STD-461A limits. Since the equipments were only tested to the spec limits, it is possible that they are actually much less susceptible.

The overall assessment of case-to-case is that the program essentially does what it is supposed to do with the relatively crude model for radiated interference, and that the positive integrated margins occur because of the discrepancy between measured and simulated broadband emission in the Giga-hertz region. The point margins are generally negative, consistent with compatibility.

3.5 SGR Assessment. As described previously in Section 2.1, a CEAR-survey run on the F-15 antenna ports predicted 17 cases of antenna-to-antenna coupled interference. This baseline was subsequently used as input to a Specification Generation run to determine if the IEMCAP SGR routine performed satisfactorily. The results of this run were used as a basis for the SGR assessment.

Both the CEAR baseline run and the SGR run were carried out on a mini-system with a detailed, judiciously picked frequency quantization of the emission and susceptibility spectra, with a total of 40 frequencies per equipment. As demonstrated in the Sensitivity Analysis (Section 4), the use of 90 frequencies does not change the results very much when the frequencies are picked judiciously in the first place. The integrated EMI margin was shown to be very insensitive to the addition of extra frequencies. The amount of spectrum adjustment did change when 90 frequencies were used instead of 40, usually a rather random process having to do with the way the extra frequencies are geometrically spaced. This effect is illustrated in Section 4.4.

To allow the code the widest latitude in adjusting emission and suscept-ibility spectra, an adjustment limit of 70 dB and an adjustment safety margin of 6 dB were used. This amount of adjustment may not always be practical for actual equipments, but it was chosen to see how the code treated the variety of interference situations predicted for the baseline.

A summary of the results is given in Table 11. The 17 interference situa-tions are listed by receiver, followed by each interfering transmitter and the baseline integrated EMI margin. The next two columns indicate the amount of emitter adjustment in the interfering transmitter's unrequired region and the new integrated EMI margin. The last two columns indicate the amount of recep-tor adjustment (at the tuned frequency of that particular emitter) and the final integrated margin for that emitter-receptor combination.

Beginning with the upper UHF receiver (COMUP) at the top of Table 11, the upper TACAN transmitter (TACUP) is seen to cause a 36.2 dB integrated margin in the baseline system. The TACUP unrequired emission was adjusted down by 41.6 dB in the COMUP passband, bringing the integrated margin down to -3.9 dB. This eliminated interference from the TACUP to the COMUP, and no receptor adjust-ment was necessary at the tuned frequency of the TACUP. Since there were no other interfering transmitters, the COMUP was compatible and its susceptibility spectrum was not adjusted anywhere.

118

Table 11. Summary of SGR Validation Results

Receptor	Emitter	Baseline Integrated Margin (dB)	Amount of Emitter Adjustment (dB)	Emitter Adjusted Margin (dB)	Amount of Receptor Adjustment (dB)	Receptor Adjusted Margin (dB)
COMUP	TACUP	36.2	41.6	−3.9	0	−3.9
AUX	COMUP	16.6	0	16.6	56.5	−10.0
	COMLO	50.1	27.5	50.1	56.5	20.0
ADF	COMUP	2.1	0	2.1	7.9	−1.1
	TACUP	8.1	0	7.2	13.9	−5.7
IFFUP	TACUP	40.6	27.5	40.6	47.2	1.1
IFFLO	TACLO	33.8	20.7	33.7	40.4	−1.9
TACUP	COMUP	15.9	0	15.9	22.4	−6.0
	IFFUP	41.2	47.1	24.0	31.0	3.7
TACLO	IFFLO	34.3	40.2	17.2	29.1	1.7
LOCAL	COMLO	6.4	0	6.3	12.5	−0.7
	TACLO	27.9	0	27.9	34.5	−1.8
GLIDE	COMLO	6.0	0	6.0	12.5	−2.6
	TACLO	27.9	0	27.9	34.5	−2.4
Marker Beacon	COMLO	25.5	0	25.5	32.0	3.8
	IFFLO	13.6	0	13.6	27.9	−8.2
	TACLO	20.3	0	20.3	27.9	−4.3

GP77-0342-7

119

This process is illustrated in Figure 22. The baseline received signal at the COMUP due to the TACUP, plotted with the dashed line, is compared with the susceptibility of the COMUP. At the emitter frequency of 165.54 MHz, the total received signal is less than the susceptibility. At the next emitter frequency of 323.45 MHz, the total received signal is again less than the susceptibility. However, a backsearch to the receptor frequency of 320.65 MHz reveals that the interpolated received signal greatly exceeds the susceptibility there. The emission spectrum is then adjusted down by 41.6 dB at the two emitter frequencies straddling the receptor frequency, bringing the total received signal at the receptor frequency below the susceptibility by the 6 dB safety margin, corresponding to the new integrated margin of -3.9 dB.
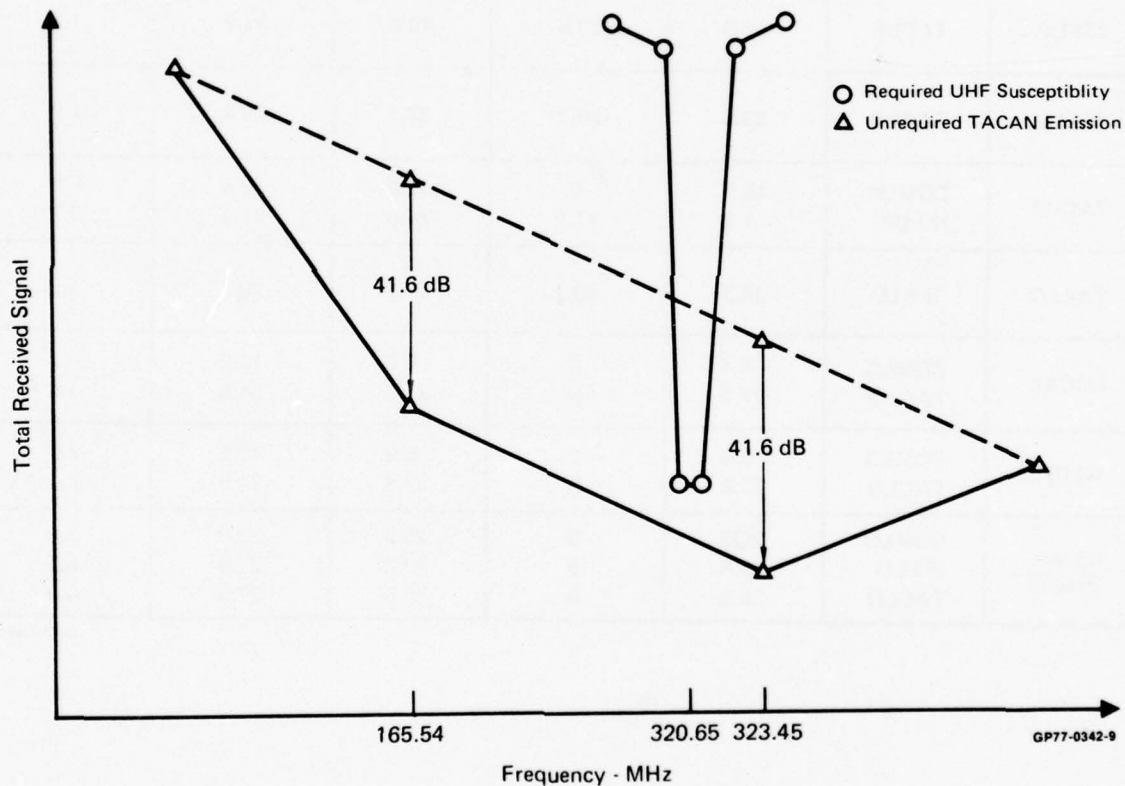
Figure 22 Example of SGR Emitters Adjustment (Back Search) Upper TACAN to Upper UHF

120

The next receptor is the AUX, with a baseline integrated margin of 16.6 dB due to the COMUP. This time there is no emitter adjustment, since the only interference is due to required COMUP emission to unrequired AUX reception. The susceptibility of the AUX is adjusted upward by 56.5 dB in the vicinity of the COMUP tuned frequency, reducing the integrated margin to -10 dB. This is possible only because the AUX was not represented as a tunable receiver. In practice, the AUX tunes over the same UHF band as the UHF transmitter and the actual interference was handled by receiver suppression when the UHF transmitter is keyed. The remaining interferer is the lower UHF transmitter (COMLO), on the same side of the fuselage as the AUX, resulting in an integrated margin of 50.1 dB. This time there is interference from unrequired COMLO emission, and the COMLO is adjusted by 27.5 dB in the region of the AUX tuned frequency. The integrated margin is not changed, however, because the dominant interference mode is still required emission to unrequired AUX susceptibility (at this point the AUX susceptibility spectra has not yet been adjusted, since the emitter adjustments are performed first). After the 56.5 dB receptor adjustment, the integrated margin is brought down to 20.0 dB. This case is illustrated in Figure 23.
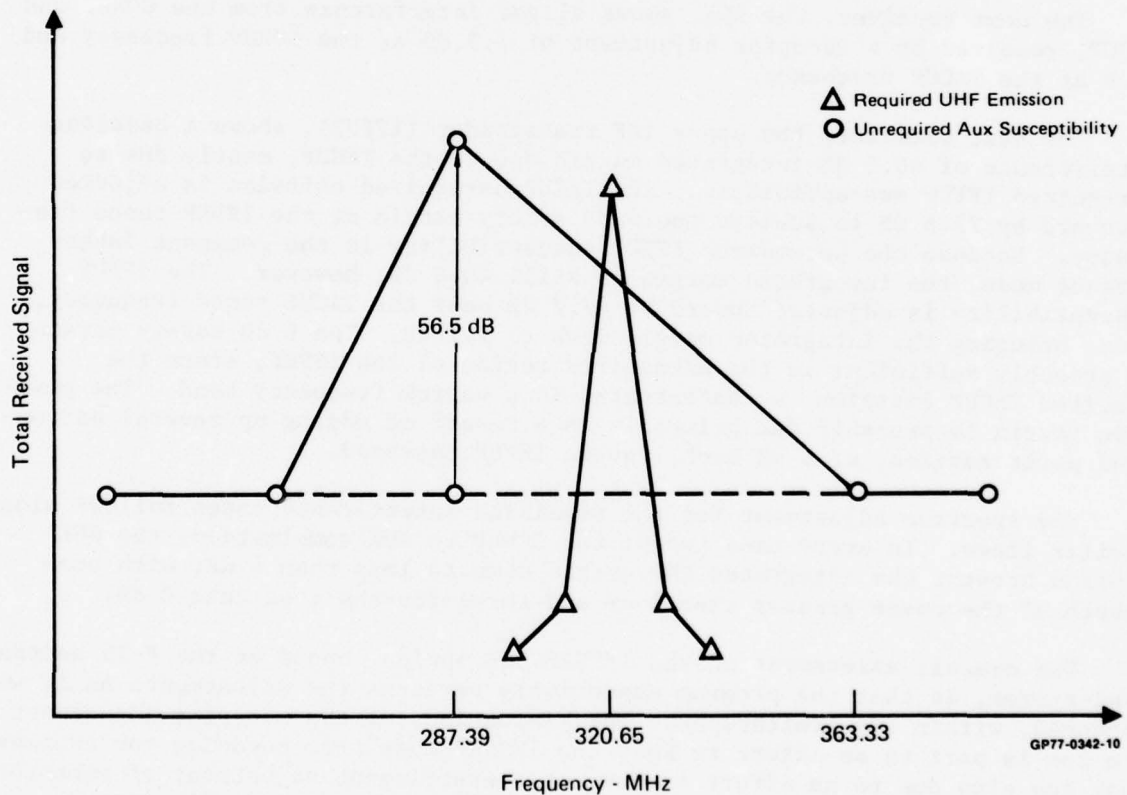
Figure 23 Example of SGR Receptor Adjustment

121

Looking at Figure 23, the required UHF emission at 320.65 MHz exceeds the baseline AUX susceptibility threshold, plotted with the dashed line. The emitter frequency is straddled by the two receptor frequencies of 287.39 Mhz and 363.33 MHz. Since the emitter frequency is slightly closer to the lower frequency, the total received signal is quantized as if it occurred at 287.39 MHz and the AUX susceptibility is adjusted upward by 56.5 dB at that point, so that it exceeds the total received signal by the 6 dB safety margin. However, when the code goes back and computes the integrated margin due to the COMLO, it uses the interpolated value of the AUX susceptibility at 320.65 MHz, which falls below the received signal at that frequency. Thus the integrated margin is still positive, 20.0 dB. This is a case where the limitations of the receptor adjustment routine make it difficult to achieve compatibility. The problem is aggravated by the fact that the emitter frequency falls almost in the exact middle of the two receptor frequencies. If the emitter frequency were closer to the lower receptor frequency, the adjustment at that receptor frequency would cause the interpolated susceptibility at the emitter frequency to be much higher. Similarly, if the emitter frequency were much closer to the upper receptor frequency, the receptor adjustment would have been performed at the upper frequency, and the interpolated susceptibility at the emitter frequency would have been higher.

The next receiver, the ADF, shows slight interference from the COMUP and TACUP, resolved by a receptor adjustment of 7.9 dB at the COMUP frequency and 13.9 at the TACUP frequency.

The next receiver, the upper IFF transponder (IFFUP), shows a baseline interference of 40.6 dB integrated margin due to the TACUP, mostly due to unrequired IFFUP susceptibility. The TACUP unrequired emission is adjusted downward by 27.5 dB to achieve the 6 dB safety margin at the IFFUP tuned frequency. Because the unrequired IFFUP susceptibility is the dominant interference mode, the integrated margin is still 40.6 dB, however. The IFFUP susceptibility is adjusted upward by 47.2 dB near the TACUP tuned frequency, then, bringing the integrated margin down to 1.1 dB. The 6 dB safety margin is probably sufficient in the unrequired region of the IFFUP, since the required TACUP emission is concentrated in a narrow frequency band. The positive margin is probably due primarily as a result of adding up several narrow-band point margins, of 6 dB each, in the IFFUP passband.

The spectrum adjustment for the remaining interference cases follows along similar lines. In every case except the COMLO to AUX combination, the SGR routine brought the integrated EMI margin down to less than 4 dB, with one-fourth of the cases greater than 0 dB and three-fourths less than 0 dB.

The overall assessment of the IEMCAP SGR option, based on the F-15 antenna mini-system, is that the program essentially performs the adjustments as it was intended, within its limitations. The limitations of the receptor adjustment are due in part to an effort to keep the IEMCAP code from becoming too complex. They are also due to an effort to prevent overstringent adjustment of receptor spectra over too wide a frequency band. One solution in cases like interference to the AUX, is to re-run the program with a few more receptor frequencies in the region of interest.

122

3.6 <u>Simulation of Actual Interference</u>. As part of the overall assessment of the IEMCAP with F-15 mini-systems, four documented cases of interference on the aircraft were simulated for IEMCAP analysis. All four cases of EMI were corrected by means of shielding or filtering equipment on production aircraft. The IEMCAP simulation was set up to test whether the program would predict the original interference, and also whether it would predict the elimination of that interference with the simulation of the actual shielding or filtering used. The following is a brief case history of each EMI situation and the results of the simulation.

3.6.1 Interference from external UHF antenna into AFC wiring. A test was performed on a trainer version of the F-15 to assess the electromagnetic susceptibility of the Automatic Flight Control Set (AFCS). The primary con-cern was radiation into the cockpit from transmitters on aircraft flying in close proximity above the cockpit.

The AFCS was turned on with the pilot's control stick pinned at its base so as to apply constant pressure to the stick force sensor. Antennas simu-lating F-15 transmissions were then aimed at the pilot's control stick, the most vulnerable area. The field intensity at each test frequency was slowly increased until a stabilator response was observed (1/4 inch movement) or the specification 200 volts per meter was reached.

The results showed a serious RF susceptibility throughout the UHF communi-cations band, 225 to 400 MHz, the most susceptible point occurring at 400 MHz. The RF radiation was picked up on the wire bundle leading from the AFCS stick force sensor to the cockpit floor.

The susceptibility threshold was dependent on the modulation used, the worst case being a 400 Hz tone with 100% modulation. For this case, the threshold field was 3 volts/meter, corresponding to the level that would be generated by the UHF antenna of an aircraft flying 40 feet above the victim aircraft.

The interference showed up as oscillations of the stabilator at the beat frequency between the modulation tone and the aircraft's primary power frequency. A similar effect was obtained with a low male voice.

The problem was eliminated by a modification of the stick force sensor, using a low pass filter to keep the RF out of the low frequency amplifier. The vendor performed susceptibility tests on the AFCS both before and after the insertion of a 2000 pf feedthrough capacitor. The susceptibility was found to be 0.5 volts/meter without the filter and 230 volts/meter with the filter, an effective filtering of 53.3 db.

3.6.1.1 Results of IEMCAP simulation. The control stick wire ports (Bundle B17 in Mini-system B3) were simulated as if the modulation on the receiver RF carrier was stripped off and detected by the stick force sensor amplifier with 100% efficiency. This was done by treating them as aperture-exposed RF receptor ports with a susceptibility in the 225-400 MHz UHF band of 20 dB less than the normal operating level. The low pass filter was simulated as a 4th order Butterworth filter with a bandwidth of 1.59 MHz

123

and a maximum isolation of 53.3 dB, based on the estimated impedance of 50 ohms in the vicinity of 1 MHz and the 2000 pf shunting capacitance. The interfering source was simulated as a 0.5 volt/meter entironmental field from 14 kHz to 18 GHz. The results of the simulation, with and without the low pass filter, are summarized in Table 12 for the pitch A signal wire (PASIG), the pitch A excitation wire (PAEXC), and the roll B signal wire (ROLLB). Since environmental field in IEMCAP is modeled as narrowband emission existing in every standard bandwidth interval, the point margin represents the interference due to a single UHF source at the given frequency. Without the filter, the environmental field resulted in a point margin of +2.3 dB at all frequencies between 225 and 400 MHz for the PASIG and ROLLB ports. With the filter, the environmental field resulted in a point margin of -51 dB at those frequencies. So the program predicted the original interference and also predicted the elimination of the interference by the filter. Since the 0.5 volt/meter is the threshold field, below which there is no interference to the unfiltered stick force sensor, the margin should theoretically be 0 dB. Thus, the computed margins for the PASIG and ROLLB in the unfiltered configuration overpredict the actual interference by 2.3 dB.

Table 12. Simulation of External UHF Interference to AFCS Wires
0.5 Volt/Meter Environmental Field

Receptor	Highest Point Margin (Unfiltered Configuration)	Highest Point Margin (Filtered Configuration)
PASIG (Pitch A Signal)	+2.3 (229 MHz)	−51.0 (229 MHz)
PAEXC (Pitch A Excitation)	−13.0 (252 MHz)	−66.3 (252 MHz)
ROLLB (Roll B Signal)	+2.3 (252 MHz)	−51.0 (252 MHz)

GP77-0342-1

The environmental field resulted in a point margin of -13.0 dB for the PAEXC in the unfiltered configuration, and -66.3 dB in the filtered configuration. The code did not, then, predict any interference to this port. This is not really a discrepancy, because it is not known precisely which of the wires in the bundle leading to the stick were susceptible, and which were not, as the entire bundle was irradiated in the test.

On the basis of this simulation, the program was extremely accurate in predicting interference to the AFCS and its subsequent fix, given the knowledge of a non-linear response at UHF frequencies. Of course, there is no way the program could have predicted the existence of that non-linear response in advance.

3.6.2 Interference from upper UHF antenna to fuel gauge. The problem originally manifested itself on an early F-15 with a metal speedbrake, when transmitting UHF through the upper antenna. With the speedbrake door open, the radiated field was picked up on a wire routed through the speedbrake com-

124

partment on its way from No. 2 fuel tank to the fuel quantity indicator, causing an error in the reading.

The problem was resolved by shielding all fuel gage wiring in the speed-brake area, and the use of EMI backshells. After the metal speedbrake was replaced by a composite speedbrake, however, the problem reappeared, this time whenever the speedbrake door was closed. This seeming paradox was thought to arise because the closed composite speedbrake door could not be effectively bonded to the airframe, permitting aperture coupling from the upper UHF antenna, while the open speedbrake door deflected the radiation from the wiring.

With the composite speedbrake door closed (within 8 inches) and the UHF antenna transmitting at frequencies of 386.9 to 394.9 MHz, the Tank 2 fuel indicator displayed 125 pounds fuel fluctuation, the specifications allowing only 60 pounds fluctuation. A field intensity meter showed an incident field of approximately 40 volts/meter in the vicinity of the speedbrake. The problem was eliminated by grounding the shields on the fuel gage wires to the airframe in several places, so that the fluctuations in the fuel quantity indicator were brought down to tolerable levels.

3.6.2.1 Results of IEMCAP simulation. The fuel gage, (Bundle B1 in Mini-system B2) like the AFCS, picked the modulation off an RF carrier, the modulation signal causing the interference to a low frequency circuit. In this case, the demodulated signal was very similar to the operating waveform, so that the system was very susceptible to the undesired signal. The susceptibility threshold of the fuel gauge was taken to be 40 dB under the normal operating level. Assuming 100% demodulation efficiency, the fuel gage was modeled as an RF receptor operating in the 225-400 MHz UHF band exposed through the speed-brake aperture to radiation from the upper UHF antenna. The corrective shield was modeled by replacing an unshielded twisted pair by a shielded twisted pair, ground at both ends, in the input data. The results of the IEMCAP simulation are summarized in Table 13. The integrated EMI margin at the fuel quantity indicator in the unshielded configuration, due to the upper UHF transmitter, is -8.4 dB. The integrated margin in the shielded configuration is reduced to -45.7 dB. Because the UHF interference is contained in a relatively small bandwidth centered about the tuned frequency of 320.65 MHz, this reduction is entirely due to a 37.3 reduction in the antenna-to-wire transfer function at 320.65 MHz.

Table 13. Simulation of Upper UHF Interference to Fuel Gauge Wires

Output Quantity	Original Configuration (Unshielded, Twisted)	Fixed Configuration (Shielded, Twisted)
Integrated Margin	−8.4 dB	−45.7 dB
Point Margin at 320.65 MHz	−8.9 dB	−46.3 dB
Transfer Function at 320.65 MHz	−58.8 dB	−96.1 dB

GP77-0342-2

125

The program failed to predict the original interference by an error of at least 8.4 dB, although it predicted the lack of interference in the shielded configuration. With all the worst case assumptions built into the antenna-to-wire coupling model, the assumption of a susceptibility 40 dB below operating level, and 100% demodulation efficiency, it would appear strange that the program still predicted compatibility in the unshielded configuration. However, the actual interference situation was thought to be exacerbated by a UHF resonance of the speedbrake door, so that the actual electromagnetic field incident on the wire was probably greater than the unperturbed field incident on the aperture. The code, on the other hand, simulates field to wire coupling with an idealized free-space model, assuming the wire is illuminated by an incident plane wave all along the exposed length. This simple model is not capable of predicting a resonance situation.

3.6.3 Interference from environmental field to HUD wires. The HUD set originally showed a vulnerability to a 20 volt/meter E-field in MIL-STD-462 radiated susceptibility tests of the HUD subsystem, showing up as flicker and jitter in the display. This interference was brought down to tolerable levels during the test by wrapping aluminum foil around the cables from the HUD signal processor to the HUD control panel.

The problem also showed up during ground tests of the entire aircraft conducted in a hangar; the ambient fields from electrical equipment and any other sources inside the hangar resulted in disturbances to the display.

The problem was eliminated by putting an overbraid shield over the cable of wires leading from the signal processor to the control panel. This was a dedicated cable containing only wires between the two boxes, eliminating parasitic effects due to additional wires entering the wire bundle, enabling the overbraid to serve as a fairly effective Faraday shield.

3.6.3.1 Results of IEMCAP simulation. A total of 5 HUD wires were simulated (Bundles B8 and B9 in Mini-system B2). All but one of the wires are power lines for which measured MIL-STD-461A conducted susceptibility data was used. The power lines were suspect because of the results of tests performed on the HUD indicating a susceptibility to inductive radiated susceptibility (RS02) and conducted interference (RS01 and CS02), as well as plane wave interference (RS03). The overbraid correction was simulated by substituting shielded wires for all the unshielded wires in the input data. The environmental field was simulated by a 20 volt/meter environmental field from 14 kHz to 1GHz.

The results of the simulation are summarized in Table 14, indicating the point margins at the DC relay line (DCREL), the high voltage power supply line (HVPS), the panel lighting power line (PNLIPO, the 28 volt DC power line, and the master caution light (CAUTN), both with and without the shield. Since the frequency of the ambient field causing the problem was unknown, point margins were recorded at 14 kHz, 1.79 MHz, 14.3 MHz, and 229 MHz.

126

Table 14. Simulation of Interference from Environmental Field to Hud Wires

Receptor	EMI Margin			
	14 kHz	1.79 MHz	14.3 MHz	229 MHz
DCREL				
Unshielded Configuration	−57.0	−12.7	+5.4	+18.2
Shielded Configuration	−66.2	−65.8	−48.7	−21.4
HVPS				
Unshielded Configuration	−42.8	+1.6	+19.7	+27.3
Shielded Configuration	−52.0	−51.5	−34.4	−12.3
PNLIT				
Unshielded Configuration	−46.7	−7.8	+10.3	+13.9
Shielded Configuration	−56.0	−60.9	−43.8	−25.7
DCPWR				
Unshielded Configuration	−48.7	−4.4	+13.6	+18.3
Shielded Configuration	−57.9	−57.6	−40.4	−21.3
CAUTN				
Unshielded Configuration	−72.7	−30.5	−12.4	−1.3
Shielded Configuration	−81.9	−83.6	−66.5	−40.8

GP77-0342-3

All of the power lines had positive point margins in the unshielded configuration. The CAUTN had a point margin of −1.3 dB at 229 MHz. None of the wire ports had positive margins in the shielded configuration. Based on these results, the code did predict the original interference and also the subsequent elimination of interference by shielding.

3.6.4 Interference from nose wheel steering to central computer reset. It was suspected in advance that the reset line that re-initializes the central computer would be vulnerable to EMI, because of the low threshold. The original design called for an unshielded configuration, with the understanding that a shield could always be incorporated if problems developed. Although interference was observed on the reset line in an avionics mockup of the F-15, it was decided to wait and see whether it was a problem on an actual aircraft before changing to a shielded configuration on the production aircraft.

It turned out that there really was a problem. A number of lines carrying switching transients tended to trigger the reset line, such as the seat motor, flap actuator and other lines that switch solenoids. Subsequently, the disconnect line, which runs in the same bundle as the central computer reset line, was chosen as the potential interferer in the mini-system lists.

The central computer reset line was shielded, eliminating the problem.

3.6.4.1 Results of IEMCAP simulation. The nose wheel steering disconnect line (Bundle II-4, Mini-system B1), which runs in the same bundle as the central computer reset line, was selected as the interferer. It was modeled as a 28 volt rectangular pulse with a period of 1 second. The reset line was modeled as having a required susceptibility 20 dB down from the operating level and an unrequired susceptibility of 1 watt.

127

The results of the simulation are summarized in Table 15. The integrated margin at the central computer reset port is −63 dB in the unshielded configuration and −104.0 dB in the shielded configuration. The highest point margin of −58 dB at 62.9 MHz is the response to the MIL-STD-461A emission level in the vicinity of 50 MHz, the upper frequency limit for that specification.

Table 15. Simulation of Interference From Nose Wheel Steering To Central Computer Reset Wire

Output Quantity	Original Configuration (Unshielded, Twisted)	Fixed Configuration (Shielded, Twisted)
Integrated Margin	−63.0	−104.0
Highest Point Margin (62.9 MHz)	−58.0	−119.5
Transfer Function (67.9 MHz)	−28.9	−90.4

GP77-0342-4

It is clear that the IEMCAP failed to predict the interference by a wide margin of error. The reason for this failure is that the integrated margin concept is only valid for devices that respond to average power, and the central computer reset line is a threshold − sensitive line that responds to transients. The average power coupled from the nose wheel disconnect line to the reset line is extremely small but the peak voltage coupled to the reset line is high, because of the short rise time and the inductive effects of the relay. This case serves as an example of the limitations of the code when dealing with threshold-vulnerable devices.

3.7 <u>Conclusions and Recommendations</u>. The results of IEMCAP runs on F-15 Mini-systems for the most part confirm the compatibility of the F-15 aircraft. The program performed reasonably well in the simulation of actual interference situations both before and after connector filtering or shielding, failing badly only for the case of a threshold-vulnerable device, a situation where the average power calculated by the IEMCAP is not an appropriate measure of interference. A discussion of receptor vulnerability with respect to average versus peak power is provided in Part II.

For those situations where the program incorrectly predicted interference, the cause in most cases is judged to be an overly pessimistic simulation of non-required emission (too high) and susceptibility levels (too low). For antenna-coupled interference, where measured coupling data can be directly compared with IEMCAP predictions, this conclusion is supported by the data. For interference coupled between wires, where measured coupling data is not available, it is more difficult to isolate the probable cause of positive margins, but the uncertainty in simulated emission and susceptibility levels is so large that it is bound to play a major role. The only cases of interference predicted between antennas and wires involve DC relays where the simulated susceptibility level is much lower than the actual level. Although there is no comparable measured coupling data, the results of simulating the 3 known

128

cases of antenna-to-wire interference lend confidence to the antenna-to-wire coupling predictions, supporting the conclusion that the overly pessimistic simulation of susceptibility is the probable cause of the discrepancies.

The results of the SGR runs confirm that the adjustments on emission and susceptibility levels are performed in a correct manner and also show that receptor adjustment may not always be successful in eliminating interference.

On the negative side, measured coupling data on a mock-up of the aircraft indicates that the antenna-to-antenna coupling model does not perform very well when simulating fuselage diffraction along coupling paths between antennas on opposite sides of the fuselage. The problem does not appear to be a code error, but the inadequacy of an idealized cylindrical model in attempting to simulate a more complex aircraft geometry. This problem should be looked into; however, in the absence of a more sophisticated model, the IEMCAP user should be aware of possible errors in antenna-to-antenna coupling when fuselage shading is involved.

Other than the problem with fuselage shading, the IEMCAP program appears to perform fairly satisfactorily. The source and receptor spectrum routines and coupling routines appear to function properly and work together properly and it has been demonstrated that the program is capable of processing a relatively large data base. In fact, by exercising the various routines for the multitude of equipments and configurations, a rather rigorous program shake-down resulted, uncovering a number of minor errors in both IDIPR and TART, as discussed in Section 2.4. The sensitivity analysis was especially useful in this regard. By re-running the program repeatedly with changes in input parameters under a variety of conditions, the various IEMCAP models were subjected to a great deal of scrutiny, particularly the wire-to-wire routines. This is not to say that all the bugs have been uncovered, but it can be said that the IEMCAP results seem reasonable for a variety of input configurations.

There are more considerations to an overall assessment of the IEMCAP code than just an evaluation of the printed outputs, however. The experience gained in running the IEMCAP on a real aircraft system has provided some insights into the program's strengths and weaknesses, and into its overall usefulness as an EMC tool.

The integrated EMI margin, as calculated by the IEMCAP, is used as a measure of compatibility or incompatibility of equipments whose performance is characterized in terms of average power. More precisely, the assumption is that the satisfactory performance of the device operating as part of the system as a whole can be correlated with the average received power at the detector or decision portion of the device. A more detailed explanation and physical interpretation of the integrated margin is provided in Part II of this report.

Since the validity of the integrated margin as a measure of compatibility is tied to the assumption that the performance of equipments is sensitive to average power, the usefulness of the IEMCAP as a tool in weapons system EMC analysis depends on the validity of that assumption for the equipments in the particular weapons system.

A survey of mini-system equipments used to simulate F-15 equipments was made to determine how many equipments can be characterized in terms of average power and how many cannot. This categorization was based on both the nature of each device itself (transistor logic, magnetic relay, analog amplifier, etc.) and on the relationship of the device output to satisfactory operation of the F-15 system as a whole. Outputs where an occasional error is acceptable because

129

of built-in redundancy were classified as average power-vulnerable and outputs where a single error is unacceptable were classified as threshold-vulnerable.

The survey of the F-15 equipments used in the mini-system indicated that the great majority of them (over 90%) are vulnerable to average power. All of the antenna ports and most of the wire ports can be categorized this way. In the list of wire ports, Table 1, the receptor ports that are threshold-vulnerable rather than average power-vulnerable are indicated with an asterisk. It should be noted that the central computer reset line, which was originally an actual victim of interference, is a threshold-vulnerable device that is susceptible to a transient.

Since the mini-system equipments were not selected with any bias in favor of average power-sensitive devices, they probably reflect the approximate percentage of such devices on the F-15. Thus, the integrated margin approach used in the IEMCAP is probably valid for most F-15 equipments.

It should be pointed out, though, that even though the threshold-vulnerable devices on the F-15 may be relatively few in number, they are probably the ones that are the most susceptible. In this respect, the IEMCAP is not equipped to predict possible cases of wire-to-wire interference.

It should also be pointed out, that even though the program performed very satisfactorily in the simulation of actual antenna-to-wire interference, in 2 out of 3 of those cases the results were based on the prior knowledge that those particular lines exhibited non-linear response at UHF frequencies. With this prior knowledge, it was possible to simulate the spurious response in the representation of the receptor spectra in the input deck. However, when the IEMCAP is used to analyze a weapons system without this prior knowledge, there is no way that it can predict interference due to non-linear effects. This is because the program is inherently based on a linear system model, i.e., based on the linear super-position of interfering signals at the receptor terminals. Yet RF interference picked up on exposed wires due to radiation from antennas is most likely to cause problems for lines that do exhibit non-linear responses at RF frequencies. Thus, the IEMCAP is not equipped to predict these important cases of antenna-to-wire interference.

It is not reasonable, however, to expect the IEMCAP to predict such interference without detailed information on device performance at RF frequencies. The program is only as good as the information provided to it. The simulation results indicate that as more detailed information becomes available, the antenna-to-wire routines do a fairly good job in analyzing such interference. One approach might be to initially model exposed lines as being vulnerable to such interference, and then to look more closely at lines where positive margins are predicted, obtaining more detailed information on them for further study.

The inability of the program to simulate threshold-vulnerable devices is a serious drawback, though. Even if detailed information on these devices is available, the program is not equipped to analyze interference to such devices,

130

where the average received power does not give a true indication of device performance. A possible remedy, involving a modification of the IEMCAP code, is suggested in Part II of this report. The modified code would accept both average power-vulnerable devices and threshold-vulnerable devices, as specified by the user. For the power-vulnerable devices it would calculate the integrated margin the way it normally does. For the threshold-vulnerable devices, however, it would add up all received signals as if they were in phase, integrating the current instead of the power, and compare the total received current or voltage with a threshold level. This ratio would be an integrated EMI margin based on threshold-vulnerable device performance.

131

4. SENSITIVITY STUDY

A sensitivity study was carried out on IEMCAP input parameters with the objectives of gaining insight into the effect of approximating input parameters on IEMCAP predictions. The sensitivity study was carried out as a test by varying input parameters and re-running the mini-systems to determine the sensitivity of IEMCAP output parameters to those variations.

A total of 18 input parameter types were varied and correlated with the resulting changes in up to 5 output parameters, with emphasis on the integrated margin and point margin, summarized in the overall test matrix, Table 16. The study is divided into 4 parts. The first 3 portions, antenna-to-antenna, wire-to-wire, and antenna-to-wire, deal with the effects of input parameter variations on CEAR-survey predictions for antenna-to-antenna, wire-to-wire, and antenna-to-wire coupled interference. The fourth portion, SGR, deals with the effects of input parameter variation on SGR outputs.

Table 16. Sensitivity Study Test Matrix

	Output Parameters Correlated				
Input Parameters Varied	Integrated Margin	Point Margin	Current Transfer Function	Fuselage Shading Factor	Wing Shading Factor
1. Resistance	X	X	X		
2. Shielding	X	X	X		
3. Grounding	X	X	X		
4. Twisting	X	X	X		
5. Balancing	X	X	X		
6. Wire Conductivity	X	X	X		
7. Insulation Permittivity	X	X	X		
8. Wire Separation	X	X	X		
9. Wire Common Length	X	X	X		
10. Bundle Height Above Ground	X	X	X		
11. Aperture Coordinates	X	X	X		
12. Aperture Length	X	X	X		
13. Antenna Coordinate	X	X	X	X	X
14. Pulse Width	X	X	X		
15. Pulse Rise Time	X	X	X		
16. Pulse Bit Rate	X	X	X		
17. Required Frequency Range	X				
18. Equipment Frequency Table	X				

Note:

"X" designates the output parameters that are correlated.

GP77-0342-11

132

4.1 <u>Antenna-to-Antenna Sensitivity Study</u>. Two types of input parameters
were varied in the antenna-to-antenna portion of the sensitivity study:
antenna coordinates and equipment frequency table. A summary of the test
results for these two input parameters is given in Table 17. By way of
illustration, the table shows that a variation of 7 feet in the location of the
upper UHF antenna causes the integrated margin at receptors receiving inter-
ference from that antenna to change by as much as 12 dB for one receptor and
as little as 0.2 dB for another receptor, so that the range of integrated
margin variation is 0.2-12.0 dB. The table also shows that the selection of
frequencies in the equipment frequency table can affect the integrated margin
by as much as 81.6 dB. These results are discussed in detail below.

Table 17. Summary of Antenna-To-Antenna Sensitivity Study Test Results

Input Parameter	Variation of Input Parameter	Range of Integrated Margin Variation
Upper UHF Antenna Coordinates	7 Feet	0.2 - 12.0 dB
	14 Feet	4.3 - 16.8 dB
	1 Foot	0 - 4.7 dB
Equipment Frequency Table[1]	Table A→Table B	4.8 - 81.6 dB
	Table A→Table C	0 - 0.6 dB

GP77-0342-17

1. Frequency Table A: 40 frequencies, judiciously selected
    Frequency Table B: 40 frequencies, less judiciously selected
    Frequency Table C: 90 frequencies, judiciously selected

4.1.1 <u>Antenna coordinates</u>. The results of the antenna-coordinate test
are tabulated in Table 18, where changes in the location of the upper UHF
antenna are correlated with changes in the integrated margin, point margin,
transfer function, fuselage shading and wing shading due to the upper UHF at
the other antenna ports. Results for the auxilliary receiver (AUXLO), auto-
matic direction finder (ADF), lower IFF transponder (IFFLO), upper TACAN
(TACUP), lower TACAN (TACLO), ILS localizer (LOCAL), glideslope (GLIDE), and
marker beacon (MARK) are presented in Table 18 (a) through (h), respectively.
The numbers in parenthesis in Table 18, and all other sensitivity study test
result tables, indicate the change in the output parameter relative to its
baseline value.

133

Output Parameters for COMUP → AUXLO	Value of Output Parameters			
Integrated Margin:	+16.6	16.8 (0.2)	29.3 (12.7)	16.5 (−0.1)
EMI Point Margin At 320.65 MHz: At 363.35 MHz:	+15.3 −13.2	15.5 −12.8	28.0 0	15.2 −13.3
Current Transfer Function At 320.65 MHz: At 363.35 MHz:	−55.7 −58.0	−55.5 −57.6	−43.0 −44.8	−55.8 −58.1
Fuselage Shading Factor At 320.65 MHz: At 363.35 MHz:	−20.1 −21.3	−17.9 −19.0	Fwd Edge Aft Edge −4.0 −1.7 −4.3 −1.9	−20.5 −21.6
Wing Shading Factor At 320.65 MHz: At 363.35 MHz:	0 0	0 0	Fwd Edge Aft Edge −29.7 −9.8 −30.2 −10.4	0 0

	①	②	③	④
Input Parameter Configuration: Upper UHF Antenna Coordinates:	0,158,464	0,158,548	0,158,632	0,158,452

Table 18(a) Sensitivity Study Test Results
Antenna Coordinates

Output Parameters for COMUP → ADF	Value of Output Parameters			
Integrated Margin:	2.1	−0.5 (−2.6)	−2.5 (−4.6)	2.6 (+0.5)
EMI Point Margin At 320.65 MHz At 363.35 MHz:	0.1 −6.2	−2.5 −8.8	−4.5 −10.8	0.6 −5.8
Current Transfer Function At 320.65 MHz: At 363.35 MHz:	−49.9 −51.0	−52.6 −53.6	−54.5 −55.6	−49.4 −50.5
Fuselage Shading Factor At 320.65 MHz: At 363.35 MHz:	0 0	0 0	0 0	0 0
Wing Shading Factor At 320.65 MHz: At 363.35 MHz:	0 0	0 0	0 0	0 0

Input Parameter Configuration:	①	②	③	④
Upper UHF Antenna Coordinates:	0,158,464	0,158,548	0,158,632	0,158,452

GP77-0221-41

Table 18(b) Sensitivity Study Test Results
Antenna Coordinates

135

Output Parameters for COMUP → IFFLO	Value of Output Parameters			
Integrated Margin:	−55.0	−54.2 (+1.8)	−44.9 (+10.1)	−55.3 (−0.3)
EMI Point Margin				
At 320.65 MHz:	−56.4	−55.6	−46.4	−56.6
At 1030 MHz:	−138.5	−136.3	−120.9	−139.0
Current Transfer Function				
At 320.65 MHz:	−106.4	−105.6	−96.4	−106.6
At 1030 MHz:	−187.3	−18.50	−169.6	−187.7
Fuselage Shading Factor			Fwd Edge Aft Edge	
At 320.54 MHz:	−22.2	−19.5	−4.1 −1.8	−22.7
At 1030 MHz:	−36.4	−32.2	−7.4 −3.3	−37.1
Wing Shading Factor			Fwd Edge Aft Edge	
At 320.65 MHz:	0	0	−29.1 −13.1	0
At 1030 MHz:	0	0	−34.2 −18.1	0

Input Parameter Configuration: ①   ②   ③   ④

Upper UHF Antenna Coordinates: 0,158,464   0,158,548   0,158,632   0,158,452

GP77-0221-42

Table 18(c) Sensitivity Study Test Results
Antenna Coordinates

136

Output Parameters for COMUP → TACUP	Value of Output Parameters			
Integrated Margin:	35.9	23.9 (−12)	19.1 (−16.8)	40.6 (4.7)

EMI Point Margin
  At 320.65 MHz:
  At 962 MHz:
	34.6
	−23.5
		22.6
		−35.4
			17.8
			−40.3
				39.3
				−18.7

Current Transfer Function
  At 320.65 MHz:
  At 962 MHz:
	−15.4
	−124.0
		−27.4
		−136.0
			−32.2
			−140.8
				−10.7
				−119.3

Fuselage Shading Factor
  At 320.65 MHz:
  At 962 MHz:
	0
	0
		0
		0
			0
			0
				0
				0

Wing Shading Factor
  At 320.65 MHz:
  At 962 MHz:
	0
	0
		0
		0
			0
			0
				0
				0

Input Parameter Configuration: ①   ②   ③   ④
Upper UHF Antenna Coordiantes: 0,158,464   0,158,548   0,158,632   0,158,452

GP77-0221-43

Table 18(d) Sensitivity Study Test Results
Antenna Coordinates

137

Output Parameters for COMUP → TACLO	Value of Output Parameters			
Integrated Margin:	−54.2	−53.8 (−0.4)	−41.2 (−13)	−54.2 (0) [1]
EMI Point Margin At 320.65 MHz: At 962 MHz:	−55.7 −75.9	−55.5 −74.6	−43.0 −57.1	−55.8 −76.2
Current Transfer Function At 320.65 MHz: At 962 MHz:	−105.7 −176.5	−105.5 −175.1	−93.0 −157.7	−105.8 −176.7
Fuselage Shading Factor At 320.65 MHz: At 962 MHz:	−20.1 −32.2	−17.9 −29.0	Fwd Edge Aft Edge −4.0 −1.7 −6.9 −3.0	−20.5 −32.8
Wing Shading Factor At 320.65 MHz: At 962 MHz:	0 0	0 0	Fwd Edge Aft Edge −29.7 −9.8 −34.5 −14.6	0 0

Input Parameter Configuration: ①   ②   ③   ④

Upper UHF Antenna Coordinates: 0,158,464   0,158,548   0,158,632   0,158,452

Table 18(e) Sensitivity Study Test Results
Antenna Coordinates

Output Parameters for COMUP → LOCAL	Value of Output Parameters			
Integrated Margin:	−14.5	−17.0 (−2.5)	−19.2 (−4.7)	−14.1 (+0.4)

EMI Point Margin
  At 320.65 MHz:
  At 110 MHz:
	−17.8
	−19.4
		−22.0
		−25.0
			−20.1
			−22.4
				−17.5
				−19 0

Current Transfer Function
  At 320.65 MHz:
  At 110 MHz:
	−67.8
	−51.0
		−70.1
		−54.0
			−72.0
			−56.5
				−67.5
				−50.5

Fuselage Shading Factor
  At 320.65 MHz:
  At 110 MHz:
	−19.4
	−11.9
		−17.4
		−10.6
			−15.9
			−9.7
				−19.8
				−12.1

Wing Shading Factor
  At 320.65 MHz:
  At 110 MHz:
	0
	0
		0
		0
			0
			0
				0
				0

Input Parameter Configuration: ①   ②   ③   ④
Upper UHF Antenna Coordinates: 0,158,464   0,158,548   0,158,632   0,158,452

GP77-0221-45

Table 18(f) Sensitivity Study Test Results
Antenna Coordinates

Output Parameters for COMUP → GLIDE	Value of Output Parameters			
Integrated Margin:	−16.5	−18.8 (−2.3)	−20.8 (−4.3)	−16.2 (+0.3)
EMI Point Margin At 320.65 MHz: At 332 MHz:	−17.8 −42.4	−20.1 −44.6	−22.0 −46.6	−17.5 −42.1
Current Transfer Function At 320.65 MHz: At 332 MHz:	−67.8 −68.4	−70.1 −70.6	−72.0 −72.6	−67.5 −68.1
Fuselage Shading Factor At 320.65 MHz: At 332 MHz:	−19.4 −19.7	−17.4 −17.7	−15.9 −16.2	−19.8 −20.1
Wing Shading Factor At 320.65 MHz: At 332 MHz:	0 0	0 0	0 0	0 0

Input Parameter Configuration: ①   ②   ③   ④
Upper UHF Antenna Coordinates: 0,158,464   0,158,543   0,158,632   0,158,452

GP77-0221-46

Figure 18(g) Sensitivity Study Test Results
Antenna Coordinates

140

Output Parameters for COMUP → MARK	Value of Output Parameters			
Integrated Margin:	−15.0	−14.2 (+0.8)	−6.7	−15.2 (−0.2)
EMI Point Margin At 320.65 MHz: At 75 MHz:	 −16.2 −44.5	 −15.5 −45.2	 −8.0 −40.3	 −16.5 −44.4
Current Transfer Function At 320.65 MHz: At 75 MHz:	 −66.2 −42.2	 −65.5 −42.9	 −58.0 −38.1	 −66.5 −42.2
Fuselage Shading Factor At 320.65 MHz: At 75 MHz:	 −23.6 −12.2	 −20.4 −10.5	Fwd Edge Aft Edge −4.2 −1.9 −2.1 −0.9	 −24.2 −12.6
Wing Shading Factor At 320.65 MHz: At 75 MHz:	 0 0	 0 0	 −28.8 −14.6 −22.5 −8.3	 0 0

Input Parameter Configuration: ①   ②   ③   ④
Upper UHF Antenna Coordinates: 0,158,464   0,158,548   0,158,632   0,158,452

Table 18(h) Sensitivity Study Test Results
Antenna Coordinates

These results indicate that the output parameters are not very sensitive to small changes in antenna location. Moving the upper UHF antenna from the baseline position, Configuration 1, to a point 7 feet aft, Configuration 2, changes the integrated margin by about 2 dB or less for all receptors except the upper TACAN, which shows a 12 dB change. The reason that the upper TACAN shows such a change is its proximity to the upper UHF antenna in the baseline configuration, about 2 feet away, so that an additional displacement of 7 feet has a more pronounced effect. In all cases, the change in the integrated margin closely follows the change in the point margin at 320.65 MHz, the tuned frequency of the UHF transmitter, since the dominant interference mode is required UHF emission to unrequired reception of the victim receivers. The change in the point margin, of course, follows the change in the transfer function at that frequency.

When the upper UHF antenna is moved back another 7 feet in the aft direction to Configuration 3, there is a much more pronounced change in the integrated margin for the AUXLO, IFFLO, TACLO, and MARK, but not for the ADF, TACUP, LOCAL, and GLIDE. The reason for the sudden change with respect to the former is that the additional 7-foot displacement of the upper UHF antenna caused the calculated path between it and the AUXLO, IFFLO, TACLO, and MARK to intersect the wing. Consequently, the antenna-to-antenna routine model used the wing shading model in its calculation of antenna-to-antenna coupling for these paths. The variation of the current transfer function for these cases is in the positive direction, i.e., the amount of coupling increases when wing shading is involved. Looking at Table 18 (c), for example, the results for the lower IFF indicate that the integrated margin increases by 1.8 dB when the upper UHF antenna is displaced 7 feet aft of its baseline position, and by 10.1 dB when the upper UHF antenna is displaced 14 feet aft of its baseline position. Table 18 (e) shows that the integrated margin for the TACLO decreases by 0.4 dB for the 7 foot displacement and increases by 13 dB for the 14 foot displacement.

It appears that the antenna coordinates are not an especially sensitive parameter, except for cases where two antennas are close together or when the path between them comes close to the edge of the wing, so that a change in coordinates causes a change from no wing shading to wing shading or vice versa. To further investigate the near-field situation when two antennas are close together, the upper UHF antenna was displaced 1 foot from baseline in the forward direction, bringing it to within about a foot of the upper TACAN antenna (Configuration 4). The integrated margin at the TACUP increases by 4.7 dB, but the integrated margin for all other receptor ports changes by less than 0.5 dB.

4.1.2 Equipment frequency table. The baseline run for the antenna-to-antenna sensitivity study was run with a total of 40 frequencies per equipment with a judicious choice of user-selected frequencies centered about the required spectrum of each port. To determine the effect of a less judicious choice of frequencies, the same mini-system was re-run with just a few selected frequencies in the required range, Configuration 2. The total of 40 frequencies per equipment was not changed. The results, shown in Table 19, indicate a significant change in the integrated margin, as much as 81.6 dB for the case

142

of the ILS glideslope. All of these variations in the integrated margin point out the importance of selecting a good frequency representation in the quantization of emission and susceptibility spectra, especially for RF ports where the spectra tend to be rapidly changing in the vicinity of the tuned frequency. A poor choice of frequencies tends to cause an over-approximation of emission due to worst case procedure used by the IEMCAP code in assigning the highest emission level in a given interval to each frequency, and interpolating between frequencies. A similar situation holds true for receptor spectra (worst case corresponding this time to a lower threshold). It is particularly important, under these conditions, to pick frequencies just outside the required range to bring the quantized emission level down sharply and to bring the quantized susceptibility level up sharply (See Figure 24). Failure to do so could lead to large errors in the integrated margin calculation.

A third run was made with the same judicious choice of frequencies as the baseline run, but with a total of 90 frequencies per equipment instead of 40. The results indicate little or no change in the integrated margin for any of the receptors. Clearly the extra 50 frequencies, geometrically spaced in the un-required frequency range, have very little effect as long as the important frequencies in the required range are wisely selected.

Since quantization of emission spectra tends to cause an over-approximation of emission levels and quantization of susceptibility spectra tends to cause an under-approximation of the susceptibility threshold level, a judicious choice of frequencies tends to result in less interference predicted.

Receptor	Output Parameter (Integrated Margin Due to Upper UHF)		
Aux	16.6	22.0 (5.4)	16.6 (0)
ADF	2.1	6.9 (4.8)	1.5 (−0.6)
Lower IFF	−55.0	−49.1 (5.9)	−55.1 (−0.1)
Upper Tacan	35.9	41.9 (6.0)	35.9 (0)
Lower Tacan	−54.2	−39.3 (14.9)	−54.5 (−0.2)
ILS Localizer	−14.5	7.5 (7.0)	−14.5 (0)
ILS Glidescope	−16.5	64.9 (81.6)	−16.5 (0)
ILS Marker Beacon	−15.0	−9.4 (5.6)	−15.0 (0)

Input Parameter Variation:	40 Frequencies (Baseline Run with Detailed Representation of Desired Spectra)	40 Frequencies (Less Detailed Representation of Desired Spectra)	90 Frequencies (Detailed Representation of Desired Spectra)

GP77-0221-48

Table 19 Sensitivity Study Test Results
Equipment Frequency Table

143

Legend:
———— Emission Spectrum
△ Quantized emission level at user-selected frequencies
(Maximum emission within each frequency interval)
- - - - IEMCAP representation of emission spectrum
(Integrated between user-selected frequencies)
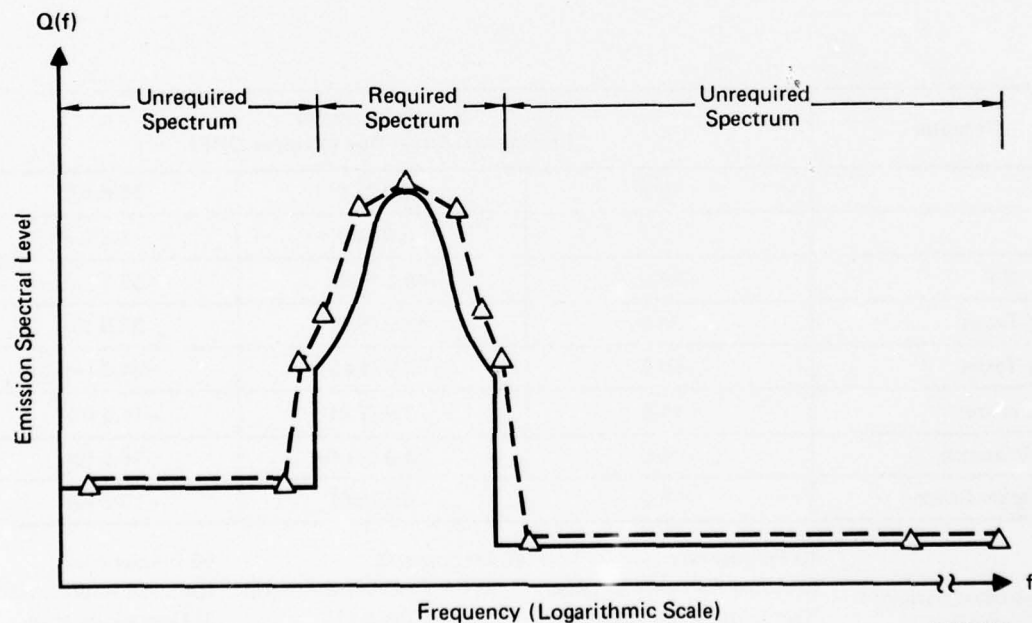
(a) "Poor" Choice of Frequencies

(b) "Good" Choice of Frequencies

GP77-0575-1

Figure 24. Effect of User-Selected Frequences on Quantized
Representation of Emission Spectrum

144

4.2 _Wire-to-Wire Sensitivity Study_. The wire-to-wire portion of the sensitivity study considers the effects of varying 15 different types of input parameters related to a victim and interferer wire as follows:

- o Termination resistance[1] (interfering wire receptor port load resistance (IWRPLR), victim wire emitter port load resistance (VWEPLR), and victim wire receptor port load resistance (VWRPLR))
- o Shield configuration (emitter and receptor wire)
- o Ground configuration (emitter and receptor wire)
- o Twisting configuration (emitter and receptor wire)
- o Balance configuration (emitter and receptor wire)
- o Conductivity (emitter and receptor wire)
- o Permittivity (emitter and receptor wire)
- o Wire separation
- o Wire common run length
- o Bundle height above ground
- o Pulse width
- o Pulse rise time
- o Pulse bit rate
- o Required frequency range (emitter and receptor)
- o Equipment frequency table

Mini-system B2 was used as a baseline for the wire-to-wire study, with the choice of one emitter and one receptor from each of the 9 wire bundles, as shown in Table 20. Thus the effect of each input parameter variation could be seen for 9 separate emitter-receptor combinations, providing information on the influence of the particular configuration on the sensitivity to a given input parameter. The results are presented in Table 22 (a) through (x), indicating changes in the integrated margin, point margin and current transfer function. The amount of variation in most input parameters in going from the baseline, Configuration 1, to Configuration 2 is +3 dB, a factor of 2. The amount of variation in going from the baseline to Configuration 3, on the other hand, depends on the results of the initial variation. If there is very little sensitivity to a 3 dB input parameter variation, the second variation may be as much as 20 dB. Onthe other hand, if a 3 dB variation has a very pronounced effect on the output, the second variation may be as little as 1 dB, to obtain more detailed information on the sensitivity.

Table 21 is a summary of the wire-to-wire sensitivity study test results, indicating the range of variation of the integrated margin for a given input variation. Each input variable is listed by the sequence number in the overall test matrix, followed by the amount that it is varied, and the range of integrated margin variation. By way of illustration, the first input parameter, interfering wire receptor port load resistance (IWRPLR), is varied by 3 dB in each of the 9 bundles, Bundle B1 through B9. In other words, the receptor port load resistance of the TRIGG, BNOGO, RUDPO, YAWBT, AILPO, RATS, ANUNC, HVPS, and DCPWR wires are all doubled. The integrated margin at the corresponding victim receptors varies by no more than 6 dB, and no less than 0 dB, so that the range of integrated margin variation due to a 3 dB variation in emitter load resistance is 0-6 dB. Because of the relative insensitivity to the 3 dB

[1]See Figure 25.

GP77-0575-6
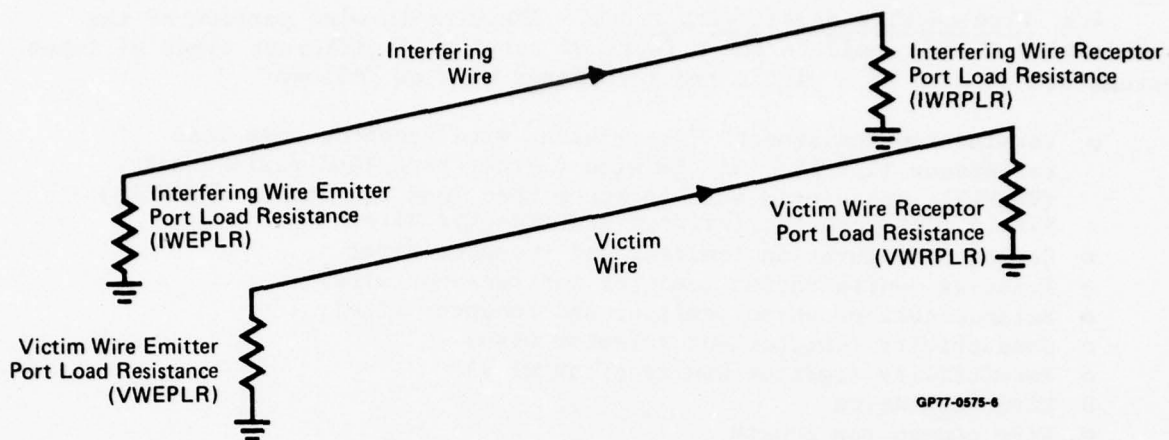
Figure 25. Illustration of Wire Termination Resistances

Table 20. Baseline For Wire-To-Wire Sensitivity Study

Bundle	Emitter Receptor Combination		
B1.	Emitter:	Hydraulic motor solenoid	(TRIGG)
	Receptor:	Tank 2 quantity indicator	(T2QNT)
B2.	Emitter:	ILS BIT no-go	(BNOGO)
	Receptor:	AIMS Code C4	(AIMS4)
B3.	Emitter:	Rudder position transducer	(RUDPO)
	Receptor:	Left bleed air overpressure sensor	(LBAO)
B4.	Emitter:	Yaw rate sensor A BIT signal	(YAWBT)
	Receptor:	Vertical acceleration, filtered	(VERTX)
B5.	Emitter:	Right aileron position transducer	(AILPO)
	Receptor:	Right flap extend	(EXTND)
B6.	Emitter:	RAM air temperature sensor	(RATS)
	Receptor:	Bypass RAM servo	(BYRAM)
B7.	Emitter:	Annunciator drive	(ANUNC)
	Receptor:	ADC AC power	(ACPWR)
B8.	Emitter:	High voltage power supply	(HVPS)
	Receptor:	HUD X-deflection	(XDEF)
B9.	Emitter:	HUD DC power	(DCPWR)
	Receptor:	Master caution light	(CAUTN)

GP77-0342-14

146

Table 21. Summary of Wire-To-Wire Sensitivity Study Test Results

	Input Parameter	Variation of Input Parameter	Range of Integrated Margin Variation
1a.	Interfering Wire Receptor Port Load Resistance	3 dB 20 dB	0-6.0 dB 0.1-17.3 dB
1b.	Victim Wire Emitter Port Load Resistance	3 dB 20 dB	0-3.0 dB 0-32.8 dB
1c.	Victim Wire Receptor Port Load Resistance	3 dB 20 dB	0-5.0 dB 3-40 dB
2a.	Receptor Shielding	Unshielded→Single Unshielded→Double	9.4-84.5 dB 9.3-93.1 dB
2b.	Emitter Shielding	Unshielded→Single	3.8-68.2 dB
3a.	*Receptor Grounding*	Both Ends→One End	0-83.8 dB
3b.	Emitter Grounding	Both Ends→One End	2.9-29.9 dB
4a.	Receptor Twisting	Untwisted→Twisted	0-84.6 dB
4b.	Emitter Twisting	Untwisted→Twisted	0-43.1 dB
5a.	Receptor Balancing	Unbalanced→Balanced	0.1-40.8 dB (But in Wrong Direction)
5b.	Emitter Balancing	Unbalanced→Balanced	0.4-54.1 dB (But in Wrong Direction)
6a.	Receptor Conductivity	3 dB 10 dB	0-3 dB 0-10 dB
6b.	Emitter Conductivity	3 dB 10 dB	0-3 dB 0-19.3 dB

147

Table 21. Summary of Wire-To-Wire Sensitivity Study Test Results (Concluded)

Input Parameter	Variation of Input Parameter	Range of Integrated Margin Variation
7a. Receptor Permittivity	3 dB 3 dB	0 dB 0 dB
7b. Emitter Permittivity	3 dB 20 dB	0-3 dB 0-22.1 dB
8. Wire Separation	Adjacent→0.5 Inches	5-28.2 dB
9. Wire Common Run Length	3 dB 10 dB	0.3-15 dB 5.9-38.1 dB
10. Bundle Height	4 Inches→8 Inches 4 Inches→36 Inches	0.1-1.6 dB 0-2.2 dB
14. Pulse Width	3 dB 13 dB	0.2-0.3 dB 0.7-8.3 dB
15. Pulse Risetime	3 dB 10 dB	2.0-2.9 dB 2.4-7.7 dB
16. Pulse Bit Rate	3 dB 10 dB	0-2.8 dB 0-15.4 dB
17a. Required Frequency Range (Receptor)	1.1 dB 3 dB	0-11.0 dB 0-17.7 dB
17b. Required Frequency Range	3 dB 20 dB	0-3.5 dB 0-8.9 dB
18. Number of Frequencies	40→65 40→90	0.1-2.8 dB 0.1-3.9 dB

GP77-0342-16

148

Table 22(a) Wire to Wire Sensitivity Study Test Results
Interfering Wire Receptor for Load Resistance

Input Parameter Value (1a. IWRPLR)		Integrated Margin (dB)		EMI Point Margin (dB)				Current Transfer Function (dB)			
				10 kHz		10 MHz		10 kHz		10 MHz	
Bundle 1											
T2QNT from TRIGG	11	−22.4		−34.7		−48.0		−36.6		−1.7	
	22 (+3 dB)	−22.1	(+0.3)	−34.7	(+0.0)	−47.6	(+0.9)	−36.6	(0.0)	−1.3	(+0.4)
	1,110 (+10 dB)	−5.1	(17.3)	−32.7	(2.0)	−32.9	(15.1)	−34.6	(2.0)	13.4	(15.1)
Bundle 2											
AIMS 4 from BNOGO	500	12.2		−13.8		−17.4		−61.3		−16.7	
	1,000 (+3 dB)	18.2	(+6.0)	−7.8	(+6.0)	−11.4	(+6.0)	−55.3	(+6.0)	−10.7	(+6.0)
	5,000 (+10 dB)	32.2	(20.0)	6.2	(20.0)	2.4	(19.9)	−41.3	(20.0)	3.2	(19.9)
Bundle 3											
LBAO from RUDPO	50,000	−47.6		−85.8		−70.4		−77.8		−14.3	
	100,000 (+3 dB)	−45.8	(+1.8)	−80.2	(+5.0)	−70.2	(+0.2)	−72.2	(+5.6)	−14.1	(+0.2)
	500,000 (+10 dB)	−37.8	(9.8)	−72.2	(13.6)	−68.8	(1.6)	−64.3	(13.5)	−12.7	(1.6)
Bundle 4											
VERTX from YAWBT	150	−137.8		−222.0		−161.9		−237.0		−128.8	
	300 (+3 dB)	−136.9	(+0.9)	−215.9	(+6.1)	−159.5	(+2.4)	−231.0	(+6.0)	−126.4	(+2.9)
	15,000 (+20 dB)	−131.3	(6.5)	−182.0	(40.0)	−157.6	(4.3)	−197.1	(39.9)	−124.5	(4.3)
Bundle 5											
EXTND from AILPO	50,000	−78.2		−186.5		−118.2		−212.6		−96.1	
	100,000 (+3 dB)	−75.2	(+3.0)	−180.8	(+5.7)	−116.1	(+2.1)	−206.8	(+5.8)	−94.0	(+2.1)
	500,000 (+10 dB)	−64.7	(13.5)	−168.2	(18.3)	−107.3	(10.9)	−194.3	(18.3)	−85.2	(10.9)
Bundle 6											
BYRAM from RATS	6,000	−92.9		−130.8		−112.9		−148.8		−82.8	
	12,000 (+3 dB)	−92.5	(+0.4)	−124.8	(+6.0)	−112.7	(+0.2)	−142.8	(+6.0)	−82.6	(+0.2)
	600,000 (20 dB)	−77.6	(15.3)	−97.9	(32.9)	−112.6	(0.3)	−115.9	(32.9)	−82.5	(0.3)
Bundle 7											
ACPWR from ANUNC	10	−28.6		−125.1		−59.1		−153.1		−42.1	
	20 (+3 dB)	−22.8	(+6.0)	−119.0	(+6.1)	−53.1	(+6.0)	−147.1	(+6.0)	−36.2	(+5.9)
	100 (+10 dB)	−13.1	(15.5)	−105.1	(20.0)	−40.0	(19.1)	−133.1	(20.0)	−23.0	(19.1)
Bundle 8											
XDEF from HVPS	218	−34.2		−38.7		−28.1		−150.8		−81.9	
	436 (+3 dB)	−29.9	(+4.3)	−32.6	(+6.1)	−24.2	(+3.9)	−144.8	(+6.0)	−78.0	(+3.9)
	2,180 (+10 dB)	−20.0	(14.2)	−18.7	(20.0)	−14.9	(13.2)	−130.8	(20.0)	−68.7	(13.2)
Bundle 9											
CAUTN from DCPWR	5	6.7		−30.8		−19.6		−69.3		−10.0	
	10 (+3 dB)	6.7	(0.0)	−30.8	(0.0)	−19.6	(0.0)	−69.3	(0.0)	−10.0	(0.0)
	500 (20 dB)	6.8	(0.1)	−30.7	(0.1)	−19.5	(0.1)	−69.2	(0.1)	−9.9	(0.1)

QP77-0221-15

149

Table 22(b) Wire to Wire Sensitivity Study Test Results
Victim Wire Emitter Port Load Resistance

Input Parameter Value (1a VWEPLR)		Integrated Margin (dB)		EMI Point Margin (dB)				Current Transfer Function (dB)			
				10 kHz		10 MHz		10 kHz		10 MHz	
Bundle 1 T2QNT from TRIGG											
11		-22.4		-34.7		-48.0		-36.6		-1.7	
22	(+3 dB)	-24.2	(-1.8)	-38.2	(-3.5)	-47.8	(+0.2)	-40.1	(-3.5)	-1.6	(+0.1)
110	(+10 dB)	-26.3	(-3.9)	-49.3	(-14.6)	-48.0	(0.0)	-51.2	(-14.6)	-1.7	(0.0)
Bundle 2 AIMS 4 from BNOGO											
100,000		12.2		-13.8		-17.4		-61.3		-16.7	
200,000	(+3 dB)	12.6	(+0.4)	-13.4	(+0.4)	-17.4	(0.0)	-60.9	(+0.4)	-16.7	(0.0)
10,000,000	(+20 dB)	12.9	(0.7)	-13.0	(0.8)	-17.4	(0.0)	-60.5	(0.8)	-16.7	(0.0)
Bundle 3 LBAO from RUDPO											
50		-47.6		-85.8		-70.4		-77.8		-14.3	
100	(+3 dB)	-47.3	(+0.3)	-89.3	(+3.5)	-71.5	(-1.1)	-81.4	(-3.6)	-15.4	(-1.1)
5,000	(+10 dB)	-53.6	(-6.0)	-119.7	(-33.9)	-92.2	(-21.8)	-111.8	(-34.0)	-36.1	(-21.8)
Bundle 4 VERTX from YAWBT											
300		-137.8		-222.0		-161.9		-237.0		-128.8	
600	(+3 dB)	-137.5	(+0.3)	-216.2	(+5.8)	-160.9	(-1.0)	-231.2	(+5.8)	-127.8	(-1.0)
30,000	(+20 dB)	-137.4	(0.4)	-193.7	(28.3)	-160.4	(1.5)	-208.8	(28.2)	-127.3	(1.5)
Bundle 5 EXTND from AILPO											
1		-78.2		-186.5		-118.2		-212.6		-96.1	
2	(+3 dB)	-78.2	(0.0)	-186.5	(0.0)	-118.2	(0.0)	-217.6	(0.0)	-96.1	(0.0)
100	(20 dB)	-45.4	(32.8)	-146.6	(39.9)	-80.0	(38.2)	-172.7	(39.9)	-57.9	(38.2)
Bundle 6 BYRAM from RATS											
10		-92.9		-130.8		-112.9		-148.8		-82.8	
20	(+3 dB)	-93.1	(-0.2)	-131.4	(-0.6)	-113.3	(-0.4)	-149.4	(-0.6)	-83.1	(-0.3)
1,000	(+20 dB)	-104.3	(-11.4)	-149.2	(-18.4)	-128.6	(-15.7)	-167.2	(-18.4)	-98.5	(-15.7)
Bundle 7 ACPWR from ANUNC											
		-28.6		-125.1		-59.1		-153.1		-42.1	
2	(3 dB)	-28.6	(0.0)	-125.1	(0.0)	-59.1	(0.0)	-153.1	(0.0)	-42.1	(0.0)
10	(20 dB)	-28.6	(0.0)	-125.5	(-0.4)	-59.3	(-0.2)	-153.6	(-0.5)	-42.3	(-0.2)
Bundle 8 XDEF from HVPS											
6		-34.2		-38.7		-28.1		-150.8		-81.9	
12	(+3 dB)	-31.2	(+3.0)	-32.7	(+6.0)	-25.4	(+2.7)	-144.8	(6.0)	-79.3	(2.6)
60	(+10 dB)	-20.8	(13.4)	-18.7	(20.0)	-15.6	(12.5)	-130.9	(19.9)	-69.5	(12.4)
Bundle 9 CAUTN from DCPWR											
1		6.7		-30.8		-19.6		-69.3		-10.0	
2	(+3 dB)	6.6	(-0.1)	-30.8	(0.0)	-19.7	(-0.1)	-69.3	(0.0)	-10.0	(0.0)
100	(+20 dB)	4.5	(-2.2)	-34.6	(-3.8)	-23.0	(-3.4)	-73.1	(-3.8)	-13.3	(-3.3)

150

GP77-0221-16

Table 22(c) Wire to Wire Sensitivity Study Test Results
Victim Wire Receptor Port Load Resistance

Input Parameter Value (1a VWRPLR)		Integrated Margin (dB)	EMI Point Margin (dB)		Current Transfer Function (dB)	
			10 kHz	10 MHz	10 kHz	10 MHz
Bundle 1 T2QNT from TRIGG	11	−22.4	−34.7	−48.0	−36.6	−1.7
	22 (+3 dB)	−21.5 (+0.9)	−35.2 (+0.5)	−45.1 (2.9)	−40.1 (−3.5)	−1.8 (−0.1)
	1,100 (+20 dB)	−11.6 (10.8)	−48.8 (−14.1)	−37.5 (10.5)	−70.7 (−34.1)	−11.2 (−9.5)
Bundle 2 AIMS 4 from BNOGO	10,000	12.2	−13.8	−17.4	−61.3	−16.7
	20,000 (+3 dB)	14.1 (+1.9)	−11.5 (2.3)	−20.2 (−2.8)	−62.0 (−0.7)	−22.5 (−5.8)
	100,000 (+10 dB)	10.5 (4.3)	−9.0 (4.8)	−26.9 (−9.5)	−66.5 (−5.2)	−36.2 (−19.5)
Bundle 3 LBAO from RUDPO	50	−47.6	−85.8	−70.4	−77.8	−14.3
	100 (+3 dB)	−45.6 (+2.0)	−86.3 (−0.5)	−68.6 (1.8)	−81.4 (−3.6)	−15.5 (−1.2)
	500 (+10 dB)	−43.0 (4.6)	−90.6 (−4.8)	−69.7 (0.7)	−92.6 (−14.8)	−23.6 (−9.3)
Bundle 4 VERTX from YAWBT	10,000	−137.8	−222.0	−161.9	−237.0	−128.8
	20,000 (+3 dB)	−140.8 (−3.0)	−224.8 (−2.8)	−164.9 (−3.0)	−242.9 (−5.9)	−134.8 (−6.0)
	20,000	−140.8 (−3.0)	−224.8 (−2.8)	−164.9 (−3.0)	−242.9 (−5.9)	−134.8 (−6.0)
Bundle 5 EXTND from AILPO	10,000	−78.2	−186.5	−118.2	−212.6	−96.1
	20,000 (+3 dB)	−81.2 (−3.0)	−189.5 (−3.0)	−121.2 (−3.0)	−218.6 (−6.0)	−102.1 (−6.0)
	100,000 (+40 dB)	−88.2 (−10.0)	−196.5 (−10.0)	−128.2 (−10.0)	−232.6 (−20.0)	−116.1 (−20.0)
Bundle 6 BYRAM from RATS	125	−92.9	−130.8	−112.9	−148.8	−82.8
	250 (+3 dB)	−92.5 (+0.4)	−133.5 (−2.7)	−113.8 (−0.9)	−154.5 (−5.7)	−86.7 (−3.9)
	12,500 (+20 dB)	−105.1 (−12.2)	−150.1 (−19.3)	−129.5 (−16.6)	−188.1 (−39.3)	−119.4 (−36.6)
Bundle 7 ACPWR from ANUNC	185	−28.6	−125.1	−59.1	−153.1	−42.1
	270 (+3 dB)	−23.4 (+5.0)	−125.1 (0.0)	−56.7 (2.4)	−159.1 (−6.0)	−45.7 (−3.6)
	1,850 (+10 dB)	−17.8 (10.8)	−125.1 (0.0)	−55.5 (3.6)	−173.1 (−20.0)	−58.5 (−16.4)
Bundle 8 XDEF from HVPS	10,000	−34.2	−38.7	−28.1	−150.8	−81.9
	20,000 (+3 dB)	−34.2 (0.0)	−38.7 (0.0)	−28.1 (0.0)	−156.8 (−6.0)	−87.9 (−6.0)
	1,000,000 (+20 dB)	−74.2 (−40.0)	−78.7 (−40.0)	−68.1 (−40.0)	−190.8 (−40.0)	−121.9 (−40.0)
Bundle 9 CAUTN from DCPWR	175	6.7	−30.8	−19.6	−69.3	−10.0
	350 (+3 dB)	6.1 (−0.6)	−33.8 (−3.0)	−22.1 (−2.5)	−75.3 (−6.0)	−15.5 (−5.5)
	17,500 (+20 dB)	−2.3 (−9.0)	−50.7 (−19.9)	−38.9 (−19.3)	−109.2 (−39.9)	−49.2 (−39.2)

GP77-0221-17

151

Table 22(d) Wire to Wire Sensitivity Study Test Results
Receptor Shielding

Input Parameter Value (2a. Receptor Shielding)		Integrated Margin (dB)	EMI Point Margin (dB)		Current Transfer Function (dB)	
			10 kHz	10 MHz	10 kHz	10 MHz
Configuration	None	−22.4	−34.7	−48.0	−36.6	−1.7
Bundle 1	Single	−39.7 (−17.3)	−42.7 (−8.0)	−95.7 (−47.7)	−44.6 (−11.0)	−49.4 (−47.7)
T2QNT from TRIGG	Double	−40.1 (−17.7)	−43.1 (−8.4)	−96.3 (−48.3)	−44.9 (−11.3)	−50.0 (−48.3)
Configuration	None	12.2	−13.8	−17.4	−61.3	−16.7
Bundle 2	Single	−49.8 (−62.0)	−81.4 (−67.6)	−108.6 (−91.2)	−128.9 (−67.6)	−107.9 (−91.2)
AIMS 4 from BNOGO	Double	−50.2 (−62.4)	−81.9 (−68.1)	−109.6 (−92.2)	−129.3 (−68.0)	−108.9 (−92.2)
Configuration	None	−47.6	−85.8	−70.4	−77.8	−14.3
Bundle 3	Single	−79.5 (−31.9)	−99.6 (−13.8)	−140.7 (−70.3)	−91.7 (−13.9)	−84.6 (−70.3)
LBAO from RUDPO	Double	−79.1 (−32.1)	−100.0 (−14.2)	−141.2 (−70.8)	−92.0 (−14.2)	−85.1 (−70.8)
Configuration	Single	−137.8	−222.0	−161.9	−237.0	−128.8
Bundle 4	None	−53.3 (84.5)	−192.6 (29.4)	−86.3 (75.6)	−207.6 (29.4)	−53.2 (75.6)
VERTX from YAWBT	Double	−138.1 (−0.3)	−222.1 (−0.1)	−162.1 (−0.2)	−237.2 (−0.2)	−129.0 (−0.2)
Configuration	None	−78.2	−186.5	−118.2	−212.6	−96.1
Bundle 5	Single	−149.2 (−71.0)	−222.0 (−35.5)	−198.2 (−80.0)	−248.0 (−35.4)	−176.1 (−80.0)
EXTND from AILPO	Double	−171.3 (−93.1)	−222.1 (−35.6)	−201.5 (−83.3)	−248.2 (−35.6)	−179.4 (−83.3)
Configuration	Single	−92.9	−130.8	−112.9	−148.8	−82.8
Bundle 6	None	−69.8 (23.1)	−125.0 (5.8)	−104.0 (8.9)	−143.0 (5.8)	−73.9 (8.9)
BYRAM from RATS	Double	−94.3 (−1.4)	−132.2 (−1.4)	−114.3 (−1.4)	−150.2 (−1.4)	−84.2 (−1.4)
Configuration	None	−28.6	−125.1	−59.1	−153.1	−42.1
Bundle 7	Single	−107.4 (−78.8)	−138.9 (−13.8)	−129.4 (−70.3)	−166.9 (−13.8)	−112.4 (−70.3)
ACPWR from ANUNC	Double	−107.7 (−79.1)	−139.2 (−14.1)	−129.7 (−70.6)	−167.3 (−14.2)	−112.8 (−70.7)
Configuration	Double	−34.2	−38.7	−28.1	−150.8	−81.9
Bundle 8	None	−6.9 (27.3)	−4.7 (34.0)	−1.7 (26.4)	−116.9 (33.9)	−55.5 (26.4)
XDEF from HVPS	Single	−30.6 (3.6)	−36.9 (1.8)	−24.3 (3.8)	−149.1 (1.7)	−78.2 (3.7)
	None	6.7	−30.8	−19.6	−69.3	−10.0
Bundle 9	Single	−2.7 (−9.4)	−40.2 (−9.4)	−41.4 (−21.8)	−78.7 (−9.4)	−31.7 (−21.7)
CAUTN from DCPWR	Double	−2.6 (−9.3)	−40.5 (−9.7)	−41.7 (−22.1)	−79.0 (−9.7)	−32.0 (−22.0)

GP77-0221-18

Table 22(e) Wire to Wire Sensitivity Study Test Results
Emitter Shielding

Input Parameter Value (2b. Emitter Shielding)[1]		Integrated Margin (dB)		EMI Point Margin (dB)			Current Transfer Function (dB)		
				10 kHz		10 MHz	10 kHz		10 MHz
Bundle 1 T2QNT from TRIGG	None	−22.4		−34.7		−48.0	−36.6		−1.7
	Single	−19.0	(3.4)	−29.3	(5.4)	−48.1 (0.1)	−31.2	(5.4)	−1.9 (−0.2)
	Double	−19.2	(3.2)	−29.6	(5.1)	−48.4 (0.4)	−31.4	(5.2)	−2.1 (−0.4)
Bundle 2 AIMS 4 from BNOGO	None	12.2		−13.8		−17.4	−61.3		−16.7
	Single	−32.1	(−44.3)	−68.0	(−54.2)	−60.8 (−43.4)	−115.5	(−54.2)	−60.1 (−43.4)
	Double	−32.5	(−44.7)	−68.4	(−54.6)	−61.2 (−43.8)	−115.6	(−54.3)	−60.5 (−43.8)
Bundle 3 LBAO from RUDPO	Single	−47.6		−85.8		−70.4	−77.8		−14.3
	None	9.3	(56.9)	−31.3	(54.5)	−19.5 (50.9)	−23.4	(54.4)	36.6 (−22.3)
	Double	−49.9	(−2.3)	−86.0	(−0.2)	−10.9 (−0.5)	−78.1	(−0.3)	−14.8 (−0.5)
Bundle 4 VERTX from YAWBT	Single	−137.8		−222.0		−161.9	−237.0		−128.8
	None	−107.9	(29.9)	−195.1	(26.9)	−137.4 (24.5)	−210.2	(26.8)	−104.3 (24.5)
	Double	−138.7	(−0.9)	−222.2	(−0.2)	−162.8 (−0.9)	−237.2	(−0.2)	−129.7 (−0.9)
Bundle 5 EXTND from AILPO	Single	−78.2		−186.5		−118.2	−212.6		−96.1
	None	−25.6	(52.6)	−66.4	(120.1)	−54.5 (63.7)	−92.4	(120.2)	−32.4 (63.7)
	Double	−82.9	(−4.7)	−198.4	(−11.9)	−121.3 (−3.1)	−224.5	(−11.9)	−99.2 (−3.1)
Bundle 6 BYRAM from RATS	Single	−92.9		−130.8		−112.9	−148.8		−82.8
	None	−54.1	(38.8)	−123.5	(7.3)	−79.6 (33.3)	−141.5	(7.3)	−49.4 (33.4)
	Double	−94.3	(−1.4)	−132.2	(−1.4)	−114.3 (−1.4)	−150.2	(−1.4)	−84.2 (−1.4)
Bundle 7 ACPWR from ANUNC	Single	−28.6		−125.1		−59.1	−153.1		−42.1
	None	−27.8	(0.8)	−121.7	(3.4)	−58.6 (0.5)	−149.8	(3.3)	−41.6 (0.5)
	Double	−29.4	(−0.8)	−125.7	(−0.6)	−60.0 (−0.9)	−153.8	(−0.7)	−43.0 (−0.9)
Bundle 8 XDEF from HVPS	None	−34.2		−38.7		−28.1	−150.8		−81.9
	Single	−43.2	(−9.0)	−40.3	(−1.6)	−38.2 (−10.1)	−152.2	(−1.7)	−92.0 (−10.1)
	Double	−43.5	(−9.3)	−40.7	(−2.0)	−38.6 (−11.5)	−152.8	(−2.0)	−92.4 (−10.5)
Bundle 9 CAUTN from DCPWR	None	6.7		−30.8		−19.6	−69.3		−10.0
	Single	8.3	(1.6)	−25.3	(5.5)	−19.2 (0.4)	−63.8	(5.5)	−9.5 (0.5)
	Double	8.0	(1.3)	−25.6	(5.2)	−19.5 (0.1)	−64.1	(5.2)	−9.8 (0.2)

1. These results are superceded by results from re-test with corrected code, Table 23.

GP77-0221-19

153

Table 22(f) Wire to Wire Sensitivity Study Test Results
Receptor Grounding

Input Parameter Value (3a. Receptor Grounding)		Integrated Margin (dB)	EMI Point Margin (dB)		Current Transfer Function (dB)	
			10 kHz	10 MHz	10 kHz	10 MHz
Bundle 1 T2QNT from TRIGG	Unshielded	-22.4	-34.7	-48.0	-36.6	-1.7
	Both Ends	-39.7	-42.7	-95.7	-44.6	-49.4
	One End	-23.0 (16.7)	-35.3 (7.4)	-48.9 (46.9)	-37.1 (7.5)	-2.6 (46.8)
Bundle 2 AIMS 4 from BNOGO	Configuration Unshielded	12.2	-13.8	-17.4	-61.3	-16.7
	Both Ends	-49.8	-81.4	-108.6	-128.9	-107.9
	One End	-33.3 (16.5)	-74.0 (7.4)	-62.2 (46.4)	-121.5 (7.4)	-61.5 (46.4)
Bundle 3 LBAO from RUDPO	Unshielded	-47.6	-85.8	-70.4	-77.8	-14.3
	Both Ends	-79.5	-99.6	-140.7	-91.7	-84.6
	One End	-50.1 (29.4)	-86.7 (13.4)	-71.0 (69.7)	-78.7 (13.5)	-14.9 (69.7)
Bundle 4 VERTX from YAWBT	Both Ends	-137.8	-222.0	-161.9	-237.0	-128.8
	One End	-54.0 (83.8)	-204.1 (17.9)	-87.0 (74.9)	-219.1 (17.9)	-53.9 (74.9)
Bundle 5 EXTND from AILPO	Unshielded	-78.2	-186.5	-118.2	-212.6	-96.1
	Both Ends	-149.2	-222.0	-198.2	-248.0	-176.1
	One End	-83.8 (65.4)	-199.2 (22.8)	-177.0 (76.2)	-225.2 (22.8)	-93.3 (82.8)
Bundle 6 BYRAM from RATS	Both Ends	-92.9	-130.8	-112.9	-148.8	-82.8
	One End	-92.9 (0)	-130.8 (0)	-112.4 (0)	-148.8 (0)	-82.8 (0)
Bundle 7 ACPWR from ANUNC	Unshielded	-28.6	-125.1	-59.1	-153.1	-42.1
	Both Ends	-107.4	-138.9	-129.4	-166.9	-112.4
	One End	-29.0 (78.4)	-175.4 (13.5)	-59.5 (69.9)	-153.5 (13.4)	-47.5 (69.9)
Bundle 8 XDEF from HVPS	Both Ends	-34.2	-38.7	-28.1	-150.8	-81.9
	One End	-34.2 (0)	-38.7 (0)	-28.1 (0)	-150.8 (0)	-81.9 (0)
Bundle 9 CAUTN from DCPWR	Unshielded	6.7	-30.8	-19.6	-69.3	-10.0
	Both Ends	-2.7	-40.2	-41.4	-78.7	-31.7
	One End	-6.2 (3.5)	-31.3 (8.9)	-20.1 (21.3)	-69.8 (8.9)	-10.5 (21.2)

GP77-0221-20

154

Table 22(g) Wire to Wire Sensitivity Study Test Results
Emitter Grounding

Input Parameter Value (3b. Emitter Grounding)[1]		Integrated Margin (dB)	EMI Point Margin (dB) 10 kHz	EMI Point Margin (dB) 10 MHz	Current Transfer Function (dB) 10 kHz	Current Transfer Function (dB) 10 MHz
Bundle 1 T2QNT from TRIGG	Unshielded	−22.4	−34.7	−48.0	−36.6	−1.7
	Both Ends	−19.0	−29.3	−48.1	−31.2	−1.9
	One End	−23.3 (−4.3)	−35.3 (−6)	−48.9 (−0.8)	−37.2 (−6)	−2.6 (−0.7)
Bundle 2 AIMS 4 from BNOGO	Unshielded	12.2	−13.8	−17.4	−61.3	−16.7
	Both Ends	−32.1	−68.0	−60.8	−115.5	−60.1
	One End	−33.2 (−1.1)	−74.0 (−6)	−62.1 (−1.3)	−121.5 (−6)	−61.4 (−1.3)
Bundle 3 LBAO from RUDPO	Both Ends	−47.6	−85.8	−70.4 −70.4	−77.8	−14.3
	One End	−46.2 (1.4)	−91.8 (−6.0)	−70.8 (−0.4)	−83.8 (−6.0)	−14.7 (−0.4)
Bundle 4 VERTX from YAWBT	Both Ends	−137.8	−222.0	−161.9 −161.9	−237.0	−178.8
	One End	−111.1 (26.7)	−221.9 (0.1)	−139.6 (22.3)	−237.0 (0)	−106.5 (22.3)
Bundle 5 EXTND from AILPO	Both Ends	−78.2	−186.5	−118.2 −118.2	−212.6	−96.1
	One End	−75.3 (2.9)	−182.4 (4.1)	−116.4 (2.8)	−208.5 (4.1)	−94.3 (1.8)
Bundle 6 BYRAM from RATS	Both Ends	−92.9	−130.8	−112.9 −112.9	−148.8	−82.8
	One Word	−63.0 (29.9)	−130.6 (0.2)	−86.9 (26.0)	−148.6 (0.2)	−56.7 (26.1)
Bundle 7 ACPWR from ANUNC	Both Ends	−28.6	−125.1	−59.1	−153.1	−42.1
	One Word	−29.0 (−0.4)	−131.0 (−5.9)	−59.8 (−0.7)	−159.1 (−6.0)	−42.8 (−0.7)
Bundle 8 XDEF from HVPS	Unshielded	−34.2	−38.7	−28.1	−150.8	−81.9
	Both Ends	−43.2	−40.3	−38.2	−152.5	−92.0
	One End	−37.8 (5.4)	−40.3 (0)	−31.9 (6.3)	−152.5 (0)	−85.7 (6.3)
Bundle 9 CAUTN from DCPWR	Unshielded	6.7	−30.8	−19.6	−69.3	−10.0
	Both Ends	8.3	−25.3	−19.2	−63.8	−9.5
	One End	6.2 (−2.1)	−31.3 (−6)	−20.1 (−0.9)	−69.8 (−6)	−10.5 (−1)

1. These test results are superceded by results from re-test with corrected code, Table 23

GP77-0221-21

155

Table 22(h) Wire to Wire Sensitivity Study Test Results
Receptor Twisting

Input Parameter Value (4a. Receptor Twisting)[1]		Integrated Margin (dB)		EMI Point Margin (dB)		Current Transfer Function (dB)	
				10 kHz	10 MHz	10 kHz	10 MHz
Bundle 1 T2QNT from TRIGG	Untwisted	−22.4		−34.7	−48.0	−36.6	−1.7
	Twisted	−15.4	(7.0)	−86.3 (−51.6)	−53.2 (5.2)	−88.1 (−51.5)	−7.0 (−5.3)
Bundle 2 AIMS 4 from BNOGO	Untwisted	12.2		−13.8	−17.4	−61.3	−16.7
	Twisted	12.2	(0)	−13.8 (0)	−17.3 (0.1)	−61.3 (0)	−16.6 (0.1)
Bundle 3 LBAO from RUDPO	Untwisted	−47.6		−85.8	−70.4	−77.8	−14.3
	Twisted	−49.4	(−1.8)	−160.5 (−74.7)	−88.5 (−18.1)	−152.5 (−74.7)	−32.4 (−18.2)
Bundle 4 VERTX from YAWBT	Twisted	−137.8		−222.0	−161.9	−237.0	−128.8
	Untwisted	−120.9	(16.9)	−151.6 (70.4)	−144.3 (17.6)	−166.7 (71.3)	−111.2 (17.6)
Bundle 5 EXTND from AILPO	Twisted	−78.2		−186.5	−118.2	−212.6	−96.1
	Untwisted	−38.1	(40.1)	−83.8 (102.7)	−66.7 (51.5)	−109.9 (102.7)	−44.6 (51.5)
Bundle 6 BYRAM from RATS	Twisted	−92.9		−130.8	−112.9	−148.8	−82.8
	Untwisted	−77.6	(15.3)	−97.8 (33.0)	−114.5 (−6.6)	−115.8 (33.0)	−89.4 (−6.6)
Bundle 7 ACPWR from ANUNC	Untwisted	−28.6		−125.1	−59.1	−153.1	−42.1
	Twisted	−84.8	(−56.2)	−251.9 (−126.8)	−133.0 (−73.9)	−280.0 (−126.9)	−116.1 (−74.0)
Bundle 8 XDEF from HVPS	Twisted	−34.2		−38.7	−28.1	−150.8	−81.9
	Untwisted	−27.0	(7.2)	−41.3 (−2.6)	−20.6 (7.5)	−153.4 (−2.6)	−74.4 (7.5)
Bundle 9 CAUTN from DCPWR	Untwisted	6.7		−30.8	−19.6	−69.3	−10.0
	Twisted	−45.7	(−52.4)	−109.4 (−78.6)	−83.0 (−78.6)	−147.9 (−78.6)	−73.4 (−63.4)

1. These test results are superceded by results from re-test with corrected code, Table 23.

GP77-0221-22

156

Table 22(i) Wire to Wire Sensitivity Study Test Results
Emitter Twisting

Input Parameter Value (4b. Emitter Twisting)		Integrated Margin (dB)	EMI Point Margin (dB)		Current Transfer Function (dB)	
			10 kHz	10 MHz	10 kHz	10 MHz
Bundle 1 T2QNT from TRIGG	Untwisted	−22.4	−34.7	−48.0	−36.6	−1.7
	Twisted	−41.7 (−19.3)	−86.2 (−51.5)	−70.3 (−22.3)	−88.1 (−51.5)	−24.0 (−22.3)
Bundle 2 AIMS 4 from BNOGO	Untwisted	12.2	−13.8	−17.4	−61.3	−16.7
	Twisted	12.2 (0)	−13.8 (0)	−17.5 (−0.1)	−61.3 (0)	−16.8 (−0.1)
Bundle 3 LBAO from RUDPO	Twisted	−47.6	−85.8	−70.4	−77.8	−14.3
	Untwisted	−31.6 (−16.0)	−59.5 (26.3)	−58.1 (12.3)	−51.6 (26.2)	−2.0 (12.3)
Bundle 4 VERTX from YAWBT	Twisted	−137.8	−222.0	−161.9	−237.0	−128.8
	Untwisted	−101.6 (36.2)	−138.3 (83.7)	−139.6 (22.3)	−153.4 (83.6)	−106.5 (22.3)
Bundle 5 EXTND from AILPO	Twisted	−78.2	−186.5	−118.2	−212.6	−96.1
	Untwisted	−65.7 (12.5)	−169.9 (16.6)	−105.7 (12.5)	−196.0 (16.6)	−83.6 (12.5)
Bundle 6 BYRAM from RATS	Twisted	−92.9	−130.8	−112.9	−148.8	−82.8
	Untwisted	−54.8 (38.1)	−80.4 (50.4)	−90.0 (22.9)	−98.4 (50.4)	−59.9 (22.9)
Bundle 7 ACPWR from ANUNC	Twisted	−28.6	−125.1	−59.1	−153.1	−42.1
	Untwisted	3.9 (32.5)	−26.3 (98.8)	−19.3 (39.8)	−54.3 (98.8)	−2.3 (39.8)
Bundle 8 XDEF from HVPS	Twisted	−34.2	−38.7	−28.1	−150.8	−81.9
	Untwisted	−20.7 (13.5)	−17.5 (21.2)	−15.8 (12.3)	−129.7 (21.1)	−69.7 (12.2)
Bundle 9 CAUTN from DCPWR	Untwisted	6.7	−30.8	−19.6	−69.3	−10.0
	Twisted	−36.4 (−43.1)	−109.3 (−78.5)	−71.1 (−51.5)	−147.8 (−78.5)	−61.4 (−51.4)

GP77-0221-23

157

Table 22(j) Wire to Wire Sensitivity Study Test Results
Receptor Balancing

Input Parameter Value (5a. Receptor Balancing)[1]		Integrated Margin (dB)	EMI Point Margin (dB)		Current Transfer Function (dB)	
			10 kHz	10 MHz	10 kHz	10 MHz
Bundle 1 T2QNT from TRIGG	Unbalanced	−15.4	−86.3	−53.2	−88.1	−7.0
	Balanced	−38.2 (−22.8)	−60.9 (25.4)	−65.3 (−12.2)	−62.8 (25.3)	−19.0 (−12.0)
Bundle 2 AIMS 4 from BNOGO	Unbalanced	12.2	−13.8	−17.3	−61.3	−16.6
	Balanced	18.2 (6)	−7.8 (6)	−11.5 (5.8)	−55.3 (6)	−10.8 (5.8)
Bundle 3 LBAO from RUDPO	Unbalanced	−49.4	−160.5	−88.5	−152.5	−32.4
	Balanced	−51.2 (−4.8)	−124.3 (36.2)	−97.2 (−8.7)	−116.4 (36.1)	−41.1 (−8.7)
Bundle 4 VERTX from YAWBT	Unbalanced	−137.8	−222.0	−161.9	−237.0	−128.8
	Balanced	−108.7 (29.1)	−183.0 (39.0)	−136.1 (25.8)	−198.0 (39.0)	−103.0 (25.8)
Bundle 5 EXTND from AILPO	Unbalanced	−78.2	−186.5	−118.2	−212.6	−96.1
	Balanced	−78.1 (0.1)	−117.4 (69.1)	−113.6 (4.6)	−143.4 (69.2)	−91.5 (4.6)
Bundle 6 BYRAM from RATS	Balanced	−92.9	−130.8	−112.9	−148.8	−82.8
	Unbalanced	−133.7 (−40.8)	−204.0 (−73.2)	−164.3 (−51.4)	−222.0 (−73.2)	−134.2 (−51.4)
Bundle 7 ACPWR from ANUNC	Unbalanced	−84.8	−251.3	−133.0	−280.0	−116.1
	Balanced	−88.6 (0.2)	−163.8 (88.1)	−114.7 (18.3)	−191.8 (88.2)	−97.8 (18.3)
Bundle 8 XDEF from HVPS	Balanced	−34.2	−38.7	−28.1	−150.8	−81.9
	Unbalanced	−47.6 (−13.4)	−44.7 (−6.0)	−42.5 (−14.4)	−156.9 (−6.1)	−96.3 (−14.4)
Bundle 9 CAUTN from DCPWR	Unbalanced	−45.7	−109.4	−83.0	−147.9	−73.4
	Balanced	−16.9 (28.8)	−54.4 (55.0)	−43.2 (39.8)	−97.9 (55.0)	−33.6 (39.8)

1. These test results are superceded by results from retest with corrected code, Table 23.

GP77-0221-24

158

Table 22(k) Wire to Wire Sensitivity Study Test Results
Emitter Balancing

Input Parameter Value (5b. Emitter Balancing)		Integrated Margin (dB)	EMI Point Margin (dB)		Current Transfer Function (dB)	
			10 kHz	10 MHz	10 kHz	10 MHz
Bundle 1 T2QNT from TRIGG	Untwisted	-22.4	-34.7	-48.0	-36.6	-1.7
	Unbalanced	-41.7	-86.2	-70.3	-88.1	-24.0
	Balanced	-41.9 (-0.2)	-55.8 (+30.4)	-67.4 (+2.9)	-57.7 (30.4)	-21.1 (2.9)
Bundle 2 AIMS 4 from BNOGO	Untwisted	12.2	-13.8	-17.4	-61.3	-16.7
	Unbalanced	12.2	-13.8	-17.5	-61.3	-16.8
	Balanced	-41.9 (-54.1)	-19.8 (-6.0)	-23.5 (-6.0)	-67.3 (-6.0)	-22.8 (-6.0)
Bundle 3 LBAO from RUDPO	Unbalanced	-47.6	-85.8	-70.4	-77.8	-14.3
	Balanced	-52.4 (-14.8)	-98.7 (-12.9)	-91.7 (-21.3)	-90.8 (-13.0)	-35.6 (-21.3)
Bundle 4 VERTX from YAWBT	Unbalanced	-137.8	-222.0	-161.9	-237.0	-128.8
	Balanced	-137.4 (0.4)	-188.7 (33.3)	-163.0 (-1.1)	-203.8 (33.2)	-129.9 (-1.1)
Bundle 5 EXTND from AILPO	Unbalanced	-78.2	-186.5	-118.2	-212.6	-96.1
	Balanced	-90.4 (-12.2)	-194.5 (-8.0)	-132.9 (-14.7)	-220.6 (-8.0)	-110.8 (-14.7)
Bundle 6 BYRAM from RATS	Unbalanced	-92.9	-130.8	-112.9	-148.8	-82.8
	Balanced	-45.9 (47.0)	-79.5 (51.3)	-70.3 (42.6)	-97.5 (51.3)	-40.2 (42.6)
Bundle 7 ACPWR from ANUNC	Unbalanced	-28.6	-125.1	-59.1	-153.1	-42.1
	Balanced	-30.7 (-2.1)	-65.5 (59.6)	-53.9 (5.2)	-93.5 (59.6)	-36.9 (5.2)
Bundle 8 XDEF from HVPS	Unbalanced	-34.2	-38.7	-28.1	-150.8	-81.9
	Balanced	-18.9 (15.3)	-15.7 (23.0)	-14.0 (14.1)	-127.9 (22.9)	-67.9 (14.0)
Bundle 9 CAUTN from DCPWR	Untwisted	6.7	-30.8	-19.6	-69.3	-10.0
	Unbalanced	-36.4	-109.3	-71.1	-147.8	-61.4
	Balanced	-16.9 (19.5)	-54.5 (54.9)	-43.2 (27.9)	-97.9 (54.9)	-33.6 (27.8)

159

GP77-0221-25

Table 22(I) Wire to Wire Sensitivity Study Test Results
Receptor Conductivity

Input Parameter Value (6a. Receptor Conductivity)		Integrated Margin (dB)		EMI Point Margin (dB) 10 kHz		EMI Point Margin (dB) 10 MHz		Current Transfer Function (dB) 10 kHz		Current Transfer Function (dB) 10 MHz	
Bundle 1											
T2QNT from TRIGG	0.85	−22.4		−34.7		−48.0		−36.6		−1.7	
	1.7 (3 dB)	−22.4	(0)	−34.7	(0)	−48.0	(0)	−36.6	(0)	−1.7	(0)
	0.0085 (20 dB)	−22.4	(0)	−34.7	(0)	−48.0	(0)	−36.6	(0)	−1.7	(0)
Bundle 2											
AIMS 4 from BNOGO	0.85	12.2		−13.8		−17.4		−61.3		−16.7	
	1.7 (3 dB)	12.2	(0)	−13.8	(0)	−17.4	(0)	−61.3	(0)	−16.7	(0)
	0.0085 (−20 dB)	12.2	(0)	−13.8	(0)	−17.4	(0)	−61.3	(0)	−16.7	(0)
Bundle 3											
LBAO from RUDPO	0.85	−47.6		−85.8		−70.4		−77.8		−14.3	
	1.7 (3 dB)	−47.6	(0)	−85.8	(0)	−70.4	(0)	−77.8	(0)	−14.3	(0)
	0.0085 (−20 dB)	−47.6	(0)	−85.8	(0)	−70.4	(0)	−77.8	(0)	−14.3	(0)
Bundle 4											
VERTX from YAWBT	0.85	−137.8		−222.0		−161.9		−237.0		−128.8	
	1.7 (3 dB)	−140.8	(−3.0)	−227.8	(−5.8)	−164.9	(−3.0)	−242.8	(−5.8)	−131.8	(−3.0)
	0.085 (−10 dB)	−127.8	(10.0)	−210.7	(11.3)	−151.9	(10.0)	−225.8	(11.8)	−118.8	(10.0)
Bundle 5											
EXTND from AILPO	1	−78.2		−186.5		−118.2		−212.6		−96.1	
	2 (3 dB)	−78.2	(0)	−186.5	(0)	−118.2	(0)	−212.6	(0)	−96.1	(0)
	0.01 (−20 dB)	−78.2	(0)	−186.5	(0)	−118.2	(0)	−212.6	(0)	−96.1	(0)
Bundle 6											
BYRAM from RATS	0.85	−92.9		−130.8		−112.9		−148.8		−82.8	
	1.7 (3 dB)	−92.9	(0)	−130.8	(0)	−112.9	(0)	−148.8	(0)	−82.8	(0)
	0.0085 (20 dB)	−90.6	(2.3)	−130.8	(0)	−112.8	(0.1)	−148.8	(0)	−82.7	(0.1)
Bundle 7											
ACPWR from ANUNC	0.85	−28.6		−125.1		−59.1		−153.1		−42.1	
	1.7 (3 dB)	−28.6	(0)	−125.1	(0)	−59.1	(0)	−153.1	(0)	−42.1	(0)
	0.0085 (20 dB)	−28.6	(0)	−125.1	(0)	−59.1	(0)	−153.1	(0)	−42.1	(0)
Bundle 8											
XDEF from HVPS	0.85	−34.2		−38.7		−28.1		−150.8		−81.9	
	1.7 (3 dB)	−34.2	(0)	−38.7	(0)	−28.1	(0)	−150.8	(0)	−81.9	(0)
	0.0085 (20 dB)	−34.1	(0.1)	−38.7	(0)	−28.0	(0.1)	−150.8	(0)	−81.8	(0.1)
Bundle 9											
CAUTN from DCPWR	1	6.7		−30.8		−19.6		−69.3		−10.0	
	2 (3 dB)	6.7	(0)	−30.8	(0)	−19.6	(0)	−69.3	(0)	−10.0	(0)
	0.01 (−20 dB)	6.7	(0)	−30.8	(0)	−19.6	(0)	−69.3	(0)	−10.0	(0)

GP77-0221-26

Table 22(m) Wire to Wire Sensitivity Study Test Results
Emitter Conductivity

Input Parameter Value (6b. Emitter Conductivity)	Integrated Margin (dB)	EMI Point Margin (dB) 10 kHz	EMI Point Margin (dB) 10 MHz	Current Transfer Function (dB) 10 kHz	Current Transfer Function (dB) 10 MHz
Bundle 1 T2QNT from TRIGG					
1	-22.4	-34.7	-48.0	-36.6	-1.7
2 (3 dB)	-22.4 (0)	-34.7 (0)	-48.0 (0)	-36.6 (0)	-1.7 (0)
0.01 (-20 dB)	-22.4 (0)	-34.7 (0)	-48.0 (0)	-36.6 (0)	-1.7 (0)
Bundle 2 AIMS 4 from BNOGO					
0.85	12.2	-13.8	-17.4	-61.3	-16.7
1.7 (3 dB)	12.2 (0)	-13.8 (0)	-17.4 (0)	-61.3 (0)	-16.7 (0)
0.0085 (-20 dB)	12.2 (0)	-13.8 (0)	-17.4 (0)	-61.3 (0)	-16.7 (0)
Bundle 3 LBAO from RUDPO					
0.85	-47.6	-85.8	-70.4	-77.8	-14.3
1.7 (3 dB)	-48.3 (-0.7)	-85.9 (-0.1)	-70.7 (-0.3)	-77.9 (-0.1)	-14.5 (-0.2)
0.0085 (-20 dB)	-20.6 (27.0)	-85.6 (0.2)	-54.2 (16.2)	-77.7 (0.1)	2.0 (16.3)
Bundle 4 VERTX from YAWBT					
0.85	-137.8	-222.0	-161.9	-237.0	-128.8
1.7 (3 dB)	-140.8 (-3.0)	-222.1 (-0.1)	-164.9 (-3.0)	-237.2 (-0.2)	-131.8 (-3.0)
0.085 (-10 dB)	-118.5 (19.3)	-221.9 (0.1)	-143.2 (18.7)	-236.9 (0.1)	-110.1 (18.7)
Bundle 5 EXTND from AILPO					
0.85	-78.2	-186.5	-118.2	-212.6	-96.1
1.7 (3 dB)	-79.4 (-1.2)	-191.2 (-4.7)	-217.3 (-0.9)	-217.3 (-4.7)	-97.0 (-0.9)
0.0085 (-20 dB)	-46.6 (31.6)	-146.8 (39.7)	-82.1 (36.1)	-172.9 (39.7)	-60.0 (36.1)
Bundle 6 BYRAM from RATS					
1	-92.9	-130.8	-112.9	-148.8	-82.8
2 (3 dB)	-95.9 (-3.0)	-131.3 (-0.5)	-115.9 (-3.0)	-149.3 (-0.5)	-85.8 (-3.0)
0.1 (-10 dB)	-83.0 (9.9)	-130.6 (0.2)	-103.0 (9.9)	-148.6 (0.2)	-72.8 (10.0)
Bundle 7 ACPWR from ANUNC					
0.85	-28.6	-125.1	-59.1	-153.1	-42.1
1.7 (3 dB)	-28.7 (-0.1)	-125.2 (-0.1)	-59.3 (-0.2)	-153.2 (-0.1)	-42.3 (-0.2)
0.0085 (-20 dB)	-26.2 (2.4)	-125.0 (0.1)	-55.4 (3.7)	-153.1 (0)	-38.4 (3.7)
Bundle 8 XDEF from HVPS					
1	-34.2	-38.7	-28.1	-150.8	-81.9
2 (3 dB)	-34.2 (0)	-38.7 (0)	-28.1 (0)	-150.8 (0)	-81.9 (0)
0.01 (-20 dB)	-34.2 (0)	-38.7 (0)	-28.1 (0)	-150.8 (0)	-81.9 (0)
Bundle 9 CAUTN from DCPWR					
1	6.7	-30.8	-19.6	-69.3	-10.0
2 (3 dB)	6.7 (0)	-30.8 (0)	-19.6 (0)	-69.3 (0)	-10.0 (0)
0.01 (-20 dB)	6.7 (0)	-30.8 (0)	-19.6 (0)	-69.3 (0)	-10.0 (0)

GP77-0221-27

161

Table 22(n) Wire to Wire Sensitivity Study Test Results
Receptor Permittivity

Input Parameter Value (7a. Receptor Permittivity)		Integrated Margin (dB)		EMI Point Margin (dB)				Current Transfer Function (dB)			
				10 kHz		10 MHz		10 kHz		10 MHz	
Bundle 1											
T2QNT from TRIGG	2.8	−22.4	(0)	−34.7	(0)	−48.0	(0)	−36.6	(0)	−1.7	(0)
	5.6 (3 dB)	−22.4	(0)	−34.7	(0)	−48.0	(0)	−36.6	(0)	−1.7	(0)
	280 (20 dB)	−22.4	(0)	−34.7	(0)	−48.0	(0)	−33.6	(0)	−1.7	(0)
Bundle 2											
AIMS 4 from BNOGO	2.8	12.2	(0)	−13.8	(0)	−17.4	(0)	−61.3	(0)	−16.7	(0)
	5.6 (3 dB)	12.2	(0)	−13.8	(0)	−17.4	(0)	−61.2	(0)	−16.7	(0)
	280 (20 dB)	12.2	(0)	−13.8	(0)	−17.4	(0)	−61.3	(0)	−16.7	(0)
Bundle 3											
LBAO from RUDPO	2.8	−47.6	(0)	−85.8	(0)	−70.4	(0)	−77.8	(0)	−14.3	(0)
	5.6 (3 dB)	−47.6	(0)	−85.8	(0)	−70.4	(0)	−77.8	(0)	−14.3	(0)
	280 (20 dB)	−47.6	(0)	−85.8	(0)	−70.4	(0)	−77.8	(0)	−14.3	(0)
Bundle 4											
VERTX from YAWBT	2.8	−137.8	(0)	−222.0	(0)	−161.9	(0)	−237.0	(0)	−128.8	(0)
	5.6 (3 dB)	−137.8	(0)	−222.0	(0)	−161.9	(0)	−237.0	(0)	−128.8	(0)
	280 (20 dB)	−137.8	(0)	−221.9	(0.1)	−161.9	(0)	−237.0	(0)	−128.8	(0)
Bundle 5											
EXTND from AILPO	2.8	−78.2	(0)	−186.5	(0)	−118.2	(0)	−212.6	(0)	−96.1	(0)
	5.6 (3 dB)	−78.2	(0)	−186.5	(0)	−118.2	(0)	−212.6	(0)	−96.1	(0)
	280 (20 dB)	−78.2	(0)	−186.5	(0)	−118.2	(0)	−212.6	(0)	−96.1	(0)
Bundle 6											
BYRAM from RATS	2.8	−92.9	(0)	−130.8	(0)	−112.9	(0)	−148.8	(0)	−82.8	(0)
	5.6 (3 dB)	−92.9	(0)	−130.8	(0)	−112.9	(0)	−148.8	(0)	−82.8	(0)
	280 (20 dB)	−92.8	(0)	−130.8	(0)	−112.9	(0)	−148.8	(0)	−82.8	(0)
Bundle 7											
ACPWR from ANUNC	2.8	−28.6	(0)	−125.1	(0)	−59.1	(0)	−153.1	(0)	−42.1	(0)
	5.6 (3 dB)	−28.6	(0)	−125.1	(0)	−59.1	(0)	−153.1	(0)	−42.1	(0)
	280 (20 dB)	−28.6	(0)	−125.1	(0)	−59.1	(0)	−153.1	(0)	−42.1	(0)
Bundle 8											
XDEF from HVPS	2.8	−34.2	(0)	−38.7	(0)	−28.1	(0)	−150.8	(0)	−81.9	(0)
	5.6 (3 dB)	−34.2	(0)	−38.7	(0)	−28.1	(0)	−150.8	(0)	−81.9	(0)
	280 (20 dB)	−34.2	(0)	−38.7	(0)	−28.1	(0)	−150.8	(0)	−81.9	(0)
Bundle 9											
CAUTN from DCPWR	2.8	6.7	(0)	−30.8	(0)	−19.6	(0)	−69.3	(0)	−10.0	(0)
	5.6 (3 dB)	6.7	(0)	−30.8	(0)	−19.6	(0)	−69.3	(0)	−10.0	(0)
	280 (20 dB)	6.7	(0)	−30.8	(0)	−19.6	(0)	−69.3	(0)	−10.0	(0)

GP77-0221-28

162

Table 22(o) Wire to Wire Sensitivity Study Test Results
Emitter Permittivity

Input Parameter Value (7b. Emitter Permittivity)		Integrated Margin (dB)		EMI Point Margin (dB)				Current Transfer Function (dB)			
				10 kHz		10 MHz		10 kHz		10 MHz	
Bundle 1											
T2QNT from TRIGG											
2.8		−22.4		−34.7		−48.0		−36.6		−1.7	
5.6	(3 dB)	−22.4	(0)	−34.7	(0)	−48.0	(0)	−36.6	(0)	−1.7	(0)
280	(20 dB)	−22.4	(0)	−34.7	(0)	−48.0	(0)	−36.6	(0)	−1.7	(0)
Bundle 2											
AIMS 4 from BNOGO											
2.8		12.2		−13.8		−17.4		−61.3		−16.7	
5.6	(3 dB)	12.2	(0)	−13.8	(0)	−17.4	(0)	−61.3	(0)	−16.7	(0)
280	(20 dB)	12.2	(0)	−13.8	(0)	−17.4	(0)	−61.3	(0)	−16.7	(0)
Bundle 3											
LBAO from RUDPO											
2.8		−47.6		−85.8		−70.4		−77.8		−14.3	
5.6	(3 dB)	−45.9	(1.7)	−85.8	(0)	−70.2	(0.2)	−77.8	(0)	−14.1	(0.2)
280	(20 dB)	−25.5	(27.1)	−85.7	(0.1)	−60.6	(9.8)	−77.7	(0.1)	−4.5	(9.8)
Bundle 4											
VERTX from YAWBT											
2.8		−137.8		−222.0		−161.9		−237.0		−128.8	
5.6	(3 dB)	−137.7	(0.1)	−222.0	(0)	−161.9	(0)	−237.0	(0)	−128.8	(0)
280	(20 dB)	−136.4	(1.4)	−221.9	(0.1)	−161.6	(0.3)	−237.0	(0)	−128.5	(0.3)
Bundle 5											
EXTND from AILPO											
2.8		−78.2		−186.5		−118.2		−212.6		−96.1	
5.6	(3 dB)	−75.2	(3.0)	−181.7	(4.8)	−116.1	(2.1)	−207.8	(4.8)	−94.0	(2.1)
280	(20 dB)	−58.1	(20.1)	−149.1	(37.4)	−91.0	(27.2)	−175.2	(37.4)	−68.9	(27.2)
Bundle 6											
BYRAM from RATS											
2.8		−92.9		−130.8		−112.9		−148.8		−82.8	
5.6	(3 dB)	−92.9	(0)	−130.8	(0)	−112.9	(0)	−148.8	(0)	−82.8	(0)
280	(20 dB)	−91.0	(1.9)	−130.8	(0)	−112.9	(0)	−148.8	(0)	−82.7	(0.1)
Bundle 7											
ACPWR from ANUNC											
2.8		−28.6		−125.1		−59.1		−153.1		−42.1	
5.6	(3 dB)	−28.6	(0)	−125.1	(0)	−59.1	(0)	−153.1	(0)	−42.1	(0)
280	(20 dB)	−28.6	(0)	−125.1	(0)	−59.1	(0)	−153.1	(0)	−42.1	(0)
Bundle 8											
XDEF from HVPS											
2.8		−34.2		−38.7		−28.1		−150.8		−81.9	
5.6	(3 dB)	−34.2	(0)	−28.1	(0)	−28.1	(0)	−150.8	(0)	−81.9	(0)
280	(20 dB)	−34.2	(0)	−38.7	(0)	−28.1	(0)	−150.8	(0)	−81.9	(0)
Bundle 9											
CAUTN from DCPWR											
2.8		6.7		−30.8		−19.6		−69.3		−10.0	
5.6	(3 dB)	6.7	(0)	−30.8	(0)	−19.6	(0)	−69.3	(0)	−10.0	(0)
280	(20 dB)	6.7	(0)	−30.8	(0)	−19.6	(0)	−69.3	(0)	−10.0	(0)

163

Table 22(p) Wire to Wire Sensitivity Study Test Results
Wire Separation

Input Parameter Value (8. Wire Separation)	Integrated Margin (dB)	EMI Point Margin (dB)		Current Transfer Function (dB)	
		10 kHz	10 MHz	10 kHz	10 MHz
Bundle 1 T2QNT from TRIGG — Adjacent	−22.4	−34.7	−48.0	−36.6	−1.7
2 in. Bundle	−28.4 (−6.0)	−40.4 (−5.7)	−53.9 (−5.9)	−42.3 (−5.7)	−7.7 (−6.0)
Bundle 2 AIMS4 from BNOGO — Adjacent	12.2	−13.8	−17.4	−61.3	−16.7
2 in. Bundle	3.0 (−9.2)	−28.2 (−14.4)	−21.0 (−3.6)	−75.7 (−14.4)	−20.3 (−3.6)
Bundle 3 LBAO from RUDPO — Adjacent	−47.6	−85.8	−70.4	−77.3	−14.3
2 in. Bundle	−53.8 (−6.2)	−90.8 (−5.0)	−75.6 (−5.2)	−82.9 (−5.1)	−19.5 (−5.2)
Bundle 4 VERTX from YAWBT — Adjacent	−137.8	−222.0	−161.9	−237.0	−128.8
2 in. Bundle	−142.2 (−4.4)	−226.3 (−4.3)	−166.3 (−4.4)	−214.4 (22.6)	−133.2 (−4.4)
Bundle 5 EXTND from AILPO — Adjacent	−78.2	−186.5	−118.2	−212.6	−96.1
2 in. Bundle	−84.6 (−6.4)	−195.4 (−8.9)	−123.8 (−5.6)	−221.5 (−9.2)	−101.7 (−5.6)
Bundle 6 BYRAM from RATS — Adjacent	−92.9	−130.8	−112.9	−148.8	−82.8
2 in. Bundle	−121.1 (−28.2)	−159.1 (−28.3)	−141.3 (−28.4)	−177.2 (−28.4)	−111.1 (−28.3)
Bundle 7 ACPWR from ANUNC — Adjacent	−28.6	−125.1	−59.1	−153.1	−42.1
2 in. Bundle	−33.6 (−5.0)	−130.1 (−5.0)	−64.1 (−5.0)	−158.1 (−5.0)	−47.2 (−5.1)
Bundle 8 XDEF from HVPS — Adjacent	−34.2	−38.7	−28.1	−150.8	−96.8
2 in. Bundle	−48.2 (−14.0)	−46.2 (−7.5)	−43.0 (−14.9)	−158.4 (−7.6)	−96.8 (−14.9)
Bundle 9 CAUTN from DC PWR — Adjacent	6.7	−30.8	−19.6	−69.3	−10.0
2 in. Bundle	1.0 (−5.7)	−36.4 (−5.6)	−25.3 (−5.7)	−74.9 (−5.6)	−15.6 (−5.6)

GP77-0221-30

164

Table 22(q) Wire to Wire Sensitivity Study Test Results
Wire Common Length

Input Parameter Value (9. Wire Common Length)		Integrated Margin (dB)	EMI Point Margin (dB)		Current Transfer Function (dB)	
			10 kHz	10 MHz	10 kHz	10 MHz
Bundle 1						
T2QNT from TRIGG						
192	(3 dB)	−22.4	−34.7	−48.0	−36.6	−1.7
384	(3 dB)	−17.9 (+4.5)	−28.7 (6.0)	−47.6 (0.4)	−30.6 (6.0)	−1.3 (0.4)
19.2	(−10 dB)	−28.3 (−5.9)	−54.7 (−20.0)	−49.4 (−1.4)	−56.6 (−20.0)	−3.1 (−1.4)
Bundle 2						
AIMS 4 from BNOGO						
56		12.2	−13.8	−17.4	−61.3	−16.7
112	(3 dB)	17.8 (+5.6)	−7.8 (6.0)	−17.1 (0.3)	−55.2 (6.1)	−16.5 (0.2)
5.6	(−10 dB)	0.6 (−11.6)	−33.8 (−20.0)	−24.2 (−6.8)	−81.3 (−20.0)	−23.5 (−6.8)
Bundle 3						
LBAO from RUDPO						
80		−47.6	−85.8	−70.4	−77.8	−14.3
160	(3 dB)	−39.6 (+8.0)	−74.2 (11.6)	−68.4 (2.0)	−66.2 (11.6)	−12.3 (2.0)
8.0	(−10 dB)	−57.2 (−9.6)	−125.6 (−39.8)	−84.8 (−14.4)	−117.7 (−39.9)	−28.7 (−14.4)
Bundle 4						
VERTX from YAWBT						
320		−137.8	−222.0	−161.9	−237.0	−128.8
640	(3 dB)	−130.2 (+7.6)	−203.9 (18.1)	−152.3 (9.6)	−219.0 (18.0)	−119.2 (9.6)
32	(−10 dB)	−175.9 (−38.1)	−282.0 (−60.0)	−212.7 (−50.8)	−297.0 (−60.0)	−179.6 (−50.8)
Bundle 5						
EXTND from AILPO						
130		−78.2	−186.5	−118.2	−212.6	−96.1
260	(3 dB)	−63.2 (+15)	−168.7 (17.8)	−104.0 (14.2)	−194.8 (17.8)	−81.9 (14.2)
65	(−3 dB)	−92.2 (−14.0)	−204.5 (−18.0)	−131.6 (−13.4)	−230.6 (−18.0)	−109.5 (−13.4)
Bundle 6						
BYRAM from RATS						
75		−92.9	−130.8	−112.9	−148.8	−82.8
150	(3 dB)	−89.1 (+3.8)	−118.7 (12.1)	−109.9 (3.0)	−136.8 (12.0)	−79.8 (3.0)
7.5	(−10 dB)	−107.0 (−14.1)	−170.8 (−40.0)	−131.9 (−19.0)	−188.8 (−40.0)	−101.8 (−19.0)
Bundle 7						
ACPWR from ANUNC						
108		−28.6	−125.1	−59.1	−153.1	−42.1
216	(3 dB)	−28.3 (+0.3)	−125.0 (0.1)	−59.0 (0.1)	−153.0 (0.1)	−42.0 (0.1)
1080	(10 dB)	−57.7 (−29.1)	−165.1 (−40.0)	−95.5 (−36.4)	−193.1 (−40.0)	−78.5 (−36.4)
Bundle 8						
XDEF from HVPS						
145		−34.2	−38.7	−28.1	−150.8	−81.9
290	(3 dB)	−27.8 (+6.4)	−38.6 (0.1)	−21.8 (6.3)	−150.8 (0)	−75.6 (6.3)
14.5	(−10 dB)	−41.8 (−7.6)	−38.7 (0)	−36.8 (−8.7)	−150.9 (−0.1)	−90.6 (−8.7)
Bundle 9						
CAUTN from DCPWR						
72		6.7	−30.8	−19.6	−69.3	−10.0
	(3 dB)	9.5 (+2.8)	−24.8 (6.0)	−15.2 (4.4)	−63.3 (16.0)	−5.5 (4.5)
3.6	(−10 dB)	−9.9 (−16.6)	−50.8 (−20.0)	−39.0 (−19.4)	−89.3 (−20.0)	−29.3 (−19.3)

165

GP77-0221-31

Table 22(r) Wire to Wire Sensitivity Study Test Results
Bundle Height

Input Parameter Value (10. Bundle Height)	Integrated Margin (dB)		EMI Point Margin (dB)				Current Transfer Function (dB)			
			10 kHz		10 MHz		10 kHz		10 MHz	
Bundle 1										
T2QNT from TRIGG										
4	−22.4		−34.7		−48.0		−36.6		−1.7	
8	−21.7	(0.7)	−33.7	(0.1)	−47.8	(0.2)	−35.5	(1.1)	−1.5	(0.2)
36	−20.2	(2.2)	−31.7	(3.0)	−47.4	(0.6)	−33.6	(3.0)	−1.1	(0.6)
Bundle 2										
AIMS4 from BNOGO										
4	12.2		−13.8		−17.4		−61.3		−16.7	
8	12.3	(0.1)	−13.7	(0.1)	−17.4	(0)	−61.2	(0.1)	−16.7	(0)
36	12.2	(0)	−13.8	(0)	−17.4	(0)	−61.2	(0.1)	−16.7	(0)
Bundle 3										
LBAO from RUDPO										
4	−47.6		−85.8		−70.4		−77.8		−14.3	
8	−47.8	(−0.2)	−85.5	(0.3)	−70.5	(−0.1)	−77.5	(0.3)	−14.4	(−0.1)
36	−48.2	(−0.6)	−85.0	(0.8)	−70.9	(−0.5)	−77.0	(0.8)	−14.8	(−0.5)
Bundle 4										
VERTX from YAWBT										
4	−137.8		−222.0		−161.9		−237.0		−128.8	
8	−138.0	(−0.2)	−223.4	(−1.4)	−162.2	(−0.3)	−238.4	(−1.4)	−129.1	(−0.3)
36	−138.5	(−0.7)	−226.1	(−4.1)	−162.9	(−1.0)	−241.2	(−4.2)	−129.8	(−1.0)
Bundle 5										
EXTND from AILPO										
4	−78.2		−186.5		−118.2		−212.6		−96.1	
8	−78.4	(−0.2)	−186.6	(−0.1)	−118.5	(−0.3)	−212.7	(−0.1)	−96.4	(−0.3)
36	−78.8	(−0.6)	−186.8	(−0.3)	−119.0	(−0.8)	−212.9	(−0.3)	−96.9	(−0.8)
Bundle 6										
BYRAM from RATS										
4	−92.9		−130.8		−112.9		−148.8		−82.8	
8	−91.3	(1.6)	−131.6	(−0.8)	−113.0	(−0.1)	−149.7	(−0.9)	−82.8	(0)
36	−93.5	(−0.6)	−133.3	(−2.5)	−113.2	(−0.3)	−151.3	(−2.5)	−83.1	(−0.3)
Bundle 7										
ACPWR from ANUNC										
4	−28.6		−125.1		−59.1		−153.1		−42.1	
8	−29.0	(−0.4)	−124.7	(0.4)	−59.2	(−0.1)	−152.8	(0.3)	−42.3	(−0.2)
36	−29.9	(−1.3)	−124.3	(0.8)	−59.6	(−0.5)	−152.3	(0.8)	−42.7	(−0.6)
Bundle 8										
XDEF from HVPS										
4	−34.2		−38.7		−28.1		−150.8		−81.9	
8	−34.6	(−0.4)	−38.4	(0.3)	−28.5	(−0.4)	−150.6	(0.2)	−82.4	(−0.5)
36	−35.3	(−1.1)	−38.1	(0.6)	−29.3	(−1.2)	−150.3	(0.5)	−83.2	(−1.3)
Bundle 9										
CAUTN from DCPWR										
4	6.7		−30.8		−19.6		−69.3		−10.0	
8	7.3	(0.6)	−29.7	(1.1)	−18.7	(−0.9)	−68.2	(1.1)	−9.0	(1.0)
36	8.4	(1.7)	−27.8	(3.0)	−17.1	(2.5)	−66.2	(3.1)	−7.4	(2.6)

Table 22(s) Wire to Wire Sensitivity Study Test Results
Pulse Width

Input Parameter Value (14. Pulse Width)		Integrated Margin (dB)		EMI Point Margin (CdB)			
				100 kHz		50 MHz	
Bundle 8 HVPS from YDEF	0.5×10^{-6}	-96.0		-149.9		-114.7	
	0.25×10^{-6}	-95.7	$(+0.3)$	-155.9	(-6)	-111.7	$(+3)$
	0.025×10^{-6}	-96.7	(-0.7)	-175.9	(-26)	-110.7	$(+4)$
Bundle 8 XDEF from YDEF	0.5×10^{-6}	-20.5		-47.8		-108.1	
	0.25×10^{-6}	-20.7	(-0.2)	-50.8	(-3)	-105.1	$(+3)$
	0.025×10^{-6}	-28.8	(-8.3)	-63.8	(-16)	-104.2	$(+3.9)$

$\tau_r = 10^{-8}$ sec

$(f_{low}, f_{high}) = (30\ Hz, 100\ MHz)$

GP77-0221-33

Table 22(t) Wire to Wire Sensitivity Study Test Results
Pulse Rise Time

Input Parameter Value (15. Pulse Rise Time)		Integrated Margin (dB)		EMI Point Margin (CdB)			
				10MHz		50 MHz	
Bundle 8 HVPS from YDEF	0.1×10^{-6}	-103.7		-122.9		-134.7	
	0.05×10^{-6}	-100.8	$(+2.9)$	-116.9	$(+6.0)$	-128.7	$(+6.0)$
	0.01×10^{-6}	-96.0	$(+7.7)$	-114.3	$(+8.6)$	-114.7	$(+20.0)$
Bundle 8 XDEF from YDEF	0.1×10^{-6}	-22.9		-39.2		-128.1	
	0.05×10^{-6}	-20.9	$(+2.0)$	-33.2	$(+6.0)$	-122.1	$(+6.0)$
	0.01×10^{-6}	-20.5	$(+2.4)$	-30.5	$(+8.7)$	-108.1	$(+20.0)$

$(f_{low}, f_{high}) = (30\ Hz, 100\ MHz)$

GP77-0221-34

Table 22(u) Wire to Wire Sensitivity Study Test Results
Pulse Bit Rate

Input Parameter Value (16. Pulse Bit Rate)		Integrated Margin (dB)		EMI Point Margin (dB)			
				10MHz		50 MHz	
Bundle 8 HVPS from YDEF	1×10^{6}	-75.4		-122.9		-79.1	
	0.5×10^{6}	-75.4	(0)	-125.9	(-3.0)	-79.1	(0)
	0.01×10^{6}	-75.4	(0)	-142.9	(-20.0)	-79.1	(0)
Bundle 8 XDEF from YDEF	1×10^{6}	-23.0		-39.2		-72.5	
	0.5×10^{6}	-25.8	(-2.8)	-42.2	(-3.0)	-72.5	(0)
	0.01×10^{6}	-38.4	(-15.4)	-59.2	(-20.0)	-72.5	(0)

$\tau_r = 10^{-7}$ sec

$(f_{low}, f_{high}) = (30\ Hz, 100\ MHz)$

GP77-0221-35

167

Table 22(v) Wire to Wire Sensitivity Study Test Results
Receptor Required Frequency Range

Input Parameter Value (17a. Required Frequency Range, Receptor)	Integrated Margin (dB)	EMI Point Margin (dB)			Current Transfer Function (dB)		
		10 kHz	10 MHz	10 MHz	10 kHz	10 kHz	10 MHz
Bundle 2 AIMS4 from BNOGO							
10^3	12.2						
2×10^3	27.0 (14.8)						
1.3×10^3	23.2 (11.0)						
Bundle 3 LBAO from RUDPO							
10^3	−47.6						
2×10^3	−47.6 (0)						
10×10^3	−47.6 (0)						
Bundle 4 VERTX from YAWBT							
10^3	−137.8						
2×10^3	−137.8 (0)						
10×10^3	−137.8 (0)						
Bundle 5 EXTND from AILPO							
10^3	−78.2						
2×10^3	−78.2 (0)						
10×10^3	−78.2 (0)						
Bundle 6 BYRAM from RATS							
10^3	−92.9						
2×10^3	−92.4 (0.5)						
10×10^3	−92.4						
Bundle 8 XDEF from HVPS							
10^7	−34.2						
2×10^7	−16.5 (17.7)						
1.3×10^7	−31.5 (2.7)						
Bundle 9 CAUTN from DCPWR							
10^3	6.7						
2×10^3	8.0 (1.3)						
10×10^3	6.6 (−0.1)						

GP77-0221-36

168

Table 22(w) Wire to Wire Sensitivity Study Test Results
Emitter Required Frequency Range

Input Parameter Value (17b. Required Frequency Range, Emitter)	Integrated Margin (dB)	EMI Point Margin (dB)			Current Transfer Function (dB)		
		10 kHz	10 MHz	10 MHz	10 kHz	10 kHz	10 MHz
Bundle 1 T2QNT from TRIGG	10^3 −22.4 (0) 2×10^3 −22.4 (0) 10^5 −25.7 (−3.3)						
Bundle 2 AIMS4 from BNOGO	10^3 12.2 2×10^3 8.7 (−3.5) 10^5 3.3 (−8.9)						
Bundle 3 LBAO from RUDPO	10^3 −47.6 2×10^3 −47.6 (0) 10^5 −47.7 (−0.1)						
Bundle 4 VERTX from YAWBT	10^3 −137.8 2×10^3 −137.8 (0) 10^5 −137.8 (0)						
Bundle 5 EXTND from AILPO	10^3 −78.2 2×10^3 −78.2 (0) 10^5 −78.2 (0)						
Bundle 6 BYRAM from RATS	10^3 −92.9 2×10^3 −92.9 (0) 10^5 −93.0 (−0.1)						
Bundle 7 ACPWR from ANUNC	10^3 −28.6 2×10^3 −28.6 (0) 10^5 −28.6 (0)						

GP77-0221-37

169

Table 22(x) Wire to Wire Sensitivity Study Test Results
Number of Frequencies

Input Parameter Value (18. Number of Frequencies)	Integrated Margin (dB)		EMI Point Margin (dB)		Current Transfer Function (dB)	
			10 kHz	10 MHz	10 kHz	10 MHz
Bundle 1						
T2QNT from TRIGG						
40	−22.4					
65	−23.1	(−0.7)				
90	−23.3	(−0.9)				
Bundle 2						
AIMS 4 from BNOGO						
40	12.2					
65	12.1	(−0.1)				
90	12.1	(−0.1)				
Bundle 3						
LBAO from RUDPO						
40	−47.6					
65	−46.6	(1.0)				
90	−46.1	(1.5)				
Bundle 4						
VERTX from YAWBT						
40	−137.8					
65	−137.1	(0.7)				
90	−136.8	(1.0)				
Bundle 5						
EXTND from AILPO						
40	−78.2					
65	−75.4	(2.8)				
90	−74.3	(3.9)				
Bundle 6						
BYRAM from RATS						
40	−92.9					
65	−92.6	(0.3)				
90	−92.5	(0.4)				
Bundle 7						
ACPWR from ANUNC						
40	−28.6					
65	−27.1	(1.5)				
90	−26.5	(2.1)				
Bundle 8						
XDEF from HVPS						
40	−34.2					
65	−32.8	(1.4)				
90	−33.6	(0.6)				
Bundle 9						
CAUTN from DCPWR						
40	6.7					
65	7.3	(0.6)				
90	7.5	(0.8)				

170

GP77-0221-38

variation in resistance in many bundles, the final variation in resistance was increased to 20 dB, or a factor of 100, for those cases. The table shows that the corresponding range of integrated margin variation is 0.1 - 17.3 dB.

The sensitivity study test results for each of the 15 input parameter types are discussed below.

4.2.1 Termination resistance. The largest variation in integrated margin due to a 3 dB variation in IWRPLR, VWEPLR and VWRPLR is 6 dB, 3 dB and 5 dB, respectively. Thus the output is slightly more sensitive to IWRPLR and less sensitive to VWEPLR, with VWRPLR somewhere in between. On the other hand, the variation in integrated margin due to a 20 dB variation in resistance shows the greatest sensitivity to VWRPLR and the least sensitivity to IWRPLR.

These results can be better understood by looking at the variation in the current transfer function and point margin at 10 kHz and 10 MHz. A 3 dB variation in resistance tends to cause a greater variation in the transfer function at 10 kHz than at 10 MHz. Typically the variation at 10 kHz is about 6 dB and at 10 MHz is somewhat less. Thus the point margin, as a ratio, is proportional to the square of the resistance at lower frequencies, and less sensitive at higher frequencies. The result of integrating the margin density is essentially an averaging process, weighted at the higher frequencies where coupling is usually higher, and the integrated margin tends to vary slightly less than the square of the resistance. The wide range in variation of the integrated margin for the 9 separate bundles indicates its dependence on the particular configuration. For example, in Bundle B7 doubling the ACPWR VWEPLR from 0.1 ohms to 0.2 ohms has no effect on the integrated margin, because such a small resistance is overwhelmed by the 185 ohm termination on the end of the wire. Increasing this resistance to 10 ohms likewise has no effect. In this example, the ACPWR line is a low impedance circuit where inductive coupling is dominant, and the induced current depends only on the total series circuit impedance. Thus, the small contribution of the emitter port impedance to the total loop impedance accounts for lack of sensitivity to this parameter. In another example, doubling the EXTND VWEPLR from 1 to 2 dB has no effect but increasing it to 100 ohms causes the integrated margin to increase by 32.8 dB, the point margin and current transfer function at 10 kHz increasing by about 40 dB. This strikingly different outcome is the result of capacitive coupling to a higher impedance line, where the inductively coupled component is relatively small because of the 10K impedance at the receptor's load end.

On the basis of the test results for termination resistance, the IEMCAP outputs are not especially sensitive to this parameter. A 3 dB uncertainty in the input causes no more than a 6 dB variation in the integrated margin, which can be said to have a quadratic dependence.

4.2.2 Shield configuration. The test data for receptor wire shielding, Table 22 (d), indicate that putting a shield on a receptor wire, grounded at both ends, reduces the integrated margin by as much as 84.5 dB and by as little as 9.4 dB. In all cases but the XDEF, variation of the current transfer function is more pronounced at 10 MHz than at 10 kHz and 22.7 dB at 10 MHz. The test data further indicates that putting a double shield on a receptor wire reduces the integrated margin by as much as 93.1 dB and as little as 9.3 dB. In all cases but the EXTND, a double shield is only slightly more effec-

171

tive than a single shield in reducing the interference; the difference in the integrated margin between a single shield and double shield is usually less than 1 dB. The integrated margin at the EXTND is reduced 71 dB by a single receptor shield, and reduced an additional 22.1 dB by the second shield.

The test results for emitter wire shielding, Table 22 (e), revealed that there were anomalies in the wire-to-wire coupling portion of the IEMCAP code. In Bundle B1 and Bundle B9, putting a shield on the emitter wire increases the integrated margin by 3.4 dB and 1.6 dB, respectively. The current transfer function for the shielded configuration at 10 kHz increases by 5.4 dB and 5.5 dB, respectively. Errors were also found relating to emitter shield grounding, receptor twisting, receptor balancing and emitter balancing; the effect of shielding, grounding, twisting, and balancing wires, in a number of cases, was to increase rather than decrease the amount of interference. Errors in the IEMCAP code were subsequently found and corrected by RADC pertaining to shielding, grounding, and twisting. The problem with balancing, however, was found to be due to an inadequacy in the mathematical model itself, and not any error in the code. Work is proceeding on an improved coupling model for balanced wires at RADC. The improved model will be implemented in the IEMCAP code as soon as possible. The affected portion of the sensitivity study having to do with emitter wire shielding, emitter shield grounding, receptor wire twisting and receptor wire balancing, was re-run at the RADC facility with a corrected version of the code. The corrected test results are summarized in Table 23.

The corrected test results for emitter wire shielding indicate that putting a shield on the emitter wire, grounded at both ends decreases the integrated margin by as much as 68.2 dB and as little as 3.8 dB. In 6 out of the 9 bundles, the margin was reduced by better than 28 dB. In the other 3 bundles (Bundle B1, B8, and B9) the emitter wire is a relatively low impedance circuit, although it is not certain that this has a bearing on the shielding effectiveness. It is clear, however, that shielding generally reduces the integrated margin by a substantial amount and that the shield configuration is a very sensitive input parameter.

4.2.3 Ground configuration. The effect of grounding the shield on the receptor wire, Table 22(f) , is a reduction of the integrated margin by as much as 83.8 dB and as little as 0 dB. Grounding a shield at both ends tends to reduce inductive coupling but has no effect on capacitive coupling, so the effect of grounding depends on which coupling mode is dominant.

The effect of grounding the emitter shield, shown in the corrected sensitivity study test results, Table 23, is a reduction in the integrated margin by as much as 29.9 dB and as little as 2.9 dB.

Grounding, like shielding, is a very sensitive input parameter.

Table 23. Corrected Sensitivity Study Results For Shielding, Grounding, Twisting and Balancing

Emitter-Receptor Combination		Integrated Margin Value			
		Emitter Shielding (①= Unshielded ②= Shielded)	Emitter Grounding (①= One End ②= Both Ends)	Receptor Twisting (①= Untwisted ②= Twisted)	Receptor Balancing (①= Unbalanced ②= Balanced)
1. T2QNT from TRIGG	①	−22.4	−23.3	−22.4	−15.4
	②	−26.2 (−3.8)	−26.2 (−2.9)	−15.4 (7.0)	−38.2 (−22.8)
2. AIMS4 from BNOGO	①	12.1	−33.2	12.2	12.2
	②	−47.2 (−59.4)	−47.2 (−14)	12.2 (0)	18.2 (+6.0)
3. LBAO from RUDPO	①	9.3	−46.2	9.3	−59.4
	②	−58.9 (−68.2)	−58.9 (−12.7)	−59.4 (−68.7)	−54.2 (+5.2)
4. VERTX from YAWBT	①	−107.9	−111.1	−120.9	−137.8
	②	−137.8 (−29.9)	−137.8 (−26.7)	−137.8 (−16.9)	−108.7 (+29.1)
5. EXTND from AILPO	①	−25.6	−75.3	−63.8	−85.3
	②	−85.3 (−59.7)	−85.3 (−10)	−85.3 (−21.5)	−78.1 (+7.2)
6. BYRAM from RATS	①	−54.1	−63.0	−77.6	−133.7
	②	−92.9 (−38.8)	−92.9 (−29.9)	−133.7 (−56.1)	−92.9 (+40.8)
7. ACPWR from ANUNC	①	−27.8	−29.0	−27.8	−112.4
	②	−55.9 (−28.1)	−55.9 (−26.9)	−112.4 (−84.6)	−88.6 (+23.8)
8. YDEF from HVPS	①	−34.2	−37.8	−27.0	−47.6
	②	−43.2 (−9)	−43.2 (5.4)	47.6 (−20.6)	−34.2 (+13.4)
9. CAUTN from DCPWR	①	6.7	5.4	6.7	−45.7
	②	−1.2 (−7.9)	−1.2 (−6.6)	−45.7 (−39.0)	−16.9 (+28.8)

GP77-0342-8

Notes: ① = Integrated EMI margin for configuration no. 1
         ② = Integrated EMI margin for configuration no. 2

173

4.2.4 Twist configuration. The effect of twisting the receptor wire, shown in the corrected sensitivity study test results, Table 23, is a reduction in the integrated margin of as much as 84.6 dB and as little as 0 dB. Twisting the emitter wire, Table 22 (i), reduces the integrated margin by as much as 43.1 dB and as little as 0 dB. The only case where twisting the receptor wire or emitter wire has no effect is in Bundle B2, BNOGO to AIMS4, where the receptor circuit has a total loop impedance of 110,000 ohms, mostly due to the source end resistance. Apparently this is too high for inductive coupling, and twisting either wire does not affect the capacitive coupling.

Twisting appears to be generally a very sensitive parameter, comparable with shielding and grounding.

4.2.5 Balance configuration. The result of receptor wire balancing, shown in the corrected test results, Table 23, may be an increase in the integrated margin by as much as 40.8 dB. Emitter wire balancing, Table 22 (h), increases the integrated margin by as much as 47.0 dB. These obviously incorrect results, as discussed previously, reflect an inadequacy in the mathematical model used by the IEMCAP for coupling to or from balanced wires, and are not to be taken as a true indication. In order to obtain a reasonable indication of the sensitivity to this input parameter, this portion of the sensitivity study would have to be re-run with an improved balanced coupling model incorporated in the code.

4.2.6 Conductivity. Test results for receptor wire and emitter wire conductivity are contained in Table 22 (1) and (m). No amount of variation in the conductivity has any affect on the integrated margin for unshielded receptor wires, as would be expected, since it is the shield conductivity that really matters. For shielded receptor wires, a 3 dB increase in conductivity reduces the integrated margin by 3 dB in Bundle B4; a 10 dB decrease in conductivity increases the integrated margin by 10 dB. In Bundle B6, a 3dB increase in conductivity has no effect, and a 20 dB decrease in conductivity increases the margin by 2.3 dB. In Bundle B8, a 3 dB increase in conductivity has no effect, and a 20 dB decrease in conductivity increases the integrated margin by only 0.1 dB.

For unshielded emitter wires, variation in the conductivity has no effect. For the shielded emitter wires, a 3 dB increase in the conductivity reduces the integrated margin by as little as 0.1 dB and as much as 3.0 dB. A 10 dB decrease in conductivity increases the margin by as much as 19.3 dB and as little as 2.4 dB.

It is difficult to generalize the effect of conductivity on the current transfer function at 10 kHz and 10 MHz. In some cases, there is more variation at the lower frequency, in others at the higher frequency. The conductivity does not appear to be an especially sensitive input parameter, and moreover is a parameter whose uncertainty is not likely to be very great in the first place.

4.2.7 Permittivity. The test results for permittivity are contained in Table 22 (n) and (o). Changes in the receptor wire permittivity have no effect

174

on the integrated margin. A 3 dB increase in emitter wire permittivity increases the integrated margin by 3 dB in Bundle B5, by 1.7 dB in Bundle B3, by 0.1 dB in Bundle B4, and has no effect in the remaining 6 bundles. A 20 dB increase in permittivity in Bundle B5 increases the integrated margin by 20.1 dB, but a 20 dB increase in permittivity in the other bundles has little or no effect on the margin. Apparently the permittivity is a very insensitive input parameter. It is also one whose uncertainty is bound not to be very great.

4.2.8 Wire separation. The wire separation test results are contained in Table 22 (p). In the baseline configuration, each emitter wire-receptor wire combination are modeled as a pair of wires with a common run length in a small bundle of 3 or 4 wires. The IEMCAP wire model assumes that the separation between any two wires is equal to one quarter of the bundle diameter, unless that quantity is less than the sum of the outer radii of the two wires. Since two wires cannot be moved closer together than their physical dimensions permit, the program then assumes that they are adjacent to each other. The wire bundles selected for the F-15 mini-systems, however, were small representative samples of very large wire bundles, and the probability of two given wires being adjacent to each other is extremely small. In order to determine the error introduced by the worst case assumption of adjacent wires, a run was performed in which each bundle was simulated as having a 2 inch diameter. This was accomplished by letting the third wire in the bundle, not used in the sensitivity study, have a very large outer diameter, which then averaged with the diameters of the other wires, brings the average bundle diameter up to 2 inches.

The test results, then, show the variation in the integrated margin when the wire separation is changed from adjacent (on the order of about 40 mils) to 0.5 inches (corresponding to one quarter the bundle diameter). The effect on the integrated margin is typically a decrease of about 6 dB. The greatest variation is for Bundle B6, where the margin decreases by 28.2 dB; the smallest variation is for Bundle B7, where the margin decreases by 5 dB. The variation in the current transfer function is generally about the same at both 10 kHz and 10 MHz. These results indicate that wire separation can be a very sensitive input parameter in some cases, and not very sensitive in other cases.

4.2.9 Wire common run length. The wire common run length test result, contained in Table 22 (q), indicates that it is a generally very sensitive input parameter. A 3 dB increase in common run length increases the integrated margin by 15 dB in Bundle B5 and by about 8 dB in Bundles B3 and B4. A 10 dB decrease in run length decreases the integrated margin by 38.1 dB in Bundle B5. Generally there is more variation in coupling at 10 kHz than at 10 MHz.

It should be noted that the common run length is a sensitive input parameter that is not likely to be known to any degree of accuracy in the initial design stage.

4.2.10 Bundle height above ground. The test results, contained in Table 22 (r), indicate that bundle height is a very insensitive input parameter. Increasing bundle height above ground from 4 inches to 8 inches changes the integrated margin less than 1 dB for all but one of the 9 bundles, the exception being Bundle B6 with a variation of 1.6 dB. Increasing bundle

175

height from 4 inches to 36 inches causes the margin to vary by about 1 dB in most cases. Bundle height is clearly a very insensitive input parameter for wire-to-wire coupling.

4.2.11 Pulse width. The baseline for the pulse parameter tests consists of one meitter, the YDEF in Bundle B8, and two receptors, the HVPS and the XDEF. The YDEF is the y-deflection voltage to the HUD display oscilloscope, simulated as a trapezoidal pulse with a pulse width of 0.5 microseconds, a rise-time of 0.01 microseconds, and a bit rate of 10^6 pulses per second.

The test results for pulse width are contained in Table 22 (s). Decreasing the XDEF pulse width from 0.5 to 0.25 microseconds causes the integrated margin at the HVPS to increase by 0.3 dB, and causes the integrated margin at the YDEF to decrease by 0.2 dB. Decreasing the XDEF pulse width from 0.5 to 0.025 microseconds causes the integrated margin at the HVPS to decrease by 0.7 dB and at the XDEF to decrease by 8.3 dB.

Looking at the data for the point margins, it is seen that reducing the emitter pulse width causes the point margin to decrease at 100 kHz and increase at 50 MHz. These two effects tend to cancel each other out, so that the integrated margin changes very little.

According to the test data, reducing the pulse width by half causes a 6 dB point margin decrease at 100 kHz at the HVPS, but only 3 dB at the XDEF. The reason for the difference is that HVPS receptor is a power line, with no required susceptibility, and the point margin at 100 kHz is calculated by IEMCAP on the basis of the total received power in a standard bandwidth. Multiplying the pulse width by 1/2 is equivalent to multiplying the power spectral density by 1/4, but the bandwidth stays the same, so the total received power is multiplied by 1/4, a 6 dB decrease. On the other hand, the XDEF receptor is a signal line with a required bandwidth greater than the emitter bandwidth, so in that case the point margin at 100 kHz is calculated by IEMCAP on the basis of the emitter bandwidth. Multiplying the pulse width by 1/2 again is equivalent to multiplying the power spectral density by 1/4, but also re-sults in doubling the emitter bandwidth, so the total received signal is multi-plied by 1/2, a 3 dB decrease.

At 50 MHz, cutting the pulse width in half results in a 3 dB increase in the point margin for both the HVPS and XDEF. At that frequency, the power spectral density of the trapezoidal pulse is independent of the pulse width but the emitter bandwidth is less than the standard bandwidth, and is conse-quently used by the program in calculating the total received signal. Thus cutting the pulse width in half doubles the bandwidth, and so doubles the point margin.

On the basis of these results, the pulse width is not a very sensitive input parameter.

4.2.12 Pulse risetime. The test results, contained in Table 22 (t), in-dicate that the pulse risetime is not a sensitive parameter. Reducing the UDEF risetime from .1 to .05 microseconds increases the integrated margin at the HVPS by 2.9 dB, and at the XDEF by 2.0 dB. Reducing the risetime from .1

to .01 microseconds increases the integrated margins by 7.7 dB and 2.4 dB. At high frequencies, such as 50 MHz, the power spectral density is inversely proportional to the square of the risetime, so a 3 dB decrease in risetime results in a 6 dB increase in the point margin, and a 10 dB decrease in risetime results in a 20 dB increase in point margin. At intermediate frequencies, such as 10 MHz, decreasing the pulse rise time has less effect on the point margin. Since there appears to be more interference at 10 MHz than at 50 MHz, the change in the integrated margin more closely tracks the point margin at the lower frequency.

On the basis of the integrated margin, the pulse risetime is a relatively insensitive input parameter, but on the basis of the point margin it is somewhat sensitive. This may be of concern, particularly if the risetime is not known with any degree of accuracy.

4.2.13 Pulse bit rate. Results for the bit rate are contained in Table 22 (v). Changing the YDEF bit rate has no effect at all on the integrated margin at the HVPS, because the interference occurs predominantly at 50 MHz where the emission spectrum of the YDEF is unrequired, taken from measured data. On the other hand, the interference at the XDEF occurs more at lower frequencies, where the power spectral density is directly proportional to the bit rate. Thus, the integratedmargin is slightly less than linearly related to the bit rate, a 3 dB variation in bit rate causing a 2.8 dB variation in the integrated margin, and a 20 dB variation causing a 15.4 dB variation.

The bit rate, based on these results, is not a sensitive input parameter.

4.2.14 Required frequency range. This test included the effects of varying the required frequency range for both receptors and emitters, the test results given in Table 22 (v) and (w). Out of 7 receptors having a required range to begin with, 5 of them showed little or no change in the integrated margin, but 2 were very sensitive. For Bundle B8, increasing the required range of the XDEF from 10 MHz to 20 MHz resulted in a 17.7 dB increase in the integrated margin. For Bundle B2, increasing the required range of the AIMS4 from 1 kHz to 2 kHz resulted in a 14.8 dB increase in the integrated margin.

The results for emitter required frequency range, on the other hand, indicate much less sensitivity. Doubling the required range had no effect at all except for the BNOGO in Bundle B2, which causes a 3.5 dB decrease in the integrated margin at the AIMS4.

The results can be explained by the fact that most of the interference in the baseline mini-system is due to unrequired emission at high frequencies, so that changing the required frequency range in the kilohertz region has little effect. However, as indicated, there may be situations where the required frequency range is a very sensitive input parameter.

4.2.15 Equipment frequency table. The results for variation of the frequency table are contained in Table 22 (x). The baseline run was performed with 40 frequencies per equipment, geometrically spaced between 30 Hz and 50 MHz. A second run was performed with 65 frequencies and a third run with 90 frequencies per equipment. In both cases, there is very little change in the

177

integrated EMI margin, usually less than 1 dB. These results are not unexpected, since the emission and susceptibility spectra for the signal/control and power line ports are such slowly varying functions of frequency, in fact log-linear, that increasing the number of points in the numerical integration beyond 40 has very little effect. Based on these results, the total number of frequencies is a very insensitive input parameter.

4.3 <u>Antenna-to-wire sensitivity study</u>. The test configuration for the antenna-to-wire sensitivity analysis includes the upper UHF antenna, the upper TACAN antenna, and 8 receptor ports connected to aperture-exposed wires, listed in Table 24. The baseline run was performed with 40 frequencies per equipment between 14 kHz and 18 GHz, and the sensitivity of 7 input-parameter types, indicated below, was tested.

- o Termination resistance (VWEPLR and VWRPLR)
- o Shield configuration
- o Twisting configuration
- o Bundle height above ground
- o Aperture coordinates
- o Aperture dimensions
- o Equipment frequency table

Table 24. Baseline For Antenna-To-Wire Sensitivity Study

Emitters		
1. Upper UHF Transmitter	(COMUP)	
2. Upper TACAN Transmitter	(TACUP)	
Receptors		
1. Fuel Tank No. 2 Quantity Indicator	(T2QNT)	Through Speedbrake Door
2. Left Bleed Air Overpressure Sensor	(LBAO)	Through Nose Wheel Well
3. HUD X-Deflectors	(XDEF)	
4. High Voltage Power Supply	(HVPS)	
5. HUD DC Relay	(DCREC)	Through Canopy
6. Master Caution Light	(CAUTN)	
7. Panel Light Power	(PNLIT)	
8. HUD DC Power	(DCPWR)	

GP77-0342-18

The sensitivity study test results are contained in Table 26(a) through (h), indicating the variations of integrated margin, point margin and transfer function due to variations in these input parameters. Both point margin and transfer function data were recorded at the tuned frequency of the UHF and TACAN transmitters. A summary of the test results is given in Table 25, indicating the range of integrated margin variation for each input parameter variation, the largest variation and the smallest variation.

178

Table 25. Summary of Antenna To Wire Sensitivity Study Test Results

Input Parameter	Variation of Input Parameter	Range of Integrated Margin Variation	"Typical" Integrated Margin Variation
1a. Victim Wire Receptor Port Load Resistance	3 dB 10 dB	0-3.1 dB 0-10.0 dB	3 dB 10 dB
1b. Victim Wire Emitter Port Load Resistance	3 dB 10 dB	0-3.5 dB 0-14.8 dB	3.5 dB 14.8 dB
2. Shielding	Unshielded → Single Unshielded → Double	29.7-37.4 dB 44.5-56.0 dB	35 dB 50 dB
4. Twisting	Untwisted → Twisted	36.9-48.3 dB	48 dB
10. Bundle Height	4 in. to 8 in. 4 in. to 36 in.	0-6.1 dB 0-11.6 dB	
11. Aperture Coordinates	2 ft Fwd 10 ft Aft	0-1.8 dB 0-19.3 dB	1 dB 1 dB
12. Aperture Dimensions	3 dB 10 dB	0-3.9 dB 0-16.3 dB	
18. Number of Frequencies	40 → 65 40 → 90	0-1.2 dB 0-2.1 dB	0 dB 0 dB

GP77-0342-20

179

Table 26(a) Antenna to Wire Sensitivity Study Test Results
Load Resistance

Input Parameter Value (1a. Victim Wire Receptor Port Load Resistance)	Output Values Due to COMUP			Output Values Due to TACUP		
	Integrated Margin (dB)	Point Margin at 320.65 MHz (dB)	Transfer Function at 320.65 MHz (dB)	Integrated Margin (dB)	Point Margin at 1025 MHz	Transfer Function at 1025 MHz
1. T2QNT 11	19.8	19.3	−10.5	−4.6	−4.0	−10.5
22	22.3 (2.5)	21.8 (2.5)	−14.1 (−3.6)	−5.1 (−0.5)	−4.5 (−0.5)	−14.0 (−3.5)
110	25.0 (5.2)	24.5 (2.7)	−25.3 (−11.2)	−9.2 (−4.6)	−8.8 (−4.8)	−25.3 (−14.8)
2. LBAO 50	−32.0	−32.6	−52.6	−34.3	−33.6	−70.3
100	−32.5 (−0.5)	−33.1 (−0.5)	−56.1 (−3.5)	−34.8 (−0.5)	−34.1 (−0.5)	−73.8 (−3.5)
5,000	−46.1 (−14.1)	−46.6 (−14.0)	−86.6 (−34.0)	−48.3 (−14.0)	−47.7 (−14.1)	−104.4 (−34.1)
3. XDEF 10,000	−126.1	−126.7	−169.7	−98.3	−97.7	−157.4
20,000	−129.1 (−3.0)	−129.7 (−3.0)	−175.7 (−6.0)	−101.3 (−3.0)	−100.7 (−3.0)	−163.4 (−6.0)
100,000	−136.1 (−10.0)	−136.7 (−10.0)	−189.7 (−20.0)	−108.3 (−10.0)	−107.7 (−10.0)	−177.4 (−20.0)
4. HVPS 218	−28.9	−29.4	−79.2	−90.0		
436	−28.9 (0)	−29.4 (0)	−82.2 (−6.0)	−90.0 (0)		
21,800	−28.9 (0)	−29.4 (0)	−119.2 (40.0)	−90.0 (0)		
5. DCREL 47	16.8	16.3	−20.2	−44.3		
94	16.8 (0)	16.3 (0)	−26.2 (−6.0)	−44.3 (0)		
4,700	16.8 (0)	16.3 (0)	−60.2 (−40.0)	−44.3 (0)		
6. CAUTN 175	−2.6	−3.1	−28.6	13.9	14.5	−27.6
350	−5.5 (−2.9)	−6.1 (−3.0)	−34.6 (−6.0)	10.9 (−3.0)	11.6 (−2.9)	−33.6 (−6.0)
1,750	−12.5 (−9.9)	−13.1 (−10.0)	−48.5 (−19.9)	4.3 (−9.6)	4.9 (−9.6)	−47.2 (−20.0)
7. PNLIT 3	12.5	12.0	−0.6	−47.2		
6	15.6 (3.1)	15.0 (3.0)	−3.6 (−3.0)	−44.7 (2.5)		
30	19.5 (7.0)	18.9 (6.9)	−13.6 (−13.0)	−41.4 (5.8)		
8. DCPWR 5	17.0	16.4	−0.6	−43.3		
10	17.3 (0.3)	16.8 (0.4)	−6.3 (−5.7)	−43.0 (0.3)		
500	19.9 (2.9)	19.3 (2.9)	−37.7 (−37.1)	−41.2 (1.1)		

180

GP77-0221-7

Table 26(b) Antenna to Wire Sensitivity Study Test Results
Source Resistance

Input Parameter Value (1b. Victim Wire Emitter Port Load Resistance)	Output Values Due to COMUP			Output Values Due to TACUP		
	Integrated Margin (dB)	Point Margin at 320.65 MHz (dB)	Transfer Function at 320.65 MHz (dB)	Integrated Margin (dB)	Point Margin at 1025 MHz	Transfer Function at 1025 MHz
1. T2QNT 11	19.8	19.3	−10.5	−4.6	−4.0	−10.5
22	16.3 (−3.5)	15.8 (−3.5)	−14.1 (−3.6)	−8.1 (−3.5)	−7.5 (−3.5)	−14.0 (−3.5)
110	5.0 (−14.8)	4.5 (−14.8)	−25.3 (−14.8)	−19.4 (−14.8)	−18.8 (−14.8)	−25.3 (−14.8)
2. LBAO 50	−32.0	−32.6	−52.6	−34.3	−33.6	−70.3
100	−35.5 (−3.5)	−36.1 (−3.5)	−56.1 (−3.5)	−37.8 (−3.5)	−37.2 (−3.6)	−73.8 (−3.5)
500	−46.8 (−14.8)	−47.4 (−14.8)	−67.4 (−14.8)	−49.1 (−14.8)	−48.4 (−14.8)	−85.1 (−14.8)
3. XDEF 6	−126.1	−126.7	−169.7	−98.3	−97.7	−157.4
12	−126.1 (0)	−126.7 (0)	−169.7 (0)	−98.3 (0)	−97.7 (0)	−157.4 (0)
600	−113.4 (12.7)	−114.0 (12.7)	−157.0 (12.7)	−85.6 (12.7)	−85.0 (12.7)	−144.7 (12.7)
4. HVPS 0.05	−28.9	−29.4	−79.2	−90.0		
0.1	−28.9 (0)	−29.4 (0)	−79.2 (0)	−90.0 (0)		
5	−29.1 (−0.2)	−29.6 (−0.2)	−79.4 (−0.2)	−90.2 (−0.2)		
5. DCREL 0.1	16.8	16.3	−20.2	−44.3		
0.2	15.2 (0)	16.2 (−0.1)	−20.2 (0)	−44.4 (0)		
10	15.2 (−1.6)	14.6 (−1.7)	−21.8 (−1.6)	−46.6 (−2.3)		
6. CAUTN 1	−2.6	−3.1	−28.6	13.9	14.5	−27.6
2	−2.6 (0)	−3.2 (−0.1)	−28.6 (0)	13.8 (−0.1)	14.4 (−0.1)	−27.7 (−0.1)
100	−6.4 (−3.8)	−7.0 (−3.9)	−32.7 (−3.8)	+10.1 (−3.8)	10.7 (−3.8)	−31.4 (−3.8)
7. PNLIT 0.1	12.5	12.0	−0.6	−47.2		
0.2	12.5 (0)	12.0 (0)	−0.6 (0)	−47.3 (−0.1)		
10	8.3 (−4.2)	7.7 (−4.3)	−4.9 (−4.3)	−53.0 (−5.8)		
8. DCPWR 0.1	17.0	16.4	−0.6	−43.3		
0.2	16.8 (−0.2)	16.2 (−0.2)	−0.7 (−0.1)	−43.3 (0)		
10	9.4 (−7.6)	8.8 (−7.6)	−8.2 (−7.6)	−51.3 (−8.0)		

GP77-0221-8

181

Table 26(c) Antenna to Wire Sensitivity Study Test Results
Shielding

Input Parameter Value (2. Shielding)		Output Values Due to COMUP			Output Values Due to TACUP		
		Integrated Margin (dB)	Point Margin at 320.65 MHz (dB)	Transfer Function at 320.65 MHz (dB)	Integrated Margin (dB)	Point Margin at 1025 MHz	Transfer Function at 1025 MHz
1. T2QNT	None	19.8	19.3	−10.5	−4.6	−4.0	−10.5
	Single	−17.5 (−37.3)	−18.0 (−37.3)	−47.9 (−37.4)	−34.4 (−29.8)	−33.8 (−29.8)	−40.3 (−29.8)
	Double	−36.1 (−55.9)	−3.67 (−56.0)	−66.5 (−56.0)	−49.3 (−44.7)	−48.7 (−44.7)	−55.2 (−44.7)
2. LBAO	None	−32.0	−32.6	−52.6	−34.3	−33.6	−70.3
	Single	−69.3 (−37.3)	−69.9 (−37.3)	−89.9 (−37.3)	−64.0 (−29.7)	−63.4 (−29.8)	−100.1 (−29.8)
	Double	−88.0 (−56.0)	−88.6 (−56.0)	−108.6 (−56.0)	−78.3 (−44.6)	−78.3 (−44.7)	−115.0 (−44.7)
3. XDEF	Double	−126.7	−126.7	−169.7	−98.3	−97.7	−157.4
	Single	−107.5 (18.6)	−108.1 (18.6)	−151.1 (18.6)	−83.5 (14.8)	−82.9 (14.8)	−142.6 (14.8)
	None	−70.2 (55.9)	−70.8 (55.9)	−113.8 (55.9)	−53.8 (44.5)	−53.1 (44.6)	−112.8 (44.6)
4. HVPS	None	−28.9	−29.4	−79.2	−90.0		
	Single	−66.2 (−37.3)	−66.8 (−37.4)	−116.5 (−37.3)	−130.1 (−40.1)		
	Double	−84.9 (−56.0)	−85.4 (−56.0)	−135.2 (−56.0)	−149.0 (−59.0)		
5. DCREL	None	16.8	16.3	−20.2	−44.3		
	Single	−20.5 (−37.3)	−21.1 (−37.4)	−57.5 (−37.3)	−84.4 (−40.1)		
	Double	−39.2 (−56.0)	−39.7 (−56.0)	−76.2 (−56.0)	−103.3 (−59.0)		
6. CAUTN	None	−2.6	−3.1	−28.6	13.9	14.5	−27.6
	Single	−39.9 (−37.3)	−40.5 (−37.4)	−65.9 (−37.3)	−15.9 (−29.8)	−15.3 (−29.8)	−57.4 (−29.8)
	Double	−58.6 (−56.0)	−59.1 (−56.0)	−84.6 (−56.0)	−30.8 (−44.7)	−30.2 (−44.7)	−72.3 (−44.7)
7. PNLIT	None	12.5	12.0	−0.6	−47.2		
	Single	−24.8 (−37.3)	−25.3 (−37.3)	−37.9 (−37.3)	−88.6 (−41.4)		
	Double	−43.5 (−56.0)	−44.0 (−56.0)	−56.6 (−56.0)	−107.6 (−60.4)		
8. DCPWR	None	17.0	16.4	−0.6	−43.3		
	Single	−20.4 (−37.4)	−20.9 (−37.3)	−37.9 (−37.3)	−84.2 (−40.9)		
	Double	−39.0 (−56.0)	−39.6 (−56.0)	−56.6 (−56.0)	−103.2 (−59.9)		

GP77-0221-9

Table 26(d) Antenna to Wire Sensitivity Study Test Results
Twisting

Input Parameter Value (4. Twisting)		Output Values Due to COMUP			Output Values Due to TACUP		
		Integrated Margin (dB)	Point Margin at 320.65 MHz (dB)	Transfer Function at 320.65 MHz (dB)	Integrated Margin (dB)	Point Margin at 1025 MHz (dB)	Transfer Function at 1025 MHz (dB)
1. T2QNT	Untwisted	19.8	19.3	−10.5	−4.6	−4.0	−10.5
	Twisted	−28.4 (−48.2)	−28.9 (−48.2)	−58.8 (−48.3)	−52.8 (−48.2)	−52.2 (−48.2)	−58.8 (−48.3)
2. LBAO	Untwisted	−32.0	−32.6	−52.6	−34.3	−33.6	−70.3
	Twisted	−80.2 (−48.2)	−80.8 (−48.2)	−100.8 (−48.2)	−82.5 (−48.2)	−81.9 (−48.3)	−118.6 (−48.3)
3. XDEF	Twisted	−126.1	−126.7	−169.7	−98.3	−97.7	−157.4
	Untwisted	−79.2 (46.9)	−79.7 (47.0)	−122.7 (47.0)	−51.3 (47.0)	−50.8 (46.9)	−110.5 (46.9)
4. HVPS	Twisted	−28.9	−29.4	−79.2	−90.0		
	Untwisted	16.8 (45.7)	16.3 (45.7)	−33.5 (45.7)	−44.3 (45.7)		
5. DCREL	Untwisted	16.8	16.3	−20.2	−44.3		
	Twisted	−31.4 (−48.2)	−32.0 (−48.3)	−68.4 (−48.2)	−92.6 (−48.3)		
6. CAUTN	Untwisted	−2.6	−3.1	−28.6	13.9	14.5	−22.6
	Twisted	−48.3 (−45.7)	−48.8 (−45.7)	−74.3 (−45.7)	−31.2 (−45.1)	−30.6 (−45.1)	−72.8 (−45.2)
7. PNLIT	Untwisted	12.5	12.0	−0.6	−47.2		
	Twisted	−24.4 (−36.9)	−24.9 (−36.9)	−37.5 (−36.9)	−85.8 (−38.6)		
8. DCPWR	Untwisted	17.0	16.4	−0.6	−43.3		
	Twisted	−26.0 (−43.0)	−26.6 (−43.0)	−43.6 (−43.0)	−87.0 (−43.7)		

GP77-0221-10

Table 26(e) Antenna to Wire Sensitivity Study Test Results
Bundle Height

Input Parameter Value (10. Bundle Height)	Output Values Due to COMUP			Output Values Due to TACUP		
	Integrated Margin (dB)	Point Margin at 320.65 MHz (dB)	Transfer Function at 320.65 MHz (dB)	Integrated Margin (dB)	Point Margin at 1025 MHz	Transfer Function at 1025 MHz
1. T2QNT 4	19.8	19.3 (3.4)	−10.5 (3.3)	−4.6	−4.0	−10.5 (3.3)
8	23.2 (3.4)	22.7 (3.4)	−7.2 (3.3)	−1.2 (3.4)	−0.6 (3.4)	−7.2 (3.3)
36	23.2 (3.4)	22.7 (3.4)	−7.2 (3.3)	−1.2 (3.4)	−0.6 (3.4)	−7.2 (3.3)
2. LBAO 4	−32.0	−32.6	−52.6	−34.3	−33.6	−70.3
8	−26.0 (6.0)	−26.5 (6.1)	−46.5 (6.1)	−28.2 (6.1)	−27.6 (6.0)	−64.3 (6.0)
36	−20.4 (11.6)	−21.0 (11.6)	−41.0 (11.6)	−22.7 (11.6)	−22.1 (11.5)	−58.7 (11.6)
3. XDEF 4	−79.2	−79.7	−122.7	−51.3	−50.8	−110.5
8	−73.1 (6.1)	−73.7 (6.0)	−116.7 (6.0)	−45.3 (6.0)	−44.7 (6.1)	−104.4 (6.1)
36	−60.1 (19.1)	−60.6 (19.1)	−103.6 (19.0)	−31.7 (19.1)	−31.7 (19.1)	−91.4 (19.1)
4. HVPS 4	16.8	16.3	−33.5	−44.3		
8	22.9 (6.1)	22.3 (6.0)	−27.5 (6.0)	−38.3 (6.0)		
36	25.9 (9.1)	25.4 (9.1)	−24.4 (9.1)	−33.7 (11.0)		
5. DCREL 4	16.8	16.3	−20.2	−44.3		
8	19.3 (2.5)	18.7 (2.4)	−17.7 (2.5)	−41.4 (2.9)		
36	19.3 (2.5)	18.7 (2.4)	−17.7 (2.5)	−38.7 (5.6)		
6. CAUTN 4	−2.6	−3.1	−28.6	13.9	14.5	−27.6
8	2.5 (5.1)	1.9 (5.0)	−23.5 (5.1)	18.9 (5.0)	19.5 (5.0)	−22.6 (5.0)
36	7.3 (9.9)	6.7 (9.8)	−18.7 (9.9)	23.7 (9.8)	24.3 (9.8)	−17.8 (9.8)
7. PNLIT 4	12.5	12.0	−0.6	−47.2		
8	12.5 (0)	12.0 (0)	−0.6 (0)	−46.0 (1.2)		
36	12.5 (0)	12.0 (0)	−0.6 (0)	−41.4 (5.8)		
8. DCPWR 4	17.0	16.4	−0.6	−43.3		
8	18.0 (1.0)	17.4 (1.0)	0.4 (1.0)	−41.7 (1.6)		
36	18.0 (1.0)	17.4 (1.0)	0.4 (1.0)	−38.9 (4.4)		

184

GP77-0221-11

Table 26(f) Antenna to Wire Sensitivity Study Test Results
Aperture Coordinates

Input Parameter Value (11. Aperture Coordinates) BL WL FS	Output Values Due to COMUP			Output Values Due to TACUP		
	Integrated Margin (dB)	Point Margin at 320.65 MHz (dB)	Transfer Function at 320.65 MHz (dB)	Integrated Margin (dB)	Point Margin at 1025 MHz	Transfer Function at 1025 MHz
1. T2QNT 0,163,530	19.8	19.3	−10.5	−4.6	−4.0	−10.5
0,163,506	19.8 (0)	19.3 (0)	−10.6 (−0.1)	−4.6 (0)	−4.0 (0)	−10.5 (0)
0,163,650	16.1 (−3.7)	15.6 (−3.7)	−14.3 (−3.8)	−9.6 (−5.0)	−9.0 (−5.0)	−15.5 (−5.0)
2. LBAO 0,93.350	−32.0	−32.6	−52.6	−34.3	−33.6	−70.3
0,93.326	−31.4 (0.6)	−32.0 (0.6)	−52.0 (0.6)	−32.5 (1.8)	−31.9 (1.7)	−68.6 (1.7)
0,93.470	−51.3 (−19.3)	−51.8 (−19.2)	−71.8 (−19.2)	−39.0 (−4.7)	−38.3 (−4.7)	−75.0 (−4.7)
3. XDEF 0,158,292	−126.1	−126.7	−169.7	−98.3	−97.7	−157.4
0,158,268	−127.2 (−1.1)	−127.8 (−1.1)	−170.7 (−1.1)	−99.0 (−0.7)	−98.5 (−0.8)	−158.2 (−0.8)
0,158,412	−125.1 (1.0)	−125.7 (1.0)	−168.7 (1.0)	98.3 (0)	−97.7 (0)	−157.4 (0)
4. HVPS 0,158,292	−28.9	−29.4	−79.2	−90.0		
0,158,268	−30.0 (−1.1)	−30.6 (−1.2)	−80.3 (−1.1)	−90.8 (−0.8)		
0,158,412	−27.9 (1.0)	−28.5 (0.9)	−78.2 (1.0)	−90.1 (−0.1)		
5. DCREL 0,158,292	16.8	16.3	−20.2	−44.3		
0,158,268	15.7 (−1.1)	15.1 (−1.2)	−21.3 (−1.1)	−45.1 (−0.8)		
0,158,412	17.8 (1.0)	17.2 (0.9)	−19.2 (1.0)	−44.4 (−0.1)		
6. CAUTN 0,158,292	−2.6	−3.1	−28.6	13.9	14.5	−27.6
0,158,268	−3.7 (−1.1)	−4.3 (−1.2)	−29.7 (−1.1)	13.1 (−0.8)	13.7 (−0.8)	−28.4 (−0.8)
0,158,412	−1.6 (1.0)	−2.2 (0.9)	−27.6 (1.0)	13.9 (0)	14.5 (0)	−17.7 (−0.1)
7. PNLIT 0,158,292	12.5	12.0	−0.6	−47.2		
0,158,268	11.4 (−1.1)	10.8 (−1.2)	−1.7 (−1.1)	−48.0 (−0.8)		
0,158,412	13.5 (1.0)	12.9 (0.9)	0.4 (1.0)	−47.2 (0)		
8. DCPWR 0,158,292	17.0	16.4	−0.6	−43.3		
0,158,268	15.8 (−1.2)	15.3 (−1.1)	−1.7 (−1.1)	−44.1 (−0.8)		
0,158,412	17.9 (0.9)	17.4 (1.0)	0.4 (1.0)	−43.3 (0)		

GP77-0221-12

185

Table 26(g) Antenna to Wire Sensitivity Study Test Results
Aperture Dimensions

Input Parameter Value (12. Aperture Dimensions)			Output Values Due to COMUP			Output Values Due to TACUP		
	w,l[1]	Diag.[2]	Integrated Margin (dB)	Point Margin at 320.65 MHz (dB)	Transfer Function at 320.65 MHz (dB)	Integrated Margin (dB)	Point Margin at 1025 MHz	Transfer Function at 1025 MHz
69" Seg	40, 114	121"	19.8	19.3	−10.5	−4.6	−10.5	−4.0
1. T2QNT	40, 57	69.6"	24.6 (4.8)	24.1 (4.8)	−5.8 (4.7)	−2.4 (2.2)	−8.3 (2.2)	−1.8 (2.2)
	4, 11.4	12.1"	13.3 (−6.5)	12.7 (−6.6)	−17.1 (−6.6)	−14.2 (−9.6)	−20.1 (−9.6)	−13.6 (−9.6)
	8, 22.8	24.2"	19.3 (−0.5)	18.8 (−0)	−11.1 (−0.6)	−8.2 (−3.6)	−14.1 (−3.6)	−7.6 (−3.6)
231" Seg	15, 82	83.4"	−32.0	−32.6	−52.6	−34.3	−33.6	−70.3
2. LBAO	15, 41	43.7"	−32.0 (0)	−32.6 (0)	−52.6 (0)	−34.3 (0)	−33.6 (0)	−70.3 (0)
	1.5, 8.2	8.3"	−38.5 (−6.5)	−39.1 (−6.5)	−59.1 (−6.5)	−42.7 (−8.4)	−42.1 (−8.5)	−78.7 (−8.4)
145" Seg	35, 150	154"	−126.1	−126.1	−169.7	−98.3	−97.7	−157.4
3. XDEF	35, 75	82.8"	−126.1 (0)	−126.7 (0)	−169.7 (0)	−97.7 (0.6)	−97.1 (0.6)	−156.8 (0.6)
	3.5, 15	15.4"	−126.1 (0)	−126.7 (0)	−169.7 (0)	−97.7 (0.6)	−97.1 (0.6)	−156.8 (0.6)
145" Seg	35, 150	154"	−28.9	−29.4	−79.2	−90.0		
4. HVPS	35, 75	82.8"	−28.9 (0)	−29.4 (0)	−79.2 (0)	−89.4 (0.6)		
	3.5, 15	15.4"	−78.9 (0)	−29.4 (0)	−79.2 (0)	−92.3 (−2.3)		
145" Seg	35, 150	154"	16.8	16.3	−20.2	−44.3		
5. DCREL	35, 75	82.8"	16.8 (0)	16.3 (0)	−20.2 (0)	−43.8 (0.5)		
	3.5, 15	15.4"	7.5 (−9.3)	6.9 (−9.4)	−29.5 (−9.3)	−52.0 (−7.7)		
134" Seg	35, 150	154"	−2.6	−3.1	−28.6	13.9	14.5	−27.6
6. CAUTN	35, 75	82.8"	−2.6 (0)	−3.1 (0)	−28.6 (0)	14.5 (0.6)	15.1 (0.6)	−27.0 (0.6)
	3.5, 15	15.4"	−6.1 (−3.5)	−6.7 (−3.6)	−32.1 (−3.5)	10.9 (−3.0)	11.5 (−3.0)	−30.6 (−3.0)
170" Seg	35, 150	154"	12.5	12.0	−0.6	−47.2		
7. PNLIT	35, 75	82.8"	11.6 (−0.9)	11.0 (−1.0)	−1.5 (−0.9)	−47.5 (−0.3)		
	3.5, 15	15.4"	0.3 (−12.1)	−0.3 (−12.3)	−17.8 (−12.1)	−55.0 (−7.8)		
263" Seg	35, 150	154"	17.0	16.4	−0.6	−43.3		
8. DCPWR	35, 75	87.8"	13.1 (−3.9)	12.5 (−3.9)	−4.5 (−3.9)	−46.5 (−3.2)		
	3.5, 15	15.4"	0.7 (−16.3)	0.2 (−16.2)	−16.8 (−16.2)	−55.1 (−11.8)		

1. Aperture width, length
2. Aperture diagonal

END
DATE
FILMED

11-77

DDC

MICROCOPY RESOLUTION TEST CHART

NATIONAL BUREAU OF STANDARDS-1963-A
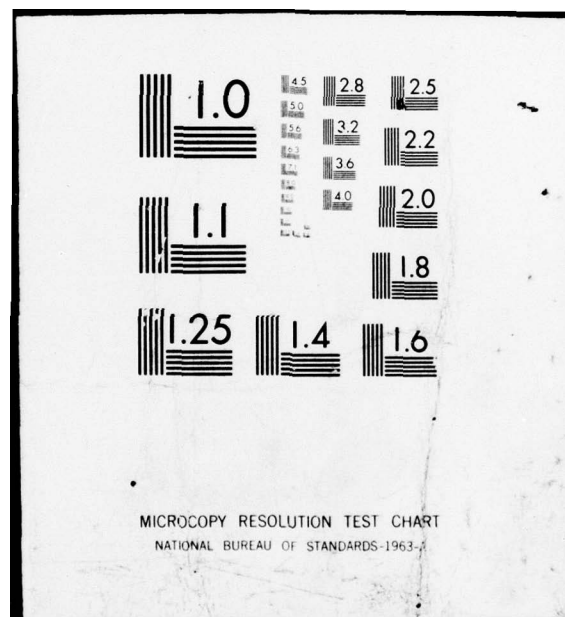
Table 26(h) Antenna to Wire Sensitivity Study Test Results
Number of Frequencies

Input Parameter Value (18. Number of Frequencies)	Output Values Due to COMUP			Output Values Due to TACUP		
	Integrated Margin (dB)	Point Margin at 320.65 MHz (dB)	Transfer Function at 320.65 MHz (dB)	Integrated Margin (dB)	Point Margin at 1025 MHz	Transfer Function at 1025 MHz
1. T2QNT 40	19.8	19.3	−10.5	−4.6	−4.0	−10.5
65	19.8 (0)	19.3 (0)	−10.5 (0)	−4.6 (0)	−4.0 (0)	−10.5 (0)
90	19.8 (0)	19.3 (0)	−10.5 (0)	−4.6 (0)	−4.0 (0)	−10.5 (0)
2. LBAO 40	−32.0	−32.6	−52.6	−34.3	−33.6	−70.3
65	−32.0 (0)	−32.6 (0)	−52.6 (0)	−34.3 (0)	−33.6 (0)	−70.3 (0)
90	−32.0 (0)	−32.6 (0)	−52.6 (0)	−34.3 (0)	−33.6 (0)	−70.3 (0)
3. XDEF 40	−126.1	−126.7	−169.7	−98.3	−97.7	−157.4
65	−126.1 (0)	−126.7 (0)	−169.7 (0)	−98.3 (0)	−97.7 (0)	−157.4 (0)
90	−126.1 (0)	−126.7 (0)	−169.7 (0)	−98.3 (0)	−97.7 (0)	−157.4 (0)
4. HVPS 40	−28.9	−29.4	−79.2	−90.0		
65	−28.9 (0)	−29.4 (0)	−79.2 (0)	−88.8 (1.2)		
90	−28.9 (0)	−29.4 (0)	−79.2 (0)	−87.9 (2.1)		
5. DCREL 40	16.8	16.3	−20.2	−44.3		
65	16.8 (0)	16.3 (0)	−20.2 (0)	−43.1 (1.2)		
90	16.8 (0)	16.3 (0)	−20.2 (0)	−42.2 (2.1)		
6. CAUTN 40	−2.6	−3.1	−28.6	13.9	14.5	−27.6
65	−2.6 (0)	−3.1 (0)	−28.6 (0)	13.9 (0)	14.5 (0)	−27.6 (0)
90	−2.6 (0)	−3.1 (0)	−28.6 (0)	13.9 (0)	14.5 (0)	−27.6 (0)
7. PNLIT 40	12.5	12.0	−0.6	−47.2		
65	12.5 (0)	12.0 (0)	−0.6 (0)	−46.3 (0.9)		
90	12.5 (0)	12.0 (0)	−0.6 (0)	−45.5 (1.7)		
8. DCPWR 40	17.0	16.4	−0.6	−43.3		
65	17.0 (0)	16.4 (0)	−0.6 (0)	−42.2 (1.1)		
90	17.0 (0)	16.4 (0)	−0.6 (0)	−41.4 (1.9)		

187

GP77-0221-14

4.3.1 Termination resistance. The test results for VWRPLR and VWEPLR resistance, contained in Table 26(a) and (b), indicate that these input parameters are not especially sensitive, on the basis of integrated or point margin variation, about 3 dB or less for a 3 dB variation in resistance. In some cases there is more sensitivity to variation in the VWRPLR, and in other cases there is more sensitivity to variation in the VWEPLR, but on the whole the results are similar. For the VWRPLR, there tends to be more variation in the current transfer function, always only in the negative direction, so that the induced current is reduced, tending to reduce the EMI margin. However, the susceptibility level (expressed in current instead of power or voltage) is lower when the receptor port load resistance, VWRPLR, is increased, tending to increase the integrated margin. The net change in the integrated margin is thus smaller than the change in the current transfer function. The change in the integrated margin due to the upper UHF was identical to the change in integrated margin due to the upper TACAN for all receptors except the T2QNT. This particular receptor is modeled as having a required susceptibility at UHF frequencies because of the known non-linear response, and an unrequired susceptibility at L-band frequencies. In the required portion of the spectrum, the susceptibility is tied to a constant voltage level $V = IR$, so the susceptibility level in terms of current is inversely proportional to the resistance, $I = V/R$. In the unrequired portion of the spectrum, the suscepti-bility level in current is inversely proportional to the square root of the resistance, $I = P/R$. For this reason, doubling the resistance decreases the current susceptibility level at the UHF frequency by 6 dB and at the TACAN frequency by 3 dB. At the same time, doubling the resistance decreases the current transfer function by 3.5 dB both at the UHF frequency and the TACAN frequency. Thus the integrated margin due to the upper UHF shows a net increase of 2.5 dB and the integrated margin due to the upper TACAN shows a net decrease of 0.5 dB.

For all other receptors, the UHF and TACAN frequencies are both in the unrequired portion of the receptor spectrum, and the variation in the inte-grated margin due to the upper UHF is always identical to the variation in the integrated margin due to the upper TACAN. No data is recorded for inter-ference to the power line receptors at the TACAN frequency, because that fre-quency exceeds the maximum frequency of interest for power lines in IEMCAP.

On the basis of the test results, the termination resistance is not a sensitive input parameter.

4.3.2 Shield configuration. The test results for shielding, Table 26(c), indicate that shield configuration is a highly sensitive input parameter.

The shielding effectiveness at every receptor wire is about 37 dB at the UHF frequency, and 30 dB at the TACAN frequency. Shielding the receptor wire results in a 37 dB reduction in integrated margin from the UHF and a 30 dB reduction in integrated margin from the TACAN, correspondingly. Double-shielding results in a 56 dB reduction in integrated margin from the UHF and 45 dB reduction in integrated margin from the UHF and 45 dB reduc-tion in integrated margin from the TACAN.

4.3.3 Twist configuration. The results for twisting, Table 26(d), indicate approximately 48 dB of reduction in the integrated margin in most cases. Twisting in this situation means that instead of having a return path through the aircraft frame or ground plane, the circuit has a return path via a second wire, twisted with the original wire. This greatly reduces the loop area of the complete circuit and its effective aperture to RF radiation. Twisting is clearly an extremely sensitive input parameter.

4.3.4 Bundle height. The results for bundle height are contained in Table 26(e). The baseline run was performed with ground returns for all receptor wires, because with twisted wires the height above ground has no effect at all. The results indicate, as expected, that the integrated margin as a ratio varies as the square of the bundle height, since the induced current is proportional to the height. This is only true up to a limiting value, obtained through considerations of maximum available power. A 3 dB change in bundle height, going from 4 inches to 8 inches, causes a maximum variation of 6 dB in the integrated margin. Bundle height appears to be a moderately sensitive parameter for wires with ground returns.

4.3.5 Aperture coordinates. The test results, Table 26(f), show that the precise aperture location is a very insensitive parameter, resulting in about 1 dB of variation for variations of up to 10 feet in fuselage station. The only exception is the LBAO receptor, exposed through the nose wheel well; a 10 foot displacement of the nose wheel well brings it behind the wing edge, resulting in wing shading, and the integrated margin is reduced by about 19 dB. Generally, though, variations of several feet in aperture coordinates have no significant effect on the IEMCAP outputs.

The results indicate that the integrated margin is very insensitive to that exact coordinates of the aperture location, as long as the aperture remains on the same side of the fuselage. Consequently, the antenna-to-wire results would be essentially unchanged if the apertures were assumed to be displaced several feet from their present positions.

4.3.6 Aperture dimensions. The test results, Table 26(g), indicate that the aperture dimensions are not a sensitive input parameter. The reason is that the original size of the apertures is much greater than a quarter of a wavelength, so that the electrical length of exposed wire is very large. In this asymptotic region, the standing waves on the line are approximated by a constant envelope, and variations in the length have no effect on the calculated induced currents. In order to appreciably change the integrated margin, then, the aperture size must be reduced to the point where the exposed length is not electrically large.

For most cases, cutting the aperture length in half does not change the integrated margin or current transfer function. There is, however, an anomaly in the results for the T2QNT. Cutting the speedbrake dimensions from 40"x114" to 40"x57" causes the integrated margin to actually increase by about 5 dB. The reasons that a smaller aperture results, in this case, in more interference, is the way the path length from the antenna to the aperture is calculated by IEMCAP. If the distance between the transmitting antenna and the center of the aperture happens to be less than the size of the aperture itself (the diagonal), then the program uses the aperture dimen-

189

sion as the average "distance" between the antenna and the aperture in its calculation of the incident electric field on the aperture. This happens to be the case for the T2QNT, since the upper UHF antenna is located right in front of the speedbrake. When the size of the speedbrake is cut in half, the program uses a smaller value of average distance between the antenna and the speedbrake aperture, resulting in a larger calculated value for the incident field on the aperture, and thus a larger induced current on the T2QNT wire and a larger integrated EMI margin.

Further reduction of the speedbrake size eventually brings the integrated margin back down to its original value, as the decreasing electrical length of the exposed wire begins to have an effect. When the aperture size is reduced from 40"x114" to 8"x22.8", the integrated margin is decreased by 0.5 dB, and when it is reduced to 4"x11.4" the margin is decreased by 6.5 dB.

This aspect of the IEMCAP code is being corrected by RADC so that reducing the size of an aperture does not have an apparently paradoxical effect on interference to exposed wires.

In general, it appears that the aperture dimensions are a very insensitive input parameter when large apertures are involved. For small apertures, the induced current is proportional to the aperture size, so a 3 dB change in aperture size could be expected to cause a 6 dB change in the integrated margin from a relatively narrow band emitter, a moderate sensitivity.

4.3.7 Equipment frequency table. The baseline run for the antenna-to-wire sensitivity study was performed with a total of 40 frequencies per equipment, with a number of judiciously selected frequencies centered about the tuned frequency of the UHF and TACAN emitters. Runs were repeated with a total of 65 frequencies and again with 90 frequencies, the extra frequencies geometrically spaced between 14 kHz and 18 GHz. There was no change at all in the integrated margin, as seen in Table 26(h) due to the UHF or TACAN. This is because virtually all of the interference is due to required UHF and TACAN emission, contained in a narrow frequency band, and the contribution from the rest of the spectrum is negligible.

For the power lines, where the receptor frequency table does not go high enough to include the required TACAN emission, this is not the case, and the integrated margin due to the TACAN does vary by 1 or 2 dB in going from 40 to 65 or 90 frequencies. As a general rule, if the required range frequencies are judiciously selected, the extra frequencies in the unrequired range have little or no effect. So the total number of frequencies is a very insensitive input parameter.

4.4 SGR sensitivity study. As a baseline for the SGR sensitivity study, an SGR run was performed on the mini-system consisting of the F-15 antenna ports. The program eliminated or greatly reduced cases of antenna-to-antenna interference by adjusting unrequired emission and susceptibility spectra up to a limit of 50 dB. The run was performed with a total of 40 frequencies per equipment, with a judicious selection of frequencies centered about the tuned frequency of each port. To determine the effect of the number of frequencies used to represent the spectra on the SGR output, a second run was performed with 65 frequencies per equipment, and a third run with 90 frequencies per equipment. These changes were correlated with the final adjusted integrated margin at each receptor port due to each emitter, and the results are tabulated in Table 27.

190

Receiver \ Transmitter		UHF Upper	UHF Lower	IFF Upper	IFF Lower	Tacan Upper	Tacan Lower
UHF Upper	① ② ③	Same Equipment	Same Equipment	Co-Located	−36.9 −36.7 (0.2) −36.7 (0.2)	11.9 12.2 (0.3) 12.3 (0.4)	−37.2 −37.0 (0.2) −37.0 (0.2)
UHF Lower	① ② ③	Same Equipment	Same Equipment	−34.0 −34.0 (0) −33.9 (0.1)	Co-Located	8.0 8.4 (0.4) 8.5 (0.5)	−5.4 −5.4 (0) −5.4 (0)
Aux Lower	① ② ③	−8.1 −18.4 (−10.3) −19.2 (−11.1)	23.5 8.8 (−14.7) 3.6 (−19.9)	−35.7 −35.6 (0.1) −35.6 (0.1)	−5.9 −5.9 (0) −5.9 (0)	8.1 8.4 (0.3) 8.5 (0.4)	Co-Located
ADF	① ② ③	−1.1 −4.9 (−3.8) −5.7 (−4.6)	−31.7 −34.0 (−2.3) −35.0 (−3.3)	−20.7 −20.8 (0.2) −20.3 (0.4)	−58.4 −58.4 (0) −58.4 (0)	−5.5 −6.0 (−0.5) −4.6 (0.9)	−73.7 −73.7 (0) −73.7 (0)
IFF Upper	① ② ③	Co-Located	−55.1 −55.1 (0) −55.1 (0)	Same Equipment	Same Equipment	1.1 2.7 (1.6) 0.5 (−0.6)	−51.7 −51.7 (0) −51.4 (0.3)
IFF Lower	① ② ③	−55.0 −55.1 (−0.1) −55.1 (−0.1)	Co-Located	Same Equipment	Same Equipment	−54.2 −53.9 (0.3) −53.1 (1.0)	−1.9 −1.1 (0.8) −1.7 (0.2)
Tacan Upper	① ② ③	−4.1 0.8 (4.9) 7.5 (4.6)	−40.5 −38.3 (2.2) −33.5 (7.0)	3.7 0.8 (−2.9) 3.8 (0.1)	−50.9 −52.3 (−1.4) −50.8 (0.1)	Same Equipment	Same Equipment
Tacan Lower	① ② ③	−54.2 −54.4 (−0.3) −54.4 (−0.2)	−19.8 −20.9 (−1.1) −20.9 (−1.1)	−46.1 −47.2 (−1.1) −46.0 (0.1)	1.7 0.8 (−0.9) 1.8 (0.1)	Same Equipment	Same Equipment
ILS Localizer	① ② ③	−17.9 −18.4 (−0.5) −18.2 (−0.3)	−0.7 −2.6 (−1.9) −1.6 (−0.9)	−40.9 −40.9 (0) −40.4 (0)	−25.2 −25.1 (0.1) −25.0 (0.2)	−8.9 −5.8 (3.1) −5.8 (3.1)	−1.8 −3.4 (−1.6) −2.5 (−0.7)
ILS Glidescope	① ② ③	−25.0 −28.5 (−3.5) −26.6 (−1.6)	−2.6 −6.1 (−3.5) −4.2 (−1.6)	−57.8 −57.8 (0) −57.7 (0.1)	−32.0 −31.6 (0.4) −31.1 (0.9)	−21.6 −21.2 (0.4) −21.1 (0.5)	−2.4 −4.8 (−2.4) −3.7 (−1.3)
ILS Marker Beacon	① ② ③	−35.9 −41.4 (−5.5) −39.0 (−3.1)	3.8 −5.0 (−8.8) −0.4 (−4.2)	−42.5 −42.5 (0) −42.5 (0)	−8.2 −7.8 (2.4) −7.3 (0.9)	−17.1 −17.6 (−0.5) −16.9 (0.2)	−4.3 −6.8 (−2.5) −5.4 (−1.1)

Input Parameter: Number of Frequencies (① = 40, ②= 65, ③= 90)

Output Parameter: Integrated Margin

GP77-0221-39

Table 27 SGR Sensitivity Study Test Results

191

In most cases, there is very little change in the integrated margin, whether 40 frequencies are used, 65 frequencies, or even 90 frequencies. In some cases, there is a slight increase in the integrated margin, and in other cases there is a decrease.

Since SGR is a very complex routine, it is difficult to describe the results without the aid of detailed computer printouts and a step-by-step account of the emitter adjustment process for each emitter-receptor combination (beginning with the first receptor, and going down the list of emitters, repeating the process for each receptor) and the receptor adjustment process. However, a pattern does emerge from all the data, and it is possible to illustrate the more fundamental effects by way of a few examples.

The major effect of changing the frequency table occurs in the receptor adjustment phase of SGR. As discussed previously in Section 2.4, the receptor adjustment is performed at the receptor frequency that is closest to the emitter frequency at which there is interference. Figure 26(a) is an example of receptor adjustment in the baseline SGR run with 40 frequencies per equipment. In this case, the program is adjusting the unrequired susceptibility of the upper TACAN receptor because of interference from the required portion of the upper UHF emitter. The total received signal from the UHF at its tuned frequency of approximately 321 MHz exceeds the unadjusted susceptibility of the TACAN, plotted with the dashed line. The two receptor frequencies straddling this emitter frequency occur at 166 MHz and 324 MHz, so the upper receptor frequency of 324 MHz is the closest. The receptor adjustment is therefore performed at 324 MHz, and the TACAN receptor spectrum is adjusted up by 42 dB at that point. The interpolated value of the adjusted susceptibility spectrum at 321 MHz is raised almost as much, so that the total received signal at 321 MHz falls below the susceptibility by 7.2 dB, and the integrated margin is calculated at -4.1 dB.

Figure 26(b) shows the same receptor adjustment process when 65 frequencies are used instead of 40. The receptor frequencies are closer together this time, since they are geometrically spaced, but this time the nearest receptor frequency is 338 MHz, and the receptor adjustment is performed at 338 MHz instead of 324 MHz. Even though the amount of adjustment is the same, 42 dB, the interpolated value of the adjusted susceptibility spectrum at 321 MHz is not raised as high this time, and the total received signal at 321 MHz is only 0.5 dB below the adjusted susceptibility level. This time the integrated margin is actually positive, 0.8 dB.

Because of the way SGR performs the receptor adjustment, the point margin and integrated margin resulting from this adjustment has a certain amount of randomness that is a function of how close the emitter frequency happens to fall to one of the two receptor frequencies straddling it. If the emitter frequency happens to fall very close to one of the receptor frequencies, the interpolated susceptibility level at the emitter frequency will be raised as much as the adjustment amount, and the point margin will be decreased as much as possible, within the adjustment limits. On the other hand, if the emitter frequency happens to fall close to the midpoint between the two receptor frequencies, the interpolated susceptibility level will be raised only about half as much as the adjustment amount, and the point margin will be decreased only about half as much.

192
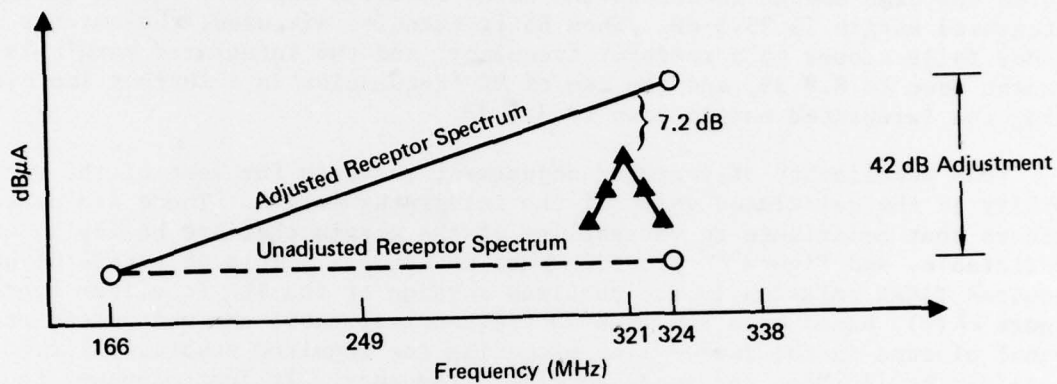
(a) Receptor Adjustment with 40 Frequencies(Integrated Margin = −4.1 dB)
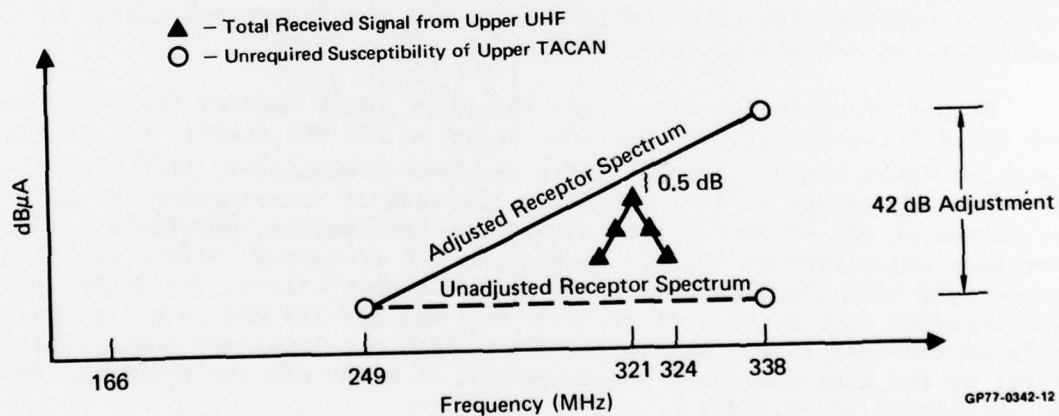
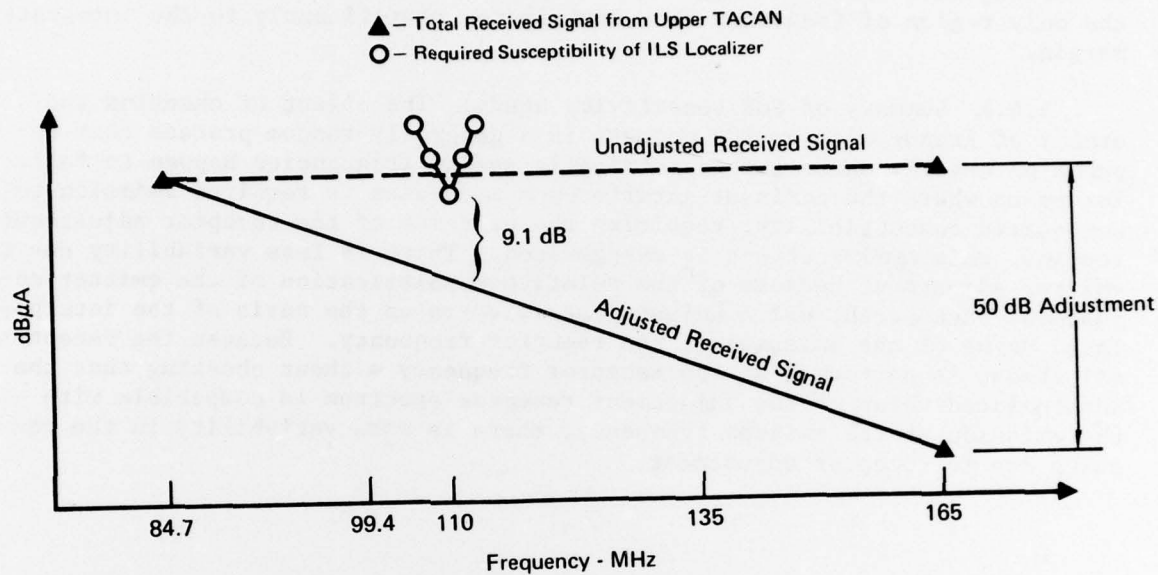(b) Receptor Adjustment with 65 Frequencies(Integrated Margin = +0.8 dB)

GP77-0342-12

Figure 26 SGR Sensitivity Study Example 1
Receptor Adjustment

193

This same random effect accounts for the large variation in the integrated margin at the AUX receiver due to the upper and lower UHF. The largest variation is the decrease of 19.9 dB in the integrated margin due to the lower UHF when 90 frequencies are used instead of 40. As discussed earlier in Section 3.4, and illustrated previously in Figure 23, when 40 frequencies are used, the UHF emitter frequency of 320.65 MHz happens to fall very close to the center of the interval, and the adjustment of the AUX susceptibility at 287.39 MHz fails to bring up the interpolated value of the susceptibility at 320.65 MHz high enough to exceed the total received signal. The adjusted integrated margin is 23.5 dB. When 65 frequencies are used, the emitter frequency falls closer to a receptor frequency, and the integrated margin is brought down to 8.8 dB, and the use of 90 frequencies is a further improvement, bring the integrated margin down to 3.6 dB.

This peculiarity of receptor adjustment accounts for most of the variability in the calculated value of the integrated margin. There are other factors that contribute to variability of the margin that are basically unpredictable, and Figure 27 provides such an example. This is a case of unrequired TACAN emission in the required portion of the ILS localizer spectrum. Figure 27(a), based on a run with 40 frequencies, shows the unadjusted received signal plotted in the dashed line exceeding the required susceptibility of the localizer at 110 MHz, the tuned receiver frequency. It just happens, though, that in a previous emitter adjustment of the TACAN because of interference from the TACAN to the UHF, the TACAN emission spectrum was adjusted down by 50 dB at 165 MHz. This brought the interpolated value of the adjusted received signal at 110 MHz down to 9.1 dB below the localizer susceptibility. The SGR routine did not have to adjust the TACAN spectrum any further in order to achieve compatibility with the localizer, and the integrated margin at the localizer was calculated at -8.9 dB.

When 65 frequencies were used, the first TACAN emitter frequency above the tuned frequency of the localizer falls at 135 MHz instead of 165 MHz as seen in Figure 27(b). Because there are more frequencies, this time the previous adjustment of TACAN emission (because of interference to the UHF) was performed at one or more of the additional frequencies, and there was no previous adjustment at 135 MHz before the SGR attempted to make the TACAN compatible with the localizer. To achieve compatibility, the TACAN emission was adjusted down by 16.4 dB at both 99.4 MHz and 135 MHz to bring the interpolated received signal at 110 MHz down below the localizer susceptibility level by the user-requested safety margin of 6 dB, and the resulting EMI margin is calculated at -5.8 dB.

The ultimate result is that the integrated margin is increased by 3.1 dB if 65 frequencies are used instead of 40. The major advantage of using more frequencies is that adjustments can be performed over smaller frequency intervals, resulting in less stringent overall specifications, tailoring the specifications more closely to the particular situation. The use of 40 frequencies resulted in an overdesigned system, with an integrated EMI margin lower than necessary.

194

▲ – Total Received Signal from Upper TACAN
○ – Required Susceptibility of ILS Localizer

(a) Emitter Adjustment with 40 Frequencies (Integrated Margin = −8.9 dB)
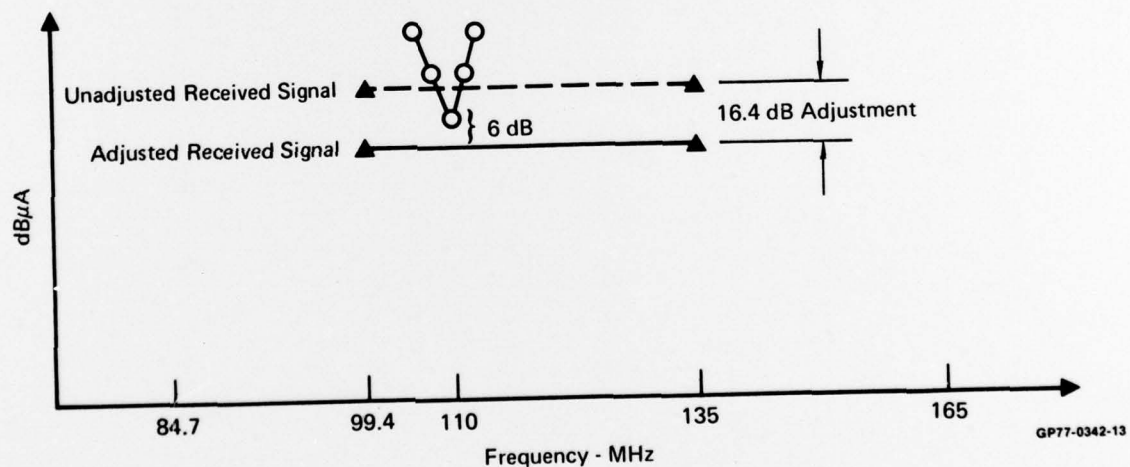
(b) Emitter Adjustment with 65 Frequencies (Integrated Margin = −5.8 dB)

Figure 27 SGR Sensitivity Study Example 2
Emitter Adjustment

195

A third run with 90 frequencies resulted in the same integrated margin as with 65 frequencies. Additional frequencies merely shrink the frequency interval over which the adjustment is performed but do not change the value of the adjusted received signal in the narrow frequency window of the receptor, the only region of frequency that contributes significantly to the integrated margin.

4.4.1 Summary of SGR sensitivity study. The effect of changing the number of frequencies on SGR outputs is a generally random process that depends on exactly where the geometrically spaced frequencies happen to fall. For cases where the dominant interference mechanism is required emission to unrequired susceptibility, requiring the exercise of the receptor adjustment routine, this random effect is exaggerated. There is less variability due to emitter adjustment because of the relative sophistication of the emitter adjustment backsearch, which adjusts the emission on the basis of the interpolated value of the emission at the receptor frequency. Because the receptor adjustment is performed at the receptor frequency without checking that the interpolated value of the adjustment receptor spectrum is compatible with the emission at the emitter frequency, there is more variability in the results due to receptor adjustment.

MISSION
of
Rome Air Development Center

RADC plans and conducts research, exploratory and advanced development programs in command, control, and communications (C^3) activities, and in the C^3 areas of information sciences and intelligence. The principal technical mission areas are communications, electromagnetic guidance and control, surveillance of ground and aerospace objects, intelligence data collection and handling, information system technology, ionospheric propagation, solid state sciences, microwave physics and electronic reliability, maintainability and compatibility.

AMERICAN REVOLUTION BICENTENNIAL 1776-1976